

THE RESPONSE OF SHEAR WALLS SUBJECTED
TO DYNAMIC LOADS

by

VITELMO V. BERTERO

Ingeniero Civil
Universidad Nacional Del Litoral
R. Argentina
1947

S.M. in C.E.
Massachusetts Institute of Technology
1953

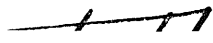
Submitted in partial fulfillment of the
requirements for the degree of

DOCTOR OF SCIENCE

at the

Massachusetts Institute of Technology
June 1957

Signature of Author:



Vitelmo V. Bertero
Department of Civil Engineering
June 1957

Signature of Professor
in Charge of Research:

Professor Robert J. Hansen
Department of Civil Engineering
June 1957

Signature of Chairman
of Departmental Committee
on Graduate Theses:

Professor Charles H. Norris
Department of Civil Engineering
June 1957

√

MASS. INST. TECH.
FEB 19 1958
LIBRARY

To my wife, whose patience and encouragement
have made this work possible.

ABSTRACT

THE RESPONSE OF SHEAR WALLS SUBJECTED TO DYNAMIC LOADS

This report deals with the experimental and theoretical study of the behavior of reinforced concrete shear walls being subjected to dynamic loads. The first part includes a brief discussion of the different factors involved in the study of such structural members. An analysis of the dynamic loading machine follows. This machine was especially designed for this investigation.

Four specimens, identical in every respect except the strength of the concrete, were tested, and attempts were made to simulate actual structural and loading conditions. The specimens were approximately 1/4 size replicas of a standard shear panel in a one-story building, one bay wide. One wall out of these four was tested under static loading. The results obtained are presented in the form of curves, tables, and photographs.

The lattice analogy was used for the theoretical analysis. The simplified lattice used for the elastic behavior during a previous investigation by Mr. Finerman, was modified for the cracked range. In order to determine the properties of the modified equivalent lattice, several assumptions were made. Making use of these assumptions, the programming for the WHIRLWIND I and IBM 704 digital computers was developed. Both programs, as well as the results they yielded, are included in the theoretical discussion.

Thesis Supervisor:

Robert J. Hansen

Title:

Professor of Structural Engineering

Feb. 19, 1958
W. J.

TABLE OF CONTENTS

CHAPTER I: INTRODUCTION	1
I. Statement of Problem	1
II. Previous Investigations	2
III. Objectives	6
IV. Summary of the Investigation	6
V. Acknowledgement	7
CHAPTER II: FACTORS INVOLVED IN THE PROBLEM OF A SHEAR WALL UNDER DYNAMIC LOAD	9
I. Wall Materials and Their Properties	9
II. Type of Wall - Proportion of Wall Components	10
III. Construction Procedures	16
IV. Support Conditions	16
V. Type of Load and Method of Load Applications	17
VI. Scale Effect	21
VII. Instrumentation and Measurements	22
VIII. Miscellaneous Considerations	23
CHAPTER III: TEST SPECIMENS	24
I. Description of Test Specimens	24
II. Properties of the Materials	24
III. Casting and Curing of Test Specimens	26
CHAPTER IV: EQUIPMENT AND INSTRUMENTATION	30
I. Loading Equipment	30
II. Measuring Equipment or Instrumentation	38
III. Miscellaneous Equipment	45
CHAPTER V: TEST OF WALLS	47
I. Wall Preparation	47
II. Test Procedure	48
III. Test Results	50
CHAPTER VI: THEORETICAL INVESTIGATION	62
I. Introduction	62
II. Elastic Behavior	63
III. Cracked Behavior	64
IV. Theoretical Results	70
CHAPTER VII: DISCUSSION OF RESULTS, GENERAL CONCLUSIONS, AND RECOMMENDATIONS FOR FUTURE RESEARCH	72
I. Discussion of the Machine's Behavior	72

II. Discussion of the Results Obtained from Tests Performed on the Walls	74
III. Discussion of the Theoretical Results	78
IV. Comparisons Between Theoretical and Experimental Results	79
V. General Conclusions	80
VI. Recommendations for Future Research	82
REFERENCES	84
FIGURES	86
APPENDIX A: GENERAL PROGRAM AND CODING FOR WHIRLWIND I	169
APPENDIX B: GENERAL PROGRAM AND CODING FOR IBM 704	201

CHAPTER I
INTRODUCTION

I. Statement of Problem

The type of framing selected for use in a particular structure depends on the amount of protection desired against the forces which one expects will act on the structure. It is obvious, therefore, that any serious attempt to design future structures which will resist atomic blast loads, wind gusts, or earthquakes, will lead to the selection of structural forms particularly suited to resist a great amount of lateral load. In this sense, the shear wall structure offers one of the most satisfactory and economical methods of construction.

All buildings which derive their principal strength for resisting lateral loads from structural walls (shear walls) capable of resisting lateral loads acting in their own plane, are understood to be shear wall structures. When forces caused by winds, earthquakes or blasts are applied to these structures, the action of the structural components subjected to lateral loads must be predicted, so that a proper design may be accomplished. Since the shear wall is one of the most important components, particular attention has to be paid to its behavior.

The shear wall is a very stiff member; that is, it has a high resistance to deformation under load. It is essentially a plate loaded in its own plane, but the analysis needed to predict its behavior is more complicated than that of simple plates, for the following reasons. The shear wall cannot act completely as an individual plate, but must deform in a manner which is consistent with the bounding frame. Secondly, the usual materials (reinforced concrete or brick) used in shear walls have

elastic and inelastic properties which are difficult to define, and which make it necessary to predict three different phases of action for any wall. Namely:

1. The elastic behavior.
2. Behavior under small deflections and partial cracking.
3. Behavior under large deflections.

In addition, the usual lateral loads produce dynamic effects which must also be considered.

From the above considerations it becomes obvious that the theoretical approach to the problem is not simple, due to the complexity of the mathematics involved.

II. Previous Investigations

Serious earthquakes have periodically stimulated engineering groups to set standards of design for structures subjected to lateral loads. These standards are usually based on the inertia of the entire structure considered. A portion of the total weight of a building is applied to each story in the form of static lateral loads. The engineer has had to rely on judgement to decide how much of the total lateral load will be carried by the shear walls. Today, the possibility of enormous lateral forces created by blasts, and the increasing desire to reduce the amount of materials used, make the previous knowledge of a dependable design criterion necessary.

Japan has suffered considerably from building failures caused by earthquakes. For this reason, Japanese engineers have devoted a considerable amount of effort in the design of shear walls. A large part of their work has been highly theoretical.

Some experimental work has also been accomplished, yielding various empirical formulas. A common practice in Japan consists of replacing a wall by an equivalent rigid frame.*⁽¹⁾⁽²⁾ Another Japanese method entails a solution of the problem by classical energy theorems.⁽³⁾ Dr. Naito⁽⁴⁾, in an investigation on seismic walls assumed that:

1. The walled frame is completely fixed at the base, and when subjected to the action of horizontal forces,
2. The walled frame would deform like a cantilever beam of I-shape.

The Japanese have conducted a considerable amount of experimental testing, but since their primary goal is earthquake study, most of the walls have been tested by reversals of loading⁽⁵⁾. For this reason, it is difficult to interpret the results in the elastic range. An experimental study which could be of some assistance is one concerning ultimate strength.⁽⁶⁾

Very little research on reinforced concrete shear walls had been done in the United States before 1949. At that time, an investigation was begun at the Massachusetts Institute of Technology, under the direction of Prof. Robert J. Hansen. The main objective of this investigation was to obtain experimental data that would help establish design procedures for structural elements which would sustain impulsive loads. Results were published in different reports.⁽⁷⁾⁽⁸⁾⁽⁹⁾⁽¹⁰⁾ Since 1951, Stanford University has carried out extensive research programs -- experimental and theoretical -- to determine the behavior of shear walls.

As a result of these investigations, several reports have been

* Numbers in parenthesis refer to entries in the Bibliography, or references.

published which shed some light on the subject. (11)(12)(13)(14)(15)(16)
(17)(18)(19)(20) However, all these investigations were made considering only the behavior of walls under static loads, and although the results obtained throw some light on the present problem, it is well known that the behavior of a structure under so called "static loads", or under very slowly applied loads, is quite different from the behavior of the same structure under rapidly-applied loads such as those which arise from wind gusts, earthquake, or blasts from the explosion of bombs. Since much attention has been paid lately to the effects of these loads, it has become increasingly important to have available methods of predicting the dynamic response of shear walls. The Massachusetts Institute of Technology, under contract to the Corps of Engineers, has undertaken recently its theoretical and experimental investigation. The principal objective of the experimental part of this investigation is to obtain sufficient data to substantiate a rational means for predicting the behavior of reinforced concrete shear walls under dynamic loads. From the theoretical side, its principal aim is to find a method that may allow, in the future, the elimination of a great part of experimental work, and act as a check for more empirical solutions. Any recommended procedure for predicting the behavior of such an element should also be based on principles which are familiar to practicing engineers, and at the same time it should be simple to apply with a fairly good degree of accuracy.

The first step of the theoretical investigation is described in the report⁽²¹⁾ submitted by Mr. Aaron Finerman, titled "The Theoretical Elastic Response of Shear Walls Subjected to Dynamic Loads". The first step in the experimental investigation was the construction of a testing machine⁽²²⁾ capable of loading dynamically to destruction

large-scale models of reinforced concrete shear walls.

Once the first step of the experimental program was completed, it was decided that this preliminary investigation would be restricted to the testing of several reinforced concrete shear walls, with the object of analyzing the behavior of the machine, and at the same time obtain some data on the parameters which can affect the dynamic resistance of the element being considered. This preliminary investigation will allow the development of a more extensive experimental research program.

The theoretical investigation may be considered as a continuation of the work made by Finerman. As the title of his report⁽²¹⁾ indicates, his work was restricted to the study of the dynamic response of walls, within the elastic range of the member. Although it is true that the designer must decide what point in the behavior of the structure he wishes to consider as the maximum permissible response, it is obvious that only rarely may he choose this point to be within the elastic range, because of the extremely heavy construction this would require. Therefore, it will be more economical to allow for a certain amount of cracking, and in some cases -- especially for certain types of blast-resistant structures -- it will be reasonable to even design for collapse, since a factor of safety may be already included in the choice of the pressure curve for which the design is to be made.

Furthermore, only under very favorable conditions may it be assumed that the first loading on a shear wall will be resisted in part by tension in the concrete. Repetition of the common live loads or unpredictable volume changes can cause cracks to develop along any section that is not constantly under compression.

From the above considerations it is evident that it is necessary to have a rational means for finding deflections and stresses not only in the elastic, but also in the inelastic ranges.

III. Objectives

This work was made in order to supplement the above-mentioned combined research program undertaken by M.I.T., and it is a theoretical and an experimental investigation covering the following points:

- A. An experimental investigation of shear wall behavior under dynamic loads.
- B. The mathematical prediction of the behavior of the tested walls.

IV. Summary of the Investigation

The mathematical prediction of shear wall behavior under dynamic loads for the phase included between the first cracking load and the ultimate load is accomplished by the use of a lattice analogy. The method consists essentially of replacing the frame and panel by a pin-connected lattice having the same resistance to deformation. The prediction of the cracked action involves a number of assumptions which are discussed in Chapter VI. The lattice analogy procedure is then used to obtain theoretical load-deflection curves and the ultimate load for the reinforced concrete shear wall.

Due to the limited time, the predictions and experimental verifications reported here have been confined to shear walls of one proportion. Four specimens were tested, and these were identical except for the strength of the concrete. In two the compressive strength at the day of the test was approximately 3,000 psi, and in the other two 5,100

and 6,300 psi respectively.

Attempts were made to simulate actual structural and loading conditions, the specimens being approximately a 1/4 scale replica of a standard shear panel in a one story building, one bay wide.

The model selected and the loading arrangement used in the tests are shown in Figure 1.

One wall was loaded by static lateral load only. This test served to check the operation of the equipment and to establish the static properties of the walls which were to be tested dynamically later. The applied load, reactions, horizontal and vertical deflections were recorded against time, during each test, with the exception of the static test. The experimental results of this investigation are presented in Chapter V, and the theoretical discussion is given in Chapter VI.

V. Acknowledgment

The experimental work described in this report was performed in the Structural Dynamics Laboratory of the Massachusetts Institute of Technology, under Contract DA-49-129-Eng 325 with the Corps of Engineers.

The author wishes to thank his advisor, Dr. Robert J. Hansen, Associate Professor of Structural Engineering, for his advice and direction of this investigation, and Howard Simpson, Associate Professor of Structural Engineering for his immediate supervision and encouragement.

The author also wishes to acknowledge the assistance of Harry Guzelimian, Research Assistant in Civil Engineering, in preparing and conducting the tests. Also the work done by Shui Ho and Christopher Caladine, Research Assistants, in preparing the program for the high-speed

computers. The recording instruments were assembled and operated by Arthur Casey, Senior Electrical Technician.

Sincere thanks are also expressed to Mr. Donald Gunn, who offered much practical advice and did the machine work for some of the apparatus, to Miss S. Carlson for typing the thesis and to E. Lawlor, A. Ostapenko, N. Durando, and K. Gentili for their help throughout the investigation.

CHAPTER II
FACTORS INVOLVED IN THE PROBLEM OF A SHEAR WALL UNDER
DYNAMIC LOAD

In planning an experimental investigation of shear walls of reinforced concrete, the following factors must be considered:

- I. Wall materials and their properties.
- II. Type of wall - Proportion of the wall components.
- III. Construction procedures.
- IV. Support conditions.
- V. Method of load application and type of load.
- VI. Scale effect.
- VII. Instrumentation and measurements.
- VIII. Miscellaneous considerations.

For the purpose of a specific series of tests designed to acquire information on a particular facet of the general problem, the importance of certain of these factors may be negligible, or for practical purposes may be considered as such. For a full understanding of the value of a series of tests and the relation of that series to the overall problem, it is necessary to define the limits within which the series falls, in terms of the above factors.

I. Wall Materials and Their Properties

Shear wall structures include articulated structural steel frames with diagonal bracing and continuous frames with masonry or reinforced concrete panels. This investigation, however, has been limited to monolithic reinforced concrete shear walls, which appear to be the

most satisfactory and economical choice for structures designed to resist heavy blasts.

The properties of the material which are important in the case of reinforced concrete are the tensile strength and modulus of elasticity of the concrete, and the yield point of the steel reinforcing.

II. Type of Wall - Proportion of the Wall Components

Although we are concerned with only one kind of shear wall -- the monolithic reinforced concrete shear walls -- many different factors must be considered. In one case, the shear wall may belong to a one story or to a multistory shear wall structure. However, since we are essentially interested in the behavior of the structural elements, our investigation will be limited solely to one-story walls. Once the dynamic response of this structural element is known, the behavior of multistory shear wall structures may be predicted by modifying certain parameters.

It is also recognized that if there exist openings in a shear wall, the dynamic response of the wall can vary over a wide range, depending on the relative size and location of the openings. However, the investigations reported herein have been conducted on solid shear walls only.

The important properties of a shear wall are:

A. Frame Effect

1. Column and beam concrete and steel areas relative to thickness and length of wall panel.
2. The steel ratio of the columns and beams.

B. The steel ratio of the wall panel and its distribution

C. Length-height (L/H) ratio of wall panel.

A. Frame Effect: Ordinarily, the greatest gains in speed of construction, cost and space usage in shear wall structures are obtained by simplifying and standardizing the wall forms by elimination of all projections and pilasters: (i.e.), they are to be constructed as monolithic, box-shaped structures without conventional framing beams and columns around shear walls. Since cross walls are ordinarily well tied to face walls and to floor and roof slabs, it is obvious the latter will impart -- acting as a frame -- considerable strength to the shear walls, in addition to that inherent in the shear wall itself.

This integral action of slab and wall must be considered in our investigation. The proportion of wall or slab that acts integrally as flanges with the shear wall in resisting bending moment and shear forces is highly debatable at this time. If one follows conventional T beam practice, the allowance would be eight times the thickness of slab or face wall on each side of the cross wall, and the maximum effective width of flange should be taken no more than one-half of the distance between shear walls. This would mean that a 6" wall or roof slab is equivalent to a 24" square column or girder, although the percentage of reinforcement would be low compared to the conventional member. It should be noted that face walls and slabs enter into the frame action for shear walls of any monolithic structure, whether or not there are framing columns and beams. However, in the case where dynamic loads are applied, the problem becomes more complex, due to the necessity of considering an equivalent mass to that of the walls and slabs.

The frame effect is an important aspect of the shear wall problem. While the general effect may be investigated by changing the frame size for a given wall, this throws little light on the actual

effect of face walls and slabs in a structure. It is obvious that if the slab develops cracks (but does not fail in flexure), the horizontal load capacity of the structure may be reduced due to the redistribution of the load which is caused by these cracks, as shown in Figure 2. When the stresses in the roof are not sufficient to cause cracking, the roof slab will supply added resistance by acting as the flange of a T beam.

The experimental approach to the problem is difficult because of the magnitude and type of loading required. Static tests on small models were carried out at Stanford University⁽¹³⁾ but the results should be considered as qualitative, owing to considerable difficulties encountered during the tests. It is hoped that a full-scale structure test program can be prepared, as it was prepared previously by the Office of the Chief of Engineers, Department of the Army.⁽²³⁾

1. The relation between column and beam areas and wall panel area is important insofar as it greatly influences the value of the load that will produce first cracking, by changing the stress pattern in the wall.

2. The steel ratio of the column and beam directly influence the ultimate strength.

In general, the frame, and particularly the columns may give rise to a different type of shear wall failure. If the column strength is insufficient to cause cracking of the shear wall, a tension failure along the base will result as shown in Figure 3. This requires a yielding of the tension column steel. If the tension column steel does not yield and produce a failure, the ultimate load can be associated either with complete wall breakdown or a shear failure of the compression column at the foundation, as it is shown in Figure 4. As far as can be

determined, reinforced concrete walls of practical proportions do not fail at ultimate by sudden panel cracking.

According to the above reasoning the investigation was programmed using shear walls whose components have been designed so as to induce progressive panel cracking, eliminating the possibility of a sudden failure.

B. The Steel Ratio of the Wall Panel and its Distribution: The design of blast-resistant structures may require the use of shear walls designed to produce as high a strength as possible. One of the basic parameters involved is the panel steel ratio.

Although it may be expected that the wall rigidity and load at first cracking would be virtually independent of the wall's steel ratio, it is obvious that the placing of reinforcing in the panel changes the mode of failure to some extent. If the percentage is small, the wall will have an ultimate load derived from two sources -- the compression column and the panel steel. As the panel strength increases with increasing percentage of steel, it tends to become the dominant influence, while the contribution of the column tends to become negligible. Studies of the strengthening factors in the panel showed that the only important parameters were the horizontal and vertical steel cross-sections. The concrete is unimportant. Furthermore, a considerable portion of the panel steel is stressed to its yield point at or before ultimate load. From static tests it was found that the yield point of the panel steel was a parameter. These same tests seem to indicate that there exists a practical limit in the neighborhood of one per cent panel steel, above which the increase in ultimate load with further increases in panel steel tends to become relatively smaller.

Standard design procedures call for equal amounts of horizontal and vertical panel steel. This steel is selected as a percentage of the wall cross-sectional area, and is uniformly distributed throughout the panel. The practice is reasonable when the steel ratio is low and large amounts of steel are not involved. However, blast design may require large amounts of steel in the panel. Some question then arises as to the efficiency of the uniformly distributed design.

Although it may have been expected, according to the stress pattern to be obtained, that the diagonal reinforcing might be more effective than that placed horizontally and vertically, the static test results obtained at Stanford University⁽¹⁶⁾⁽¹⁹⁾ indicated that in all cases the ultimate loads were smaller, in the case of a diagonal pattern than for vertical and horizontal distributions. Both concentrated and uniformly distributed patterns were studied, including an attempt to provide local strengthening of critical areas. Concentrations of steel on the diagonals and in the lower corners produced early shrinkage cracking in these locations and noticeably decreased the strength.

With uniformly distributed diagonal steel, the strength was nearly equivalent to the rectangular design. However, Mr. Whitney⁽²³⁾, after analyzing a limited number of tests conducted on concrete reinforced with 45-degree diagonal tension steel, reached the conclusion that in general it appears that the above distribution of reinforcing results in slightly stronger and stiffer shear panels, provided the walls are not subjected to a transverse load at the same time. Further studies under static loads show that uniform vertical steel is more effective than horizontal steel. Vertical steel alone appears to be fully as effective as vertical plus horizontal steel. Complete omission of hori-

zontal steel would be undesirable from a practical standpoint, since a certain amount of horizontal steel is necessary to hold the vertical steel in place. The tests at Stanford⁽¹⁹⁾ demonstrated that if it is desired to reduce the panel steel, the horizontal wall steel in the upper three quarters of the wall can be reduced substantially, without influencing the panel stiffness or strength.

The present study only takes into account walls with uniformly distributed horizontal and vertical reinforcing steel, and a steel ratio of 1/4 percent. However, it is obvious from the above considerations that in the extensive experimental program, a large number of different ratios must be taken into account.

C. Length-Height (L/H) Ratio of Wall Panel: The length-height (L/H) ratio, is an important factor in wall behavior. Static tests at Stanford University⁽¹⁵⁾, indicated that the ultimate strength in stress per unit of shear area is essentially independent of L/H, whereas the first cracking load increases greatly with the L/H ratio.

For walls with panel reinforcing, first cracking and ultimate loads become essentially equal at an L/H value somewhat greater than three.

However, these conclusions were obtained from tests on specimens in which the bottom beam can be considered as fixed. The analytical study made by Finerman⁽²¹⁾, shows that for simple-support shear walls, the first cracking load decreases after a certain L/H, instead of increasing.

In this first series of dynamic tests, the L/H ratio was not changed, but it is obvious that it would be necessary to do so in a general investigation.

III. Construction Procedures

Although shear walls, except for pre-cast elements, would be formed and poured in place in a vertical position, the models here studied were poured flat on the casting floor.

It is possible that some small difference in strength may occur from this difference in method of casting, but it is believed that this factor has no importance.

IV. Support Conditions

The support conditions of a shear wall are an important factor. Yield, sliding or other movements of the supports of a wall exposed to a blast or to a motion of the footing that restrains the building frames from sliding or rotating will act to relieve the straining parts, and must therefore be considered in the design.

The flexibility of the foundation materials and its resistance to lateral deflection and to rotation are important in determining the motion of a structure. When a structure is founded on spread footings or on footings supported by piles, the relative degree of fixity of the columns in the structure at their connection with the footings is a matter of considerable importance in determining the lateral resistance and the strength of the structure being submitted to lateral forces.

In this investigation, the walls were supported as indicated -- in a general way -- in Figure 5. Details of the support are shown in Figures 6 and 7. The type of supports used may be considered as simple supports, except for the fact that they are not entirely rigid, but have some flexibility. The deflections of the supports were determined during the first static test, and were found to be not negligible.

In a shear wall, the loads are transmitted at the bottom of the wall through a connecting shear wall, a floor slab, or the foundation. It is evident that only in the case of single-story buildings, (which are generally preferable to multistory constructions), may our supports be considered similar to those encountered in an actual structure.

V. Type of Load and Method of Load Application

As it was stated previously, the main purpose of this work is to study the behavior of shear walls which are submitted to loads produced by an atomic blast. Obviously then, attempts must be made to simulate this special kind of load.

Most of the energy released by atomic fission acts to heat the surrounding air to extremely high temperatures. The rapid expansion of this heated air exerts an enormous pressure on the surrounding atmosphere which moves outward from the center of the explosion as a conventional shock wave. This wave is characterized by a virtually instantaneous rise to peak pressure which quickly decreases in intensity to atmospheric, followed by a much less intense negative pressure. This intensity of the peak pressure, the variation with time, and the duration of the positive phase are of prime interest. These factors depend on the energy release of the weapon, the ground zero distance, and the height of burst. It is obvious that the exact loading to which any particular building may be exposed will never be accurately known. The only thing that can be done is to establish the energy level to be protected against, by the selection of an appropriate bomb and ground zero distance. Once this is done, curves of load vs. time for most types of rectangular structures

may be approximated by the methods given in⁽⁴⁾, Chapter XI; and⁽²³⁾, Appendix 1.

Evidently, the way in which impulsive loads are transmitted in an actual structure depends largely on the type of construction and the location of the wall. Figure 8 shows the typical loading on shear wall structures.

In calculating the horizontal reactions of the exterior front and rear walls, the roof and shear wall are usually assumed infinitely rigid in their own planes. Then, the reactions of the exterior walls rather than the direct blast pressures should be used in the design of shear walls, because the dynamic strains in the stiff, quick-acting shear wall are greatly affected by the rate at which the forces acting on the front and rear walls and the roof are applied on it.

In structures where large plastic deformations of the exterior blast-resistant walls are allowed, the reactions of the wall will have an impulse curve which is very different from that for the pressures acting on the exposed wall at any given time, as shown in Figure 9. This difference in the shape of the impulse curve (elimination of the peak) will, in most cases, reduce the strength needed for the structural element which supports the exterior walls.

Usually, wall spacing would be large compared to story height and the main face wall reinforcing would be in a vertical direction. Hence, face wall pressures would be transmitted primarily to the floor system and thence to the tops of the shear walls. If walls were so closely spaced that face wall pressure were transmitted primarily in a horizontal direction and distributed along vertical ends of the walls, it is questionable whether the shear walls would be very heavily loaded.

An exception would occur if large impulsive loads were applied to very heavy face walls. However, the above conditions lead us to the conclusion that the proper method of testing model shear walls is to apply the load along the top of the wall. This conclusion introduces another question: How should the load be distributed along the top of a model wall? Four possibilities are shown in Figure 10.

Japanese investigators have found that the second and third methods cause a different crack pattern than the first. The loading indicated in Figure 10-D probably comes closest to the actual conditions, since face walls and floors together act as an I-beam, the floor being the web of the beam. It would seem reasonable to believe that shear would be distributed to the cross wall by the floor in a manner consistent with the parabolic distribution of shearing stress in an I-beam web. However, this can only be true in the elastic range, because if the slab develops cracks but does not fail in flexure, the load will be redistributed according to the crack pattern on the roof, as mentioned before and shown in Figure 2.

However, the truly few static tests carried out at Stanford University⁽¹³⁾, reach the following conclusion:

"The manner in which loading is applied to the shear wall -- whether directly or through a roof -- has relatively little influence on the shear wall behavior, providing the structures are otherwise identical."

Another factor which will affect the behavior of a shear wall is the presence of vertical forces. These forces may result from heavy dead loads and the superimposed live load arising from vertical effects of the blast or other dynamic forces. Impulsive roof loads of a high order of magnitude will be present under ordinary conditions, and the

magnitude of the total vertical force will be of the order of 50 to 100% of the shear load applied to the top of the wall, depending on relative dimensions and type of construction. It is evident that the added vertical load may affect the response, because the moments of these loads affect the deflections, which in turn affect the moments of the vertical forces; but there is still another effect of the vertical load which is potentially of great importance in a problem of this kind. This effect concerns the change in the resistance properties of the cross sections of the columns, which is brought about by the simultaneous presence of direct forces and bending moments. Because the problem is a non-linear one, and both the forces and the moments are independent functions of time, enormous complexities would be introduced into any analytical considerations. These effects may be approximated in the manner suggested by Newmark and Fraenkel.⁽²⁴⁾⁽²⁵⁾

However, the tests performed under static loads at Stanford University⁽¹³⁾, indicated that the shape or magnitude of the load deflection curve is not significantly influenced by vertical loads of the same order of magnitude as the shear load, and the initial stress pattern and initial cracks are influenced very slightly by the vertical loading. The final crack pattern is similar to that of specimens subjected to shear load only.

For the effects considered above, in the present series of tests, a loading arrangement was used which subjected the panel to stresses that would occur under cantilever loading with a concentrated load at the upper corner. (Figure 6).

In a more extensive experimental program, some account of the added vertical load may be taken by considering an increased dead load

equivalent to the added vertical force.

Special consideration must also be given to the effects of various different combinations of load rise with time, peak intensity, and duration of load.

VI. Scale Effect

If the various factors mentioned before are to be explored in a satisfactory manner using full-scale shear wall models, the program immediately assumes stupendous proportions. On the other hand, it is difficult to properly simulate complex stress patterns with scale models, particularly when cracking of concrete and yielding of reinforcing steel are involved. Hence, some comparisons are needed.

For the static tests carried out at Stanford University⁽¹³⁾, concrete models geometrically scaled to $1/8$, $1/4$, and $3/8$, were used. The results of these tests indicated that in general, there is no definite indication of scale effect.

It must be noted that if no scale effect exists -- in the case of static loads -- the load will vary as the square of the scale factor, and deflections vary directly as the scale factor, with like concrete strength and modulus of elasticity.

However, these results were obtained considering that the applied load and the internal forces are closely balanced at all times, and that the acceleration is negligible.

In the case of rapidly or instantaneously applied loads, however, the internal forces resisting deflections will not be immediately and continuously equal to the applied loads, and the resultant acceleration of the member will not be negligible. The maximum stress and, more

important, the maximum displacement produced under blast loads, are a function of the intensity of the applied force, the rate of application of the force, the duration of the load, and the particular variation with time of the applied force and the resistance. These stresses and displacements are generally far different from those which would result from a static load of equal magnitude, and the prediction of the way the load and deflections will vary with the scale factor becomes very difficult. As in any dynamic problem, the solution of this one becomes a question of force, mass, stiffness, strength, and time. The scale factor between the responses of model and prototype will not only depend on the dimensional scale factor, but also on the rate of application of the force, the duration of the load, and the natural vibratory frequency of the wall.

In the present work, a reinforced concrete panel of $45 \frac{1}{8}$ " by 61" was considered to represent a $1/4$ -scale model of a prototype wall. For the reasons given above, it is obvious that in order to determine the scale effect with accuracy, it will be necessary to plan an extensive experimental program including not only different scale concrete models, but also varying the load-time function.

VII. Instrumentation and Measurements

In planning the experimental program for studying the dynamic characteristics of the shear wall, several requirements have to be met.

One set of requirements is related to the design of the testing machine, and the other set is related to the instrumentation necessary to obtain the magnitude of load and reactions, strains and deflections, of the test specimen.

Electronic, photographic, and mechanical means are used. The

accuracy of the results to be obtained will depend on the errors introduced by the different sources.

A discussion of some of these errors will be given in Chapter IV.

VIII. Miscellaneous Considerations

There are other factors which may also be considered in the case of a structure with shear wall construction, such as: horizontal construction joints, shrinkage cracks, expansion joints, etc. However, it is believed that the importance of these factors may be neglected in this investigation.

CHAPTER III TEST SPECIMENS

I. Description of Test Specimens

The specimens used in this investigation were designed to represent shear walls in a single story building, one bay wide, which was considered to represent a 1/4 scale model of a prototype wall.

The dimensions were chosen to duplicate as accurately as possible, the shear wall tested statically at Stanford University.⁽¹⁶⁾

Details of the shear wall configuration, stirrup-spacing, and steel distribution are illustrated in Figure 11. The four walls cast were identical except for the compressive strength of the concrete. For two of these walls, the compressive strength was 3,000 psi, whereas in the other two this strength was 5,100 and 6,300 psi respectively. Table I contains the important characteristics of the walls.

As shown in Figure 11, the columns were extended to provide sufficient bond for reinforcing, and to prevent local cracking failures in the places where the load was applied. As it is indicated in the same figure, special steel plates were used where the load and reactions are applied.

II. Properties of the Materials

Information concerning the properties of the materials constituting a specimen is of prime importance in an experimental investigation.

Two types of concrete were used in the construction of the specimens. The mixes used for the concrete had the following characteristics:

For wall #1 and #2

1 part by weight of high early strength Portland Cement

2.46 part by weight of sand

2.82 part by weight of 1/4" - 1/2" gravel

6 gallons of water per sack of cement

Air entraining agent - Darex 28 cc per sack of cement

For wall #3 and #4

1 part by weight of high early strength Portland Cement

3.4 part by weight of sand

3.8 part by weight of 1/4" - 1/2" gravel

7.45 gallons of water per sack of cement

Air entraining agent - Darex 28 cc per sack of cement

As can be seen above, the types of concrete used were very similar to those found in conventional practice.

Sufficient control specimens were made for each model, so that the rate of gain in strength and the strength on the day of the test could be ascertained. An attempt was made to test all specimens when the strength was approximately that desired. This was possible in all but the first two walls.

The values of the important characteristics of the concrete used in the four walls are listed in Table II.

Reinforcing Steel

Due to the small amount of steel reinforcement used in the wall panel, and in order to maintain the separation of the bars between practical limits, it was necessary to use undeformed bars for the panel reinforcing. Intermediate grade Inland Hi-Bond deformed bars were used for the frame reinforcing.

The important characteristics of the bars used in the four walls are given in Table III.

III. Casting and Curing of Test Specimens

All walls were cast on the floor, in a wood formwork especially designed so that its part could be easily removed. Two walls were cast simultaneously. The reinforcing cage and the steel plates -- where loads and reactions of the supports acted -- were held in position by welding the reinforcing of the frame to the plates, which were held in place by an auxiliary steel frame. Figure 12 shows the formwork and the reinforcement in place.

Special pins were inserted where the brackets for measuring deflections had to be attached, and bolts were inserted for the subsequent attachment of the lateral restraint mechanism.

All the concrete was mixed for three to five minutes in a mixer of 6 cu.ft. capacity. Each wall was cast from two batches of concrete of approximately the same proportions. Three 6 x 12" control cylinders were also cast from each batch. The concrete was placed in the forms and cylinder molds with the aid of a high-frequency internal vibrator.

The walls and control cylinders were stored under moist conditions for five days, after which they were removed from the forms and kept stored in the air of the laboratory until tested.

Figure 13 shows the walls and cylinders just after being cast.

TABLE I PROPERTIES OF WALLS

Specimen	Frame Dimensions				Frame Reinforcing			Stirrups	
	Top	Bottom	Columns	Columns	Beams	Columns	Beams	Columns	Columns
#1	5"x 7 1/2"	12"x 7 1/2"	5"x 7 1/2"	5"x 7 1/2"	4-1/2" \emptyset	4-1/2" \emptyset	1/8" \emptyset wire - 5" c.c.	1/8" \emptyset wire - 5" c.c.	1/8" \emptyset wire - 5" c.c.
#2	5"x 7 1/2"	12"x 7 1/2"	5"x 7 1/2"	5"x 7 1/2"	4-1/2" \emptyset	4-1/2" \emptyset	1/8" \emptyset wire - 5" c.c.	1/8" \emptyset wire - 5" c.c.	1/8" \emptyset wire - 5" c.c.
#3	5"x 7 1/2"	12"x 7 1/2"	5"x 7 1/2"	5"x 7 1/2"	4-1/2" \emptyset	4-1/2" \emptyset	1/8" \emptyset wire - 5" c.c.	1/8" \emptyset wire - 5" c.c.	1/8" \emptyset wire - 5" c.c.
#4	5"x 7 1/2"	12"x 7 1/2"	5"x 7 1/2"	5"x 7 1/2"	4-1/2" \emptyset	4-1/2" \emptyset	1/8" \emptyset wire - 5" c.c.	1/8" \emptyset wire - 5" c.c.	1/8" \emptyset wire - 5" c.c.

Specimen	Panel Reinforcing and Spacing		Age at Test (Days)	Compression (f'c) psi
	Horizontal	Vertical		
#1	1/4" \emptyset at 10" ctrs.	1/4" \emptyset at 10" ctrs.	53	5,100
#2	1/4" \emptyset at 10" ctrs.	1/4" \emptyset at 10" ctrs.	64	6,300
#3	1/4" \emptyset at 10" ctrs.	1/4" \emptyset at 10" ctrs.	7	3,000
#4	1/4" \emptyset at 10" ctrs.	1/4" \emptyset at 10" ctrs.	8	3,000

TABLE II PROPERTIES OF CONCRETE MIXES

Specimen	Batch	Cement/Sand/Gravel By Weight	Water/Cement By Weight	Compressive Strength (f'c psi)	Modulus of Elasticity E_c *(psi x 10 ⁶)	Age At Test (Days)
#1	2	1.00:2.46:2.82	0.53	5.100	4.50	53
#2	2	1.00:2.46:2.82	0.53	6.300	4.70	64
#3	2	1.00:3.40:3.80	0.66	3.000	3.80	7
#4	2	1.00:3.40:3.80	0.66	3.000	4.00	8

* E_c is Initial Tangent Modulus

TABLE III PROPERTIES OF REINFORCING BARS

Specimen	Panel Reinforcement			
	Size	Yield Point f_y (ksi)	Ultimate Strength (ksi)	Modulus of Elasticity E_s (ksi)
#1	#2 Plain bars	39.30	52.00	31,000
#2	#2 Plain bars	39.30	52.00	31,000
#3	#2 Plain bars	39.30	52.00	31,000
#4	#2 Plain bars	39.30	52.00	31,000

Specimen	Frame Reinforcement			
	Size	Yield Point f_y (ksi)	Ultimate Strength (ksi)	Modulus of Elasticity E_s (ksi)
#1	#4	47.00	83.90	30,900
#2	#4	47.00	83.90	30,900
#3	#4	47.00	83.90	30,900
#4	#4	47.00	83.90	30,900

CHAPTER IV
EQUIPMENT AND INSTRUMENTATION

The equipment and instrumentation necessary to apply the load and to record the behavior of a test specimen are as important a part of the test setup as the specimen itself. The reliability and consistency of this equipment's behavior is of prime necessity for the success of the test program. The fact that the equipment and instrumentation necessary for a dynamic test are infinitely more complicated than the equipment for the static testing of comparable specimens is perhaps not so obvious, but this fact will be attested to in the following description.

The apparatus used is designed to provide a clear picture of the behavior of a test specimen under dynamic loading, which will also serve as an adequate basis for comparison with tests of similar specimens subjected to static loading. The pulse of the loads applied should be controllable as to magnitude and duration, and the force-time shape should follow any desired function. The apparatus should also be able to record reactions, deflections and strains as functions of time.

The different parts of the apparatus may be grouped under the following three principal items:

- I. Loading equipment.
- II. Measuring equipment or instrumentation.
- III. Miscellaneous equipment.

I. Loading Equipment

The loading equipment used in this investigation may be referred to as "Dynamic Testing Machine". It was specially designed and constructed

for this experimental program, under contract with the Corps of Engineers.

This Dynamic Testing Machine consists of two basic parts:

A. The Basic Frame, and

B. The Loading Unit.

A. The Basic Frame

The supporting frame for the specimens and loading device consists of many parts. Figure 5 is a schematical diagram of the principal parts of the basic frame. Figure 14 is a side view of the heavy truss and lateral foundation beam.

As shown in Figure 5, the specimen (A) to be tested is supported vertically by two horizontal cantilever beams B and C. These beams may be moved six inches at a time allowing the support of walls from 2 to 16 feet in length.

The horizontal reaction is offered by the fixed lateral horizontal cantilever beam D, to which the reaction is transmitted by means of a strut E, composed of two channels. The three support cantilever beams transmit the forces to the two principal trusses I and II.

As it is also indicated in Figure 5, the main loading system F is supported by a lateral loading cantilever beam G. This loading beam may be moved up and down by increments of five inches allowing walls from 3ft 9 in., to 9 ft in height to be tested. This loading beam is bolted to the basic trusses; therefore when the main loading device (hydraulic jack) applies a load to the specimen, the reaction equal and opposite to the load applied is transmitted to the basic trusses, and consequently, if the applied load were static, the trusses would be under loads which equilibrate themselves and the corresponding support reactions would be zero. This is clearly shown in the sketch of Figure 15. However, since the loads

to be applied are dynamic ones, at any given time there may exist a considerable resultant force on the truss's supports, which required the addition of the support beams H and I. H is connected to the pile caps of the foundation by means of high-strength bolts, and I is cast into a mass of reinforced concrete J, which was also bolted to the pile caps. As it is shown in Figure 5 and partially indicated in figure 14, this mass of reinforced concrete consists of two lateral beams running parallel to the trusses I and II - connected together by the heavy mass of concrete poured on beam I. This special shape was required in order that the unbalanced horizontal force may be transmitted to the foundation.

For more complete information on the design, computations, and details of the basic frame, refer to report (22).

B. The Loading Unit

The loading unit is the most important feature of the dynamic testing machine. It was conceived by Professor Howard Simpson, and constructed under his direction. It is completely described in reference (22) and Figure 16 shows diagrammatically its operation.

This loading device consists of several basic sections:

1. The hydraulic loading unit, which is the basic loading device.
2. The sequence control system for the automatic control of the loading and unloading processes.
3. The pressurizing system.

1. The Hydraulic Loading Unit: This is actually a hydraulic jack and consists, essentially, of the main cylinder, main piston, and main shaft. Figure 17 shows a section of this hydraulic jack. Before a dynamic test, equal forces are applied to both faces of the main piston by the introduc-

tion of compressed oil into the chambers on either side of the piston, and pressures into the two compartments are adjusted according to the area of the piston faces (73.631 sq. in. for the push side, and 65.974 sq. in. for the pull side) and the desired value for the dynamic load, so that no load is applied to the specimen through the main shaft.

At the time of loading, the oil in one face of the piston (pull side) is permitted to escape, and the piston is acted upon by the pressure of the remaining oil on the other face (push side). This pressure is kept practically constant for small displacements of the piston, by means of four five-gallon accumulators.

The unloading process involves the flow of oil from the ten-gallon accumulator to the pull side, and as this oil is at a higher pressure than that in the push side, the piston is forced to move back, away from the specimen. The loading and unloading processes are controlled automatically as it is explained below.

2. The Sequence Control System for the Automatic Control of the Loading and Unloading Processes: The load command signal is obtained from a mechanical function generator, which consists of a rotary wiper and fifty contact points. Each contact has its own potentiometer voltage divider, so that the voltage on the wiper arm can be made to follow any desired function. Figure 18 is a schematic diagram showing the functional block diagram of the electronic control system, and Figure 19 is a photograph of the function generator control panel.

The voltage function produced by the function generator is attenuated and sent to a summing circuit where it is combined with the signal from the force transducer at the ram. The combined signal is the error or the difference between the command and the load on the specimen. The error

signal is amplified and sent to a second summing circuit, where it is combined with position feedback signals from the second and third stages of a three-stage hydraulic servo valve. This combined signal controls the first hydraulic stage. Thus, the error signal controls a feedback-stabilized hydraulic system, or inner loop. The third stage is a large three-way valve (dump valve), which controls the flow to and from the pull side of the ten-inch-diameter hydraulic cylinder. The force on the specimen is produced by the difference between the system pressure at the rear or push chamber of the cylinder, and the controllable bucking pressure at the front or pull chamber. Figure 20 shows the servo and dump valves connected together.

3. Pressurizing System: The pressurizing system consists of two pumps, a manifold, 4 five-gallon accumulators, 1 ten-gallon accumulator, 1 one-gallon accumulator, two one-pint accumulators, safety devices, filter units, 1 circulating unit, 1 transfer unit, a receiver unit or tank, the control panel, and the necessary piping and tubing. Figure 16 shows the disposition of these different parts. A photograph of the pumps can be seen in Figure 21.

The Vickers pump consists essentially of a variable-delivery piston pump, which can deliver a maximum of 48 g.p.m., the maximum operating pressure being 3000 psi. The principal purpose of this pump is to supply the oil to the servo valves. However, it is connected in such a way that it may also deliver oil to the complete system. The other pump is a Seco radial hydraulic pump, whose principal characteristics are the following:

Maximum pressure (spot rating)	10,000 psi
Maximum pressure (continuous rating)	6,000 psi
Delivery at max. pressure	.60 gpm

The principal purpose of this unit is to feed the accumulators, and the hydraulic jack.

The manifold allows the delivery of oil from the pull side to the receiver unit, or the flowing of oil from the ten-gallon accumulator to the pull side. These two operations are made through the dump valves which are directly connected to the manifold.

The principal function of the ten-gallon accumulator is to supply oil, at a determined pressure, to the pull side of the hydraulic jack -- through the dump valve -- to reduce or remove the applied load when required.

The four five-gallon accumulators are connected directly to the push side and their principal use is to act as a source of fluid power to hold the pressure behind the face of the piston when it moves forward. The one-gallon accumulator is connected to the servo valves to act as a leakage compensation and to help supply the large flows required during the test. The two one-pint accumulators are connected directly to the pull side with the object of smoothing out pulsations, should this ever prove necessary. Figure 22 shows some of the accumulators in place.

The safety devices consist of safety heads with rupture diaphragms, one of which is connected between the pull and push sides in order to prevent the ramming of the piston against the front side of the cylinder due to an unpredictable drop of pressure in the pull side and simultaneous failure of the specimen. The other safety head with rupture diaphragm is connected between the ten-gallon accumulator and the push side and it will rupture if a sudden and unpredictable drop of pressure occurs in the push side. This will permit a fast balance of pressure between push and pull sides, thus preventing the ramming of the piston against the back of the cylinder. The Barksdale valve located on the control panel may also be con-

sidered as a safety device, because if it is opened it will allow the rapid draining of the push side. To open the valve it is only necessary to hit down the lever.

The filter units consist of 10 μ filters, located at different points. One of these filters is connected to the Vickers unit, and filters all the oil that this unit pumps into the system. Another 10 μ filter is connected between the transfer unit and the Seco unit. Two 10 μ filters are also placed in parallel just before the servo valves, with the purpose of filtering all the oil that goes to these valves. In addition to these filters, it was necessary to connect a unit which filters all the oil that comes out of the system through a 1 μ filter, just before it is returned to the tank of the Vickers unit. Figure 23 shows this unit.

The transfer unit is a small pump which transfers the oil from the tank of the Vickers unit to that of the Seco unit. The receiver unit is a three-gallon tank into which the oil from the servo valve and the pull side of the cylinder is drained, before it is sent back to the tank of the Vickers unit through the circulating unit.

Figure 24 is a photograph of the control panel, the schematic diagram of which is shown in Figure 16.

Oil from any supply pump can be directed into the system through the line interlock valves which are on the control panel.

As an example of the use of the panel in a dynamic test, we may take the following description: One starts the Vickers pump with all valves closed, except for valves 10, 2, and the ^{Backdale} Braksdale valve. All the pressure gage line valves (6'; 4'; 1'; 5'; and 7), are just cracked so that the pressure in any line will be indicated at any moment. In this way, it is possible to bleed pressure into the servo system in an amount sufficient to

operate the dump valve -- approximately 2,500 psi. The test supervisor operating the electronics maintains contact with the operator of the pressurizing system control panel, and once he has stabilized the inner loops and has moved the dump valve to a position that will connect the pull side of the main cylinder and the ten-gallon accumulator, he gives the order to supply pressure to the system. At this moment the control panel operator opens valve 1, and closes valve 2. This will allow the oil to flow to any part of the system, once the line interlock valves 6,4,5,9, are opened. One starts opening valves 6 and 4, which will allow the supply of pressure to the 10 gal. accumulator and pull side of the cylinder. If the pressure required for the test is smaller than 2,500 psi, this is obtained directly by operating the Vickers pump, but if the pressure is larger than 2,500 psi, the Vickers pump is turned off at 2,500 psi pressure, and closing valve 10, the Seco unit is started, which can then give a maximum pressure of 10,000 psi. Once the pressure in the 10 gal. accumulator and the pull side of the cylinder is that desired for the test, valves 6 and 4 are closed, and then the Barksdale valve is closed at the same time that valve 4 is opened. This operation will allow the supply of pressure to the push side. Due to the fact that the diameter of the shaft is greater in the pull side than in the push side, the area of the pull face of the main piston is smaller than that of the push side. Consequently, the pressure required in the push chamber to maintain equilibrium is smaller than that required in the pull chamber by a factor of 0.896. Then, one must take the precaution that the pressure in the push side does not exceed a value equal to 0.896 times that of the pull side.

When the pressure in the push chamber has reached the desired amount, determined by the desired magnitude of load, valve 5 is closed,

and valve 9 is then opened. If the pressure desired in the 10 gal. accumulator and in the chambers of the cylinder required the use of the Seco pump, this pump must now be turned off, and the Vickers unit is to be started once more.

The operator of the control panel gives the signal of "ready for testing" to the test supervisor, and the test can then be performed as soon as the supervisor brings the ram in contact with the specimen. The test is initiated by pressing the fire button of the function generator.

To bleed off the supply lines after the test, special precaution has to be taken in extracting first the oil from the push chamber by opening the Barksdale valve, then draining the complete system by opening valves 2, 6 and 4. Servo pressure must be maintained until all push pressure has disappeared, to avoid the accidental opening of the dump valve.

II. Measuring Equipment or Instrumentation

For the complete definition of the behavior of a test specimen under dynamic loading, the measuring equipment had to be designed to provide a finished record of the applied load, reactions, deflections, and strains, all as functions of time. The instruments also had to be capable of recording the detailed shape of the mentioned quantities for force-time curves of any shape, and pulses of different magnitude and duration. However, as it was pointed out in Chapter I, the principal objective of this preliminary test program was not only the evaluation of the properties of the shear wall, but also the evaluation of the testing machine. Since one of the most important properties of the machine is the speed of the load build up and the shape of the load-time curve during build up, it was decided to run this first series of tests with a load-time variation as sketched in Figure 27,

where the load-build-up time T_r was expected to be of the order of 20 to 30 milliseconds, and the total duration of testing T was planned to be about 40 to 60 milliseconds. This fact simplified considerably the design of the necessary instruments, because, as the time T was planned to be approximately equal ⁽¹⁰⁾two to three times the time T_r , it was only necessary to design a high-speed recording system.

It must be pointed out that, as only four Cathode Ray Oscilloscopes were readily available, and this would only allow the recording of eight simultaneous signals -- without the use of special equipment -- it was decided to measure only load, reactions and deflections in this first series of tests.

The different electronic, photographic and mechanical means used, are grouped and described below, under the following items:

- A. Measurement of Load and Reactions
- B. Measurements of Deflections
- C. Recording Equipment
- D. Timing System
- E. Calibration

The functional block diagram for the instrumentation is shown in Figure 28 and Figure 29 is a view of the instruments.

A. Measurement of Load and Reactions

The measurement of load and reactions may actually be regarded as a measurement of strains, because the measurements were obtained through the use of standard SR-4 gages and strain measuring equipment. The gages were attached to Load Cells and calibrated in terms of kips of load.

1. Load: For purposes of analysis and proper functioning of the con-

trol of loading and unloading processes, it is important to know the magnitude of the load applied by the machine as a function of time. Of the various methods possible for the determination of this force-time curve, that of using sensing elements such as Baldwin SR-4 strain gages seemed to be most practical and reliable. These sensing elements have to be attached to an elastically strained member (load cell) near the point of application of load to the wall, and the change in electrical properties, such as resistance due to the strain, is converted to force by calibration with known applied load.

The design of the load cell for this particular investigation depended upon the mounting problem, and the sensitivity required. The simple column (hollow or solid), seemed to be the most advantageous and simplest load cell shape for use in this case. As the load cell had to be connected to the ram (or main shaft) of the hydraulic jack and to the element (Ram Head) which will be in direct contact with the specimen to be tested, and also had to be interchangeable (for sensitivity reasons that will be explained below), the setup shown in detail in Figure 30 was adopted solving in this way the mounting problem.

In order to satisfy the sensitivity requirements, the following steps were taken:

With the object of obtaining the maximum strain possible for a given stress intensity, aluminum alloy was selected.

Logically, the simplest method of obtaining a constant output from the load cell as the maximum load decreases, is through the use of tube with reduction of the wall thickness. With this in mind, and since it was expected for this first series of tests, that the ultimate resistance of the shear wall would not be greater than 150 kips, a drawn tube

of aluminum alloy 6062-T6, with a 4 in. outside diameter, and a wall thickness of 1/2 in., was selected.

Not only the stress in the load cell was checked, but also special precautions were taken in checking that the natural frequency (which is a direct function of the area in the form $f_n \sim \sqrt{A}$), does not go below certain limits imposed by the frequency of the wall to be tested.

The following are the equations used in order to satisfy the requirements of the shear wall to be tested.

To obtain the output of a load cell for a given force, the following expression was used:

$$V_o = \frac{GF \times PV}{E\pi(r_o^2 - r_l^2)} \quad (1)$$

V_o = output voltage

GF = gage factor of the sensing element

P = applied load

V = applied voltage

r_o = outside diameter of the cylinder

r_l = inside diameter of the cylinder

And for the frequency:

$$f_n = \frac{1}{2\pi} \sqrt{\frac{E\pi(r_o^2 - r_l^2)}{l(M + 0.33m)}} \quad (2)$$

M = lumped mass at the end of the load cell

m = mass of the cylinder gage section

E = elasticity modulus of 6062-T6

l = length of the load cell.

Past work has shown positively that SR-4 gages have little, if any, frequency restrictions below 50,000 cycles per second. Expression (1) imposes a limitation on the load cell sensitivity. Type C-10 or CB-10 are the best for high sensitivity load cells for dynamic tests. However, as they were not readily available, C-7 models with a gage factor of 3.3 were used instead. Four C-7 strain gages were mounted on the outer surface of the aluminum tube in an alternating pattern. Two of the gages were placed horizontally and parallel to the axis of the tube, and two are circumferential (vertical). As it is shown by Figure 31(a), a Wheatstone bridge circuit is formed with the horizontal gages in opposite legs. This arrangement eliminates the effect of eccentric loading, if present, and multiplies the average strain output of the horizontal leg by approximately 2.6. Consequently, a maximum voltage of 22.5 volts can be applied to this circuit. Substituting our data into equation (1), the output of the load cell is seen to be 1.3 millivolts per kip of load, which can be considered as a satisfactory sensitivity. However, the results of the preliminary tests revealed that in order to obtain better control of the loading and unloading processes it would be better to have large output voltage, for which reason it is planned - for the successive tests - to use the arrangement shown in Figure 31(b).

Equation (2) yields a natural frequency of approximately 3,000 cycles per second. If it is now considered that the wall to be tested was expected to have a maximum natural frequency of 200 cycles per second, it is possible to expect that the unit designed would probably adequately measure the load applied in the tests.

The calibration of the load cell was obtained previously in a hydraulic testing machine, as it is shown in Figure 32.

2. Reactions: The two vertical, and the horizontal reactions of a shear wall specimen are measured by special load cells. The shape of this load cell was determined by mounting requirements, and the necessity of possessing great flexibility in the plane of the wall, since they also act as supports. As it is shown in detail in Figure 33 these load cells consist of three seven and a half inch pieces of 8 WF 48 steel. Actually the design was made for an aluminum H-beam, with a depth of 8 in. and web thickness of 0.5 in. But as this standard structural shape was not readily available, it was decided to use three welded plates. Experience showed, however, that it was too difficult in practice to obtain welds of sufficient strength and it became necessary to use steel. In order to obtain the sensitivity required, eight SR-4, type C-7 strain gages are mounted as shown in Figure 33. This arrangement eliminates the effect of any eccentricity of load and results in a signal output from the bridge equal to 2.6 times the average of the vertical gage. These load cells have been calibrated statically under an axial load of 70 kips compression and tension.

B. Measurement of Deflections

Deflections of the shear wall specimen are measured at two points -- as shown in Figure 27 -- by means of electric-inductance gages of the moving-core solenoid type, conventionally termed as Linear Variable Differential Transformer (L.V.D.T.) and manufactured by the Schaevitz Engineering Company. Since previous static tests indicated that the maximum horizontal deflection before failure would not exceed 1 in., a Schaevitz gage with a maximum range of 1" was used. The gage used for measuring vertical deflections at the loading point had a maximum range of $\pm 3/8$ ", and for the one used at the support for the vertical displacement, the range was $\pm 1/4$ ". For the horizontal displacement of the support, one with a maximum range of

$\pm 1''$ was used. Due to the fact that the point at which the vertical deflection is to be measured will also move considerably in the horizontal direction, a difficult alignment problem was posed. This problem was solved by using the device that is shown in Figure 34 and which essentially consists of the use of two universal joints.

C. Recording Equipment:

The signals from the load, reactions, and deflections are detected on four DuMont type 322, Dual Beam Cathode-Ray oscilloscopes, and the permanent record of the traces from the screen of the Cathode-Ray oscilloscopes are obtained by using four DuMont Type 297 oscillograph record cameras; which operating on the Polaroid-Land principle, produce a finished print (oscillogram) 60 seconds after exposure.

D. Timing System

The number of events taking place and the short duration of the loading period made it mandatory to adopt a triggering device such that the starting of the complete instrumentation system could occur simultaneously with the initiation of the test. This is obtained by pressing the fire button of the function generator, thus sending -- 2 milliseconds prior to the function -- a voltage pulse to the external synchronization of all the Dual Beam Cathode-Ray oscilloscopes.

The plotting of load, reactions and deflections versus time, was made possible by energizing the Schaevitz with a 500-cycles voltage. This was obtained by sending a carrier wave to the Schaevitz with a Hewlett-Packard 200A audio oscillator, thus obtaining in this way a modulated wave for the deflection signal, with a time interval equal to 2 ms. between wave peaks.

As there are four deflections and four forces (one load and three reactions) to be measured, one deflection and one force signal were recorded in each oscilloscope; and since the deflection is calibrated versus time, it is possible to obtain the calibration of force vs. time.

E. Calibration

The load cells used to measure load and reactions were calibrated under static loading, using a Baldwin 200,000 lbs. hydraulic testing machine. During this calibration, shunting resistances of a precision wire wound resistance were placed across one leg of the bridge, so that their equivalent values in terms of load could be determined. In order to obtain the calibration trace on the screen of the oscilloscope, the zero reference line is established first, and then the bridge is unbalanced with the calibrated resistance.

The calibration of the Schaevitz is obtained from a linear wire wound calibrated potentiometer, whose value was determined during initial calibration of the Schaevitz, in terms of mechanical movement of an Ames Dial Gage.

III. Miscellaneous Equipment

Among the various parts of the mechanical and electrical equipment used on this experimental work, there are several small devices which are indispensable to the smooth performance of a wall test, but do not merit detailed discussion. These include:

- A. The Lateral Restraint System
- B. Deflection Gage Mount
- C. Indicator of the Ram Head Position
- D. Guide for the Ram and
- E. Restraining Strut.

A brief description of each of these auxiliary equipment follows:

A. The Lateral Restraint System

In order to prevent any lateral movement of the wall during the test, a lateral restraint system was devised for these tests. Figure 35 is an overall view of this system, connected to the specimen, and Figure 36 shows in detail the different parts of this device.

B. Deflection Gage Mount

The deflection gages were supported on an auxiliary frame, composed of two horizontal bars bolted to two poles which were fastened between floor and ceiling.

C. Indicator of the Ram Head Position

The function of this device is to indicate the position of the ram head position with respect to the specimen. It is illustrated in Figure 37, and consists essentially in a slide-wire deflection gage, whose output can be seen on the screen of an oscilloscope.

D. Guide for the Ram

Illustrated in Figure 38 is the guide for the ram, which is a device that prevents the transmission of any large bending moment to the main shaft of the hydraulic jack. This bending moment can be produced by friction between the ram head and the plate connected to the specimen. Figure 39 gives the details of this device.

E. Restraining Strut

In order to protect the load cells, used for reactions, and the ram from damage caused by a specimen overriding the stroke of the ram, a special strut of steel was placed behind the wall, limiting the total horizontal deflection of the wall to two inches. Figure 40 shows this strut in place.

CHAPTER V

TESTS OF WALLS

Although the long time static resistance of shear walls is not of major concern in this study, it was considered desirable to make an initial static test on a wall similar in properties to that to be tested dynamically. Such a test was considered to be valuable, not only because it would provide a way of comparing the static resistance of the structural element to its dynamic behavior, as well as a comparison with the static tests made previously (16); but also because it would afford an opportunity to check the correct operation of all the equipment at a loading rate slow enough to permit -- as a double-check -- the simultaneous use of Ames dial gages and Linear Variable Differential Transformer gages. This previous test would also make possible the study of the importance of the support displacements, measured by placing at the supports special Ames dial gages.

I. Wall Preparation

The preparation of the wall for testing is the same whether the test is to be made dynamically (load duration 20-100 milliseconds) or statically (load gradually applied over a period of 5-10 minutes), except that more deflection brackets and supports for Ames dial gages were necessary for the static test. Figure 42 shows schematically the location of the gages for the static test, and Figure 43 for the dynamic tests.

Three days after the wall is cast, it is removed from the formwork and stored in the laboratory until the tests on the corresponding cylinders give a compressive resistance close to that required. Then the

wall is moved into position on the reaction-measuring supports, which are already bolted in position on the supporting beams, as shown in Figure 44. The wall is then bolted by means of six 7/8" Allen Socket-Head Cap Screws per support. Then the lateral restraint mechanism is bolted on the already cast bolts, and connected with the part attached to the frame, as shown in Figure 35. The wall is then white washed in order to improve the detection of the cracks. Next, the brackets for deflections are attached to the wall on the already cast bolts. Then the frame for supporting the gages is put in place and the last step is the attachment of the gages and the making of all the electrical connections required for recording and calibrating the various measuring devices. A wall ready for testing is shown in Figure 45. It must be noted that the preparation of the wall for testing requires at least the work of two men, for a period of twelve hours.

II. Test Procedure

In a static test, after the zero value of each measuring device is read, the calibrating traces for each electronic measuring device are recorded according to the procedures for calibrating, described in Chapter IV, and the gain of each amplifier is first set so that the calibrating step representing the greatest trace deflection -- which in turn represents a value of load, reaction or deflection greater than that expected in the test -- will remain on the record.

The load is applied by allowing the gradual flow of oil into the chamber behind the main piston (push side), and readings are taken for every 50 psi of oil pressure increment, which is equivalent to a load increment of 3680 lbs.

In a preliminary step, the load is increased until an oil pressure of 300 psi is reached, and then released, with the object of checking if

all the measuring devices are working. The load is then increased until the maximum resistance of the wall has been overcome and its travel is stopped by the restraining strut placed behind the wall.

In a dynamic test, after the calibration traces have been recorded and the precharge pressure of the nitrogen in the different accumulators arranged according to the maximum pressure of oil to be applied, oil is pumped into the servo mechanism until a pressure of 2,000 psi is reached, with the object of activating the dump valve. Then the dump valve is set in neutral position by means of the balance control, and the two inner-loop gains (one corresponding to the servo, and the other to the dump valve) are set in order to obtain the stability of these two inner loops. Next, the dump valve is moved to the closed position, which will allow the pumping of oil to the pull side, and also to the ten-gallon accumulators, because they are now interconnected through the manifold and the dump valve. Once the pressure on the pull side and ten-gallon accumulators reaches a value high enough to give more force on the pull side than that which will exist on the push side under the maximum required oil pressure for the test to be performed, the control valves to the pull side and ten-gallon accumulators are closed, and oil is pumped to the push side of the loading piston. This is done until the pressure reaches the value required for the test.

Once the oil pressures in the different parts of the system are those required for testing, the man who is operating the hydraulic system gives the "ready" order to the man in charge of the electronic equipment; who then, by means of the balance control moves the dump valve to the center position (neutral), and then opens it slightly in order to move the ram towards the wall. When the ram-head position indicator indicates that the

head of the ram is close to the wall, the shutters of all the oscillograph record cameras are opened, and when the signal of the ram-head indicator shows that the ram is practically touching the wall, the man in charge of the function generator presses the fire button, which simultaneously releases the trigger on all the oscilloscopes and sends the signal to the summing point, where the output of the load-cell-ram-bridge is connected. This activates the whole system, producing the load desired. This load is established beforehand by setting the amplitude of the function generator's signal in correspondence to the magnitude of the load desired.

In these preliminary dynamic tests, it was decided to apply to each wall dynamic loads of increasing magnitude, starting from a value which is smaller than that at which cracking should be expected -- according to the static test -- and then increasing the magnitude of the peak load, until a value that produces the collapse of the wall is reached.

III. Test Results

A. Static Test

1. Specimen #1: Specimen #1 was tested under lateral static load, and the results of this test are presented in the form of curves and photographs. Figure 46 shows the complete picture of the deflections that the wall and its supports suffered, while Figure 47 shows the lateral movement of the top of the shear wall with respect to the foundation (supports), which is of primary importance.

The analysis of the curves of Figure 46 shows that although the vertical displacement of support C given by curve 8 is negligible -- which was expected due to the special precautions taken, such as the welding of the supporting beam C to the principal truss, the vertical displacement of support B, given by curve 4, was considerable, and the same can be said

with respect to the horizontal displacement given by curve 3. In spite of the special precautions taken with the connection of the supporting beam B with the trusses, such as the introduction of shims between the gusset plate of the supporting beam and the web of the two channels that form the bottom chord of the two trusses, and that the nuts of the high-strength bolts were driven in with power wrenches in order to provide a good clamping force, the large vertical displacement seems to indicate that the friction produced between the joined members was not sufficiently high to prevent vertical slipping.

The considerable horizontal movement can also be explained by horizontal slipping at the junction of the horizontal support with the web of the two channels that compose the strut E (see Figure 5).

Thus, if agreement between experimental and theoretical results is expected, it is not only necessary to measure the displacement of the support in the dynamic tests, but also to include in the theoretical analysis the effect of the rotation and sliding of the shear wall as a consequence of non-rigid supports.

The curve (a) of Figure 47, obtained by subtracting from the total displacement measured at the loading point the value obtained for the horizontal movement of the support B, plus the horizontal movement due to the rotation caused by the vertical movement of the supports; shows that the first crack in the wall occurred at a load of approximately 25 Kips. This is what actually happened during the first test, when -- in order to check the instrumentation -- the oil pressure in the push side was increased up to 350 psi. The first crack was that marked with number 1 in the picture of Figure 48. The complete test was actually carried out on a cracked wall.

The failure of the wall happened at a load of 73.6 kips, due to

failure of the welded connection of the reinforcement of the tension column with the supporting plate; as shown in Figure 48.

The maximum relative deflection recorded at the start of yielding was 0.12 in. With respect to these results, the following comparison should be made:

a. The tests carried out at Stanford University (16) on an analogous specimen -- where the only difference lay in the strength of the concrete, (3 vs. 5) $\times 10^3$ psi, and in the modulus of elasticity, (3 vs. 4.5) $\times 10^6$ psi -- gave the following results:

First crack load	24 kips	Deflection at ultimate load	0.20 in.
Ultimate load	71 kips		

The load-deflection curve obtained in this test is plotted in Figure 47, curve (b). It should be noted that the ultimate load was associated by shear failure at the base of the compression column.

b. The computation of the ultimate load -- assuming that the stress-strain relation for the steel reinforcement of the frame is the ideal plastic relation, (i.e.) neglecting the increase of stress during strain hardening -- gives an ultimate value of only 55 kips.

When the results obtained are compared with those of the Stanford University investigation, we can see that there is some difference, especially in the cracked region. Perhaps this discrepancy can be explained by the difference in concrete properties, and by the different method of holding down the tension column of the shear wall at the support. It seems that for the test performed at Stanford University, the support of the tension column was considerably stiffer than that used in this test; and furthermore, special reinforcements were introduced at the bottom of the tension column, which avoid the yielding of the column at this point.

The discrepancy between the experimental ultimate load obtained during the test, and that obtained analytically, can be explained by the presence of a vertical force at the loading point as a consequence of the considerable rotation of the wall produced by the large movement of support B.

B. Dynamic Tests

A total of three specimens (numbers 2, 3, and 4) were tested dynamically. Continuous photographic recording of the oscilloscope's trace for the applied load, reactions and deflections at four points as functions of time was obtained during each dynamic test by means of oscilloscope-record cameras. An example of this photographic recording is shown in Figure 49. It is the complete data for the test number six, performed on wall #4.

The results of the dynamic test on each specimen are presented in the form of curves, tables, and photographs, and a brief description of these results for each specimen is given as follows:

1. Specimen #2: This specimen was subjected to several load pulses. The results obtained in four of these tests are presented in Figures 50 through 57. From these figures it can be seen that the load pulse applied was not completely consistent in shape.

The sharp peaks and depressions in the load-time curves were caused by an improper gain and vibrations in the system. However, if these peaks and depressions are averaged and a curve is drawn through the average points, a smooth load pulse can be obtained; however, its shape varies from one test to another. The rise time varies from 10.0 ms. to 30.0 ms., and the total duration from 35.0 to 75.0 ms.

Figures 50, 52, 54, and 56 give the value of the load and reactions versus time, and Figures 51, 53, 55, and 57 give, respectively, the value of the deflections vs. time obtained in these tests. As it is shown in this last group of figures, only the data corresponding to the horizontal deflection at the loading point, and at the support was obtained, due to the fact that at the time the tests were started, the complete set of devices necessary for holding and attaching the Shaevitz gages was not available. Consequently, it was not possible to obtain the component of the horizontal displacement at the loading point caused by the vertical movement of the support.

The maximum value of the applied dynamic load, and the time required to reach this peak load, the lateral movement of the loading point with respect to the foundation (supports) at the time at which peak load is reached, and the maximum value of this relative lateral movement with the time at which it happens are shown in Table V-1, for each test. Also shown in this table is the static deflection obtained on specimen #1 corresponding to the value of the peak load of each dynamic test.

A comparison of the static deflection with the dynamic one, reveals that:

- a. Test No. 1 performed on an uncracked wall gives practically the same deflection as that in the static test.
- b. For the following tests, when the peak load is smaller than 30 kips, the dynamic deflections are larger than the static.
- c. For the first eight tests, when the peak load is larger than 30 kips, the dynamic deflection is smaller than the static, the difference

being quite considerable in the case that the load pulse has a short rise time and a definite and sharp peak load (see Test No. 8).

- d. After test No. 8 the dynamic deflections are larger than the static ones; the explanation of this result can be found in the fact that the wall was considerably damaged (cracked) after test No. 8.

It must also be noted that the first cracking occurred during test No. 5, at a load of 40 kips.

Because of an error when trying to precharge the ten-gallon accumulator to a higher pressure, after test No. 12, the pressure in the pull side was released without releasing that in the push side first, resulting in an unbalanced force that produced the failure of the specimen. The failure occurred by tension failure of the welding of the reinforcement of the tension column with the support plate. Figure 53 shows the cracks on the wall after test No. 6, which had a peak load of 31.5 kips. However, the cracks shown in the picture were produced by a load of 40 kips, applied during test No. 5. Figure 59 shows the wall after failure.

2. Specimen #3: Specimen #3 was submitted to several load pulses of varying magnitude and duration.

Figures 60 through 71 show the values of the load, reactions and deflections vs. time, obtained in some of these tests. From these figures it can be seen that the rise time varies from 12.5 to 25.5 milliseconds and the total duration varies from 35 to 62 milliseconds. It may also be seen that during the first tests the load did not come back to zero. The force-time shape varies considerably from one test to another and only that corresponding to test 13 can be considered as triangular in shape, if the small peaks and depressions are smoothed with an average curve.

Table V-2 gives a summary of the test results on specimen #3.

Analyzing these results and the corresponding figures, it can be seen that when there exists a definite peak load, the maximum horizontal deflection takes place almost simultaneously, the delay being only of a few milliseconds in certain cases. On the other hand, when there is no definite peak in the pulse, the maximum deflection may occur considerably before or after the instant at which the peak load is reached, and more or less coinciding with some of the other peaks.

In this case, first cracking occurred during test No. 5, at a load of 42.5 kips.

If the values of the maximum lateral deflection obtained on the tests performed on this specimen are compared with those obtained on a specimen being subjected to a similar static load, it can be seen that considerably higher deflections resulted on specimen #3. This difference can be only partially explained by the difference in the moduli of elasticity of the concrete (4.70×10^6 psi for the specimen under static loading vs. 3.80×10^6 psi for specimen #3.)

Because of an error during test 16, the vertical reaction at the fixed support and the vertical displacement at the same support were not obtained.

Figure 72 shows wall #3 after failure produced by a dynamic load with a peak value of approximately 68 kips. This failure was due to the defective welding of the reinforcement of the tension column to the support plate.

3. Specimen #4: In Figures 73 through 84, the applied load, reactions and deflections occurring on some of the several tests carried out on specimen #4 are plotted as functions of time. It can be seen from these figures that:

- a. The shape of the pulse load is not consistent, even if a smooth curve is drawn through average points of the peaks and depressions.
- b. The rise time of the pulse varies from 3 to 33.5 milliseconds.
- c. The total duration of the pulse varies from 21 to 65 milliseconds.
- d. The maximum lateral displacement of the loading point with respect to the supports for the case when the pulse has a definite peak load is reached almost simultaneously with the peak load.

Table V-3 gives a summary of all the data obtained on this specimen.

The first crack occurred at a load of 37.0 kips.

Comparing the values given in Tables V-2 and V-3, it can be seen that the maximum value for the horizontal displacement obtained in the tests performed on specimen #4 are larger than those produced by similar loads on specimen #3.

Wall #4 failed under a dynamic load whose peak value was equal to 74 kips. Figure 85 shows the crack pattern of this wall after failure, which was produced also by tension failure of the reinforcement of the tension column with the support plate.

The cause for the failure produced in the four walls tested was unexpected, (i.e.) the defective welding of the connection between reinforcement of the tension column and the support plate. In an actual shear wall construction, this kind of failure cannot happen, and consequently the question of how much more load can the specimen withstand if this premature failure is avoided, arises. In order to find a quick answer to this question it was decided to repair the connection of wall #4, chipping out the concrete at the bottom of the tension column and welding again the reinforcement to the support plate, taking special precautions to avoid failure in the welding section.





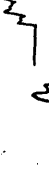



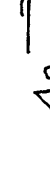



The repaired wall was then submitted to a new series of tests, starting with a peak load of 30 kips in order to check the instrumentation. Once the instrumentation was in order, two pulses with a peak load of 73 and 76 kips respectively, were applied. These peak loads were approximately equal to those at which the failure of the connection occurred. This time the wall endured the load, and when a new dynamic load with a peak value equal to 80 kips was applied, the wall also withstood it.

The failure of the wall was produced by a load of 95 kips, with a rise time of 21 ms. This time the failure was associated with a shearing off of the compression column at its junction with the beam foundation. This is the kind of failure that was expected according to the results obtained in the static tests carried out on similar walls at Stanford University. (16)

Figure 86 shows the wall after collapse. It is interesting to note the local crushing of the concrete in the panel around the corner at which failure occurred.

TABLE V-1

SUMMARY OF TEST RESULTS ON SPECIMEN #2

TEST NO.	MAXIMUM VALUE OF APPLIED LOAD		RELATIVE HORIZONTAL DEFLECTION OF LOADING POINT		STATIC DEFLECTION		
	Value in kips	Time at which it is reached (millisec)	Produced at time (in.)	MAXIMUM VALUE in inches	time at which it is reached (millisec.)	Shape of Load-Time Curves	Corresponding to the load of (2) (in.)
(1)	(2)	(3)	(4)*	(5)*	(6)'	(7)*	(8)**
1	26.0	16	0.018	0.018	16		0.019 0.008
2	23.5	15.5	0.009	0.015	19.5		0.010 0.0075
3	27	15.5	0.019	0.024	17.5		0.023 0.009
4	25.2	14.5	0.021	0.023	16.5		0.017 0.008
5	40.0	15.0	0.046	0.061	17		0.066 0.026
6	31.5	10	0.030	0.036	10.5		0.038 0.017
7	26.0	12.6	0.020	0.025	13		0.019 0.008
8	45.5	10.5	0.069	0.069	10.5		0.081 0.020
9	30.2	25.5	0.052	0.056	26		0.034 0.016
10	27.5	17.7	0.046	0.046	18		0.024 0.011
11	53	30	0.111	0.111	30		0.101 0.033
12	49	18	0.115	0.150	30		0.094 0.023

* Values obtained without subtracting the horizontal displacement caused by vertical movement of the supports.

** Values obtained from curve a of Figure 47.

TABLE V-2
SUMMARY OF THE TEST RESULTS ON SPECIMEN #3

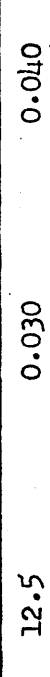
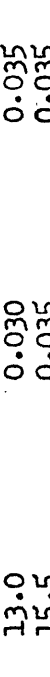
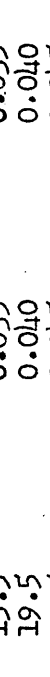
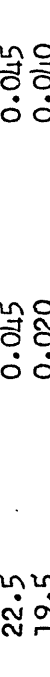
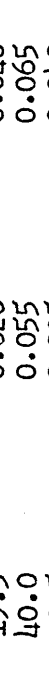
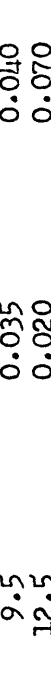
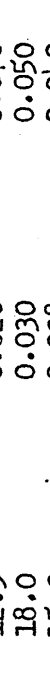
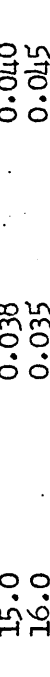
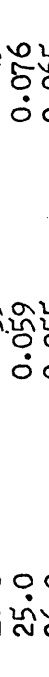
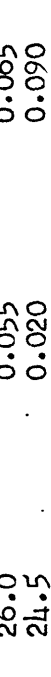












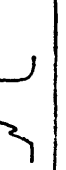


TEST NO.	MAXIMUM VALUE OF APPLIED LOAD	RELATIVE HORIZONTAL DEFLECTION OF LOADING POINT			MAXIMUM VALUE	Shape of Load-Time Curves
		Value in kips	Time at which it is reached (millisec.)	Produced at time (3)(in.)		
(1)	(2)	(3)	(4)	(5)	(6)	(7)
1	32	12.5	0.030	0.040	10	
2	34.5	13.0	0.030	0.035	14.0	
3	22.0	15.5	0.035	0.035	15.5	
4	36.0	19.5	0.040	0.040	19.5	
5	42.5	22.5	0.045	0.045	22.5	
6	34.5	19.5	0.020	0.040	21.0	
7	17.5	40.0	0.055	0.065	13.0	
8	29.0	9.5	0.035	0.040	12.0	
9	30.0	12.5	0.020	0.070	10.0	
10	25.5	18.0	0.030	0.050	21.0	
11	21.5	15.0	0.038	0.040	19.0	
12	21.5	16.0	0.035	0.045	19.0	
13	48.7	25.0	0.059	0.076	27.0	
14	36.8	26.0	0.055	0.065	28.0	
15	64.0	24.5	0.020	0.090	20.5	
16	67.8	25.5				

TABLE V-3
SUMMARY OF TEST RESULTS ON SPECIMEN #4

TEST NO.	MAXIMUM VALUE OF APPLIED LOAD	Time at which it is reached (millisec)	Produced at time (3)(in.)	RELATIVE HORIZONTAL DEFLECTION OF LOADING POINT		Shape of Load-Time Curves
				in inches	MAXIMUM VALUE	
(1)	(2)	(3)	(4)	(5)	(6)	(7)
(0)	20.0	3.0	0.020	0.035	9.0	
(1)	8.5	6.5	0.020	0.030	11.0	
(2)	18.0	3.0	0.023	0.060	8.0	
(3)	18.0	13.0	0.050	0.050	13.0	
(4)	28.4	20.0	0.050	0.060	44.0	
(5)	37.0	19.0	0.040	0.070	22.0	
(6)	50.5	29.0	0.085	0.085	29.0	
(7)	62.5	33.5	0.083	0.095	24.5	
(8)	60.0	27.0	0.080	0.095	33.0	
(9)	74.3	26.0	0.140	0.160*	22.0*	

*Values before failure of the specimen

CHAPTER VI
THEORETICAL INVESTIGATION

1. Introduction

As stated in Chapter I, the basic problem being considered is the prediction of the resistance and behavior of reinforced concrete shear walls which are subjected to dynamic loading caused by air blasts due to the explosion of nuclear weapons.

Elementary approaches to the shear wall problem assume that the wall is a beam. The beam is considered to be cantilevered from the foundation. In the case of static loads, wall deflections and stresses are then found from elementary strength of materials formulas. Results from such analysis are often quite inaccurate, and completely erroneous conclusions may be drawn. Therefore, the analysis of a shear wall must be based on a more exact solution.

The shear wall may be reduced to the problem of a plate loaded in its own plane. This is a problem in plane stress analysis. Precise mathematical solutions based on the theory of elasticity are available for only a small number of special problems. The analysis made in Chapter II of the different factors involved in the study of this specific problem, shows that its solution is complicated not only by the nature of the shear wall itself, which can take many forms, but also by the necessity to predict three phases of action for any wall, namely:

1. The elastic behavior
2. The behavior when partially cracked and subjected to small deflection, and
3. The large-deflection behavior.

If to this is added that the problem to be investigated is a dynamic one, it is obvious that an exact mathematical solution is impossible and some approximate methods must be developed to provide solutions of engineering accuracy in a reasonable amount of time.

II. Elastic Behavior

This phase was investigated by Mr. Aaron Finerman (21). The procedure followed in his studies may be summarized as follows:

Dynamic Analogy: The actual continuous wall was replaced by a concentrated mass system inter-connected by weightless springs as shown in Figure 87. The stiffness and properties of the springs were obtained by the lattice analogy method.

The fundamental concept involved in the lattice analogy is that of replacing a plate by a pin-connected lattice having the same deformations as the plate, under similar stress conditions. In this manner, the equivalent bar area of the lattice may be determined.

Equation of Motion: The equation of motion of each mass point can be developed either from considerations of the requirement of dynamic equilibrium or from the Lagrangian equations.

Numerical Integration: The set of simultaneous equations of motion was solved by numerical integration.

To obtain the numerical solution, an open type formula was used to predict the value of displacement in the succeeding time interval. This predicted value was then corrected by the use of a closed type formula which required a number of iterations.

Principal Tensile Stress Determination: After a consistent set of displacements has been obtained, it is necessary to compute the principal tensile stress at the center of each segment. The stresses are then com-

pared to the cracking stress of concrete, to determine where and when the first crack appears. Cracking may also take place in the tensile column.

The analyses were carried out until the principal tensile stress at the center of a segment exceeded the cracking stress of concrete.

III. Cracked Behavior

As was established before, one of the principal objectives of this work was to predict mathematically the cracked behavior.

The prediction of cracked action involves a number of assumptions, and considerable time was spent trying to find a method of approximate analysis that is simple to apply and yet offers a fairly high degree of accuracy. In this case, the effort made by Mr. Calladine in order to draw an analysis of the cracked behavior from the theory of elasticity must be mentioned. However, the proposed treatment was not a complete solution by the mathematical theory of elasticity. Judgement had been applied in the consideration of the stresses and slipping of the steel in the neighborhood of the crack. Difficulties in the programming of this method, in the short time available, made it impractical.

Finally, it was decided to adapt for the cracked range the simplified lattice used by Mr. Finerman for the elastic behavior. Where cracks occur in the wall panel, or in the tension column, the behavior of the wall depends on the location of the cracks, changing of modulus of elasticity, the value of Poisson's ratio, etc., and consequently it is obvious that the areas determined for the equivalent lattice bars - for the elastic phase - are no longer valid. Some further assumptions are required to determine the properties of an equivalent lattice.

In order to simplify the problem, and considering the limited computer time available and storage capacity of the high speed digital computer

Whirlwind I, the following assumptions have been made.

- 1) Poisson's ratio does not change due to cracking of wall.
- 2) Elastic modulus of the materials remains constant.
- 3) The crack extends through the whole segment.
- 4) Due to the fact that a careful study of the different crack patterns obtained in the static tests of specimens similar to those being studied showed that the cracks at the wall panel occur practically at an angle of 45 degrees, it was decided to neglect the effect of variation in the angle at what cracking occurs in a segment, and to assume that all cracks occur at that angle.
- 5) In order to satisfy the deflection of the segment once a crack occurs under assumption 4, the stiffness of all the lattice bars changes for that segment, except for the diagonal compression bar, which retains the stiffness derived under the assumption of elastic behavior.

Assumption 5 may be justified by the following reasoning: The reinforced concrete wall is considered as a laminated plate of three laminas, as shown in Figure 88, the central lamina or core being a steel lamina representing the steel reinforcement, and the other two laminas or faces being the concrete layer.

As long as the stresses acting in the plane of this laminated plate are smaller than those which will produce cracks in the concrete, the elastic isotropy of the laminated plate permits the substitution of a plate of concrete of equivalent thickness (transformed thickness) for the real plate, and then this substituted by the pin truss according to the lattice analogy.

When the stresses reach the value that will crack the concrete at

45 degrees (i.e. pure shear stresses), the collaboration of the concrete laminas in absorbing stresses disappear completely, except for the case of stresses parallel to the crack. This means that, if for a moment we neglect this unique possibility of concrete collaboration, as cracks occur, the effectiveness of the laminated plate is reduced to that of the steel lamina alone, and consequently the pin truss of the lattice analogy will be similar to that obtained for the case before cracking. The only difference will be that the area of the bars, instead of corresponding to the total transformed thickness will now be proportional to the area of the steel lamina alone. Now, taking into account the fact that for stresses parallel to the crack, the cracked laminated plate behaves as if it were not cracked, the diagonal bar of the corresponding lattice is assumed to maintain its area proportional to the total transformed thickness.

It is recognized that the assumption of neglecting completely the collaboration of the concrete with the steel due to the bond between cracks in members under tension, will result in lattice members of smaller stiffness than actual. However, if a very fine lattice is used, this assumption will not introduce appreciable error and according to the analysis of the results obtained by Galletly (10) for the case of static loads, it is expected that, even if a coarse lattice network is used, this assumption is justifiable. Later, in the discussion of the stiffness of the lattice members, a method for taking into account the collaboration of concrete is proposed.

It is evident from the above considerations that the effect of the fineness of the lattice pattern, (i.e.) how fine the lattice must be in order to obtain a fair agreement between experimental and analytical results, becomes important enough to require a more careful consideration. With this

purpose, lattices of two different sizes were investigated. (More complete information is given in appendices A and B)

6. When the strain in a bar of the lattice network has reached the value corresponding to the yield point stress, the force in that bar should then be kept constant for any increase in strain.

This assumption is also an approximation, because -- if we neglect the collaboration of the concrete -- when any unit of the continuous plate starts yielding under pure shear stresses, it would be necessary to assume in the analogous lattice -- if the requirement that deformations be equal is to be satisfied -- that not only the diagonal bar in tension is yielding, but also all the other bars, with the exception of the diagonal bar in compression; although the horizontal and vertical bars have not yet reached the yielding point. However, an exact analysis of the deformation of the unit-continuous plate under stresses that will produce yielding is not possible and it is believed that the assumption made above will not introduce any large error.

7. If at any moment the strain in a bar which is in yielding state starts to decrease, the force in the bar will decrease following Hooke's Law. If the strain continues to decrease to zero, the cracks disappear and the concrete starts to collaborate again. This is shown clearly in Figure 89.

8. The computation is carried out until the deflection at any point reaches the value for the deflection at which -- in the static test -- the load starts to decrease.

This is of course an arbitrary value, and does not mean in any way that the wall will collapse.

It is evident that a better point for stopping the computations would be the moment at which enough bars have yielded to make the structure a mechanism. However, the requirements for such a method were considered prohibitive due to their complexity.

According to the above assumptions, the stiffness of the bars is given by the following equations:

1. Elastic Range:

$$K_i = \frac{A_{t_i}}{l_i} E_c \quad (1)$$

which is the value obtained by Finerman (21); where A_{t_i} is the transformed area of the bar, l_i is the length of the bar, and E_c is the modulus of elasticity of concrete. This stiffness determines a curve of force vs. deflection like that shown in Figure 89 by line A' O A.

2. Cracked Range:

Once the segment cracks, the stiffness of the bars is given by:

$$K_i = \frac{A_{s_i}}{l_i} E_s \quad (2)$$

where A_{s_i} is the steel area of the bar in consideration, and E_s is the modulus of elasticity of steel. In Figure 89, the curve F vs. $\frac{\Delta l}{l}$ is given by line OB.

Equation (2) is valid until the strain $\frac{\Delta l}{l}$ reaches the value for which the stress in the steel is equal to the yielding limit. After that the curve F vs. $\Delta l/l$ in Figure 89 becomes the horizontal line BC.

As discussed before, the stiffnesses obtained from equation (2) are smaller than the actual due to the assumption that the collaboration of the concrete between the cracks could be neglected. Different investigators and authors, (26) (27) (28), have proposed different

methods in order to take into account the collaboration of the concrete, after concrete has cracked. Following Brice (28), whose study seems to be the most complete, the stiffness after crack can be obtained from:

$$\frac{\Delta l_i}{l_i} = \frac{1}{E_s} \left[\frac{F_i}{A_{c_i}} - \frac{f_{c_i}^t}{2.75p} \right]$$

where $f_{c_i}^t$ is the tension stress in the concrete as given by:

$$\frac{F_i}{A_{c_i} + nA_{s_i}}$$

A_{c_i} is the concrete area.

p is the percentage of steel.

It must be noted that $f_{c_i}^t / 2.75p$ is the factor that represents the collaboration of the concrete. According to this, the stiffness would be:

$$K_i = \frac{A_{s_i}}{l_i \left[1 - \frac{1}{2.75(1 + np)} \right]} E_s$$

This equation is valid until f_c^t reaches the maximum allowable value in tension; from then on, the equation that governs the deflections is given by:

$$\frac{\Delta l_i}{l_i} = \frac{1}{E_s} \left[\frac{F}{A_s} - \frac{f_c^t \max}{2.75p} \right]$$

and consequently, the F is given by:

$$F_i = A_{s_i} E_{s_i} \frac{\Delta l_i}{l_i} + \frac{f_c^t \max}{2.75p} A_{c_i}$$

This equation is valid until the strain $\Delta l_i / l_i$ is such that the stress of the steel on the cracked cross-section reaches the yield limit, in other words, until:

$$\frac{F_i}{A_{s_i}} = f_y$$

From then on, the force F_i will remain constant with increasing $\Delta l_i/l_i$. Figure 90 shows schematically the curve F vs. deflection for the different phases considered above.

If in any moment -- after cracking occurs -- the deformation in a bar starts to decrease, the force vs. deflection curve follows a line parallel to the line OB , as indicated by line CD in the figure; until the total deformation becomes zero -- point D . From then on, the F vs. $\Delta l/l$ curve becomes parallel to the OA line -- line DE in Figure 89.

With these assumptions and incorporating the program developed by Mr. Finerman (21) for the elastic range, the writing of the general program for the use of the digital computer Whirlwind I was undertaken by Mr. Ho, while Mr. Calladine undertook the writing for the new IBM computer. A complete information on the coding for these two high-speed computers, is given in appendices A and B.

IV. Theoretical Results

A. Data for the Analysis

1. Applied Load. The applied load curve is shown in Figure 91. The actual loading duration is 75 milliseconds; however, the dynamic effect to the wall is assumed to be continued until 25 seconds after the applied load is over.

2. Number of Segments. Detail of the wall is shown in Figure 1. For the Whirlwind I the wall was equally divided into six segments, each of 22" square. The dynamic model in the form used for computer solution is shown in Figure 92. As seen from the figure, two extra dummy columns and rows are added to the model for the convenience of programming.

Equivalent wall properties for the dynamic model are shown in Appendix A, item V. 0.10 milliseconds was used as time interval in this computation. For the IBM 704 computer, the wall was divided into a grid system 7 squares by 5, each square being 9.2". The time interval was equal to 0.0375 milliseconds.

B. Results

1. From the Whirlwind I program. The results of the analysis are presented on Figure 93, 94, 95 and 96.

The nomenclature used in these figures is

P = applied Load (which is equal to the static horizontal reaction)

H = horizontal reaction

V_L = vertical reaction at left support

V_R = vertical reaction at right support

V_S = vertical reaction for statically applied load = $P(\frac{L}{H})$

X_L = horizontal displacement of loaded mass point

X_R = horizontal displacement of extreme right hand mass point in top row.

Y_L = vertical displacement of loaded mass point

Y_R = vertical displacement of extreme right hand mass point in top row.

2. From the IBM 704. The more significant information is given in Figure 97 and 98. The nomenclature used in these figures is the same as that used above.

CHAPTER VII

DISCUSSION OF RESULTS, GENERAL CONCLUSIONS, AND RECOMMENDATIONS FOR FUTURE RESEARCH

I. Discussion of the Machine's Behavior

As stated in Chapter I, one of the principal objectives of this preliminary investigation was the analysis of the testing machine's behavior. In this respect, it is interesting to point out that the results obtained demonstrated the following:

A. Although in the function generator the rise time of the load was set at 15 ms., this time varied considerably from test to test. For small loads, the rise time oscillated around 12 ms., except for some of the tests carried out on wall #4. In this case, the rise time was considerably less -- perhaps this can be attributed to some impact effect. As the peak value of the load increased, the rise time also increased; oscillating between 24 and 33.5 ms. at loads greater than 50 kips.

It is felt that these variations in rise time are due to the saturation of the only dump valve used in the system, and it is hoped that with the introduction of a new dump valve and the use of higher pressure, it will be possible to obtain a rise time close to the desired value.

B. The shape of the load-time pulse varies considerably from that required and set in the function generator. From the shape of the load-time curves given in tables V-1, V-2 and V-3 it can be seen that -- if the small depressions and peaks are smoothed with an average curve -- when the load is small the shape is completely irregular, showing big oscillations. As the load increases, and for loads of approximately 30 kips,

the curve presents two definite peaks. When the peak load is larger than 30 kips, the shape of the average curve tends to be triangular.

It can be also observed that in a few tests, the load did not return to zero after the peak value was reached. A series of tests performed on a reinforced concrete column after the four tests of the preliminary investigation were completed, showed that these considerable deviations of the load-time curve were caused by the use of an improper pressure in the accumulators. It was discovered that the pressure of nitrogen in the ten-gallon accumulator was too high in comparison to the low oil pressure used for the push and pull sides, and most of the oscillations were due to the use of high gain.

Considerable improvement in the shape of the load-time curve was already obtained during the series of tests performed on the reinforced concrete column. It is believed that all difficulties will be eliminated when the appropriate nitrogen and oil pressures, and gain are determined by trial and error.

C. The duration of the load pulse varies from 35 to 75 ms. although the function generator was set for 50 ms.

The cause for this irregularity seems to lie in the same factors discussed above under 1 and 2. Above all, the saturation of the dump valve seems to be the principal reason for the greater duration of the load pulse.

D. The movement of the supports for the specimen are considerably larger than expected. This motion not only confuses the experimental results, not allowing a good comparison between theoretical and experimental results; but also has considerable influence in the behavior of the

loading unit, because a larger displacement of the ram is required, and consequently a greater flow of oil.

It is planned to stiffen the supporting beam and to make the connections more rigid, in order to minimize the displacement of the supports.

II. Discussion of the Results Obtained from Tests Performed on the Walls

It is known that the dynamic response of a member being subjected to a dynamic impulsive load is not only a function of the intensity of the applied force as in the static case, but also of the rate of application of the force, the duration of the load, and the particular variation with time of load and resistance. Then, it is believed that in order to get an idea of the shear wall's dynamic behavior from the data obtained, given in Chapter V, the following comparisons have to be made.

A. The shape of the reaction vs. time and displacement vs. time curves must be compared with the load-time curve. When this analysis is completed it can be seen that in all cases the reaction and displacement curves resemble the load curve. In fact, if the small peaks and depressions of the load-time curve are smoothed out by an average curve; and if in some cases some time shifting which is probably due to defective synchronization and calibration is accounted for; the agreement in shape is very good. It is possible to observe that any significant irregularities in the load vs. time curve were reproduced in the reaction and displacement curves.

The resemblance discussed in the preceding paragraph is important, because it reveals an almost complete absence of dynamic effect and indicates that the response of the wall is practically a static one.

The conclusions arrived at can be justified by a quick analysis of the results obtained in the theoretical computations. In effect, according to the figures obtained by the IBM 704 computer for the dynamic horizontal reaction (see Fig. 97), it can be seen that in the elastic region this reaction ("H") vibrates about the static reaction, which is equal to the applied load. However, the amplitude of this vibration is very small, and its period has a value of approximately 5 milliseconds. The cause for this oscillation may be considered to be the fundamental mode of the multi-mass system. Considering that the rise time for the load was always greater than 13 ms., (i.e.) that the rise time/natural period of the fundamental mode, ratio was always larger than 2.6, it follows that no appreciable dynamic effect can be expected. Consequently the amplitude of vibration and displacement has to be very small -- unobtainable with the sensibility of the instrumentation used in this series of tests.

B. When the values of the displacements obtained on specimen #2 are compared with those obtained on specimen #1 -- assuming that the same vertical movement of the supports occurs during the dynamic test rather than during the static test -- it can be seen that as long as wall #2 was not badly cracked by previous loads, the dynamic displacement that the specimen undergoes practically coincides with that obtained for similar static loads on wall #1. Considering that the modulus of elasticity for the concrete in both specimens was approximately the same, the reasons for this similarity follows from the former conclusion (i.e.) that there is practically no dynamic effect.

While this discussion was being written, a static test was con-

ducted on a specimen built with concrete whose characteristics were similar to those of the concrete used in specimens number three and four. A quick analysis of the results seems to also indicate a good agreement between the displacements under static and dynamic loads. It must be pointed out that in order to make a comparison of these results it is necessary to subtract from the horizontal displacement obtained in the test, the horizontal displacement due to the rotation of the wall. This rotation is caused by the considerable vertical displacement of the supports.

C. When the type of failure is analyzed it can be seen, as pointed out in Chapter V, that the collapse of all four specimens was produced by a defective welding between the reinforcement of the tension column and the support plate. However, the failure of repaired wall #4 was produced by a shearing off of the compression column at its junction with the beam. This type of failure agrees with that obtained in the static test conducted on a similar specimen at Stanford University.

D. Analysis of the Ultimate Resistance: If no appreciable dynamic effect exists, it is logical to expect a larger ultimate resistance under dynamic than under static load. Unfortunately, due to the premature failure of the specimens for reasons given above, only the results obtained during the test conducted on the repaired wall #4, may be analyzed in an attempt to shed some light on this fact of the problem. The failure of this specimen took place under a load of 95 kips. Although it is true that no report of a static test conducted on a wall similar to #4 is included here, such a static test was just completed, as mentioned before. The wall in this case failed under a load of 80 kips --

a value which agrees closely with the results obtained at Stanford University; where a similar specimen failed under a load of 71 kips. It is then significant that the repaired wall #4, although extensively cracked by numerous blows applied prior to the ultimate load, was still able to resist a load higher than that endured by a similar wall being loaded statically. If the value of 80 kips is taken as a basis for comparison, the increase in ultimate load is of the order of 20%. If the Stanford tests are taken as a basis, the increase is approximately equal to 33%.

To justify this increase in ultimate load, two factors must be considered:

1. An increase in the strength of the member due to the increase of the yield point of the material under high rate of loading.

2. The ductility of the member -- which may be defined as the ratio of the maximum deflection (just before collapse) to the yield deflection -- is an important influence in determining the resistance of a member to dynamic loads.

Ductile members -- those which can maintain their peak or near peak ultimate strength for large plastic strains -- are capable of absorbing a greater amount of energy without failure, and are less liable to fail or collapse suddenly.

The ductility of a shear wall depends on the type of failure. In the specimen being studied, failure occurred due to a shearing off of the compression column, which is a sudden type of failure. The specimen may be considered as a brittle structure member.

Consequently, the increased strength of the member under dynamic load finds its justification in the influence of the speed of loading on the yield point of the materials. What this influence is precisely, on members made of concrete and steel is difficult to evaluate, but factors of the order to 20 to 35% greater than the static strength seem reasonable.

III. Discussion of the Theoretical Results

If the results obtained from the computations carried out by the WHIRLWIND I and IBM 704 computers are compared, the following facts become evident:

A. There is a very good agreement in the values obtained for the horizontal displacement of the loading point, up to a load of 25 kips, (i.e.) while the wall behaves elastically.

B. According to the IBM 704 program, the first crack occurred at a load of approximately 25 kips; whereas, according to the results obtained from WHIRLWIND I's program, the first crack should occur at a load of approximately 43 kips. This big discrepancy is the first indication that there is something wrong in one of the two programs.

C. After cracking occurs; according to both programs, the lattice started to oscillate and practically all the segment cracked. It was felt that these oscillations and the widespread cracking which followed were due to the abrupt weakening of the elements at cracking, under the cracking hypothesis adopted. However, a second run was made by Mr. Calladine, increasing the amount of steel in the wall and beams, retaining its elastic properties but reducing its yield strength in such a way that the ultimate strength per element was unchanged, and on the whole, this

second test gave results similar to those of the first.

A third test was also run by Mr. Calladine in order to check whether an increased number of iterations would be helpful. Clearly, the elastic solution would not be improved, but it was felt that the abruptness of the cracking could be better dealt with by repeated applications of the iterative procedure. However, the desired effect was not achieved.

The trouble -- which is undoubtedly serious -- seems to be of a mathematical nature rather than a physical one, and it is hoped that a careful reappraisal of the programming will point out the error.

IV. Comparison Between Theoretical and Experimental Results

The theoretical computations run on IBM 704 yield what seem to be satisfactory results up to a load of 23 kips, and those run on WHIRLWIND I give good results up to a load of 40 kips. It is evident that a comparison of theoretical and experimental results can only encompass this region, which may be considered as the elastic range of the wall.

It is interesting to point out, in the first place, that the first cracks in specimens number three and four, occur under loads of 42.5 and 37 kips, respectively. These values are in very good agreement with the results obtained for the program run on WHIRLWIND I.

This seems to indicate that in the computations performed by IBM 704 the oscillations of the lattice obtained at a load of 23 kips are due to a mathematical error, and not to cracking.

As it was mentioned before, the theoretical and experimental results show clearly that the vibrational amplitude of reactions and displacements

is so small, that no dynamic effect is apparent.

If the theoretical and experimental values for the horizontal displacement of the loading point are compared, it may be seen that the results are inconsistent. For example; at a load of 23 kips WHIRLWIND'S I computations give a displacement of 0.0115 in., and IBM 704's computations a displacement of 0.014 in., whereas, in the static test performed on specimen #1, a value of 0.0017 was obtained for a similar load. The difference can be explained by considering that the modulus of elasticity for the concrete in wall #1 was 4.5×10^6 p.s.i., while in the theoretical computations, a value of 3×10^6 p.s.i. was used. However, if the theoretical results are compared with the experimental values obtained from test No. 3 on wall 3 and test No. 6 on wall 4, it can be seen that the latter are of the order of 0.035 in., which is considerably larger than the theoretical ones. The explanation for these inconsistent results perhaps lies in the difficulties in obtaining a good evaluation of the experimental value from the data, due to the complications introduced by the displacement of the supports.

V. General Conclusions

The conclusions that can be drawn from the former discussion may be summarized as follows:

A. Due perhaps to the use of inappropriate gain in the amplifiers, incorrect nitrogen and oil pressures, and saturation of the dump valve of the system, aggravated by the extra oil flow required by the considerable displacement of the specimen's supports; the force-time shape of the pulse, rise time of load, and duration of pulses given by the dynamic

loading machine differ from those set in and required by the function generator.

B. Although the number of walls tested so far is too small to allow the drawing of any general conclusion, the almost complete lack of vibrations in the reactions and displacements obtained from the tests on walls 2, 3, and 4 reveals that the applied load practically produces no dynamic effect.

The values for the horizontal displacement of the loading point during a dynamic test and those corresponding to a static test seem to agree quite closely, in spite of the difficulties introduced in the exact evaluation of this data by the necessity of taking into consideration the displacement of the supports. The type of failure produced on all four walls was an unexpected one--the defective welding of the tension column's reinforcement to the support plate. In the wall where the connection was repaired, failure occurred by a shearing off of the compression column, which is the type of failure expected. Although this wall was extensively cracked, it was still able to resist several blows with peak values larger than those endured by a similar wall under static loading.

C. The theoretical analysis performed on WHIRLWIND I yields satisfactory results until first cracking occurs, at a load of 40 kips. This value is in good agreement with the experimental data. After cracking, however; the lattice started to vibrate and the results are not consistent with the experimental data. Satisfactory results are given by the analysis of the IBM 704 computer up to a load of 23 kips, after which the lattice begins to vibrate. The cause of this oscillation seems to be a mathematical error in the programming.

D. The theoretical and experimental results agree in showing an almost complete lack of vibration. However, when the values for the horizontal displacement of the loading point are compared, they are found to be inconsistent.

VI. Recommendations for Future Research

This preliminary series of tests demonstrated most convincingly that considerably more experimental and theoretical work has to be done in order to reach a good understanding of the shear wall problem. It is suggested that further theoretical and experimental work be done along the following lines:

A. Introducing a new set of dump and servo valves in the system in order to investigate the possibility of decreasing the rise time and obtaining better control of the duration of pulse. Performing a series of tests in order to find the appropriate gain and the appropriate oil and nitrogen pressures to be used for different values of the peak load. Investigating the possibility of introducing modifications in the system with the aim of obtaining a better control of the pulse.

B. Investigating the possibility of improving the instrumentation used for the recording of the load, reactions, and displacements.

C. Starting an extensive series of tests in order to determine the influence of the following variables on the behavior of the shear wall:

1. Strength of concrete
2. Effect of frame
3. Amount of panel reinforcement
4. Effect of rise time

5. Variation of load pulse
6. Length/Height ratio of wall
7. Scale effect

D. From the theoretical point of view, a careful review of the programs already written is suggested, in order to find the cause for the oscillation of the system.

An investigation of the proper time interval for the numerical integration, and the effect of the grid sizes, with the aim of reducing the computation time to the minimum possible, while still obtaining a good approximation.

REFERENCES

1. K. Muto, D. W. Butler and B. Osawa, "Solution of Frames by the Consideration of Bending and Shear in the Rigid Region", Transactions of the Architectural Institute of Japan (Japanese) N-45 (Tokyo, December 1952) p. 53.
2. K. Muto and B. Osawa, "Approximate Method of Calculation of Forces in a Reinforced Concrete Wall with Openings", Transactions of the Architectural Institute of Japan (Japanese) N-45 (Tokyo, December 1952) p. 58.
3. Y. Otsuki, "Stress Analysis of a Wall with Rectangular Holes", Transactions of the Architectural Institute of Japan (English) N-41 (Tokyo, August 1953) p. 72.
4. "Massachusetts Institute of Technology", Lecture Notes on 1.559 "Structural Design for Dynamic Loads", p. 19.2.
5. K. Muto, and K. Kuromasa, "Experimental Study of Vibration-Resistant Reinforced Concrete Walls", Study of Strength and Construction of Reinforced Concrete Frames with Walls (Japanese) (Tokyo: Japanese Architectural Engineering Research Fund 1952.)
6. Dr. Tadashi Taniguchi, "The Study of Vibration-Resistant Walls", Transactions of the Architectural Institute of Japan (Japanese) N-41 (Tokyo, August 1953) p. 62.
7. Hansen, R. J., "Behaviour of Structural Elements under Impulsive Loads", Massachusetts Institute of Technology, April 1950, p. 97.
8. Hansen, R. J., "Behaviour of Structural Elements under Impulsive Loads, II", Massachusetts Institute of Technology, November 1950, p. 83.
9. Hansen, R. J., "Behaviour of Structural Elements under Impulsive Loads, III", Massachusetts Institute of Technology, July 1951, p. 89.
10. Galletly, Gerard D., "Behaviour of Reinforced Concrete Shear Walls under Static Load", Massachusetts Institute of Technology, August 1952.
11. Williams, H. A., Benjamin, J. R., "Investigation of Shear Walls, Concrete and Brick-Walled Bents under Static Shear Loading", Technical Report No. 1, Part 1, Department of Civil Engineering, Stanford University, Stanford, California, April 1952.
12. Benjamin, J. R., "Investigations of Shear Walls, Part 2 - Prediction of Behavior of Plain Concrete and Brick Walled Bents under Static Shear Loading by Lattice Analogy", Technical Report No. 1, Part 2, Stanford University, April 1952.
13. Williams, H. A., Benjamin, J. R., "Investigations of Shear Walls, Part 3 - Experimental and Mathematical Studies of the Behavior of Plain and Reinforced Concrete Walled Bents under Static Shear Loadings", Technical Report No. 1, Part 3, Stanford University, July 1, 1953.

14. Williams, H. A., Benjamin, J. R., "Investigations of Shear Walls, Experimental and Mathematical Studies of the Behavior of Brick Walled Bents under Static Shear Loading", Technical Report No. 2, Part 4, Stanford University, August 1, 1953.
15. Williams, H. and Benjamin, J., "Investigation of Shear Walls, Part 5, Prediction of the Behaviour of Plain Concrete, Reinforced Concrete, and Brick-Walled Bents under Static Loadings", Stanford University 1953.
16. Williams, H., and Benjamin, J., "Investigation of Shear Walls" Part 6, Continued Experimental and Mathematical Studies of Reinforced Concrete Walled Bents under Static Shear Loading, Stanford University, 1954.
17. Walter, J. K. et.al., "Investigation of Shear Walls", Part 7, Continued Experimental and Mathematical Studies of the Behaviour of Brick Walled Bents under Static Shear Loading, Stanford University, 1954.
18. Stivers, R., Benjamin, J. and Williams, H., "Investigation of Shear Walls", Part 8, Stresses and Deflections in Reinforced Concrete Shear Walls Containing Rectangular Openings, Stanford University, August 1954.
19. Benjamin, J. and Williams, H., "Investigation of Shear Walls," Part 9, Continued Experimental and Mathematical Studies of Reinforced Concrete Walled Bents under Static Shear Loading, Stanford University, September 1, 1955.
20. Benjamin, J., Williams, H., Erickson, R. and Campbell, R., "Investigation of Shear Walls", Part 10, Limited Study of Brick and Concrete Block Shear Walls with Steel Frame, Stanford University, September 1956.
21. Finerman, Aaron, "The Theoretical Elastic Response of Shear Walls Subjected to Dynamic Loads", Massachusetts Institute of Technology, August 1956.
22. Simpson, Howard, "A Dynamic Loading Machine", Massachusetts Institute of Technology, 1957.
23. Proceedings of the American Concrete Institute, Year 1955, p. 600.
24. Proceedings of the Conference on Building in the Atomic Age, Massachusetts Institute of Technology, June 1952.
25. Newmark, Nathan M., "An Engineering Approach to Blast-Resistant Design", Transactions of ASCE, Vol. 121, 1956, pp. 45-64.
26. Guerin, A., "Traite' de Beton Arme" Tome I, p. 238, Tome II, p. 54.
27. Telemaco van Langendouck, "Calculo de Concreto Armado", Associacas Brasileira de Cimento Portland, Vol. 1 (2nd Edition) Sao Paulo, 1954.
28. Brice, Louis Pierre, "Etude des Conditions de Formation des Fissures de Glissement et de Decohesion dans les Solides", Travant, June 1954, p. 475-506.

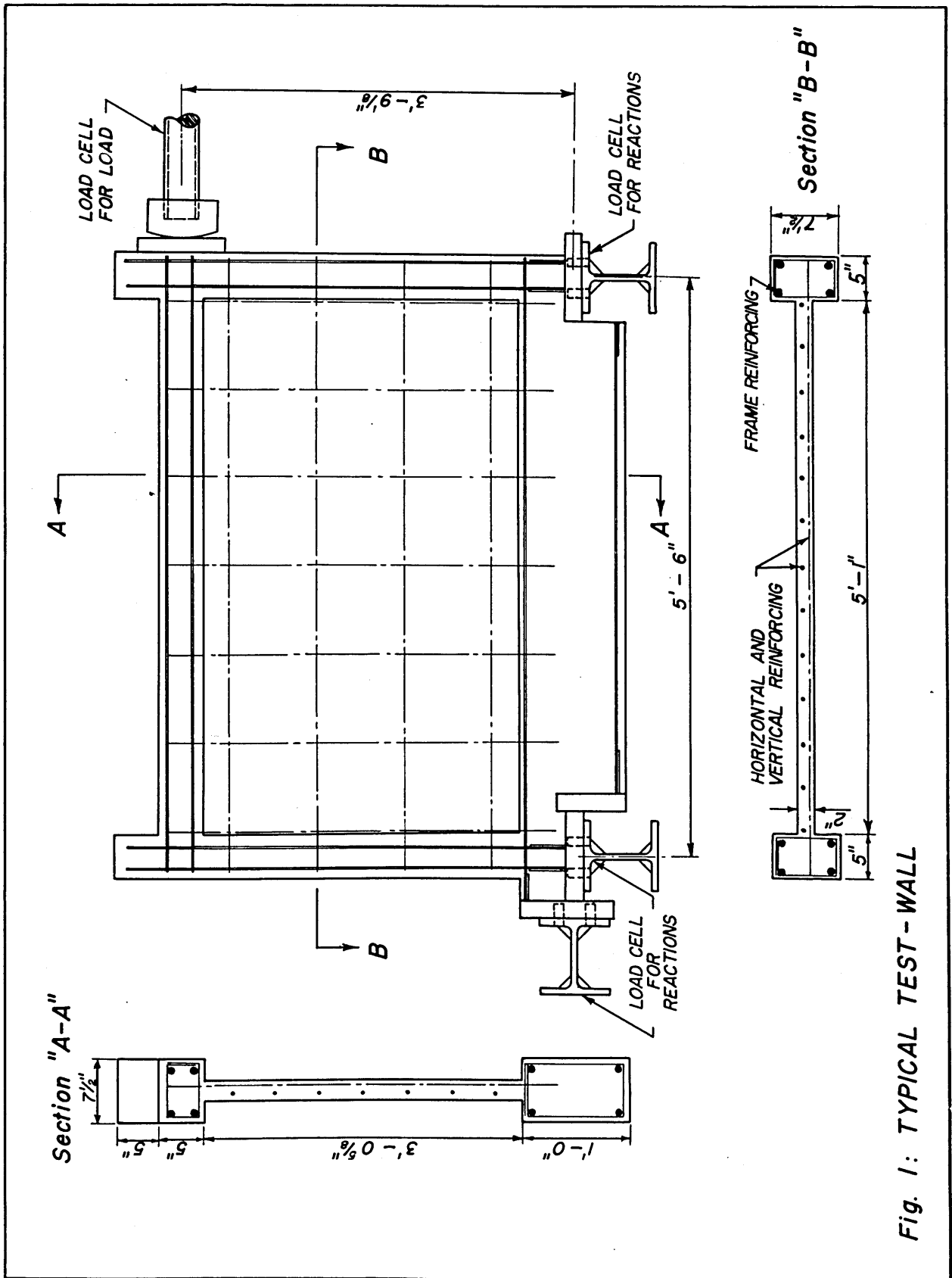


Fig. 1: TYPICAL TEST - WALL

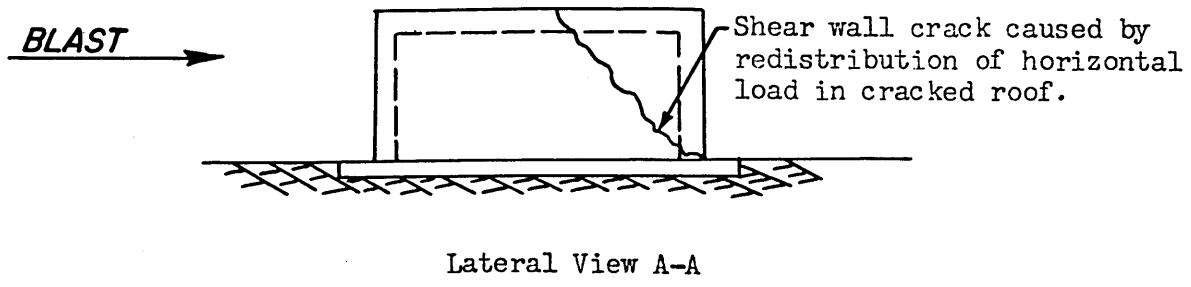
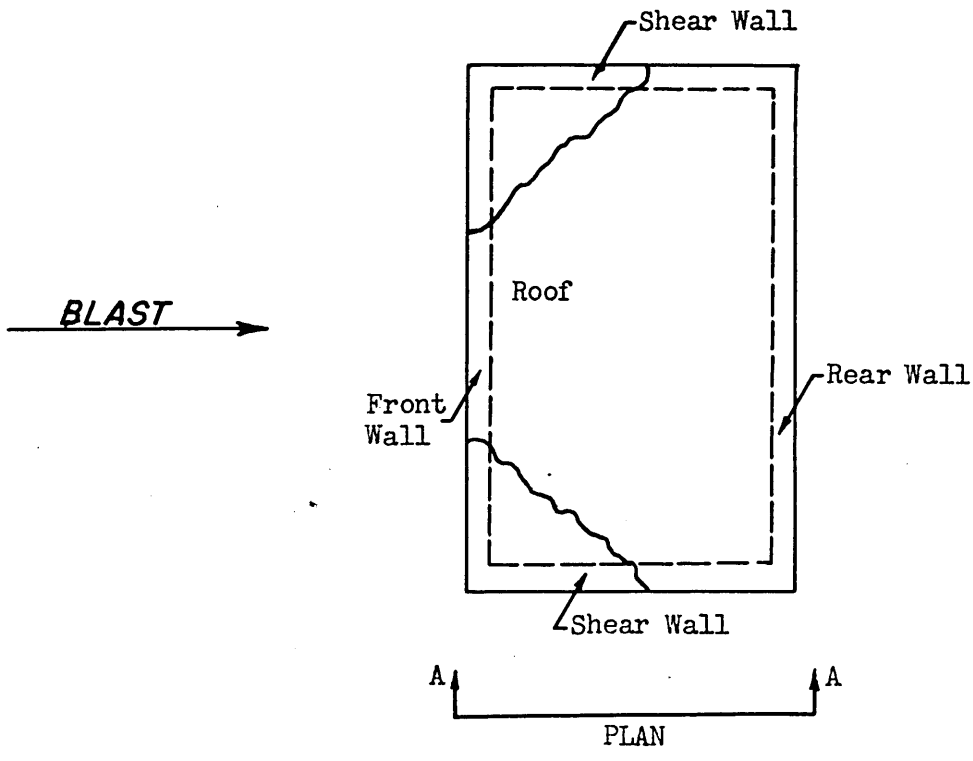


Figure 2 - Shear Wall Crack Caused by Redistribution of Horizontal Load in Cracked Roof

87

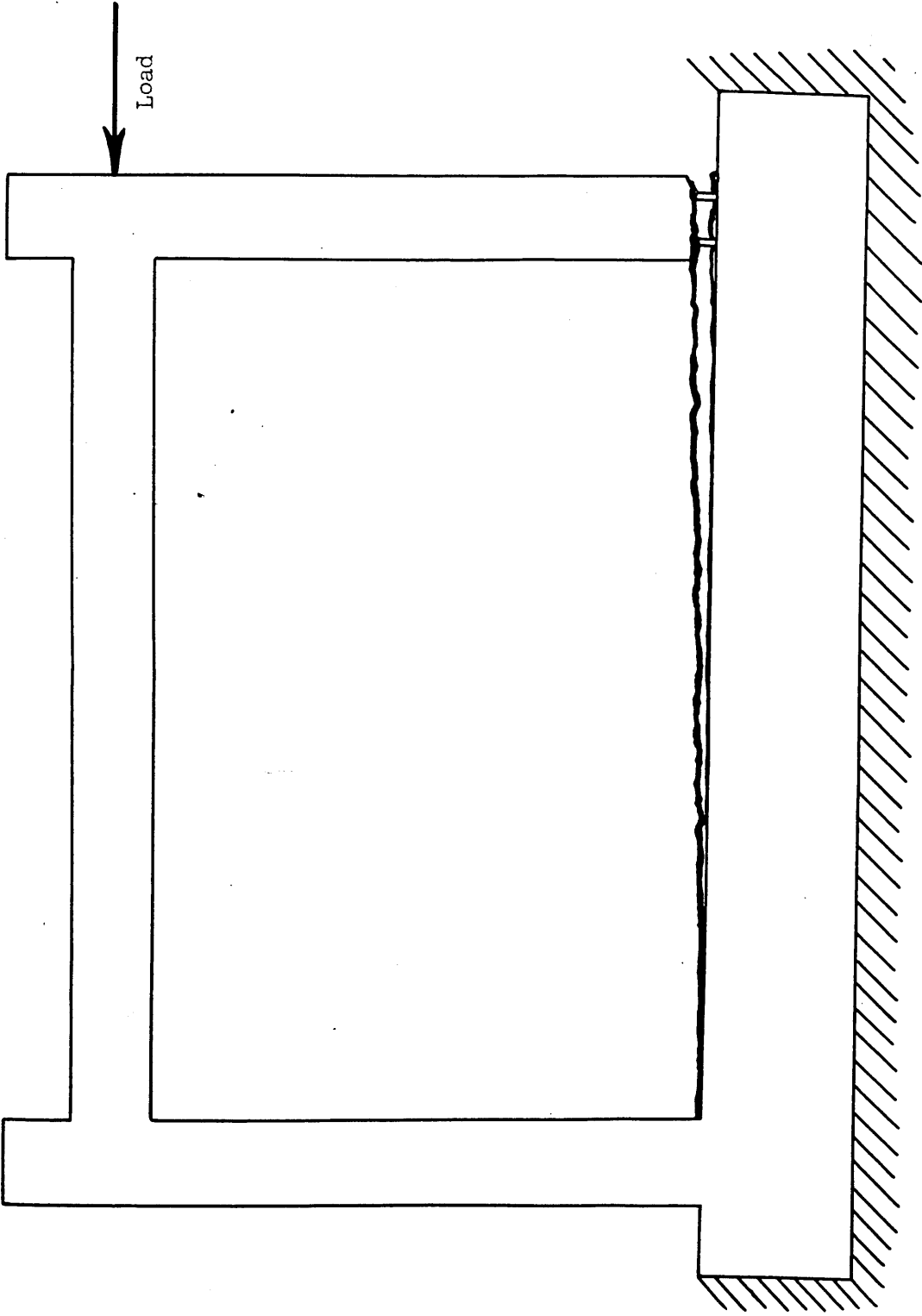


Figure 3 - Shear Wall Tension Failure

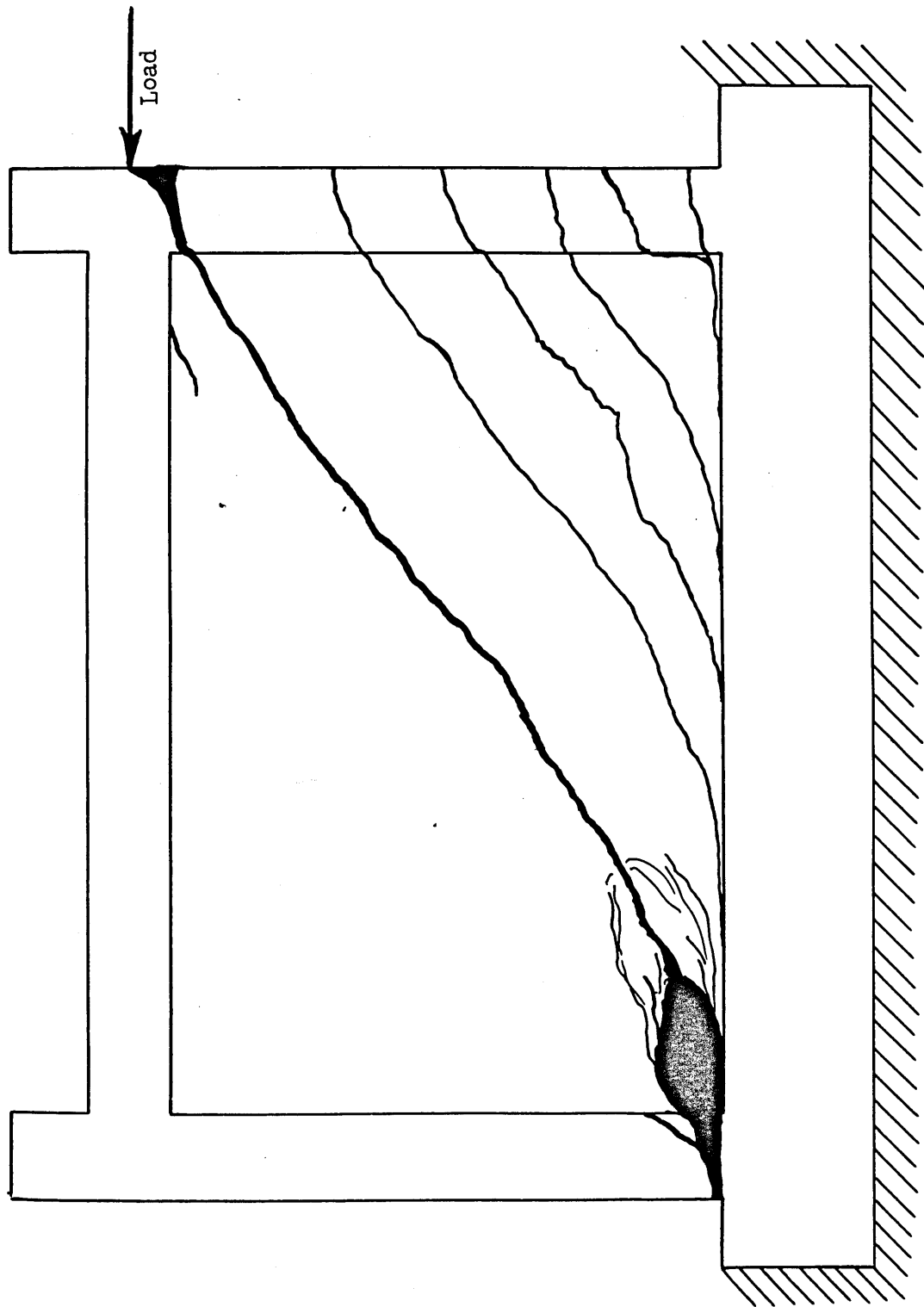


Figure 4 - Shear Wall - Shear Failure at the Base of Compression Column

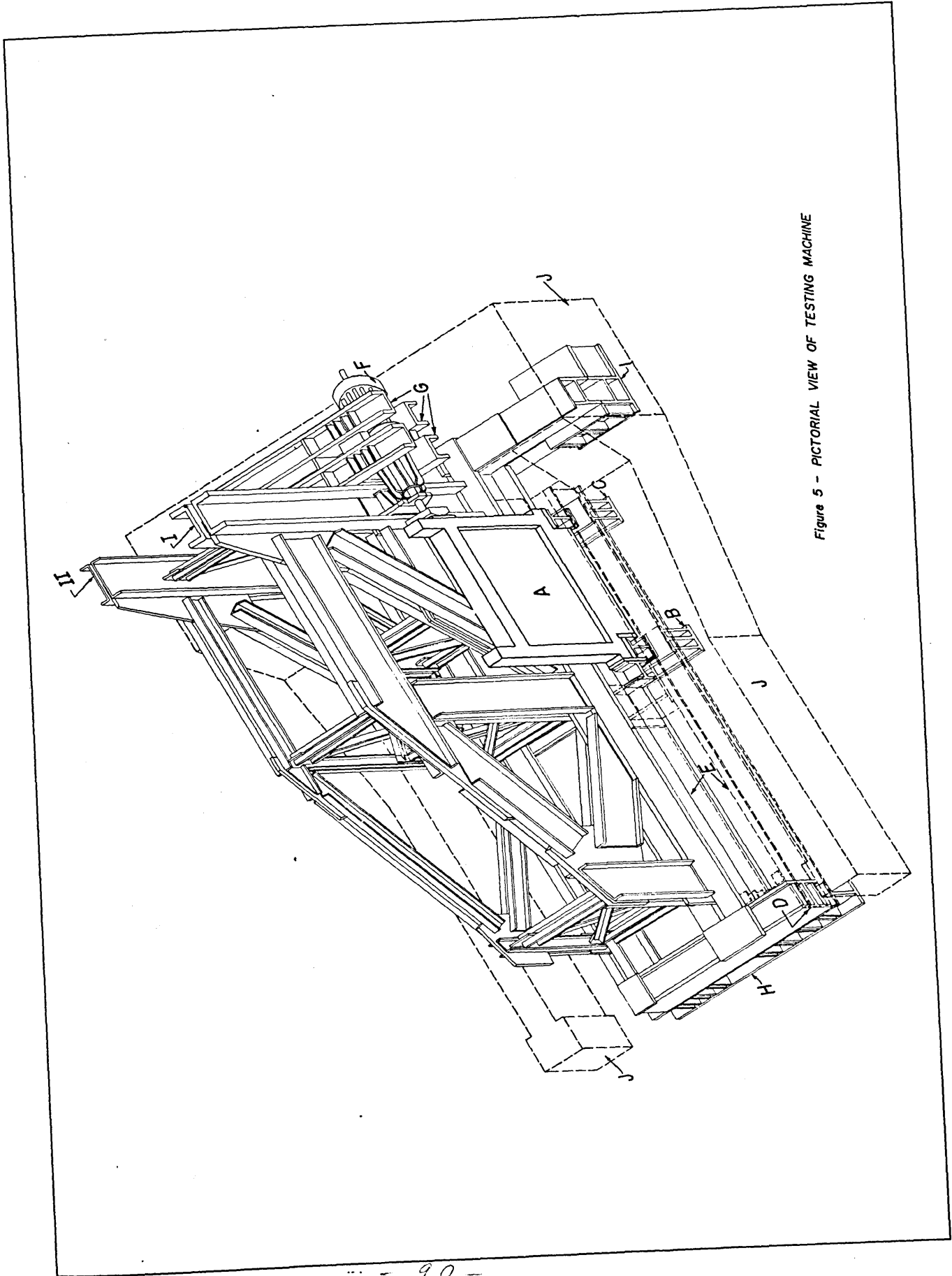


Figure 5 - PICTORIAL VIEW OF TESTING MACHINE

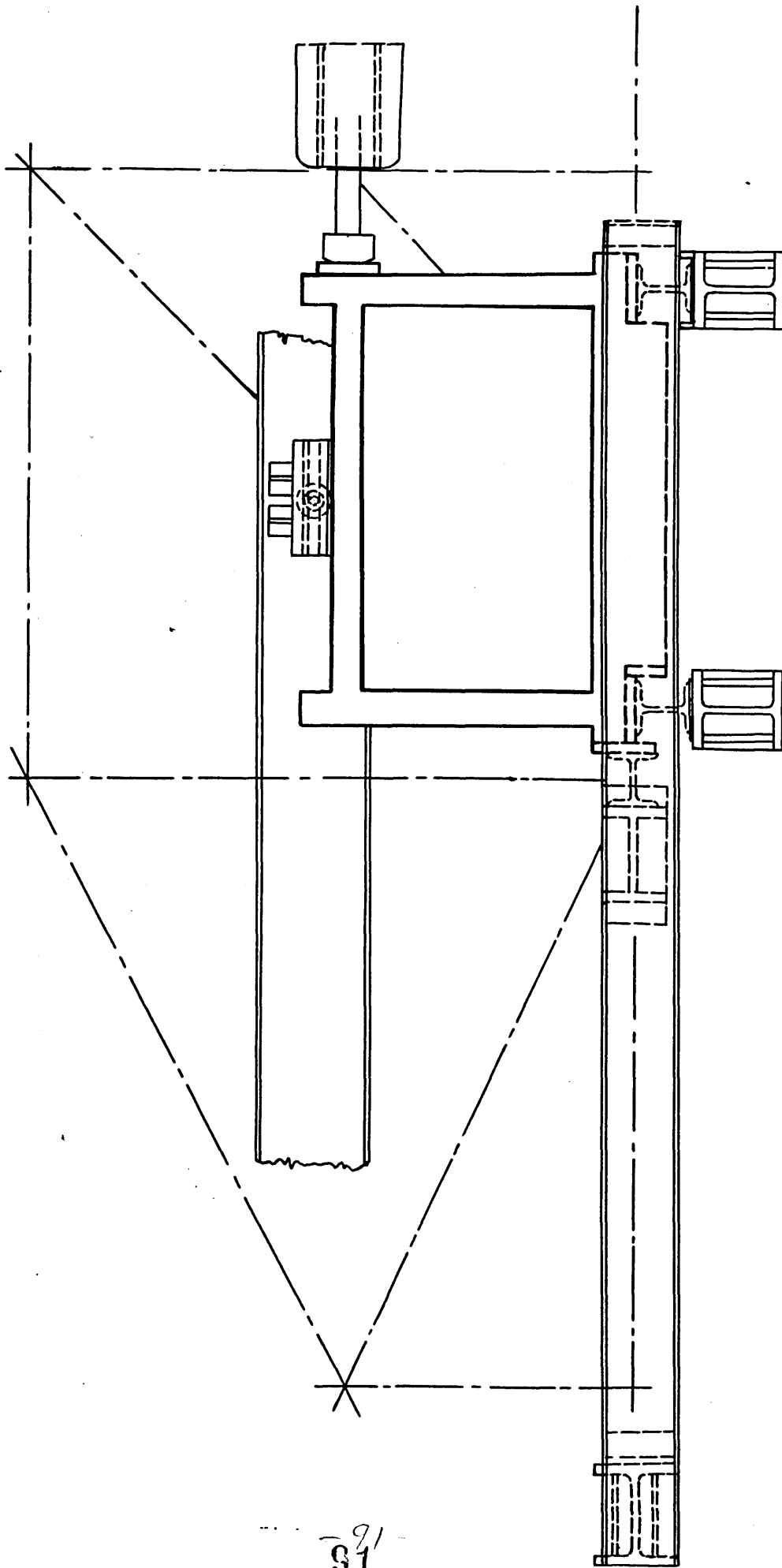


Figure 6 - Support Arrangement for the Shear Wall - Lateral View

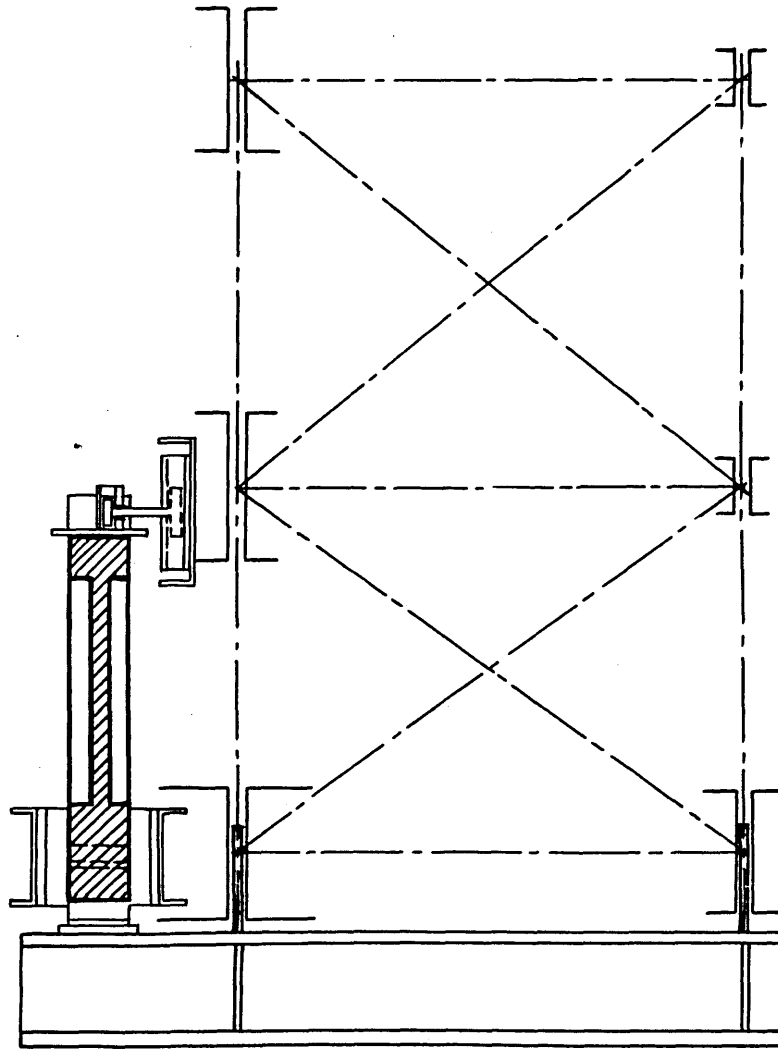
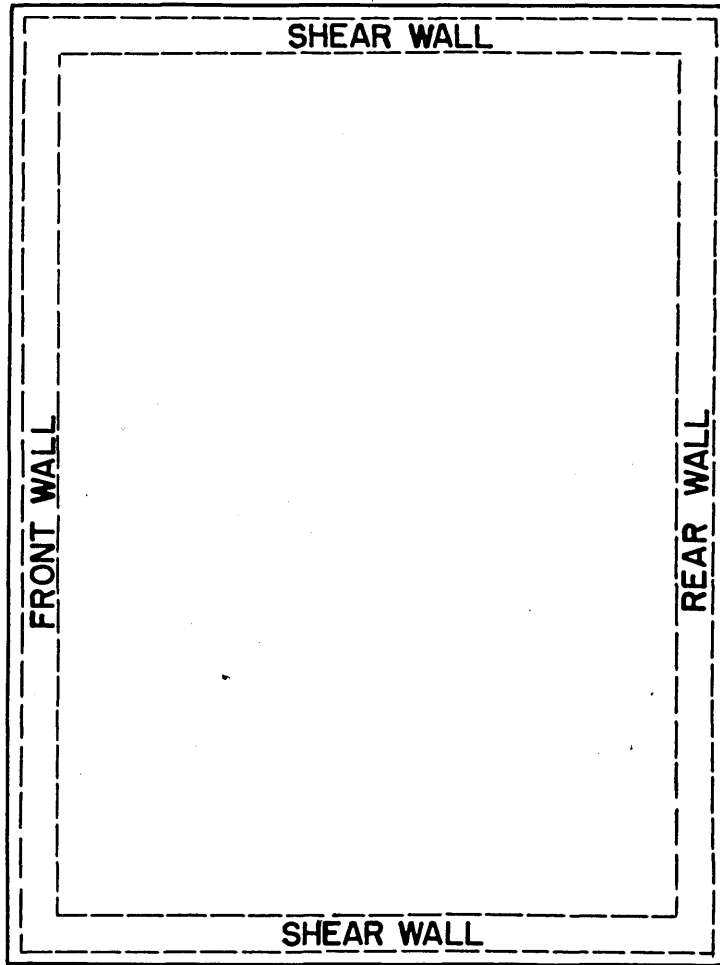
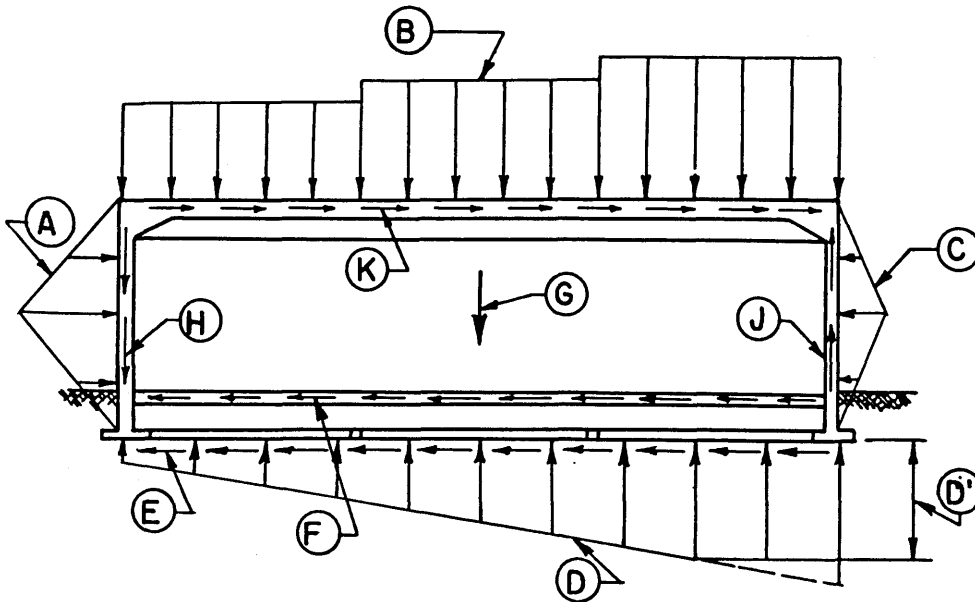


Figure 7 - Support Arrangement for the Shear Wall - Cross Section



- A - Lateral Load from Horizontal End Shear of Front Wall
- B - Vertical Load from Vertical end Shear of Roof
- C - Lateral Load from Horizontal End Shear of Rear Wall
- D - Foundation Resistance Below Shear Wall Footing
- D' - Ultimate Plastic Soil Resistance
- E - Friction on Shear Wall Footing
- F - Lateral Load from Horizontal Shear in Floor Slab
- G - Dead Load
- H - Vertical Load from Vertical Shear in Front Wall
- J - Vertical Load from Vertical Shear in Rear Wall
- K - Lateral Load from Horizontal Shear of Roof

PLAN



Section at Shear Wall

Figure 8 - Typical Loadings on Shear Wall Structure

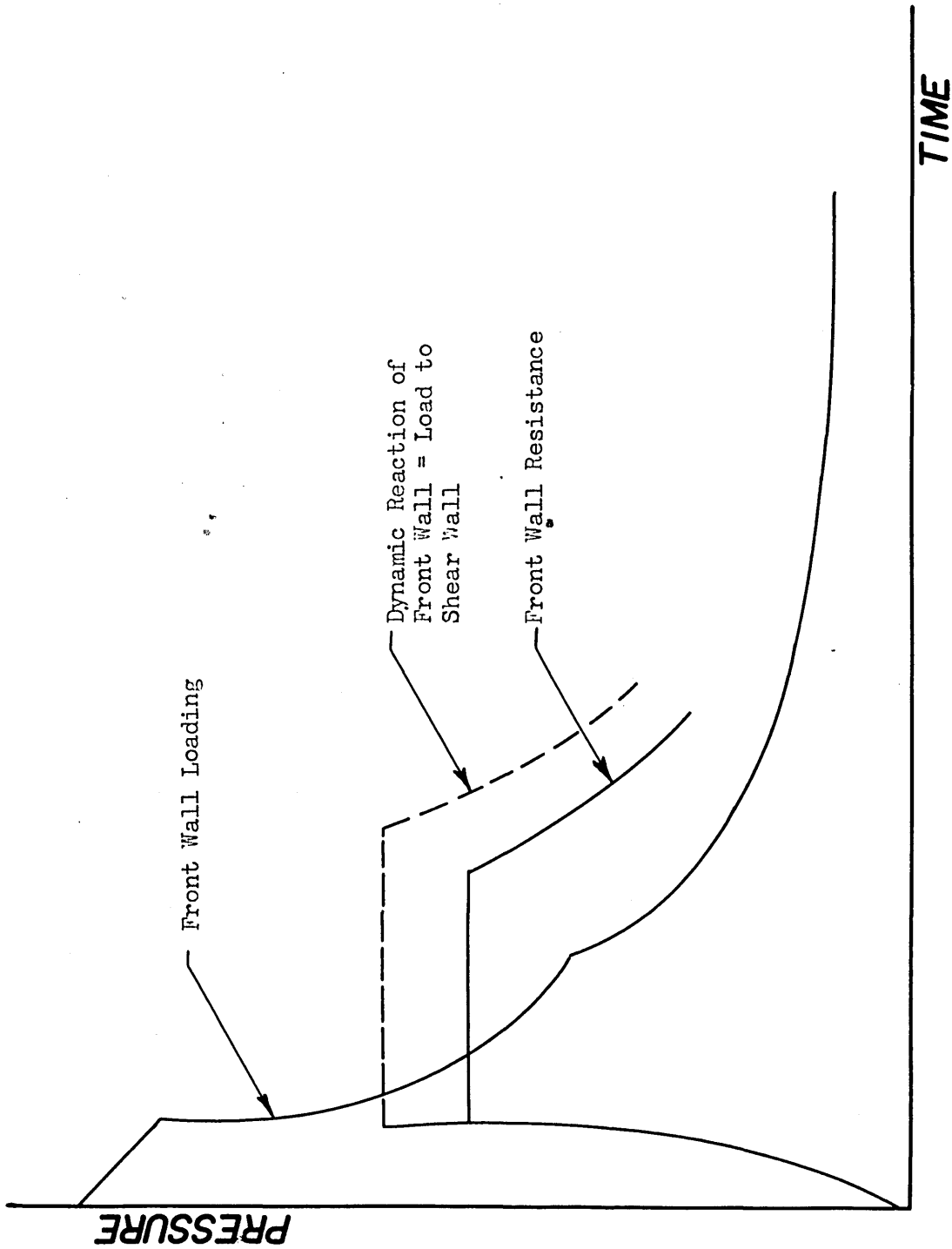


Figure 9 - Comparison of Front Wall Loading with Shear Wall Loading

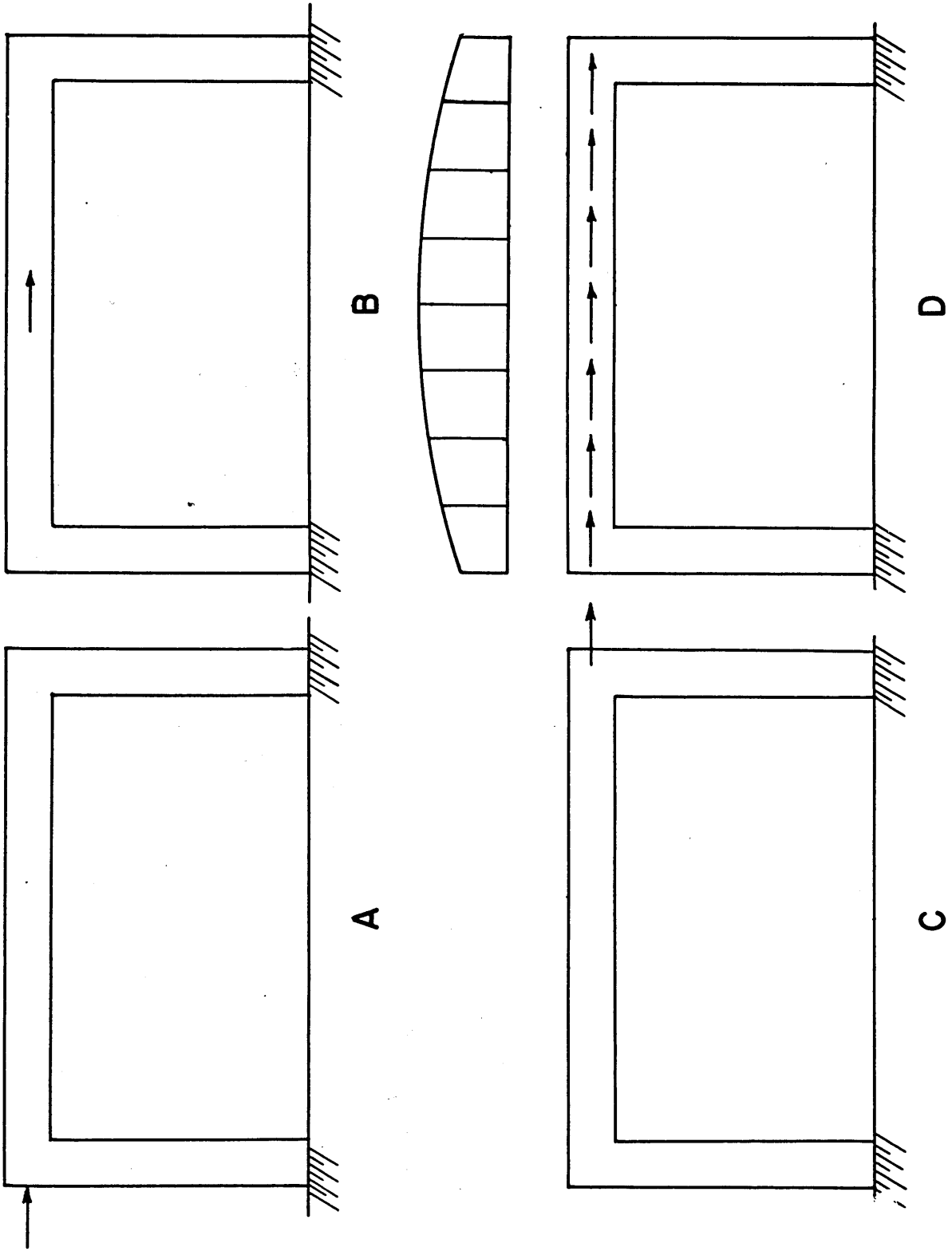


Figure 10 - Four Possibilities of Load Distribution Along the Top of a Model Wall

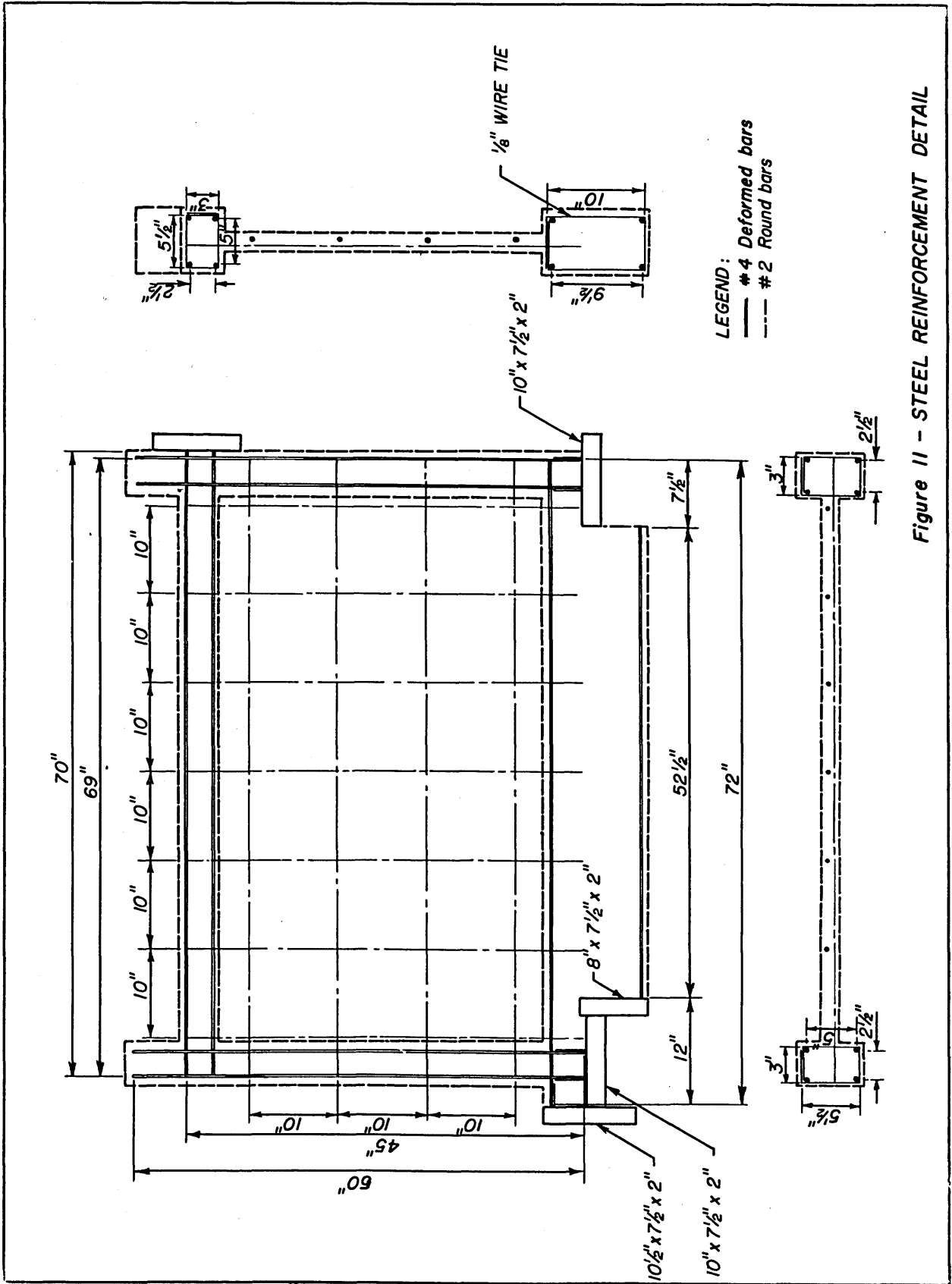


Figure 11 - STEEL REINFORCEMENT DETAIL

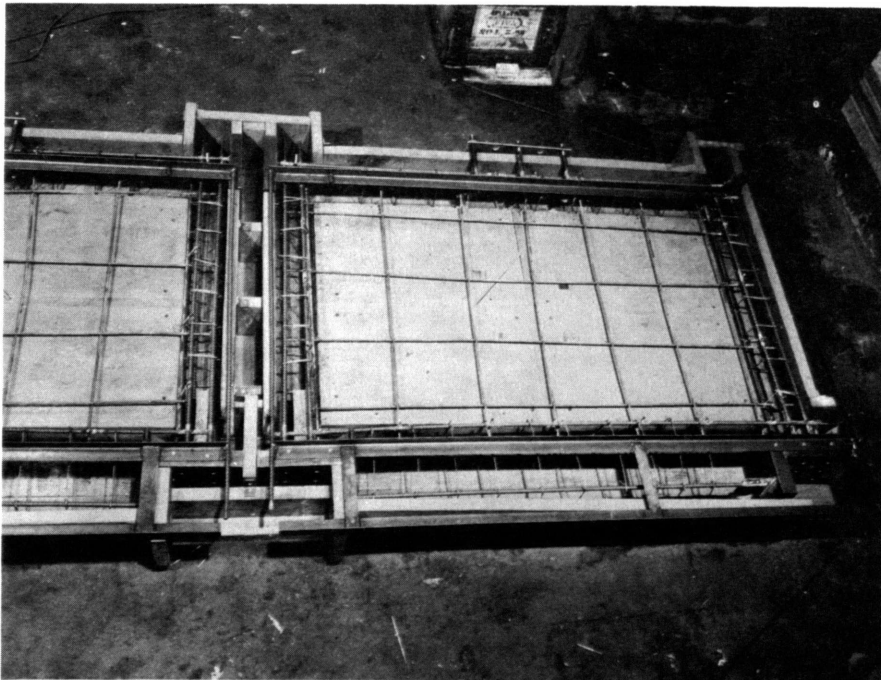
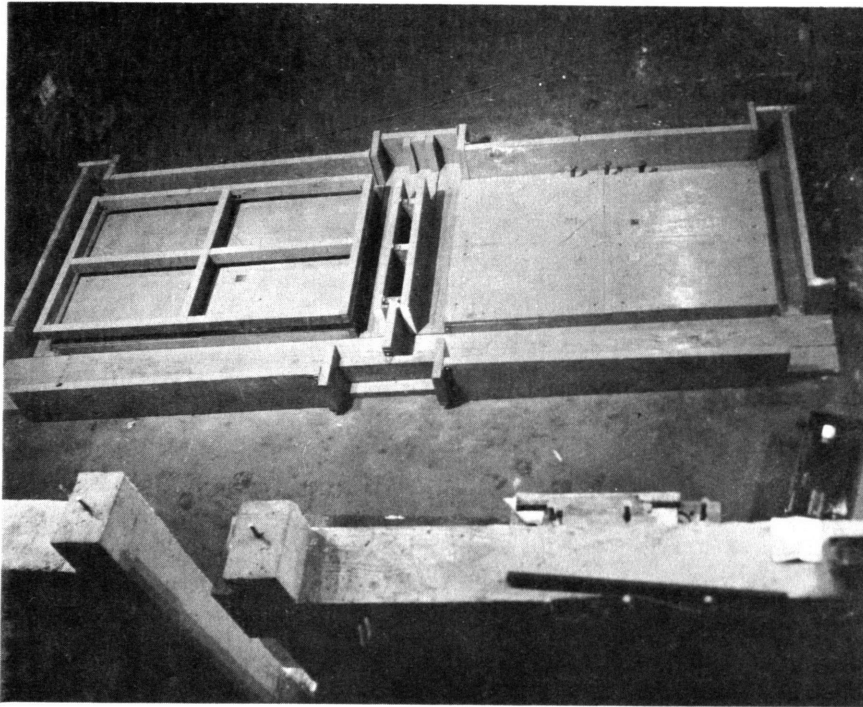


Figure 12 - Formwork and Reinforcement in Place for the Shear Wall Specimen

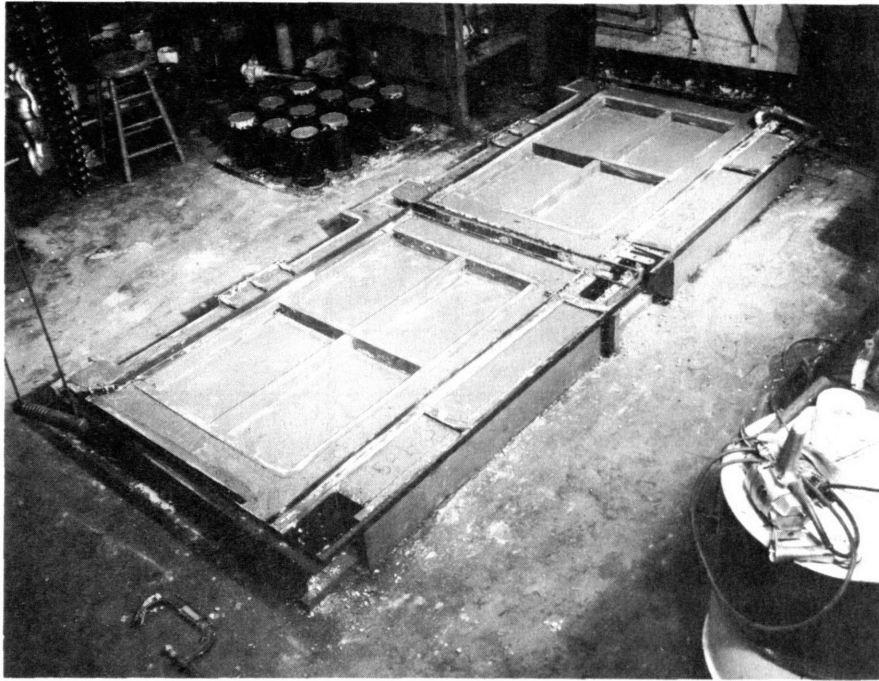


Figure 13 - Walls and Cylinder, after being Cast

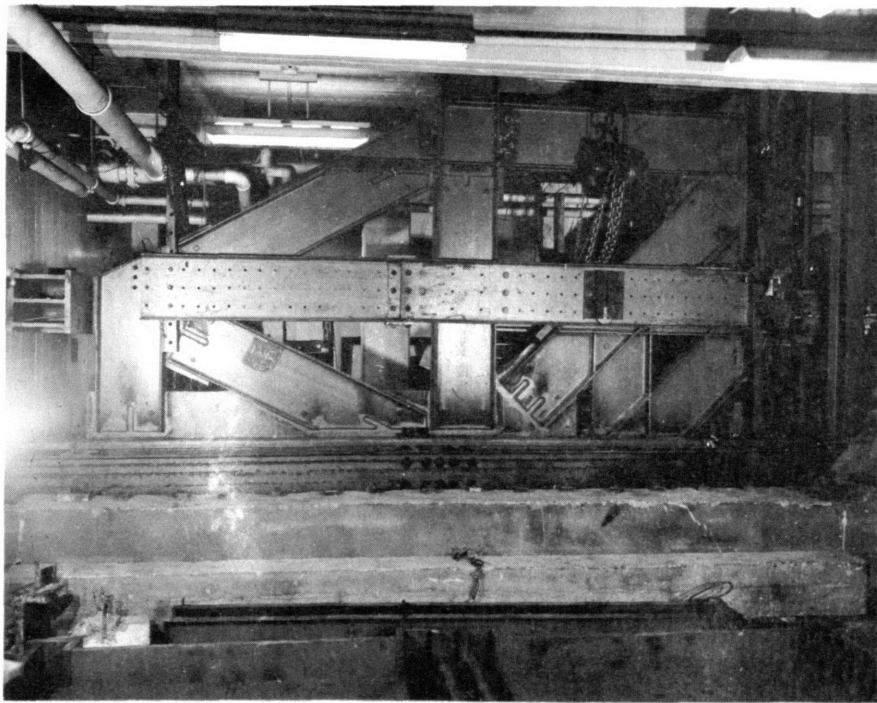


Figure 14 - Side View of Heavy Truss and Lateral Foundation Beam

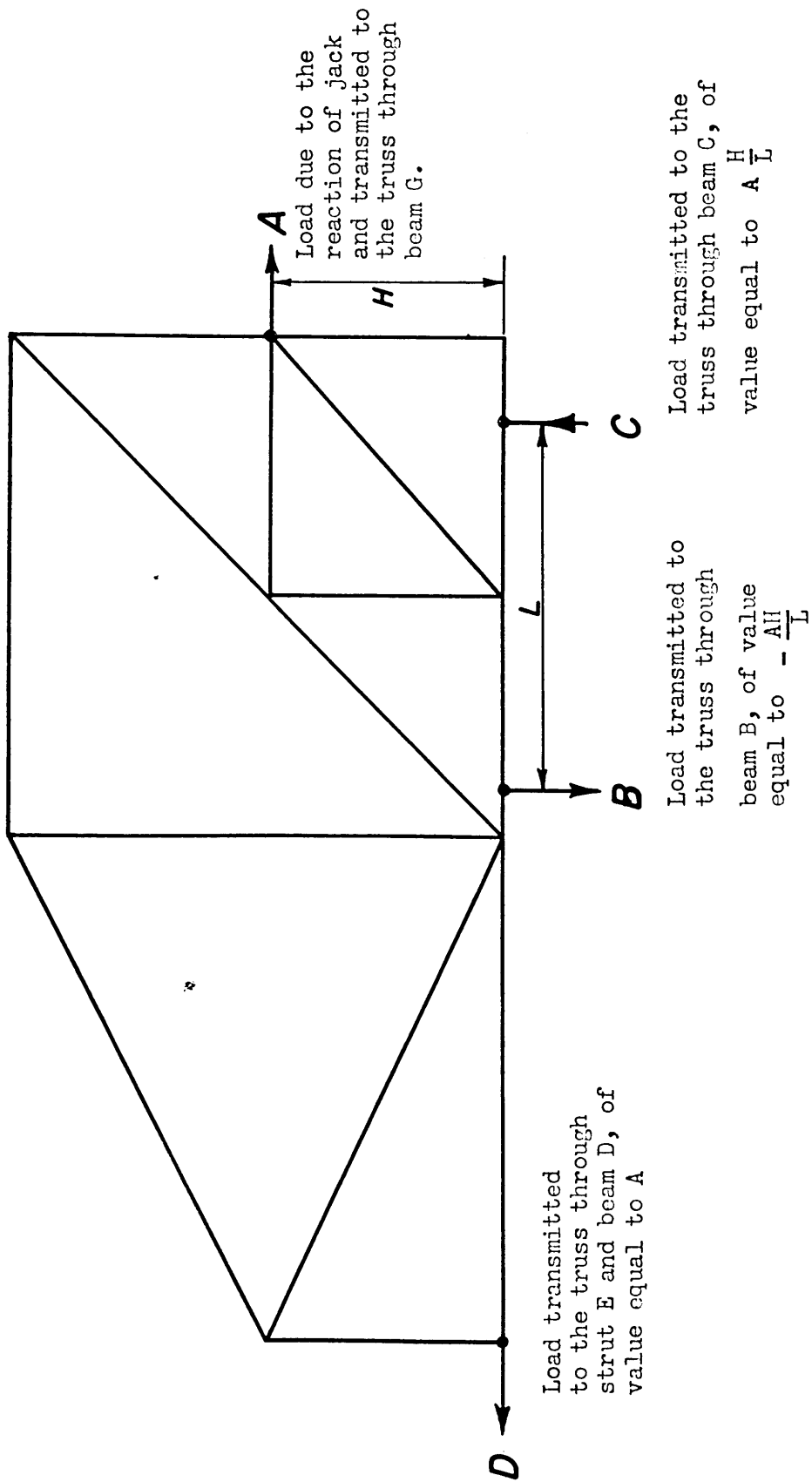


Figure 15 - Loads Acting on Trusses

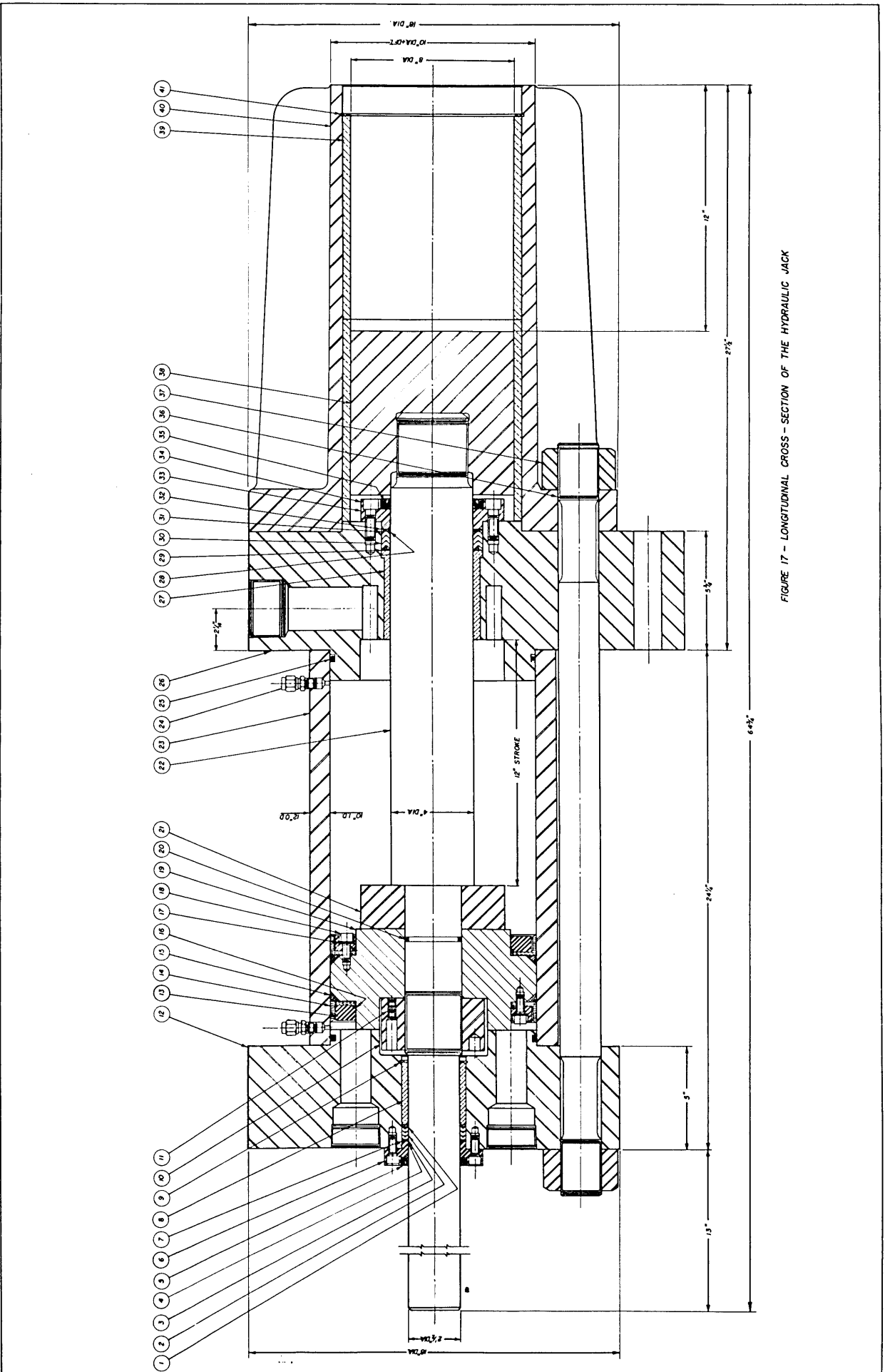


FIGURE 17 - LONGITUDINAL CROSS - SECTION OF THE HYDRAULIC JACK

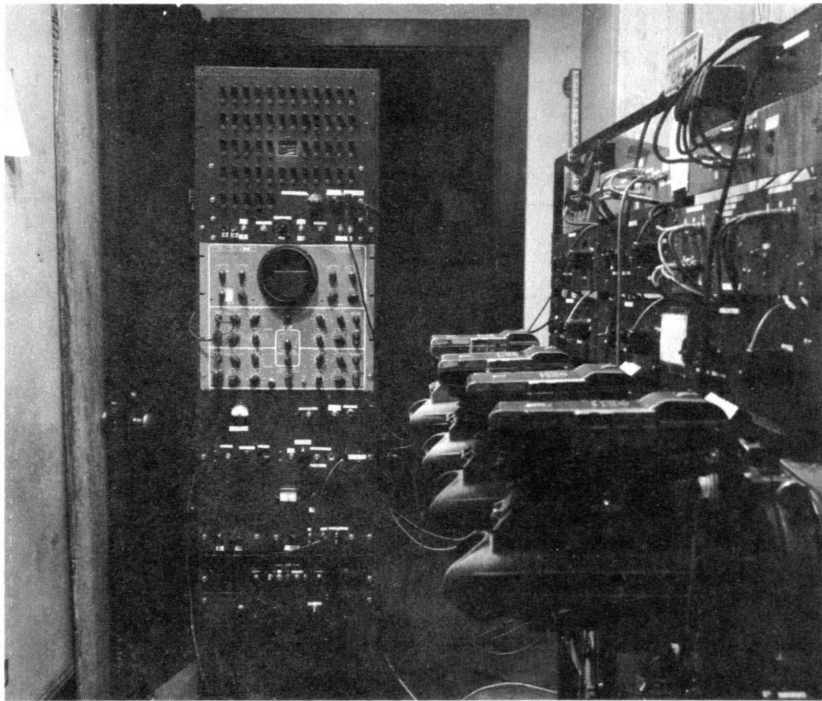


Figure 19 - View of Control Panel of the Function Generator

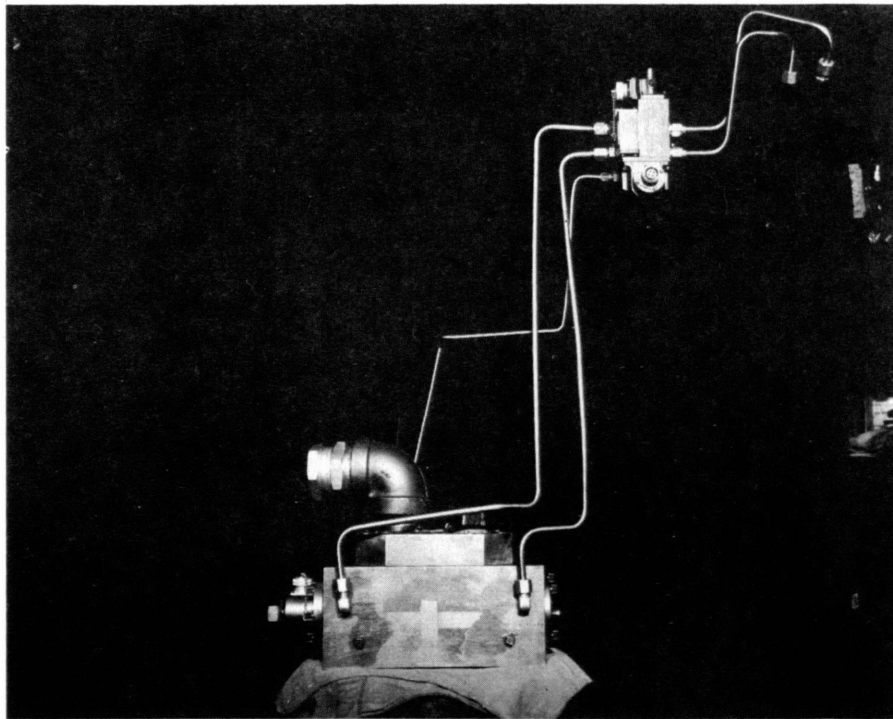


Figure 20 - View of the Servo and Dump Valves

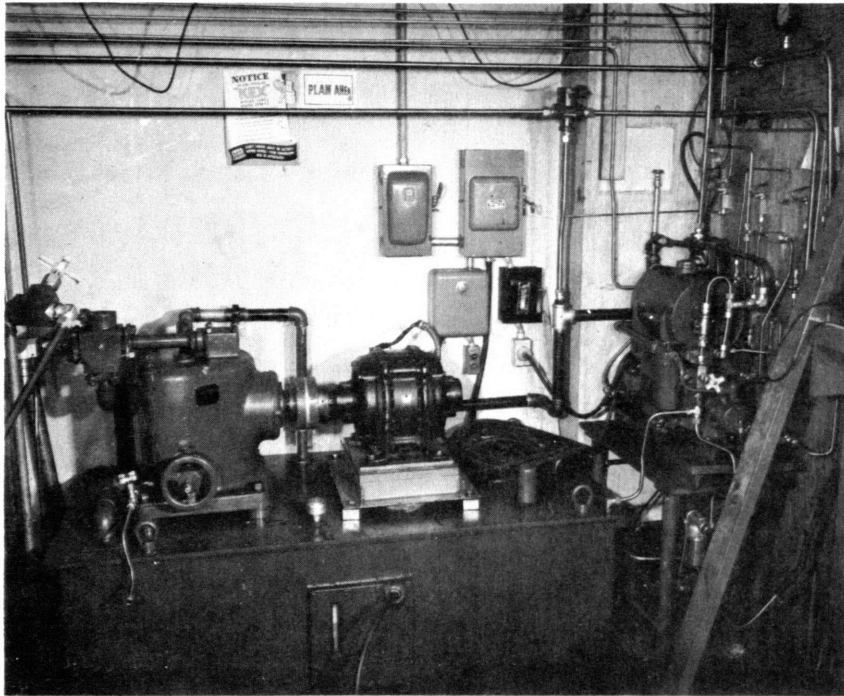


Figure 21 - General View of Pump Setup

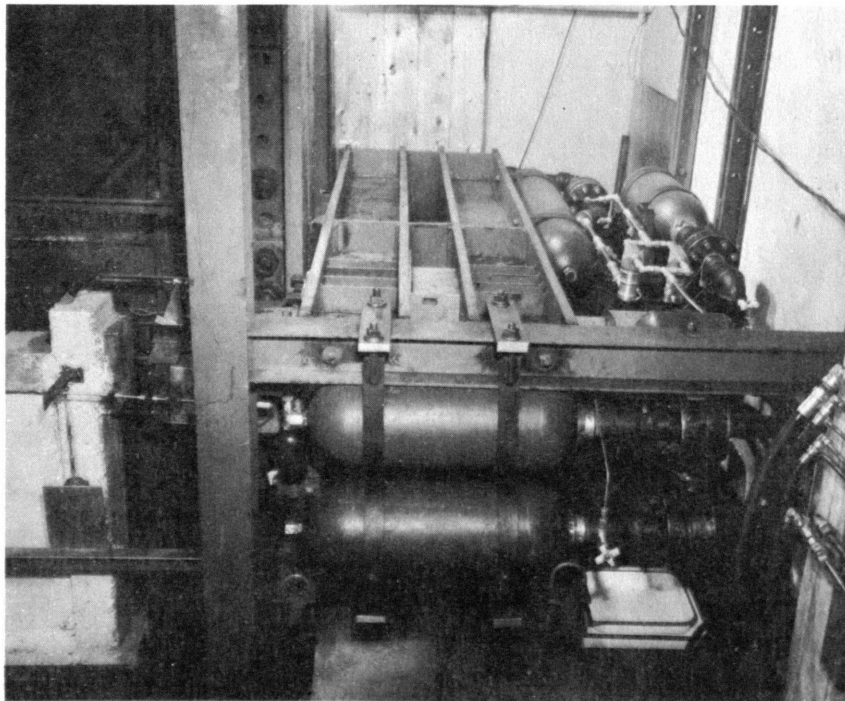


Figure 22 - View of Accumulators in Place



Figure 23 - General View of the Filter Unit

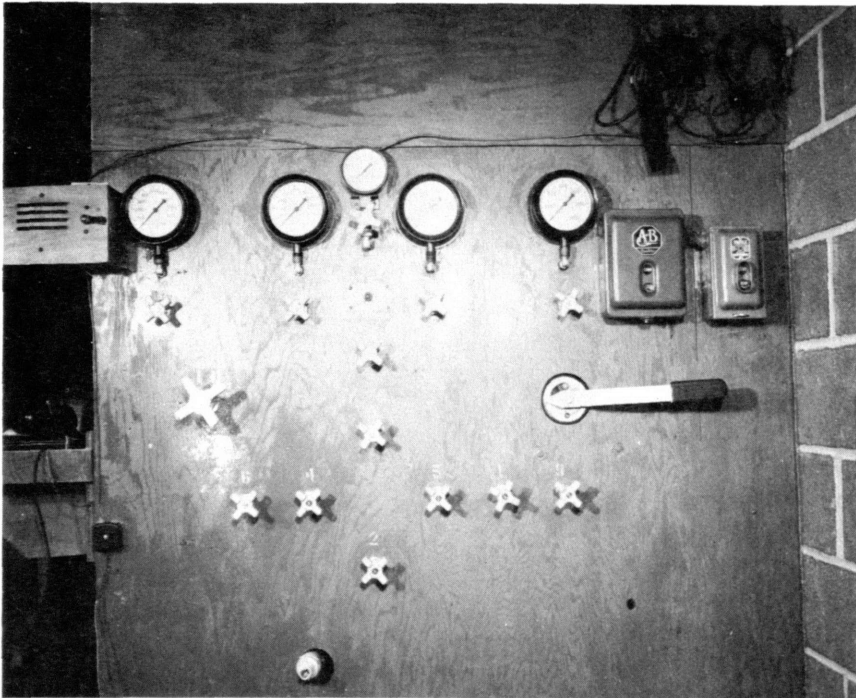


Figure 24 - View of Control Panel of the Pressurizing System

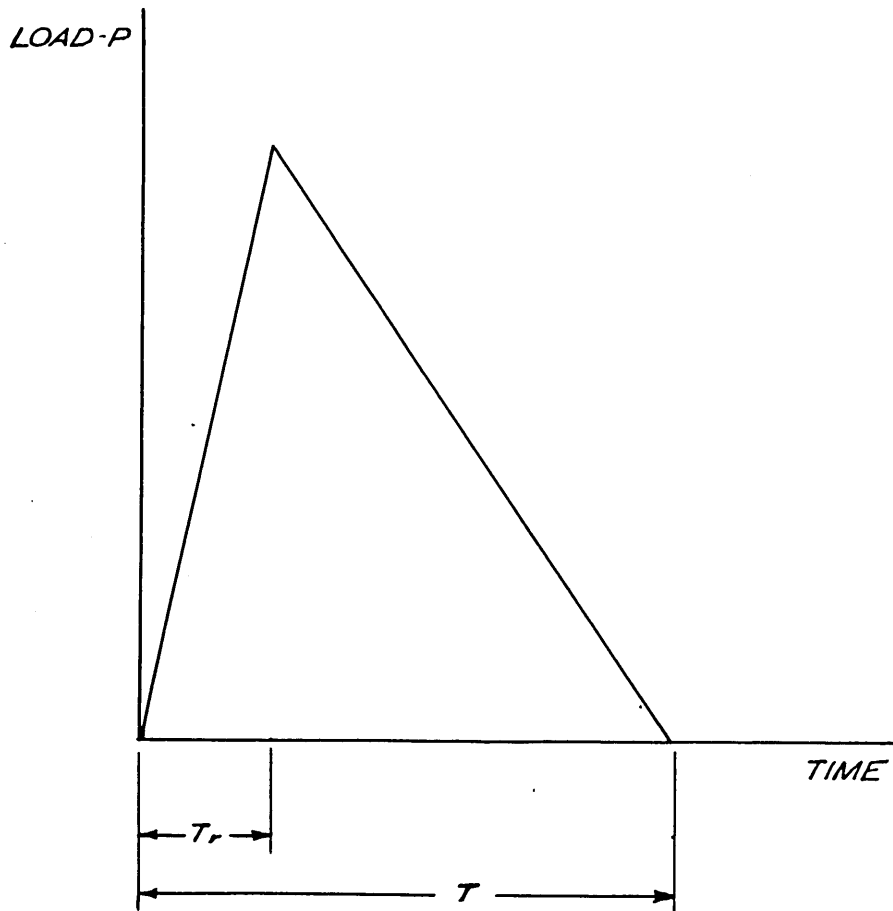


Figure 27 - Load-Time Function

TRANSDUCER FOR LOAD AND DISPLACEMENT	TYPE OF STRAIN AND OF GAGE NORMALLY EMPLOYED	SENSING CIRCUIT FOR TRANSFORMING RESISTANCE CHANGES INTO VOLT. CHANGES	SUPPLY VOLTAGE FOR SENSING CIRCUIT - 45 V. - D.C.	OSCILLATOR SUPPLY VOLTAGE 6 V. 500 ~ A.C.	MASTER SELECTOR CONTROL SWITCH	INDICATOR DUAL BEAM OSCILLOSCOPE	RECORDER CAMERA
--------------------------------------	--	--	---	---	--------------------------------	----------------------------------	-----------------

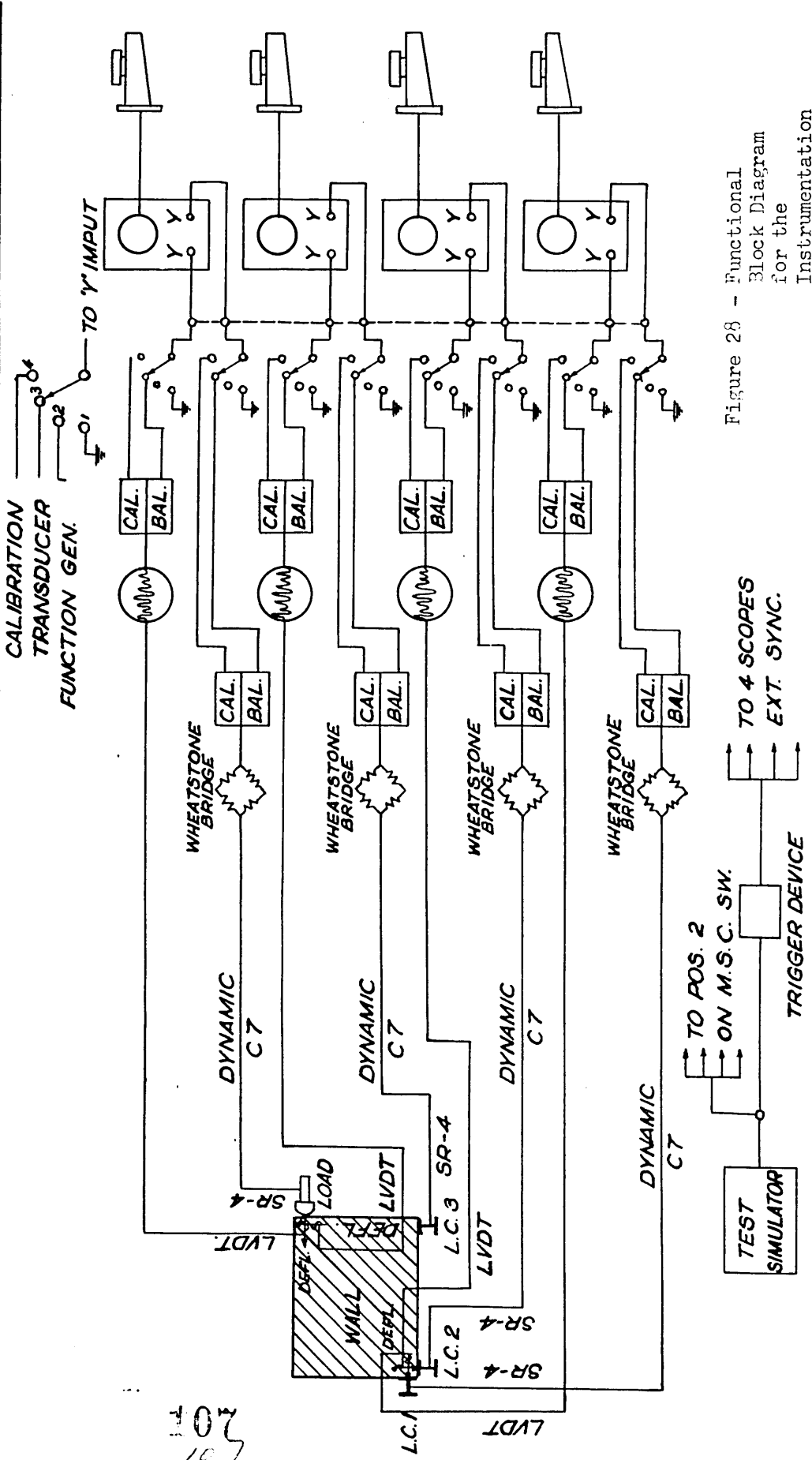


Figure 28 - Functional Block Diagram for the Instrumentation

201

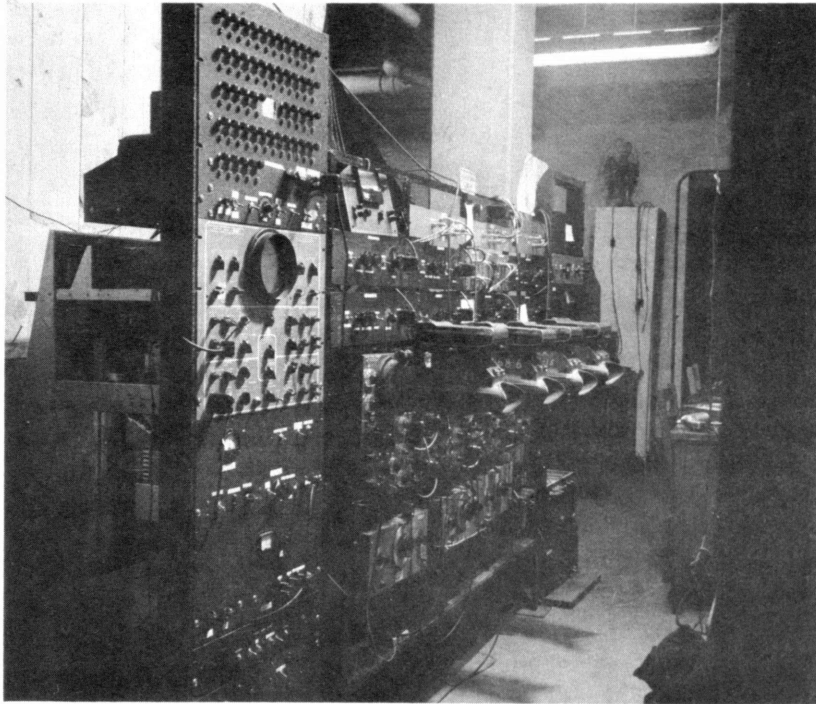


Figure 29 - General View of Instruments

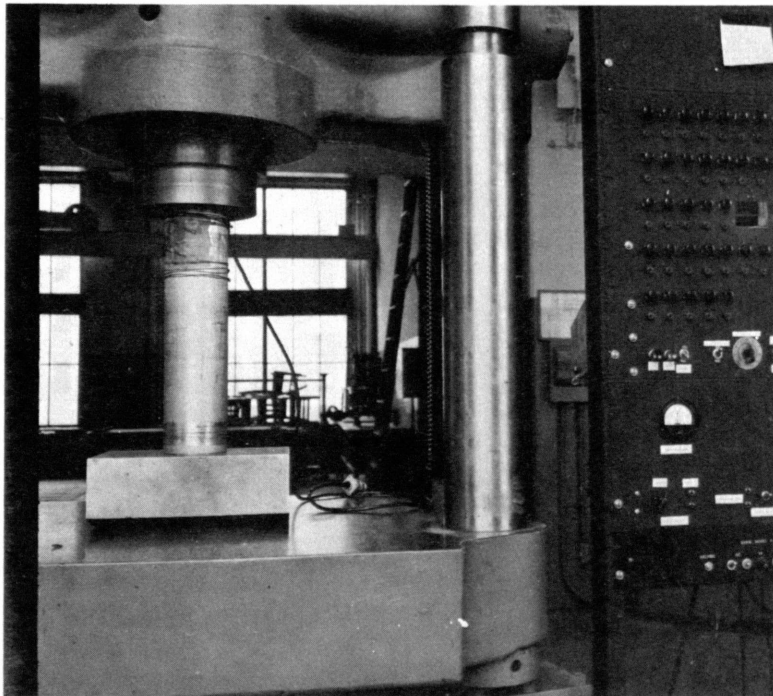


Figure 32 - Calibration of Ram Load Cell

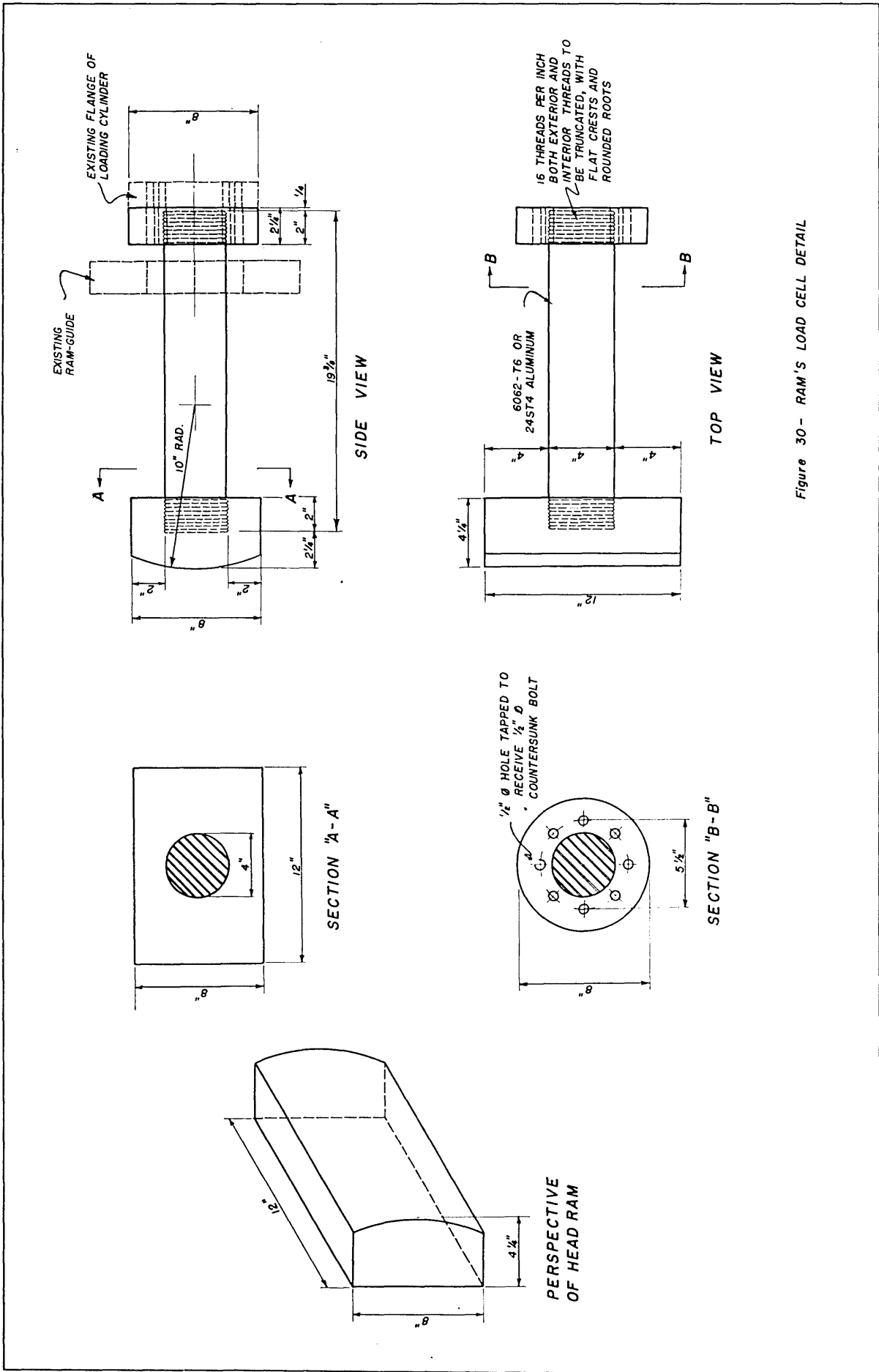


Figure 30 - RAM'S LOAD CELL DETAIL

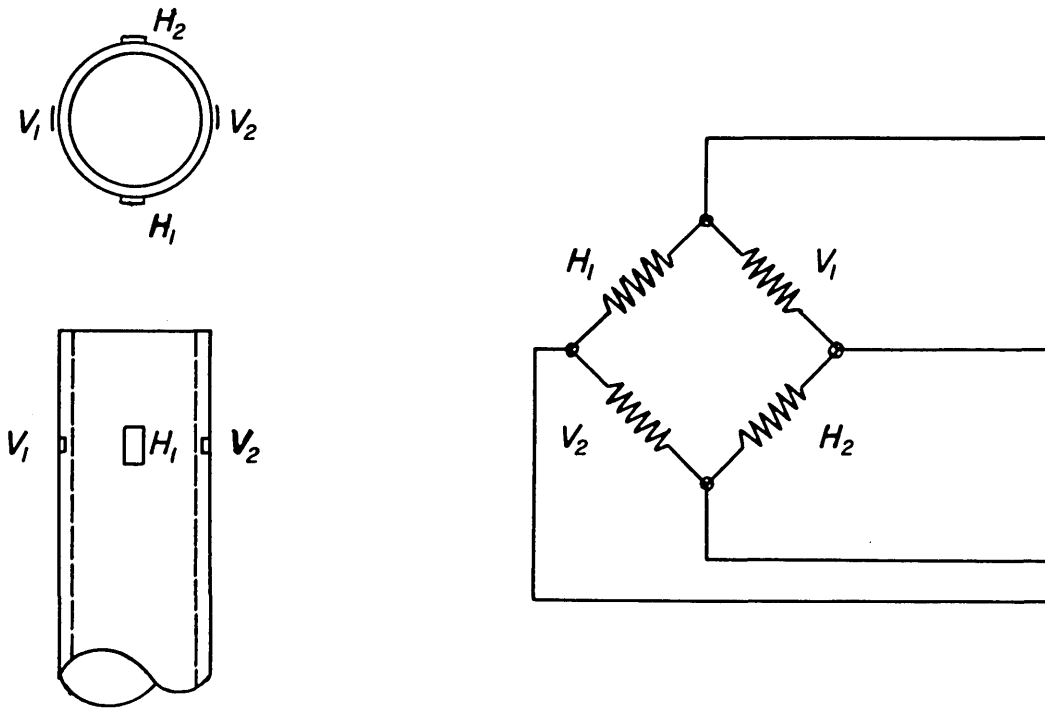


Figure 31-(a)

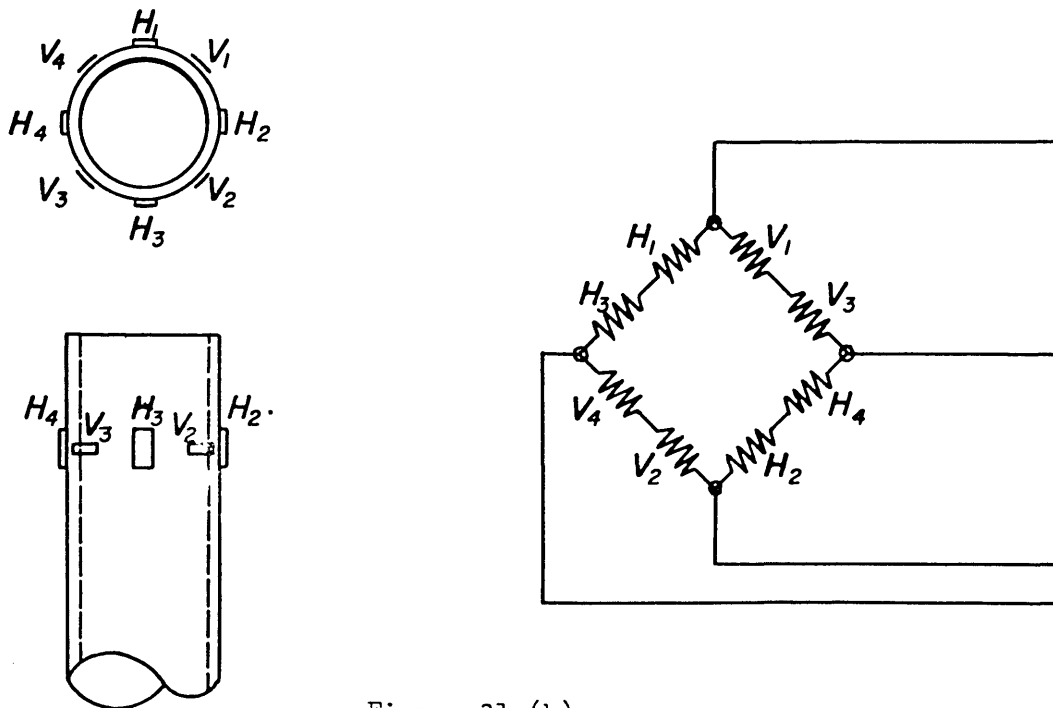
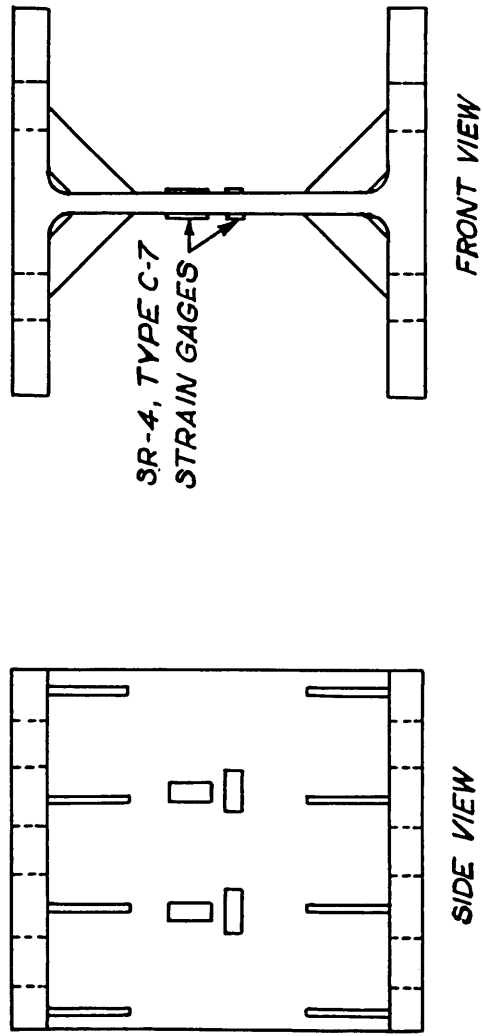


Figure 31-(b)

Figure 31 - Gage arrangement and circuits for ram load cell



WF 8 - 48

Figure 33 - Gage Arrangement for Reaction-Load Cell

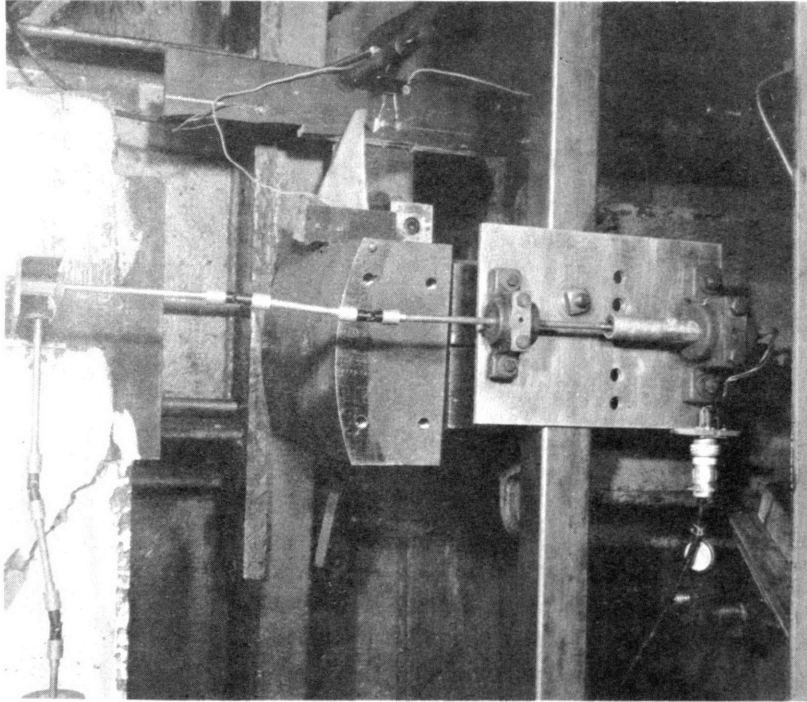


Figure 34 - View of the Device used to Connect the L.V.D.T. with the Specimen

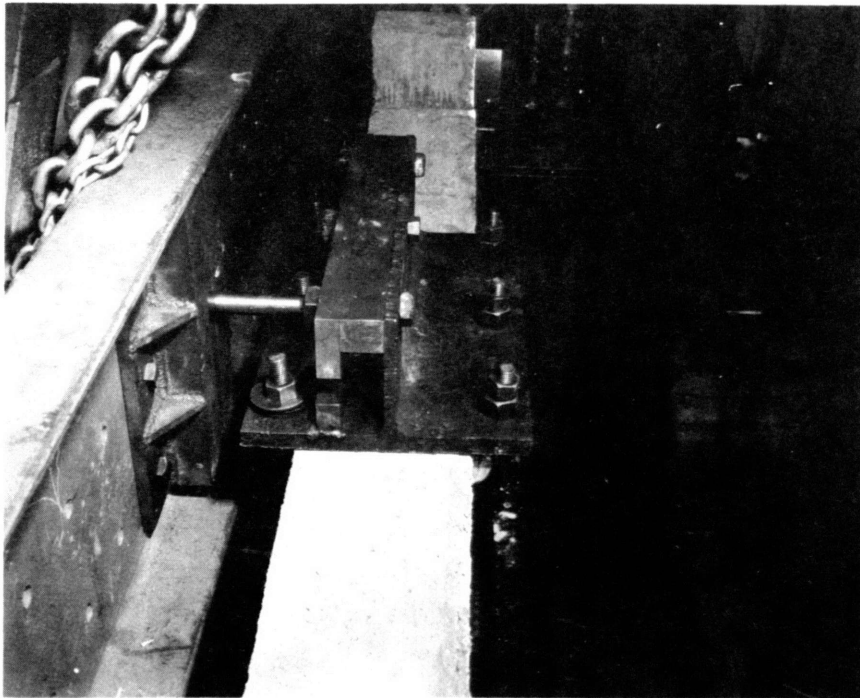


Figure 35 - View of the Lateral Restraint System

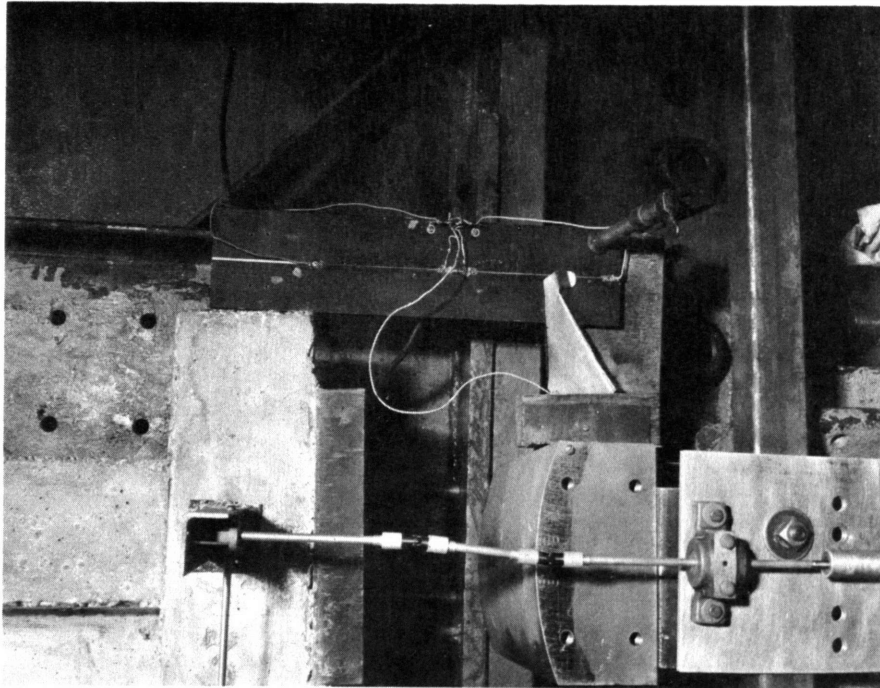


Figure 37 - View of Indicator of the Ram Head Position

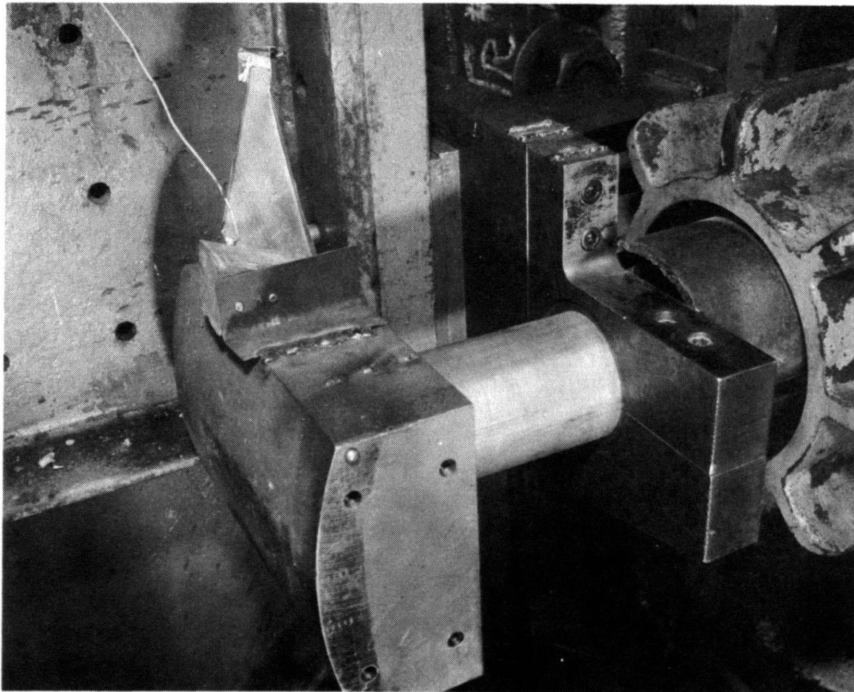
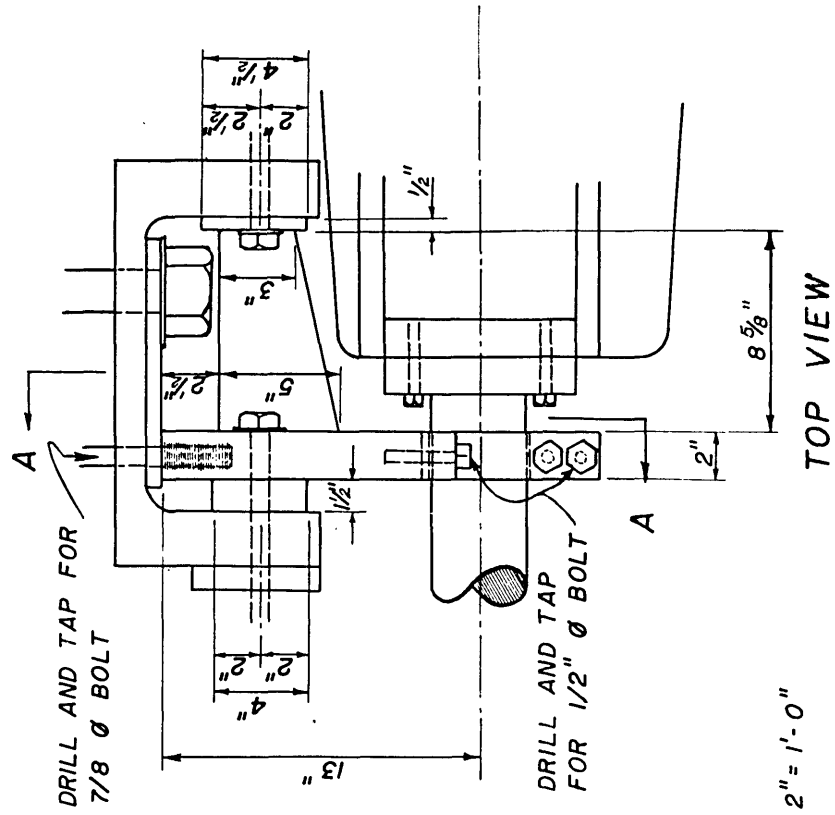
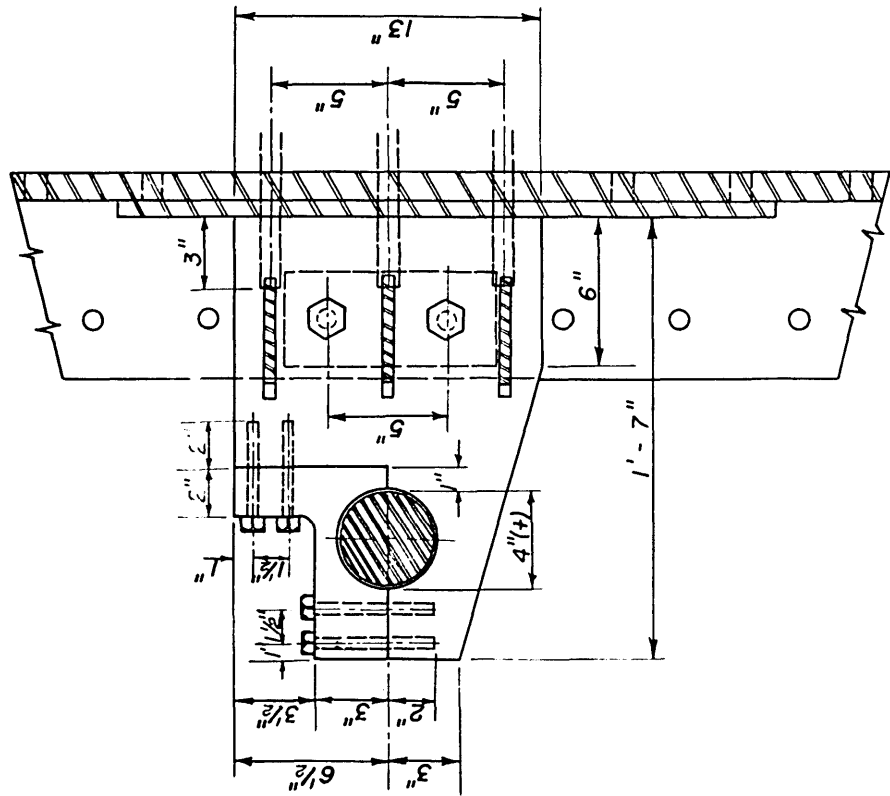


Figure 38 - View of the Guide for the Ram



SCALE: 2" = 1'-0"

Figure 39 - RAM GUIDE DETAIL

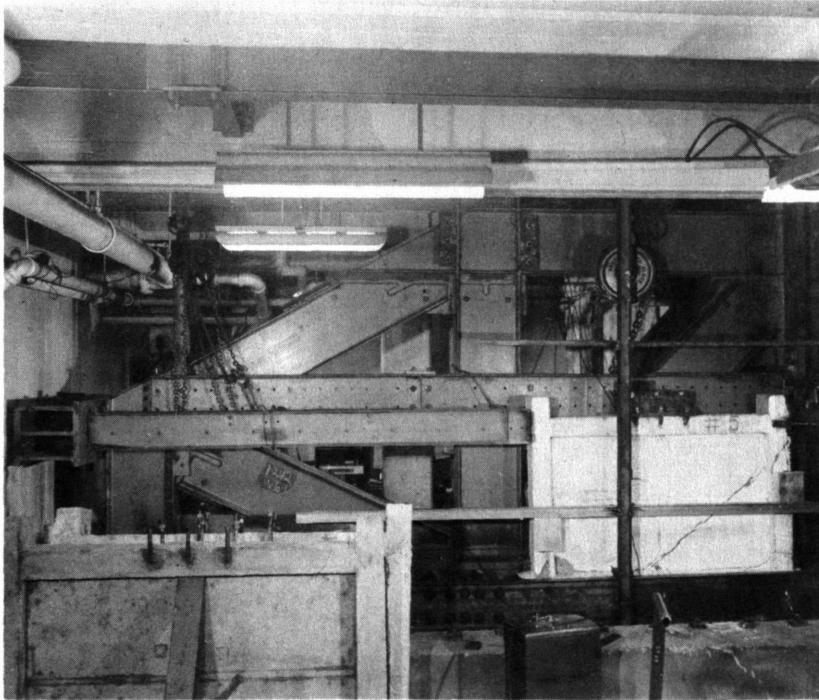


Figure 40 - View of the Restraining Strut

115.

116

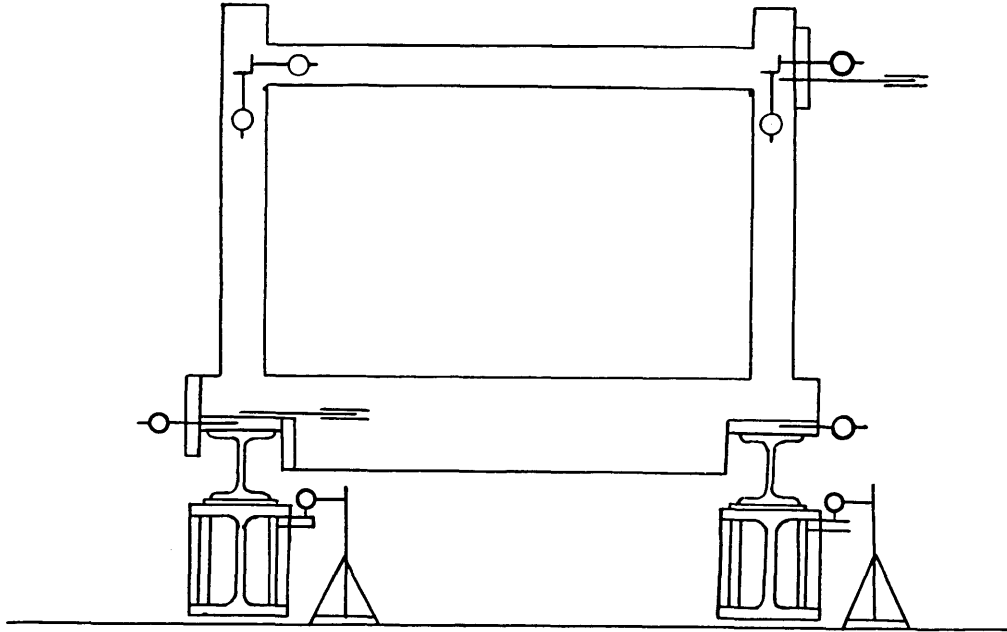


Figure 42 - Arrangement of Gages for Measuring Deflections Under Static Load

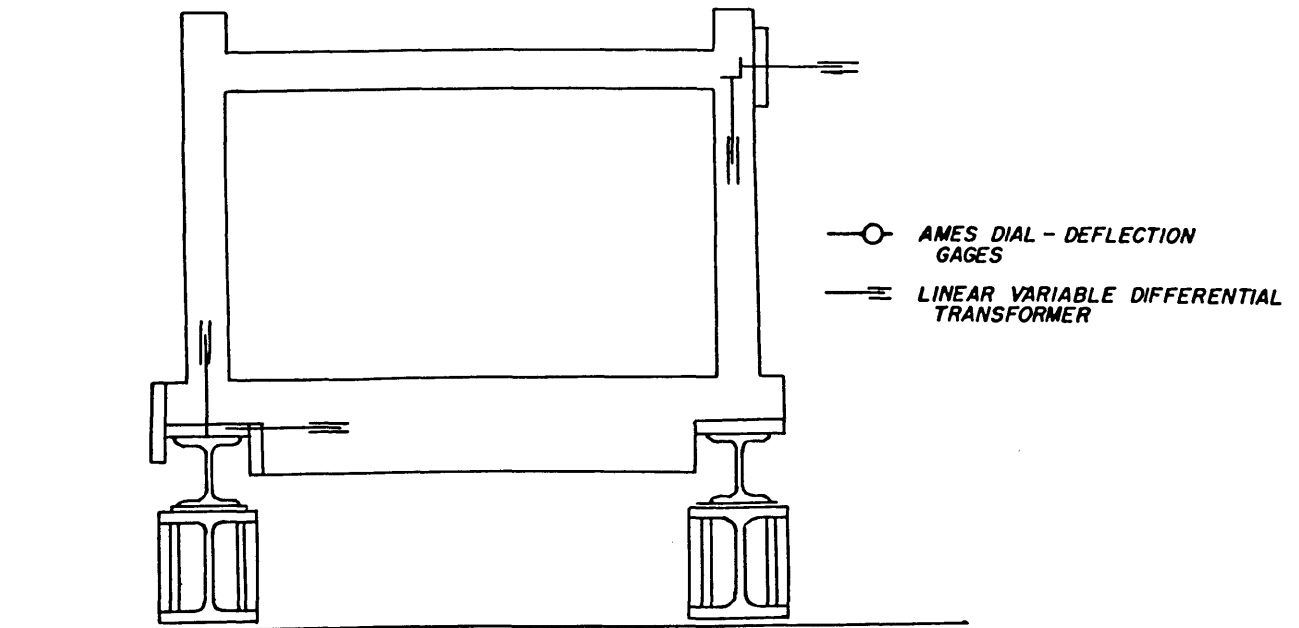


Figure 43 - Arrangement of Gages for Measuring Deflections Under Dynamic Load

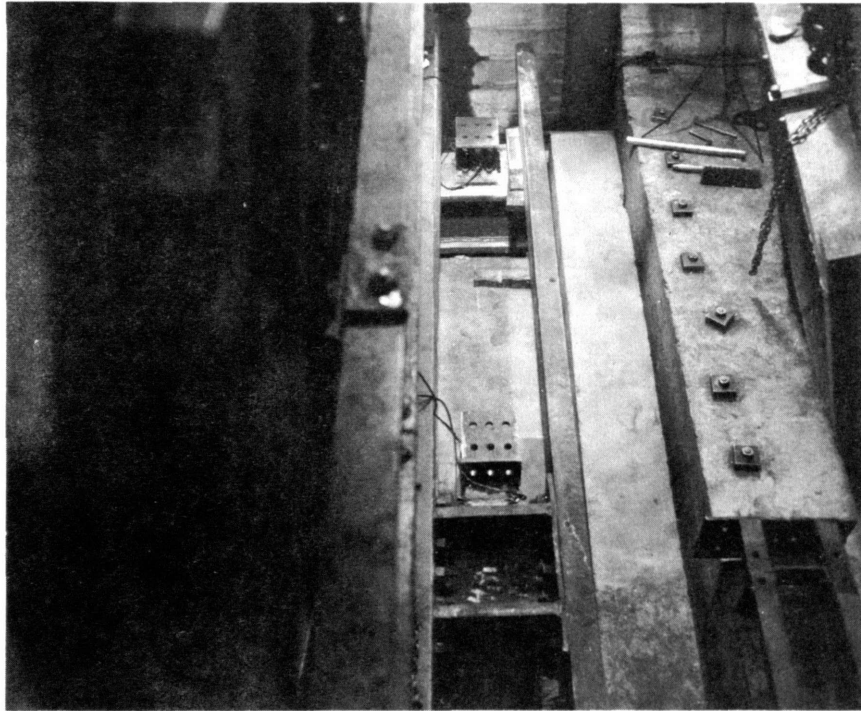


Figure 44 - Setup of Load Cells for Reactions

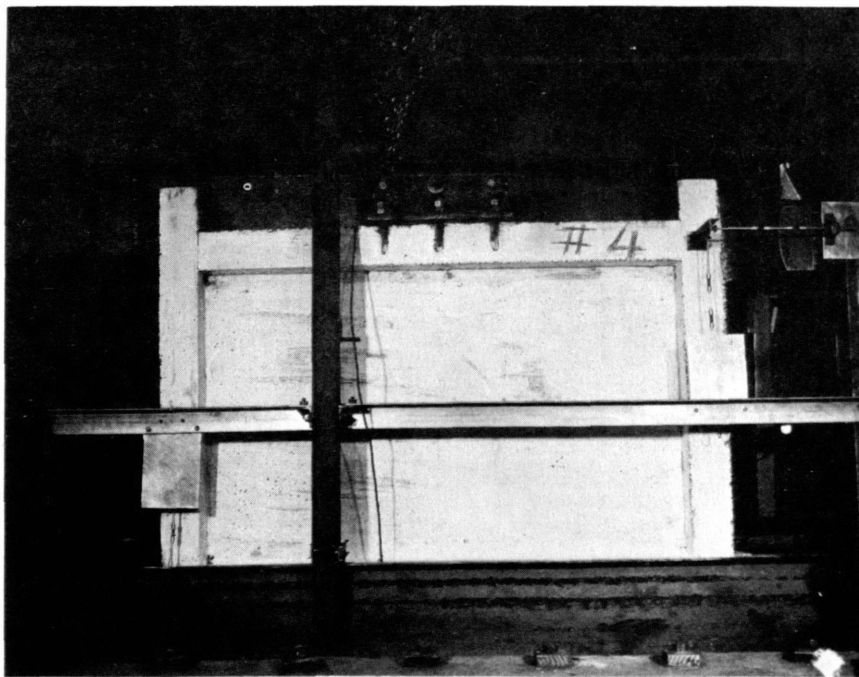


Figure 45 - A Typical Wall Ready for Testing

LOAD
(Kips)

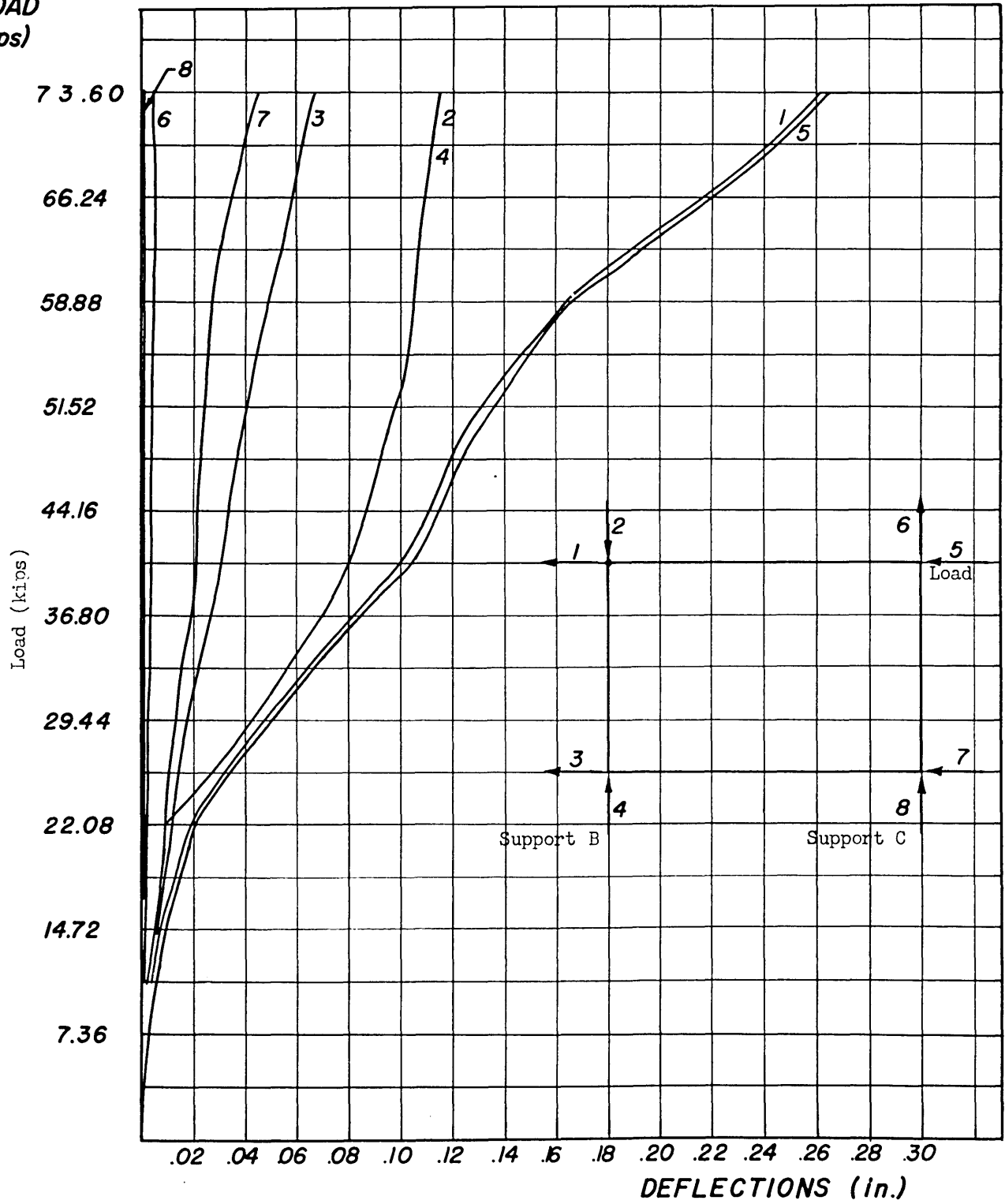


Figure 46 - Load-Deflection Curves for Wall #1 (Static Test)

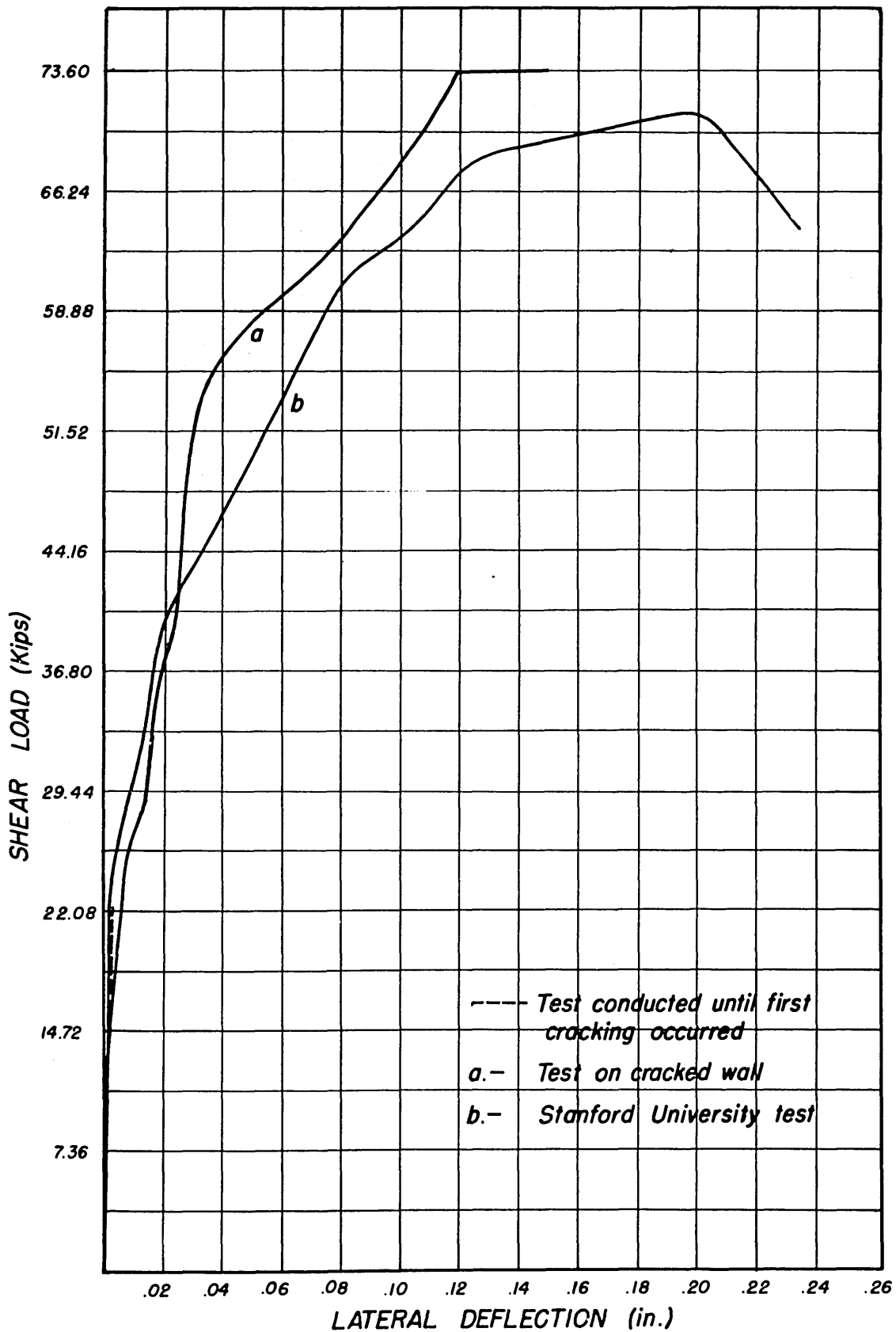


Figure 47 - Lateral Deflection of the Top of the Wall with Respect to the Supports (Wall #1 - Static Test)

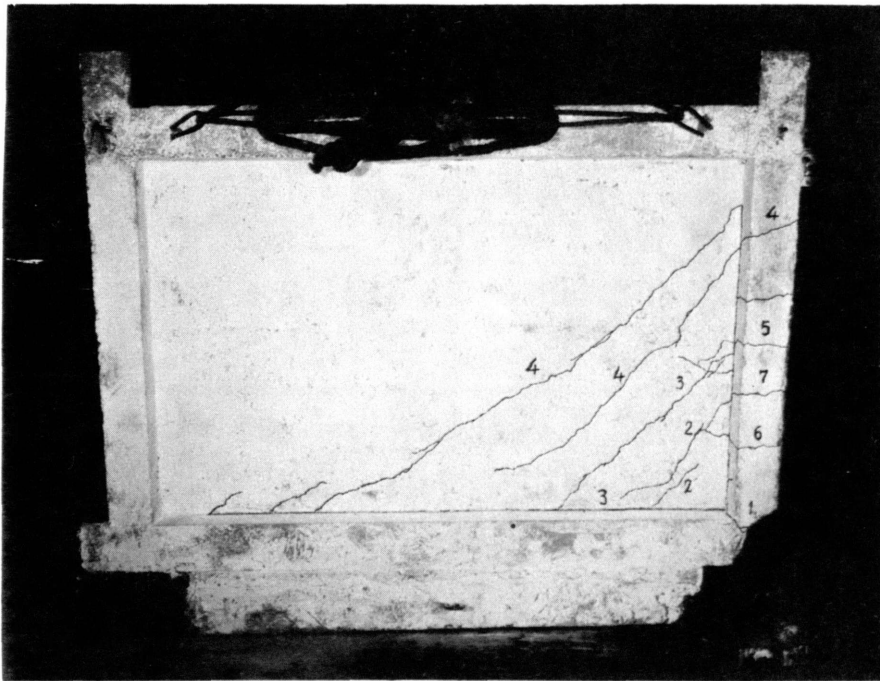
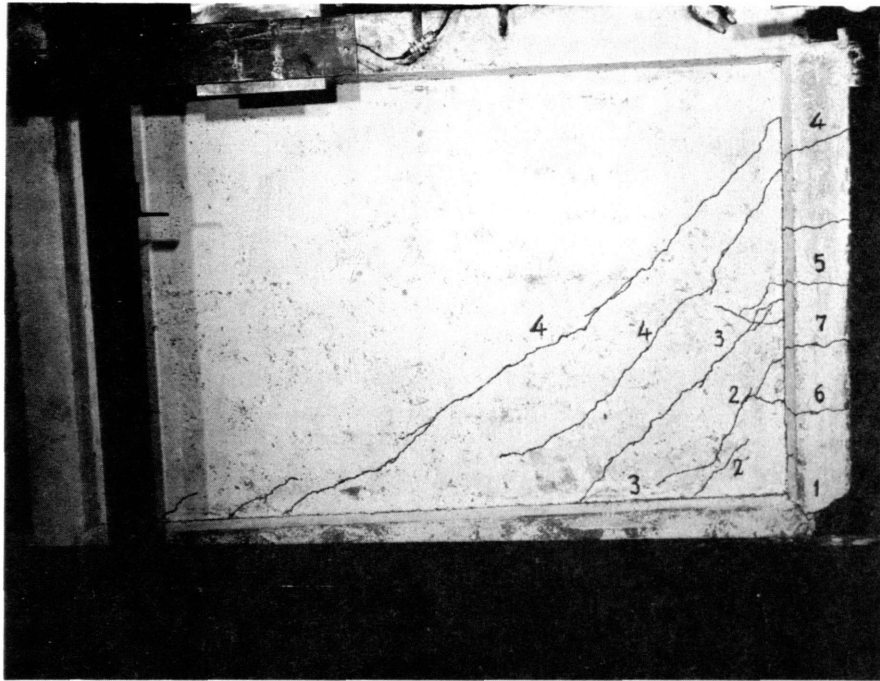
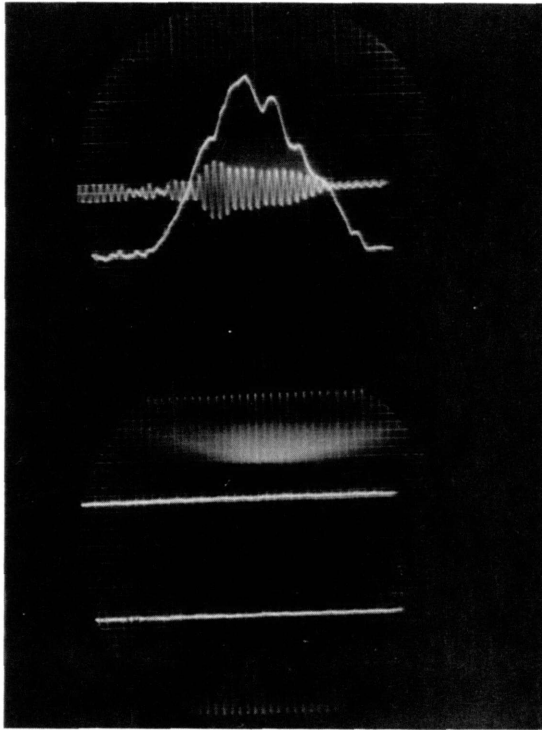
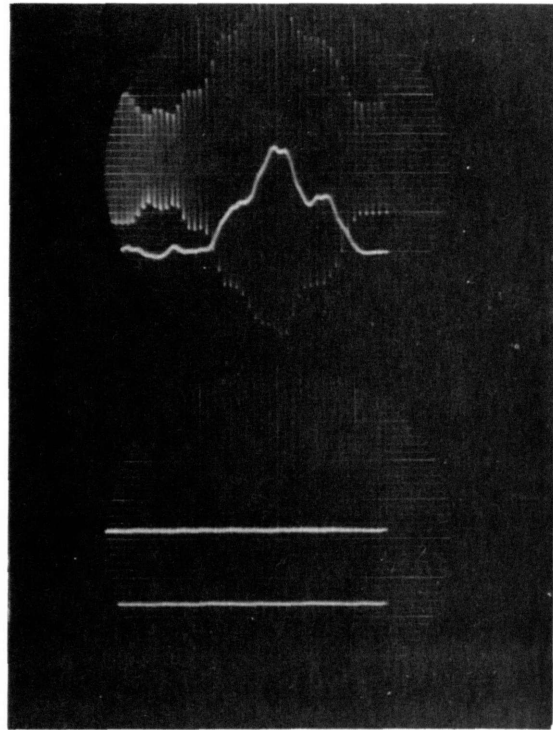


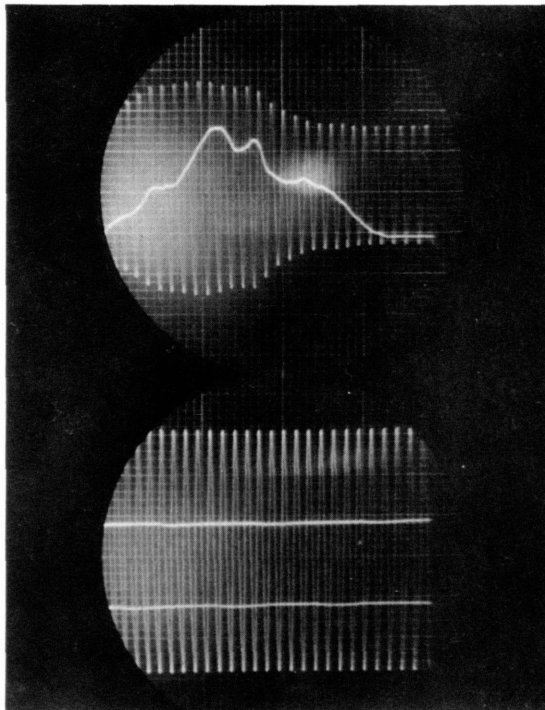
Figure 48 - STATIC TEST -
Final Condition of Wall #1



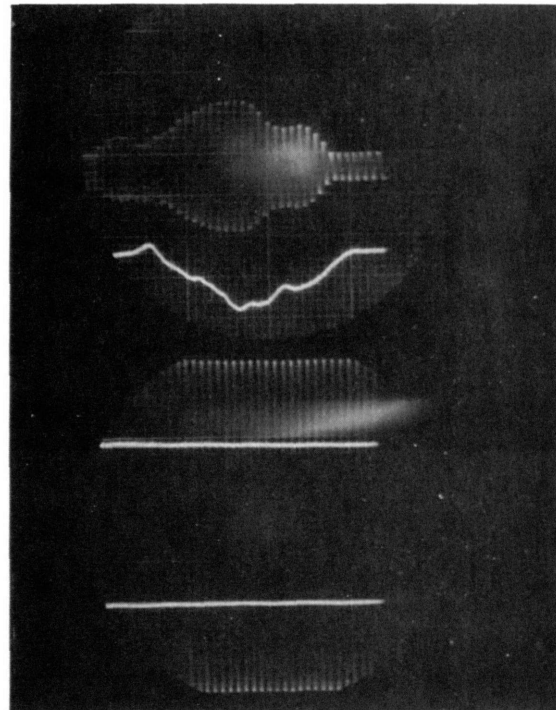
A



B



C



D

Figure 49 - Example of a Complete Record of a Test
(Test 6 on Wall #4)

A- Load and vertical deflection at loading point

B- Horizontal reaction and horizontal deflec. at loading pt.

C-vertical reaction at support C and vert. defl. at support B

D-vertical reaction at support B and horiz. deflec. at support B

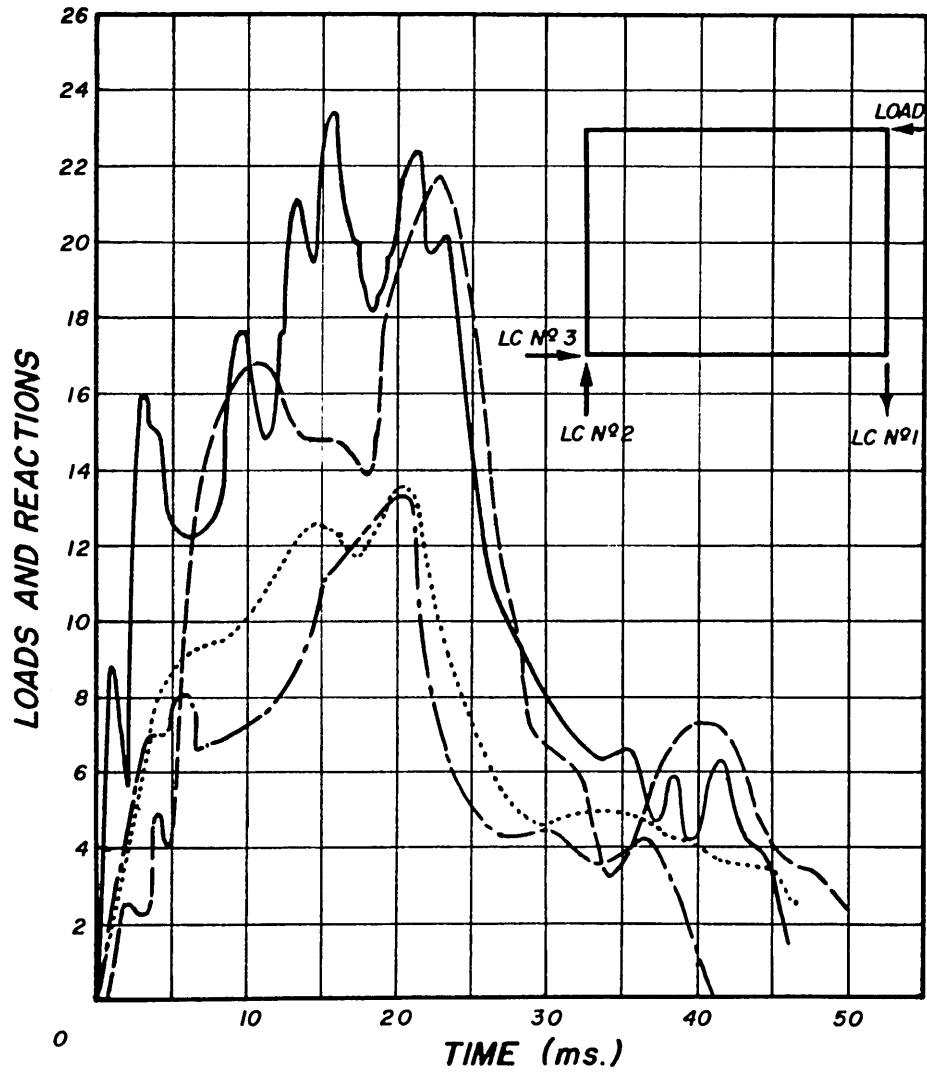


Figure 50 - Observed Load and Reactions vs Time
for Test No. 2 on Wall #2

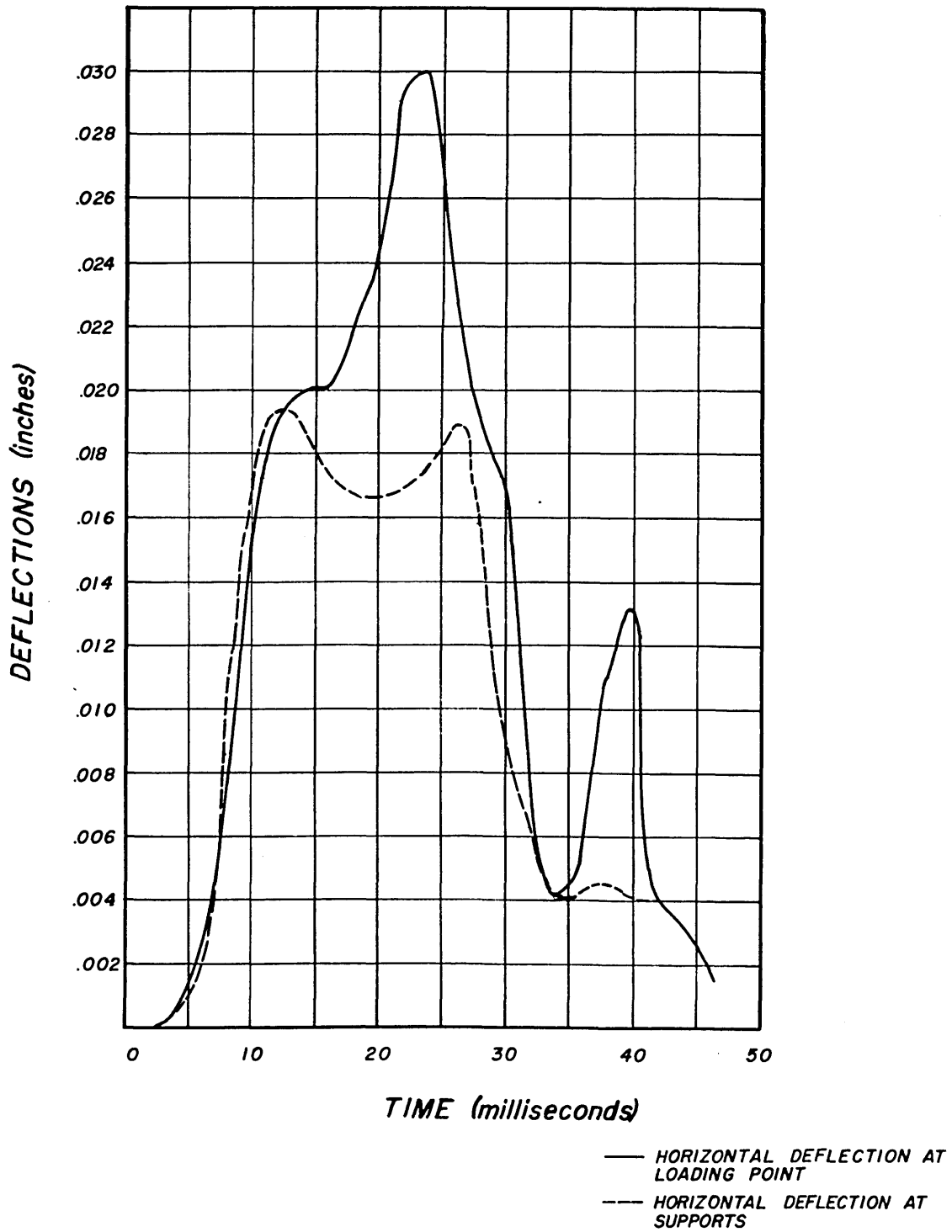


Figure 51 - Observed Deflections vs Time for Test No. 2 on Wall #2

424
124

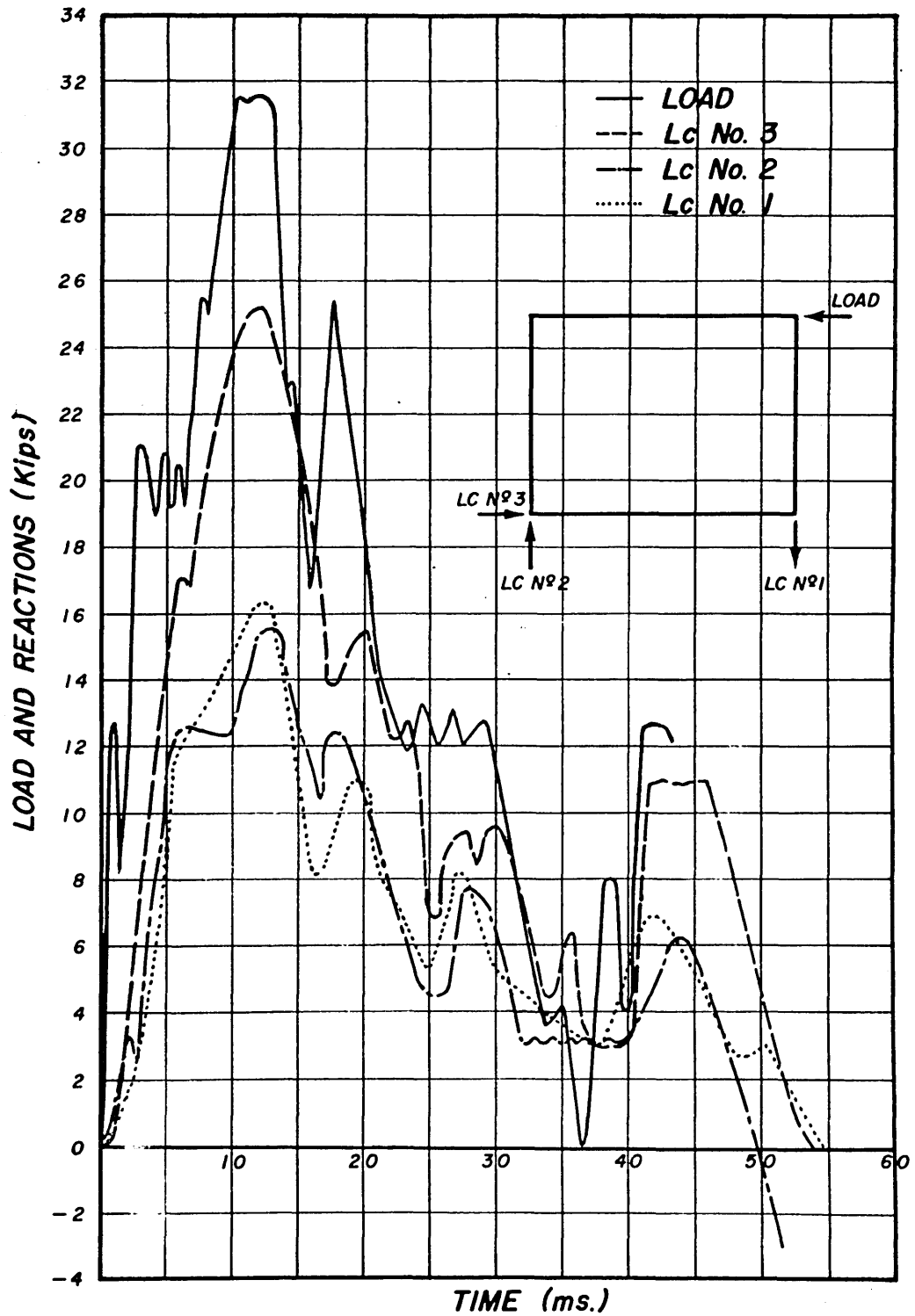


Figure 52 - Observed Load and Reactions vs Time for Test No. 6 on Wall #2

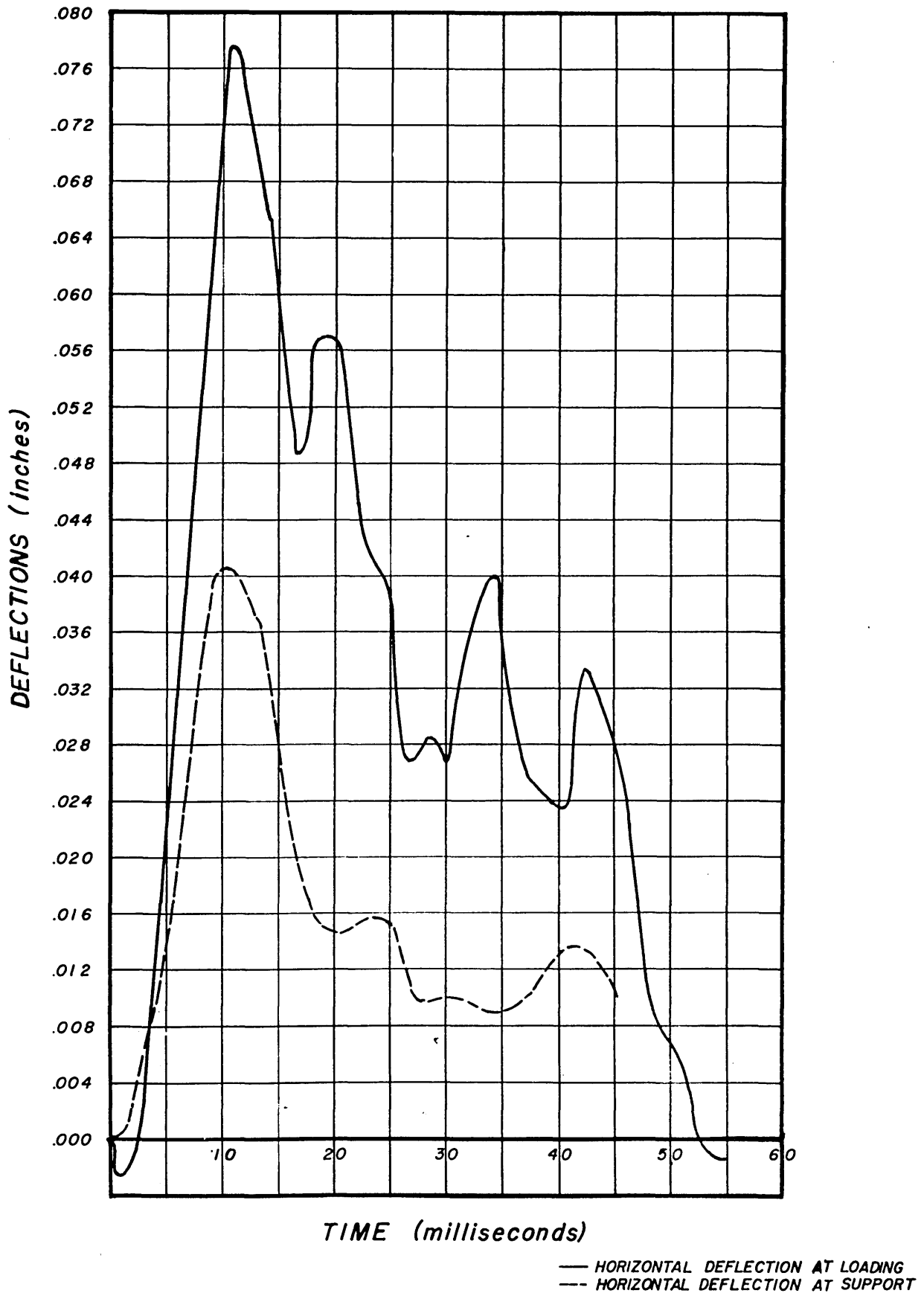


Figure 53 - Observed Deflections vs Time for Test No. 6 on Wall #2

126

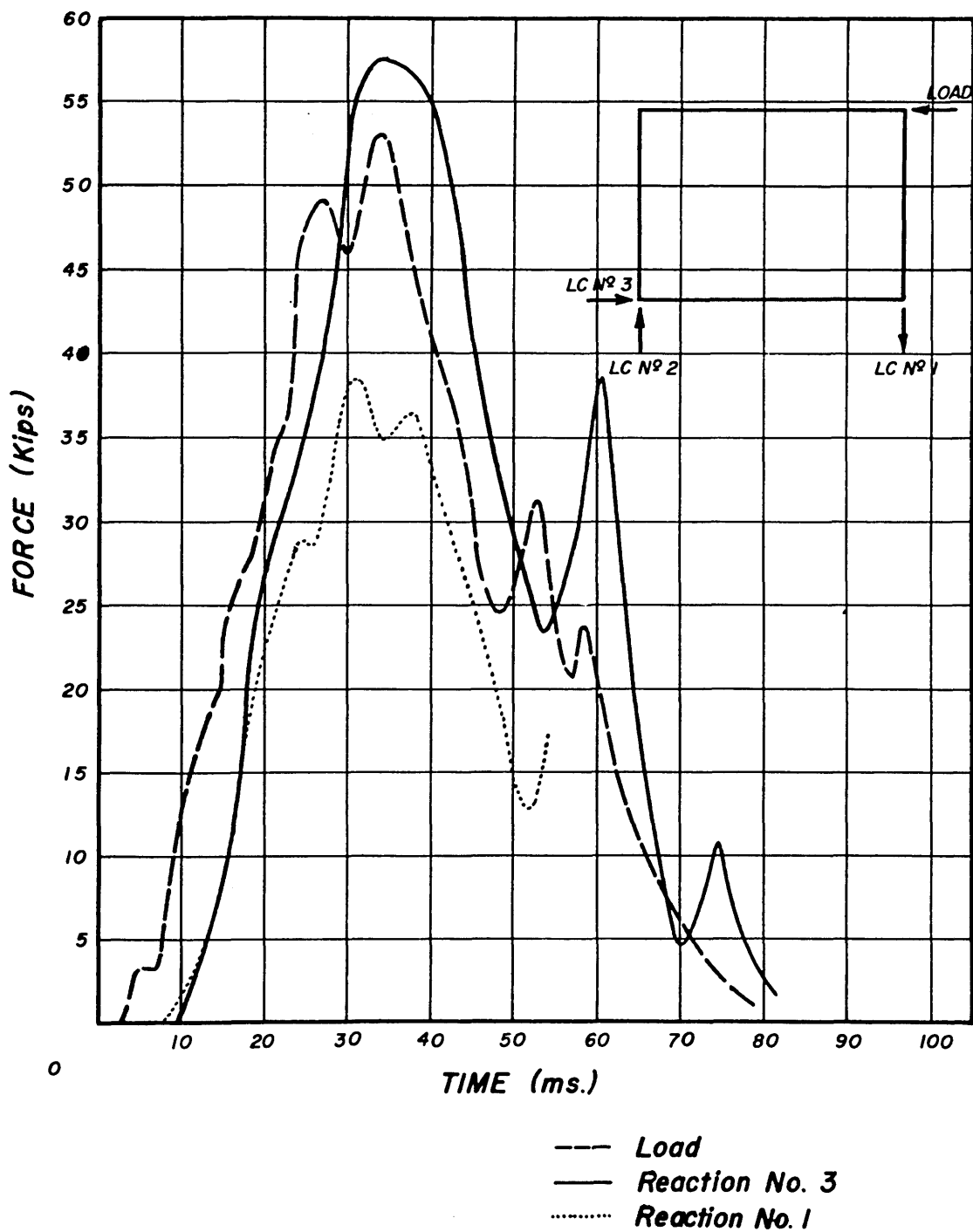


Figure 54 - Observed Load and Reactions vs Time for Test No. 11 on Wall #2

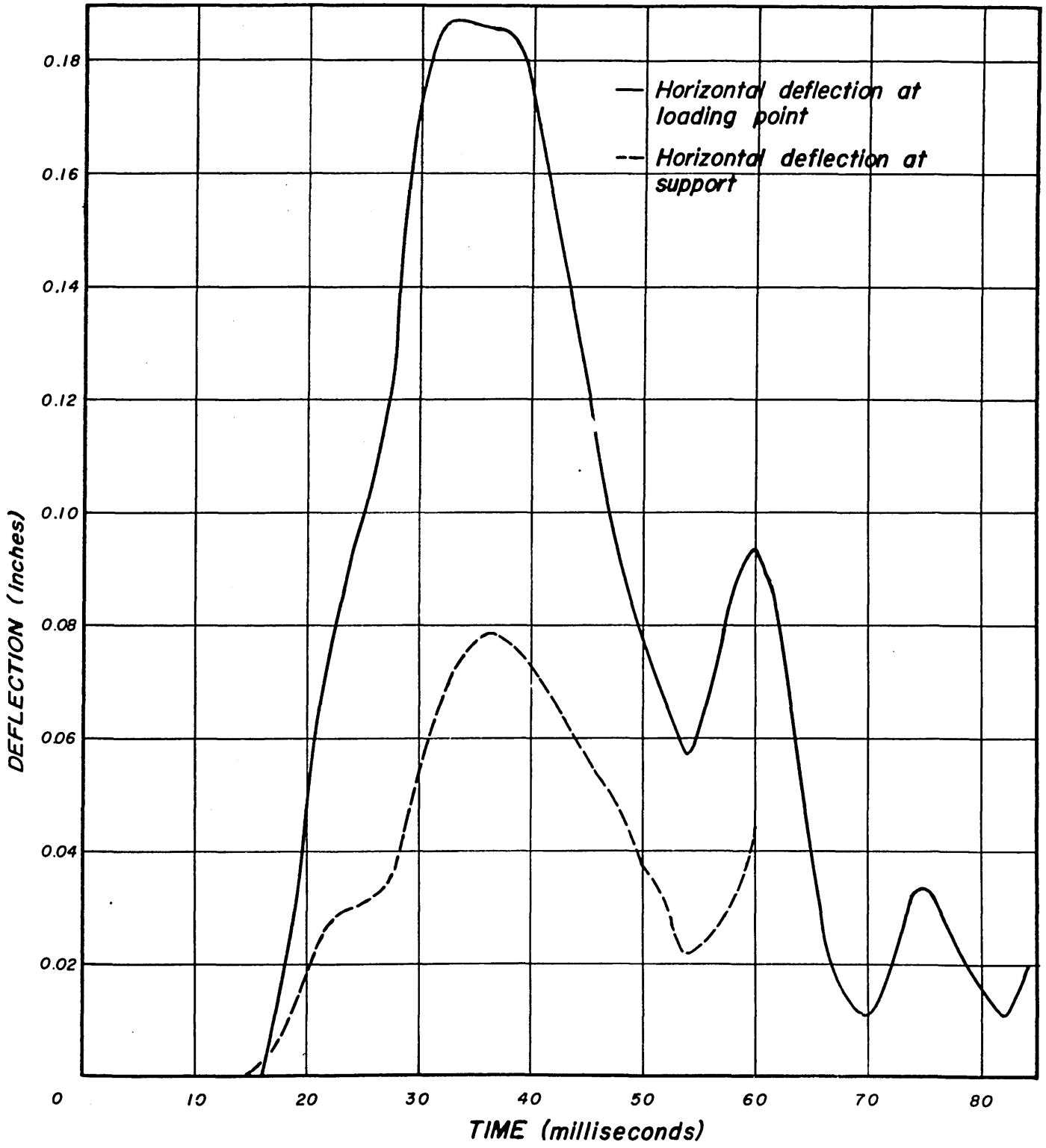


Figure 55 - Observed Deflections vs Time for Test No. 11 on Wall #2

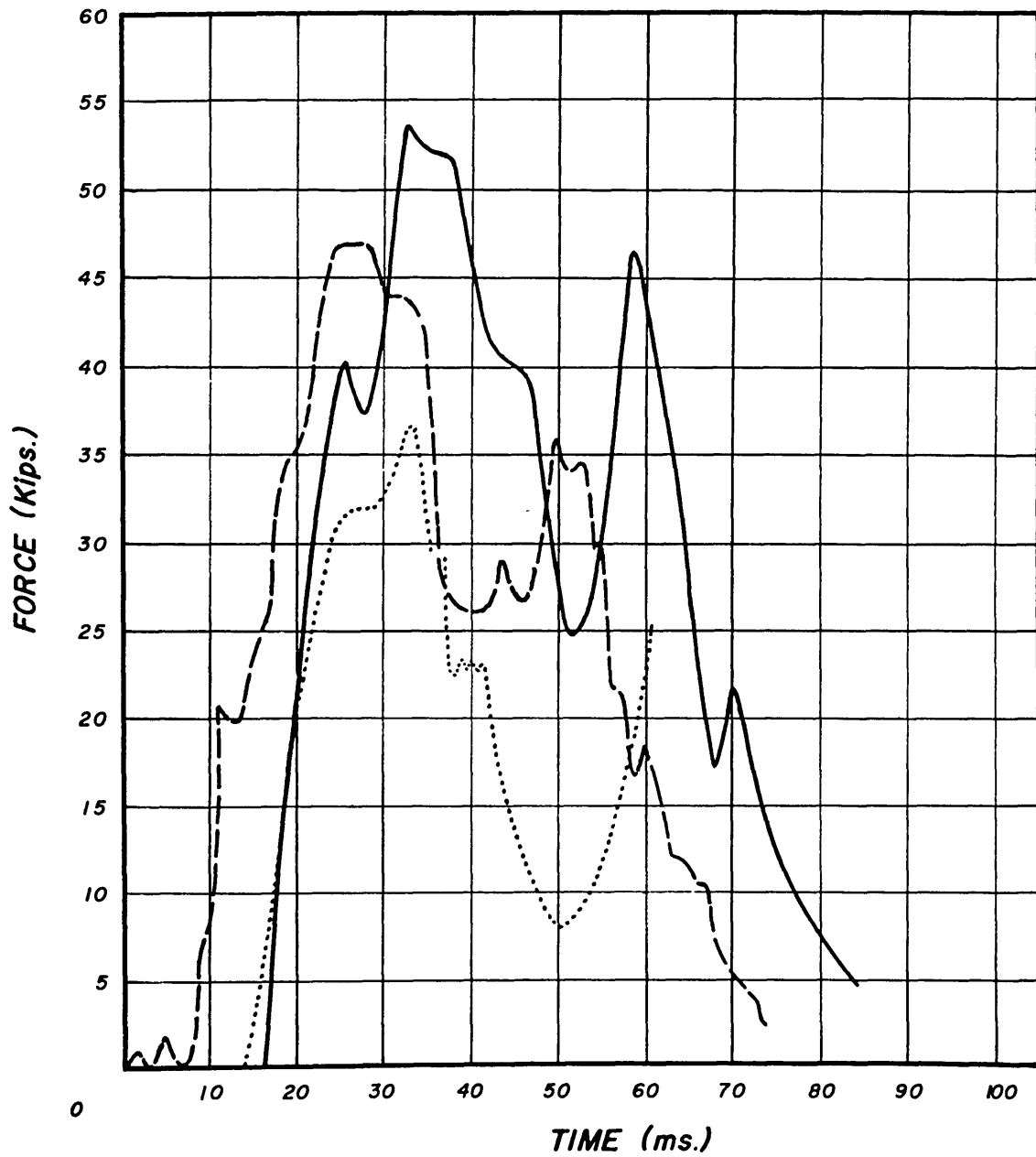


Figure 56 - Observed Loads and Reactions for Test No. 12 on Wall #2

129
129

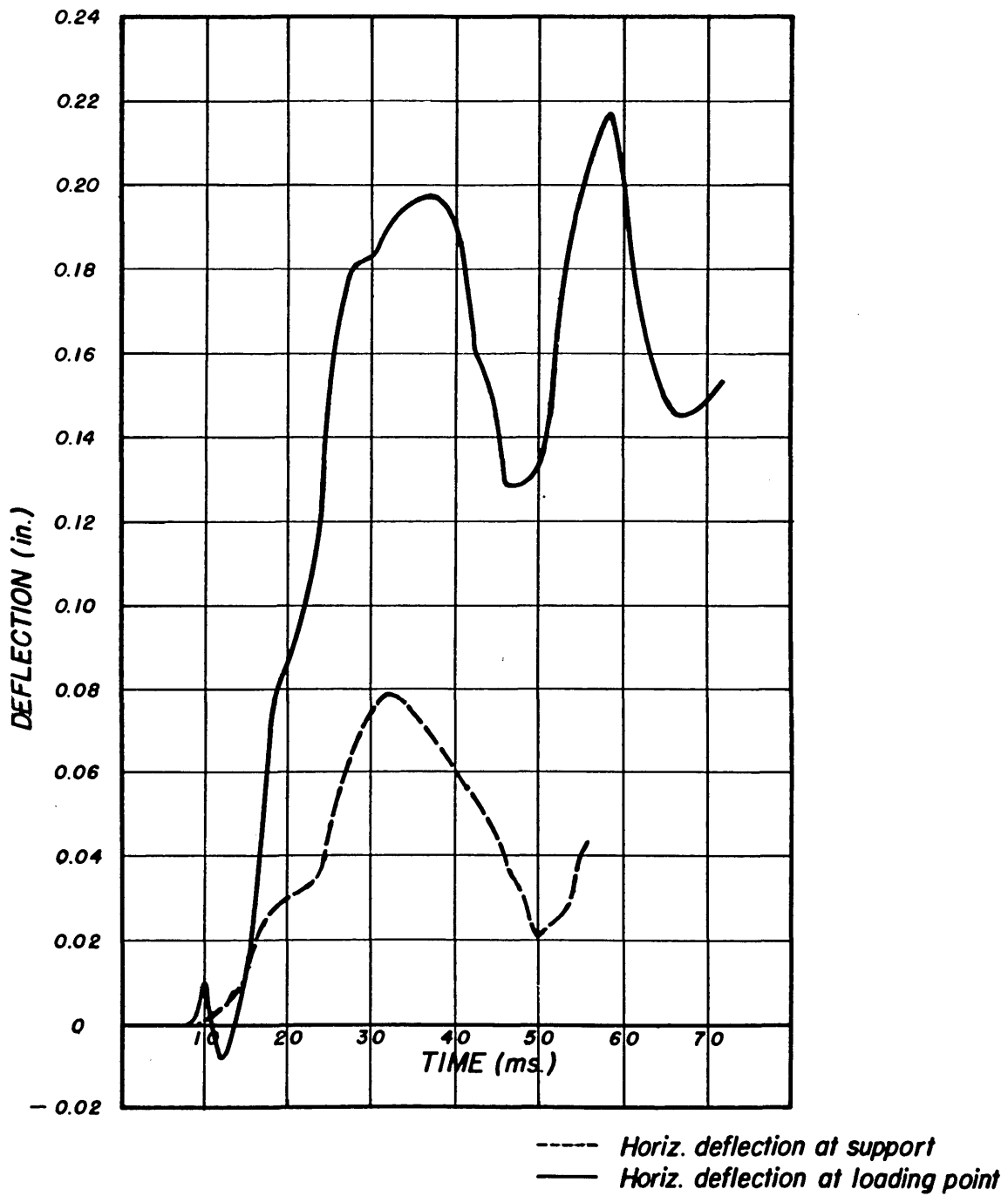


Figure 57 - Observed Deflections vs Time for Test No 12 on Wall #2

730
130

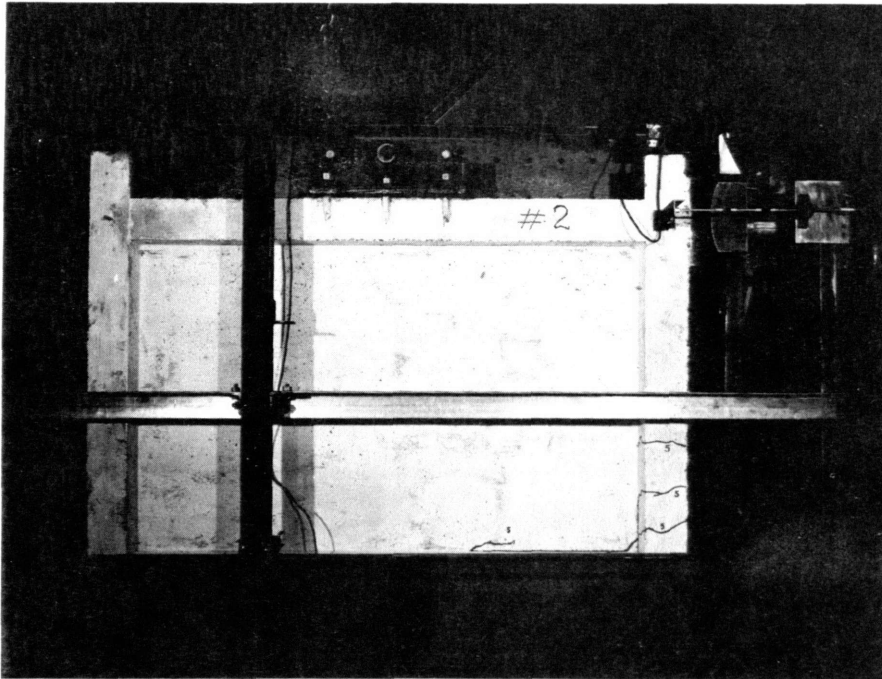


Figure 58 - Crack Pattern of Wall #2 After a Dynamic Load with a Peak Value of 31.5 kips was Applied

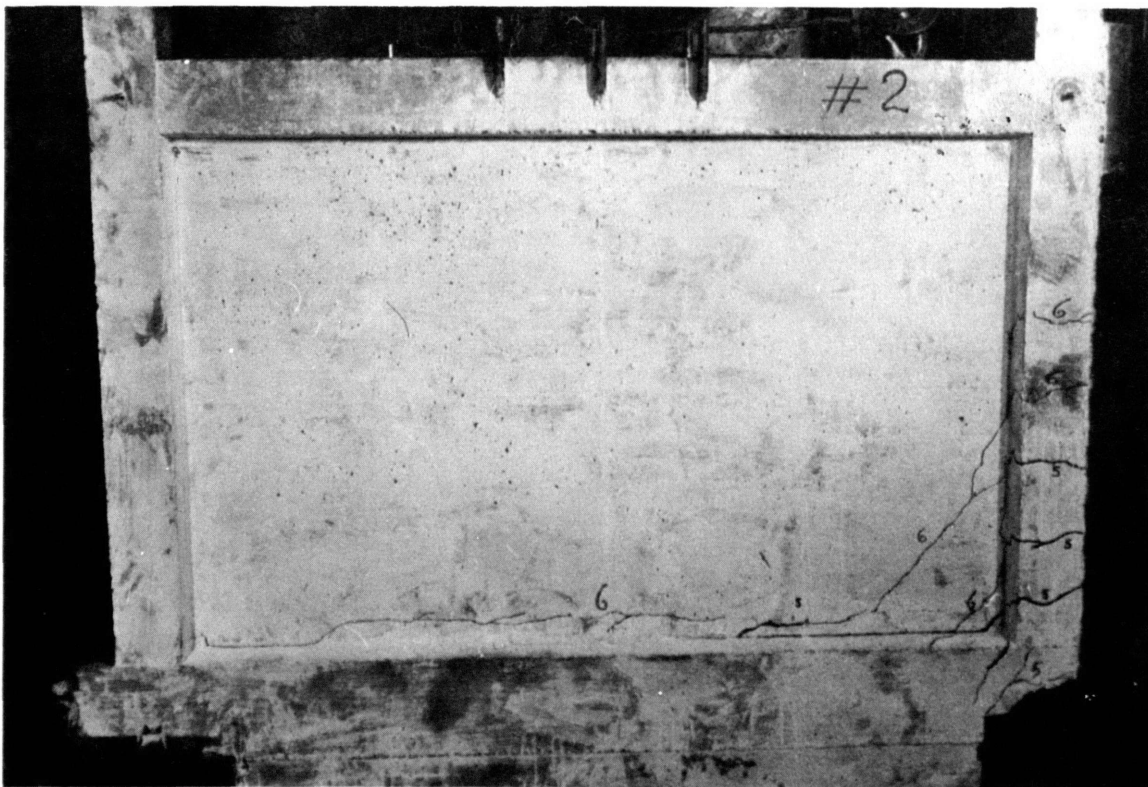


Figure 59 - Final Condition of Specimen #2

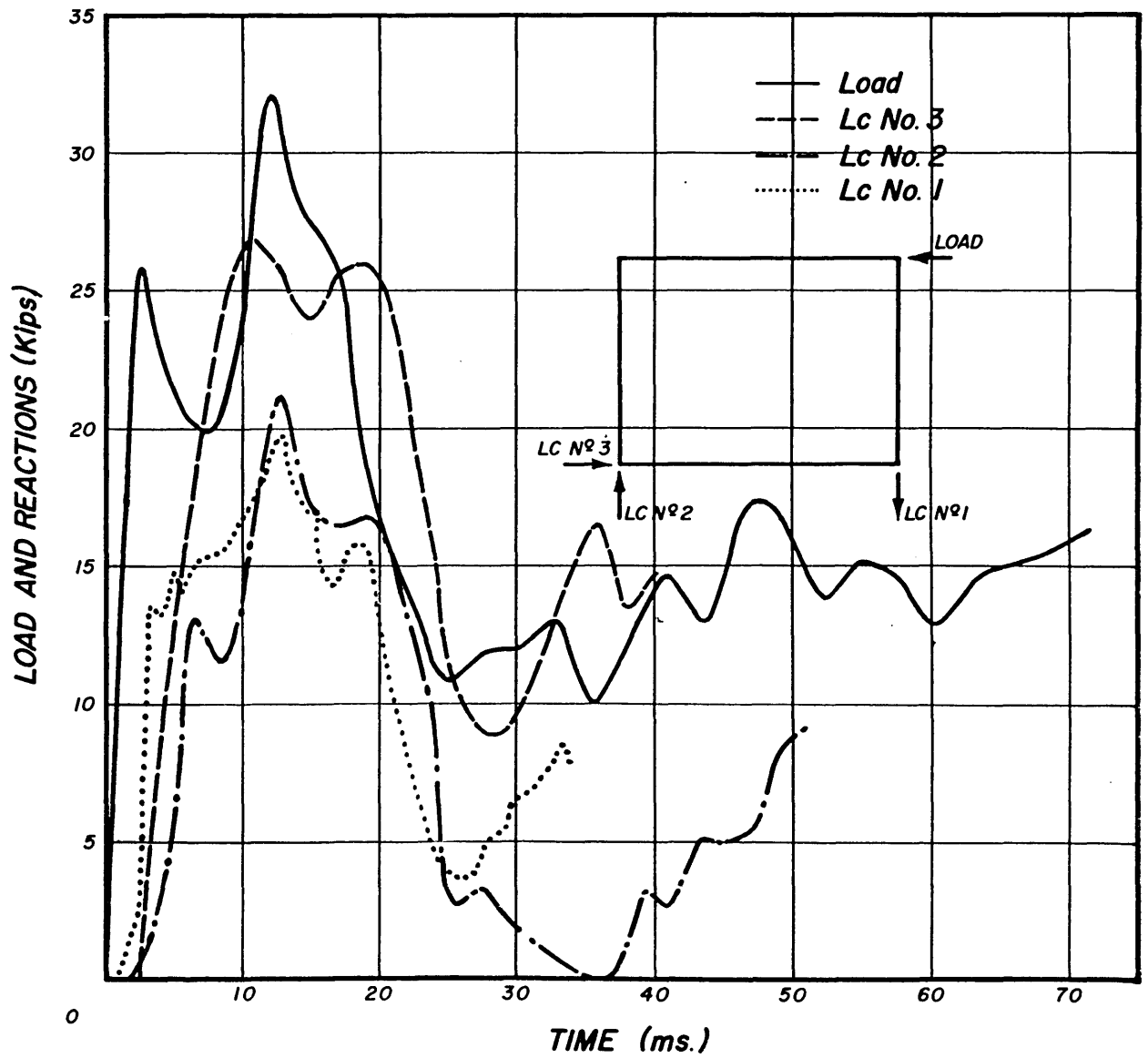


Figure 60 - Observed Load and Reactions vs Time for Test No. 1 on Wall #3

132

132

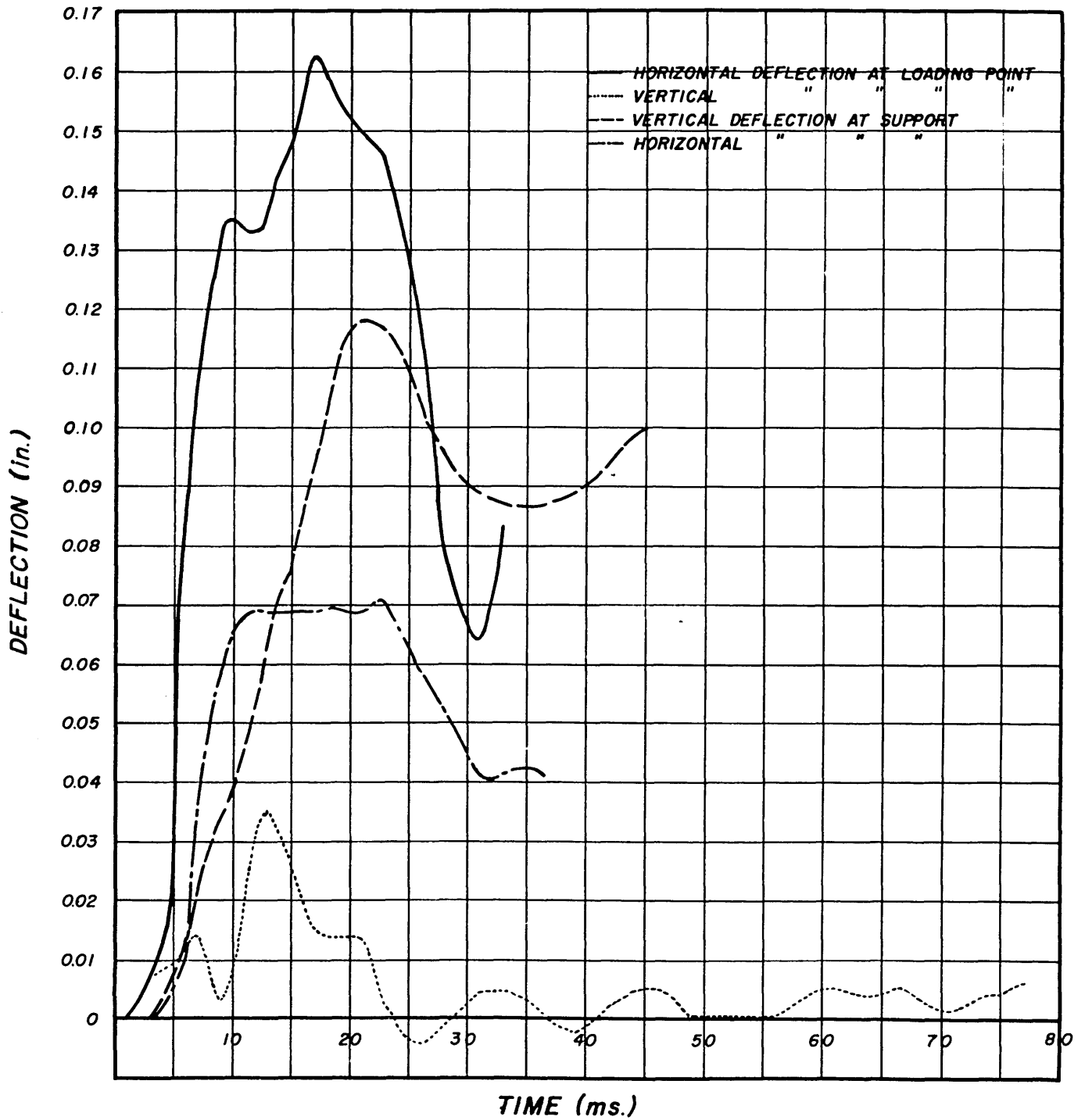


Figure 61 - Observed Deflections vs Time for Test No. 1 on Wall #3

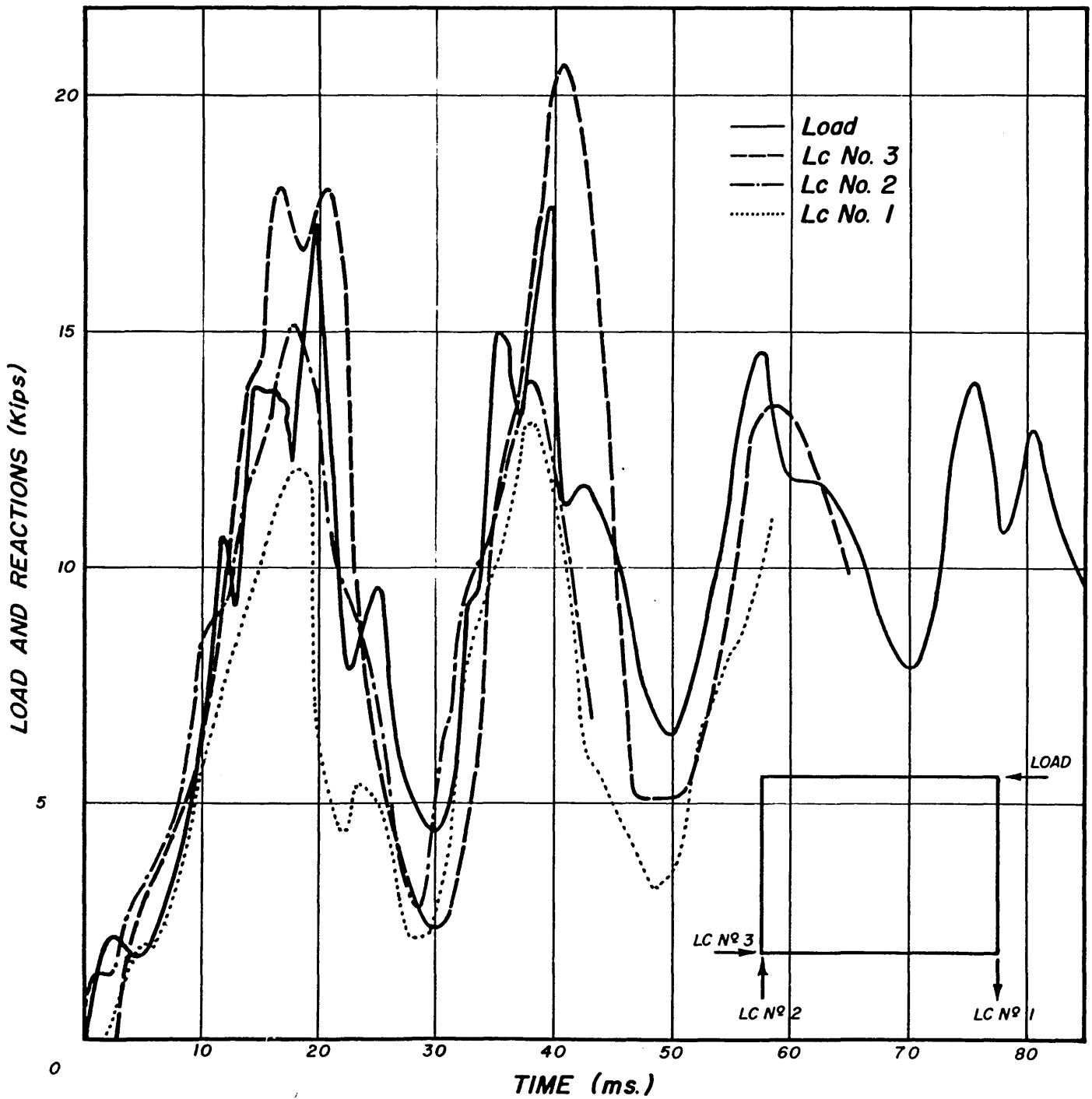


Figure 62 - Observed Load and Reactions vs Time for Test No. 7 on Wall #3

134

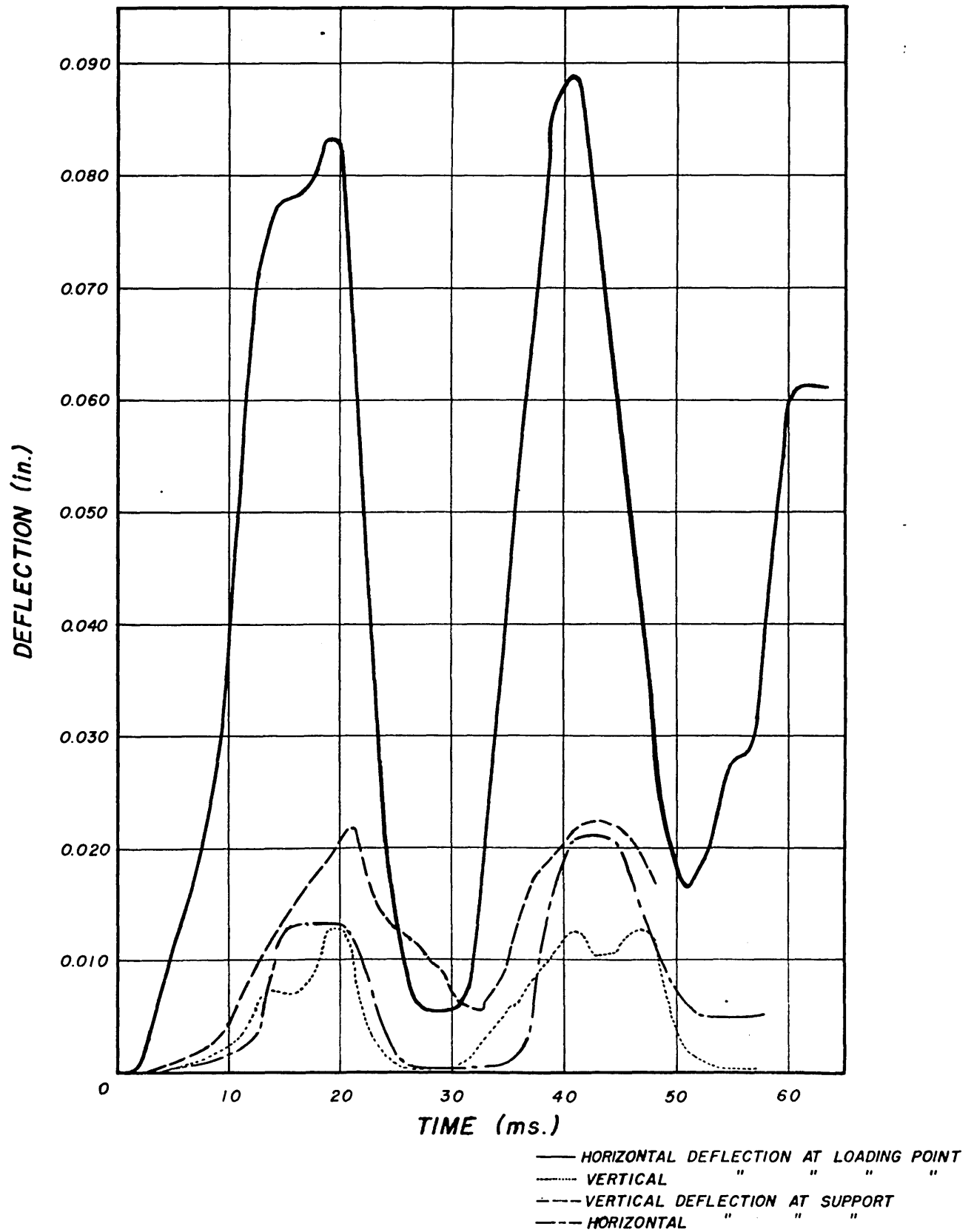


Figure 63 - Observed Deflections vs Time for Test No. 7 on Wall #3

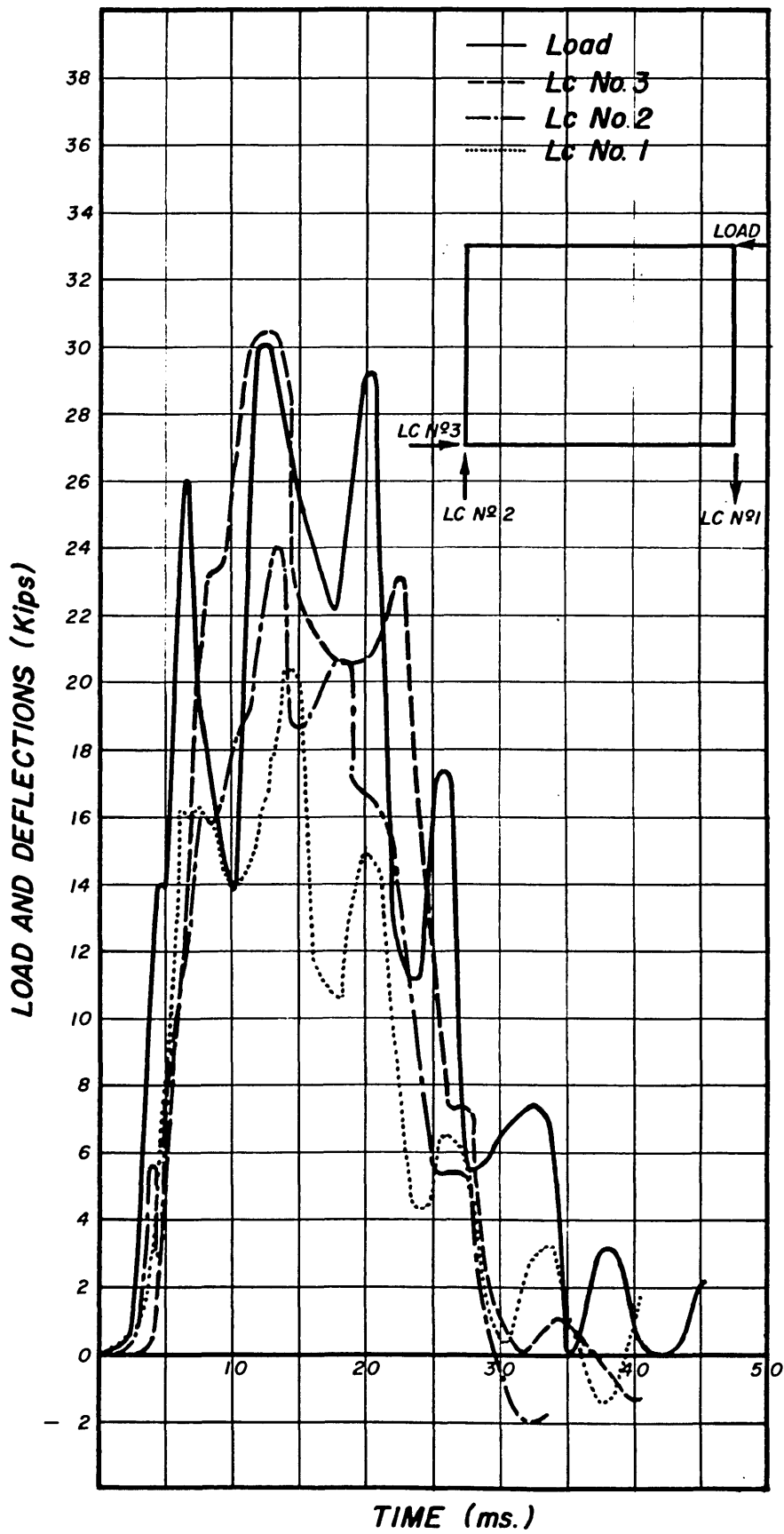
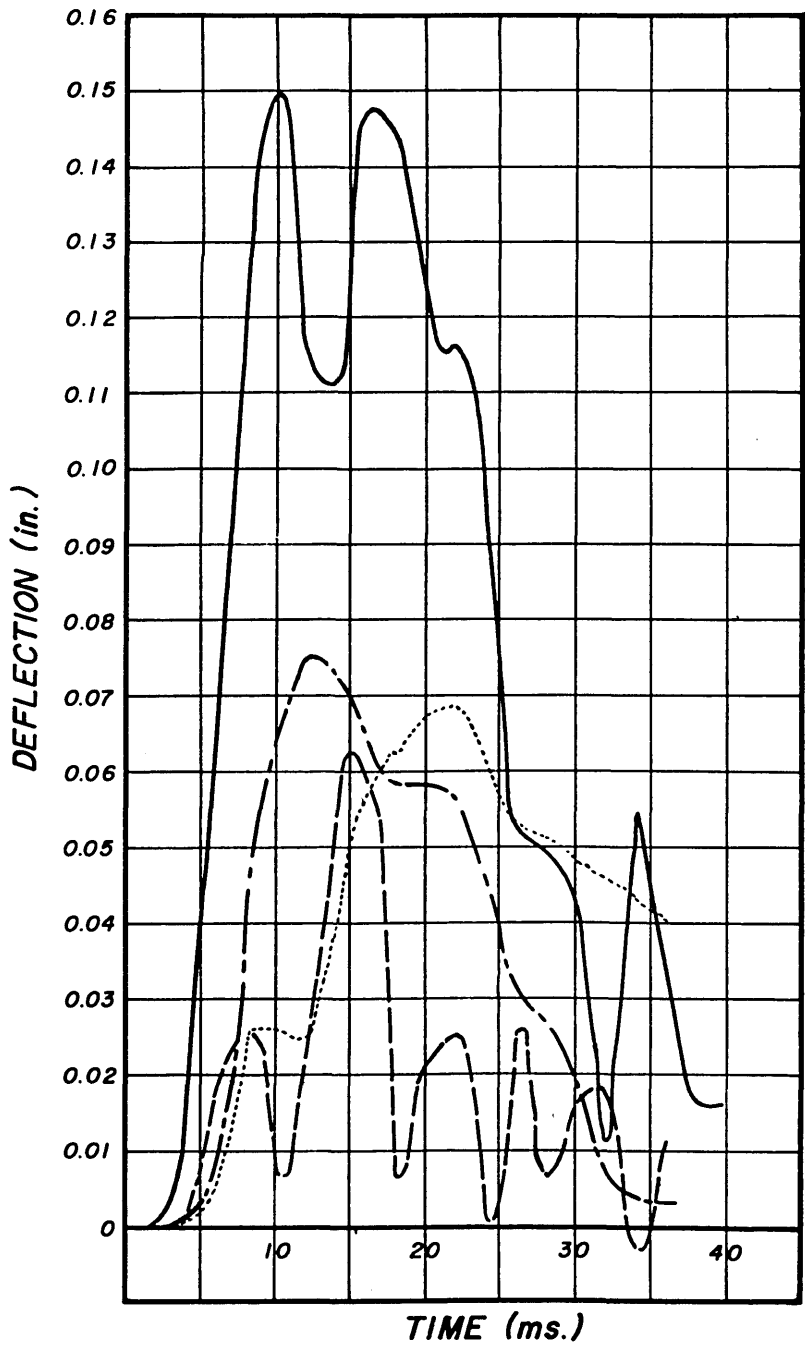


Figure 64 - Observed Load and Reactions vs Time for Test No. 9 on Wall #3



——— HORIZ. DEFLECTION AT LOADING POINT
 - - - VERTICAL " " " "
 VERTICAL DEFLECTION AT SUPPORT
 - · - HORIZ. " " " "

Figure 65 - Observed Deflections vs Time for Test No. 9 on Wall #3

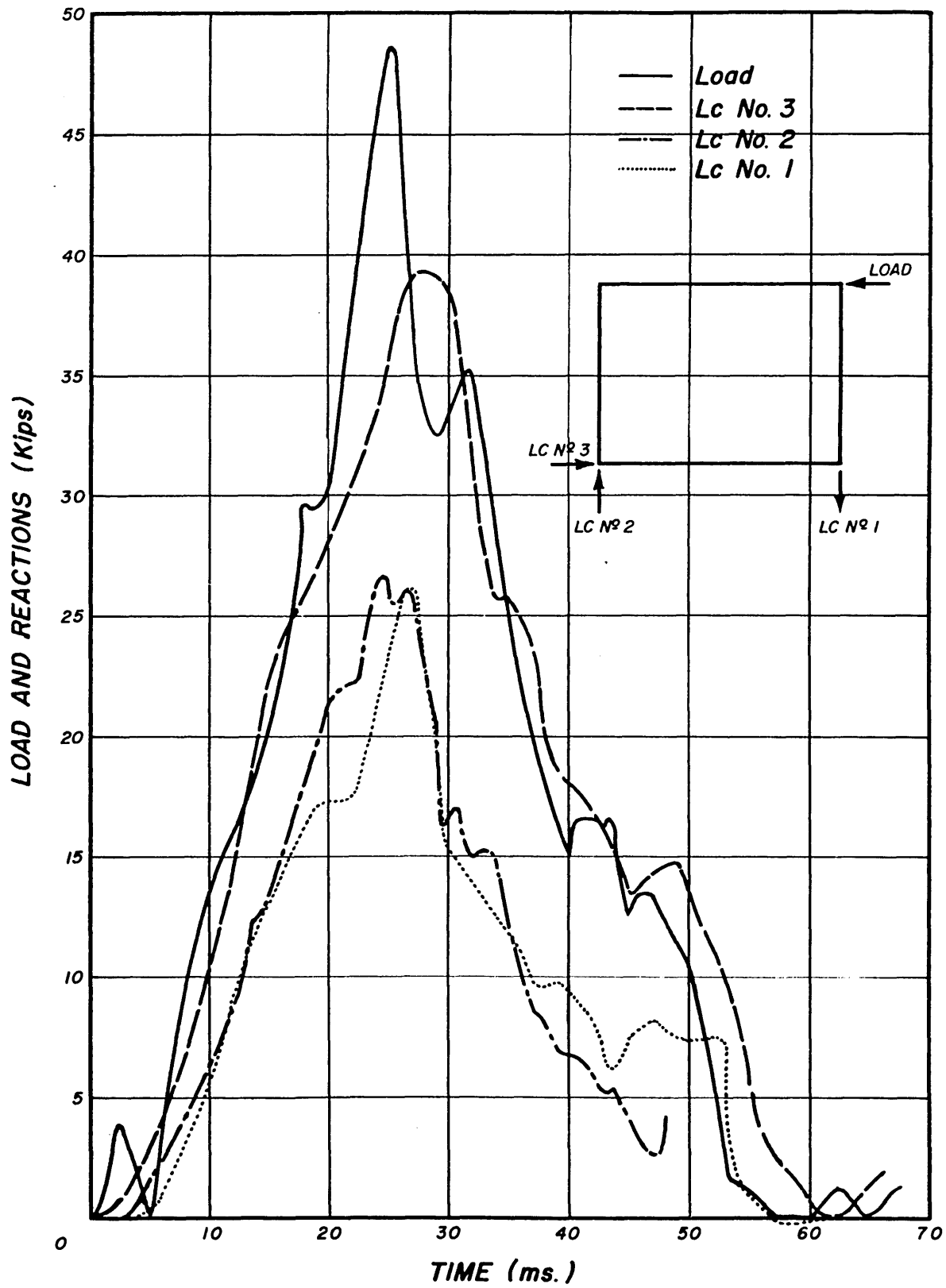


Figure 66 - Observed Load and Reactions vs Time for Test No.13 on Wall #3

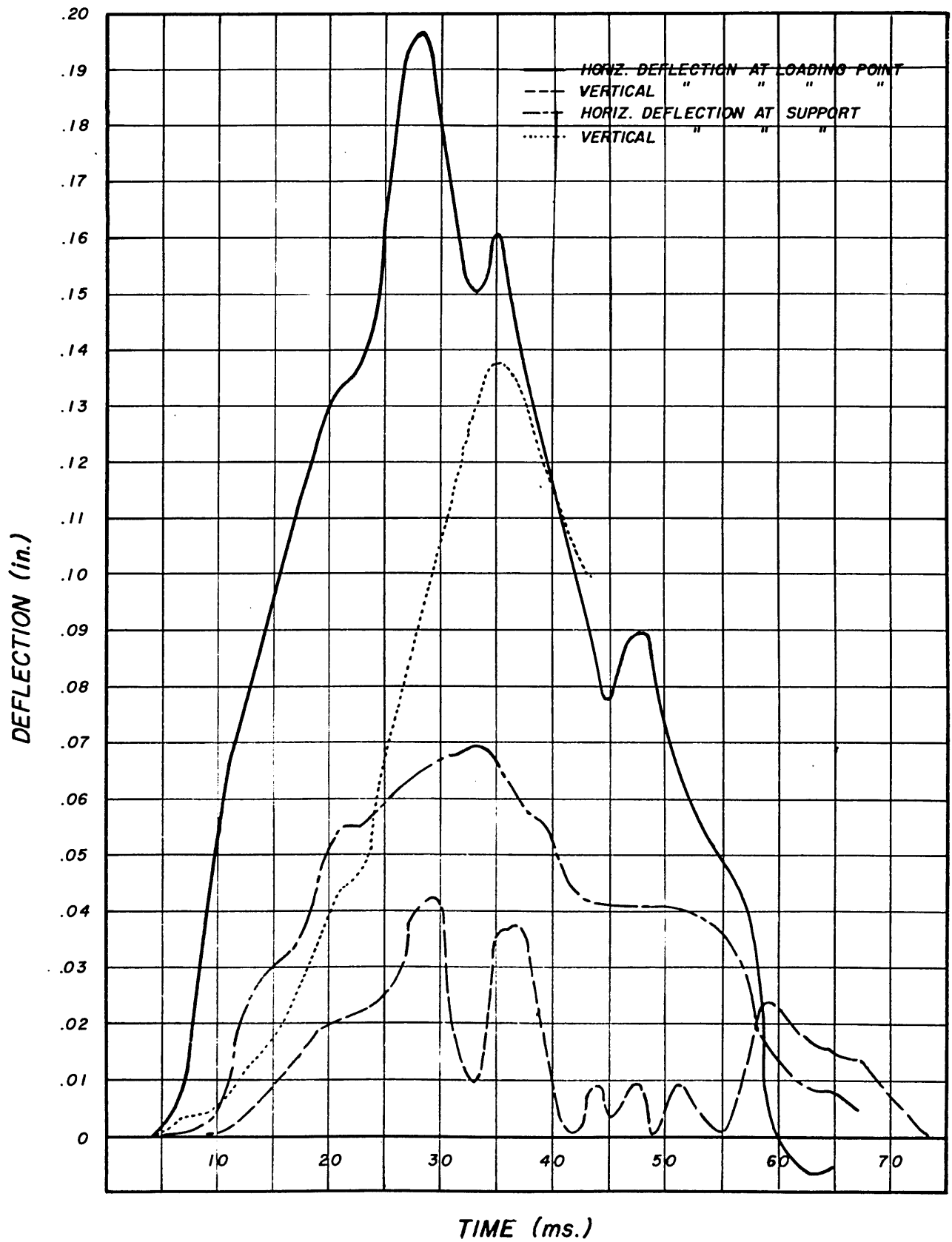


Figure 67 - Observed Deflections vs Time for Test No. 13 on Wall #3

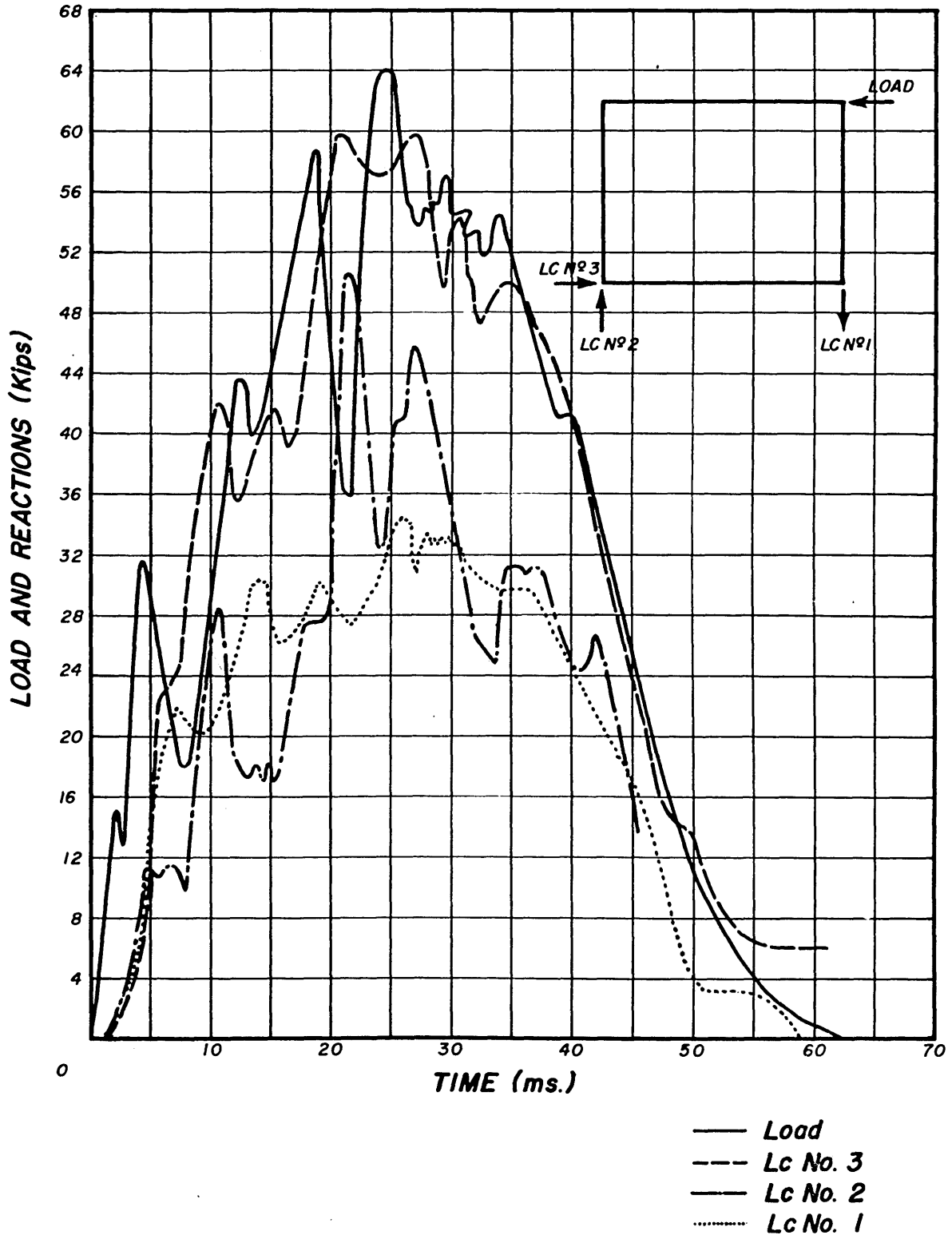


Figure 68 - Observed Load and Reactions vs Time for Test No. 15 on Wall #3

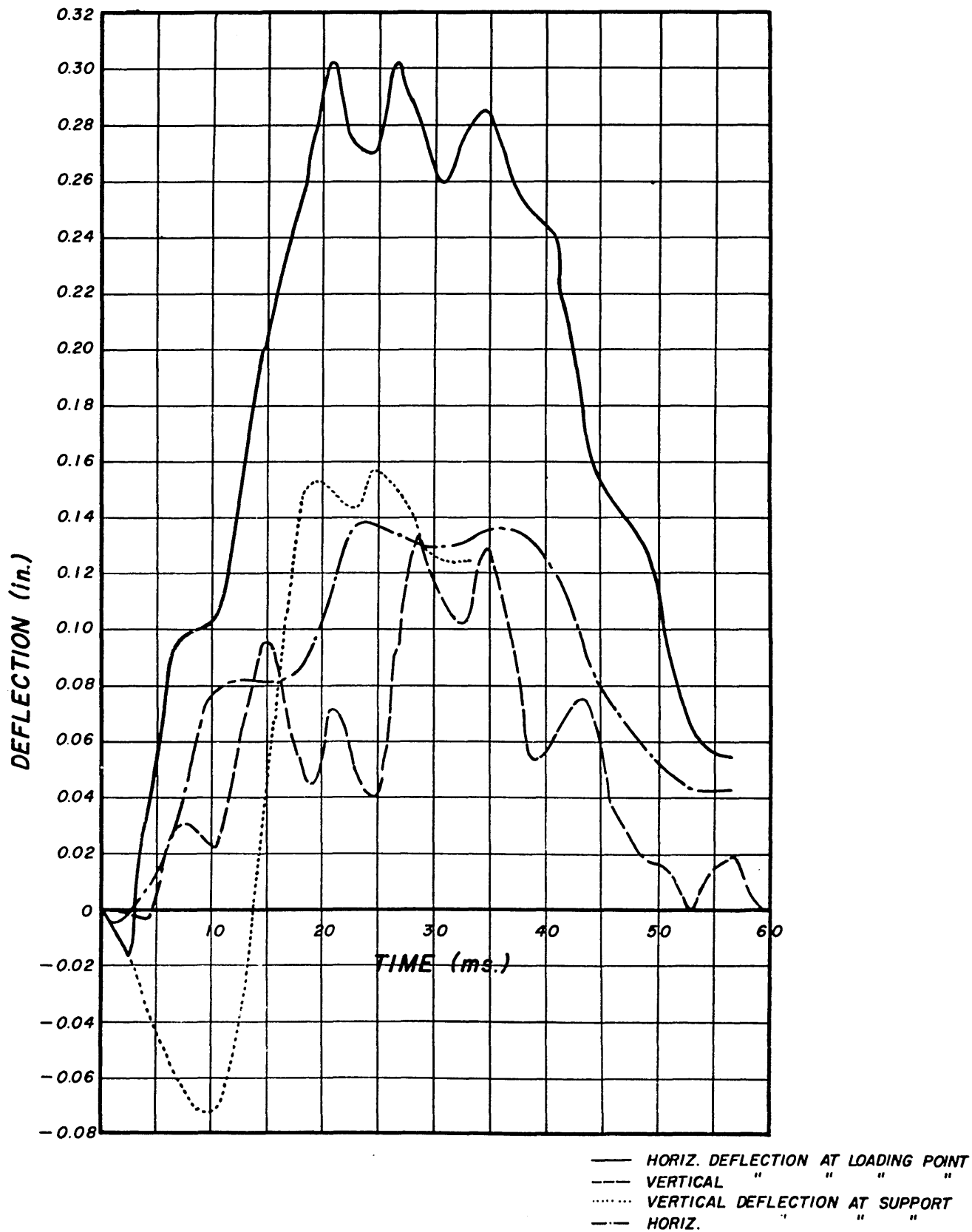


Figure 69 - Observed Deflections vs Time for Test No. 15
on Wall #3 ...

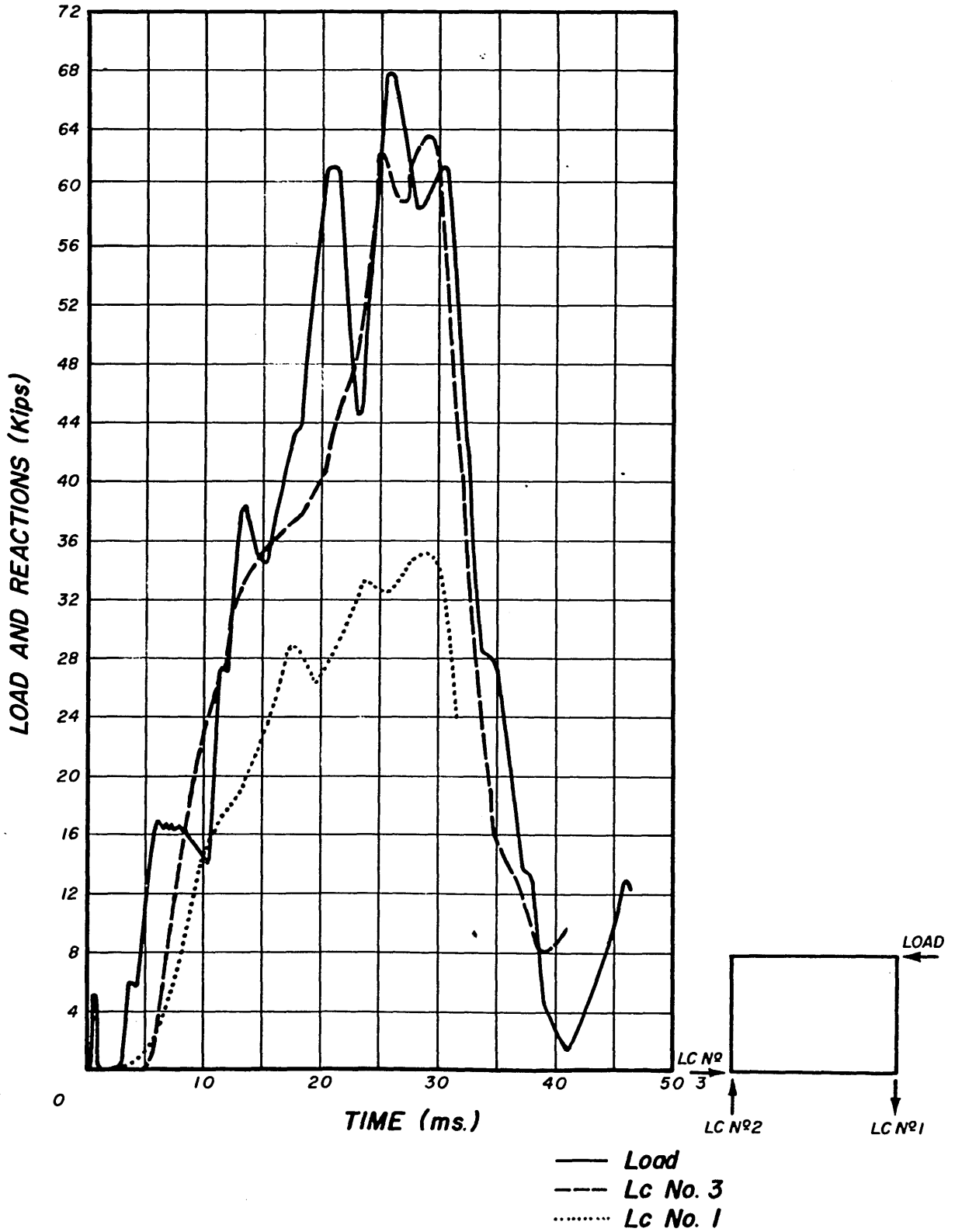


Figure 70 - Observed Load and Reactions vs Time for Test No. 16 on Wall #3

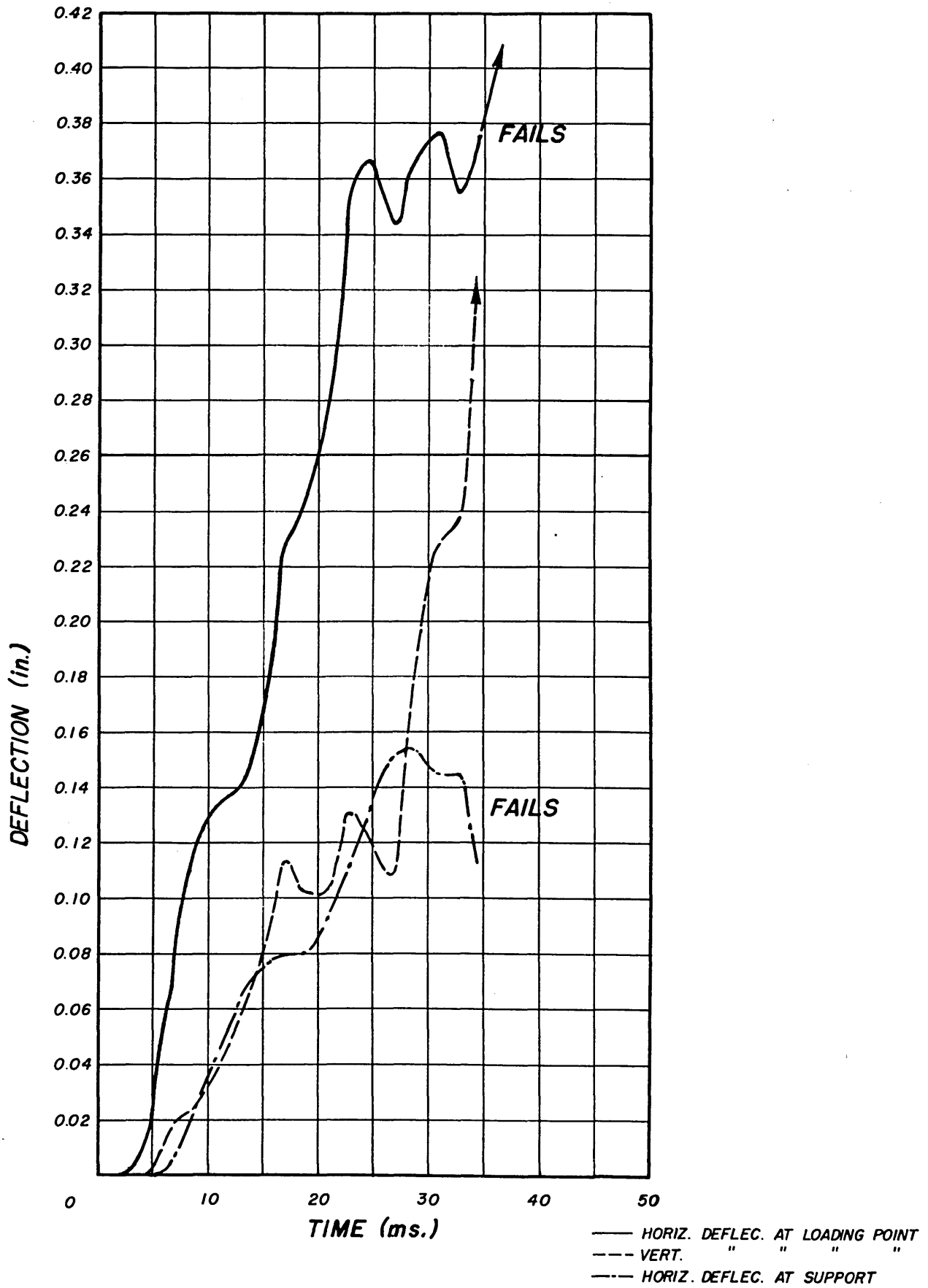


Figure 71 - Observed Deflections vs Time for Test No. 16 on Wall #3

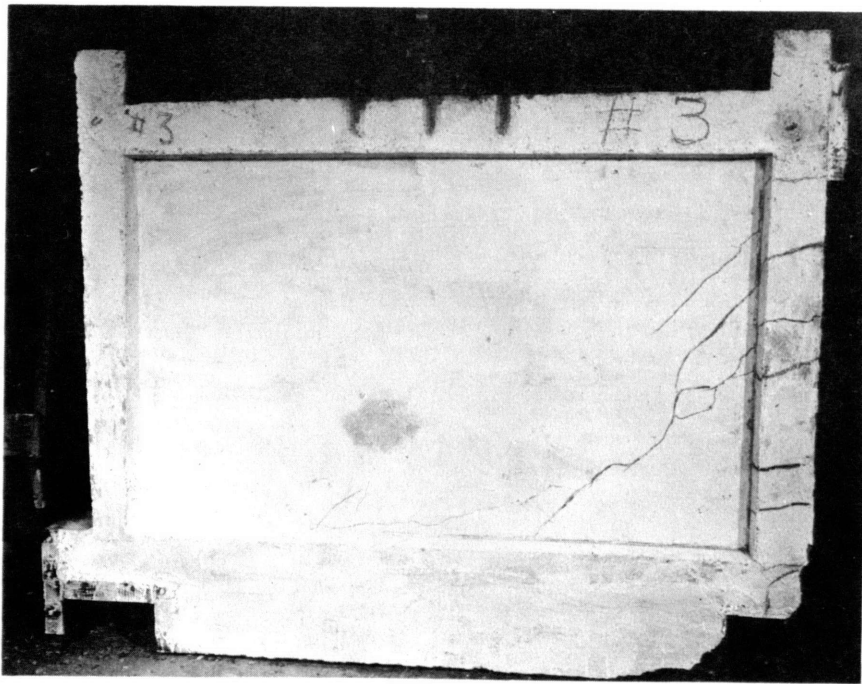


Figure 72 - Wall #3 After Failure

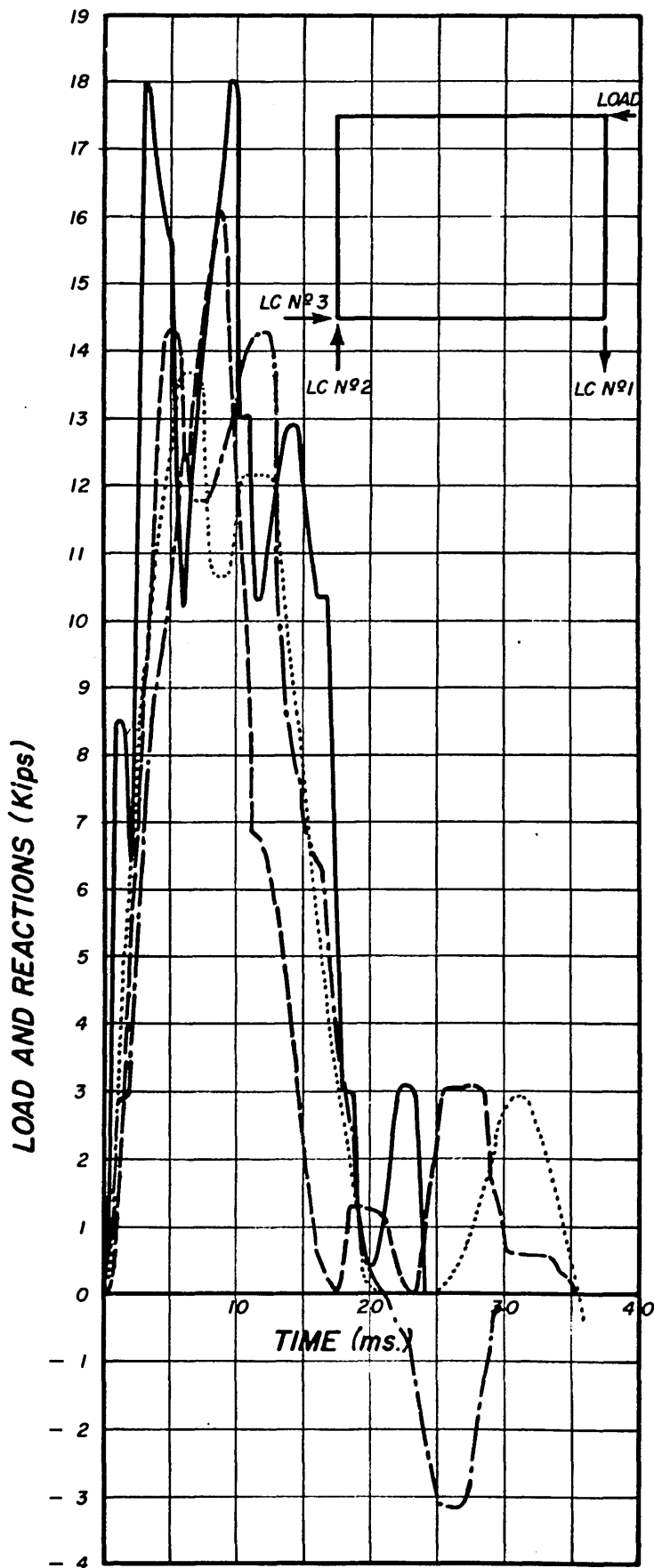
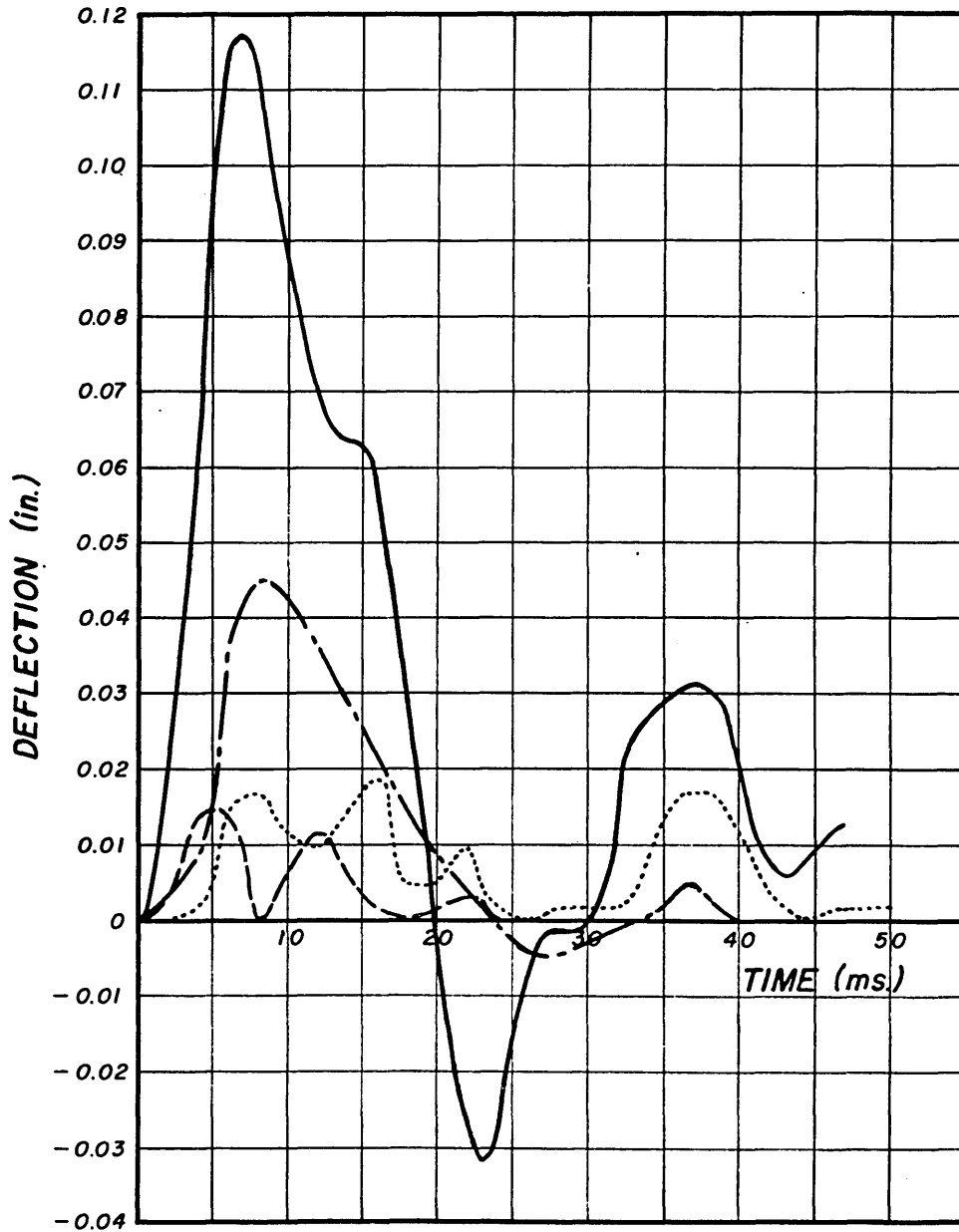


Figure 73 - Observed Load and Reactions vs Time for Test No. 2 on Wall #4

- Load
- - - Lc No. 3
- · - Lc No. 2
- Lc No. 1



— Horizontal deflection at loading point
 Vertical
 --- Vertical deflection at support
 -.- Horizontal " " "

Figure 74 - Observed Deflections vs time for Test No. 2 on Wall #4

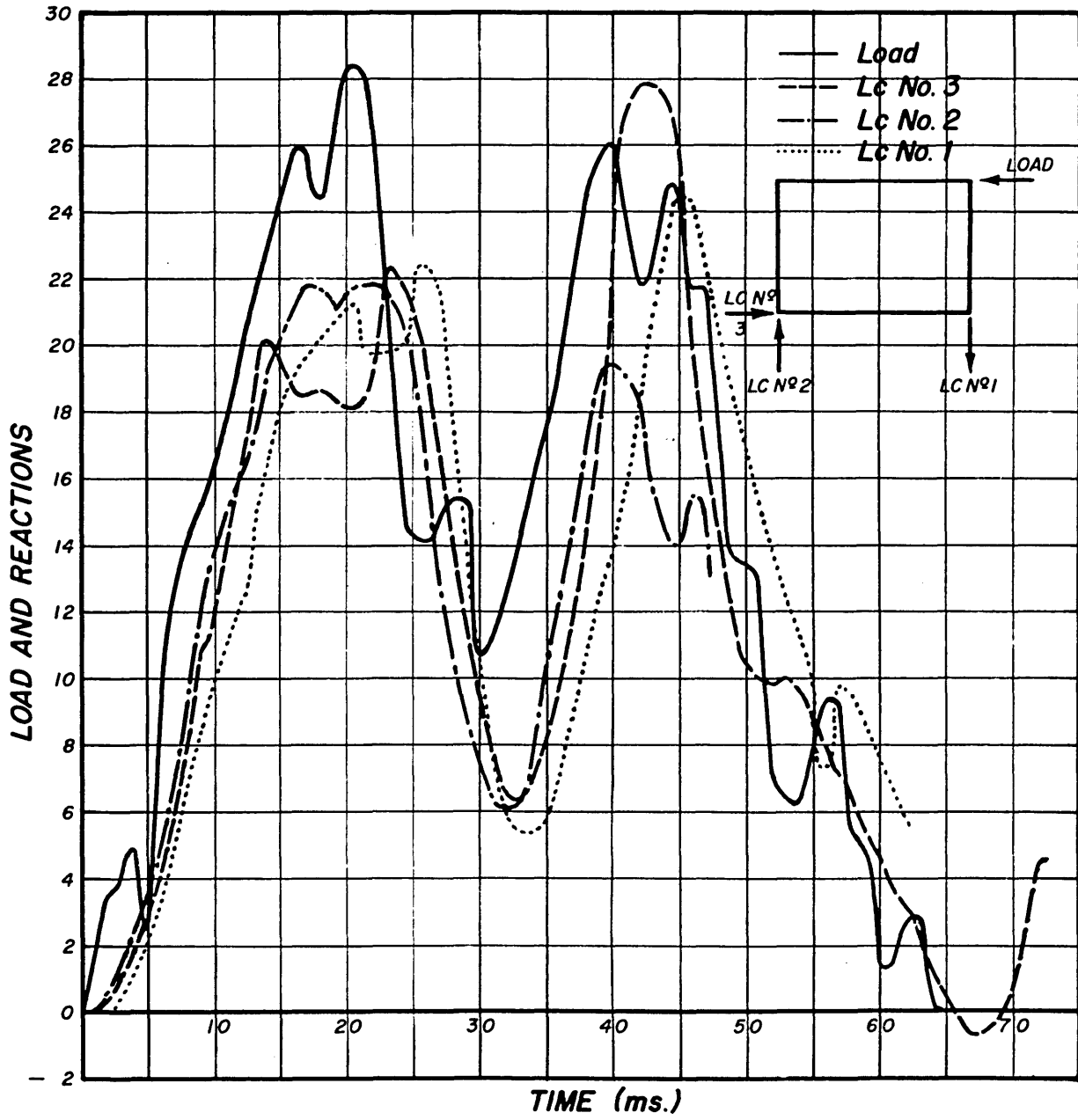


Figure 75 - Observed Load and Reactions vs Time for Test No. 4 on Wall #4

227
147

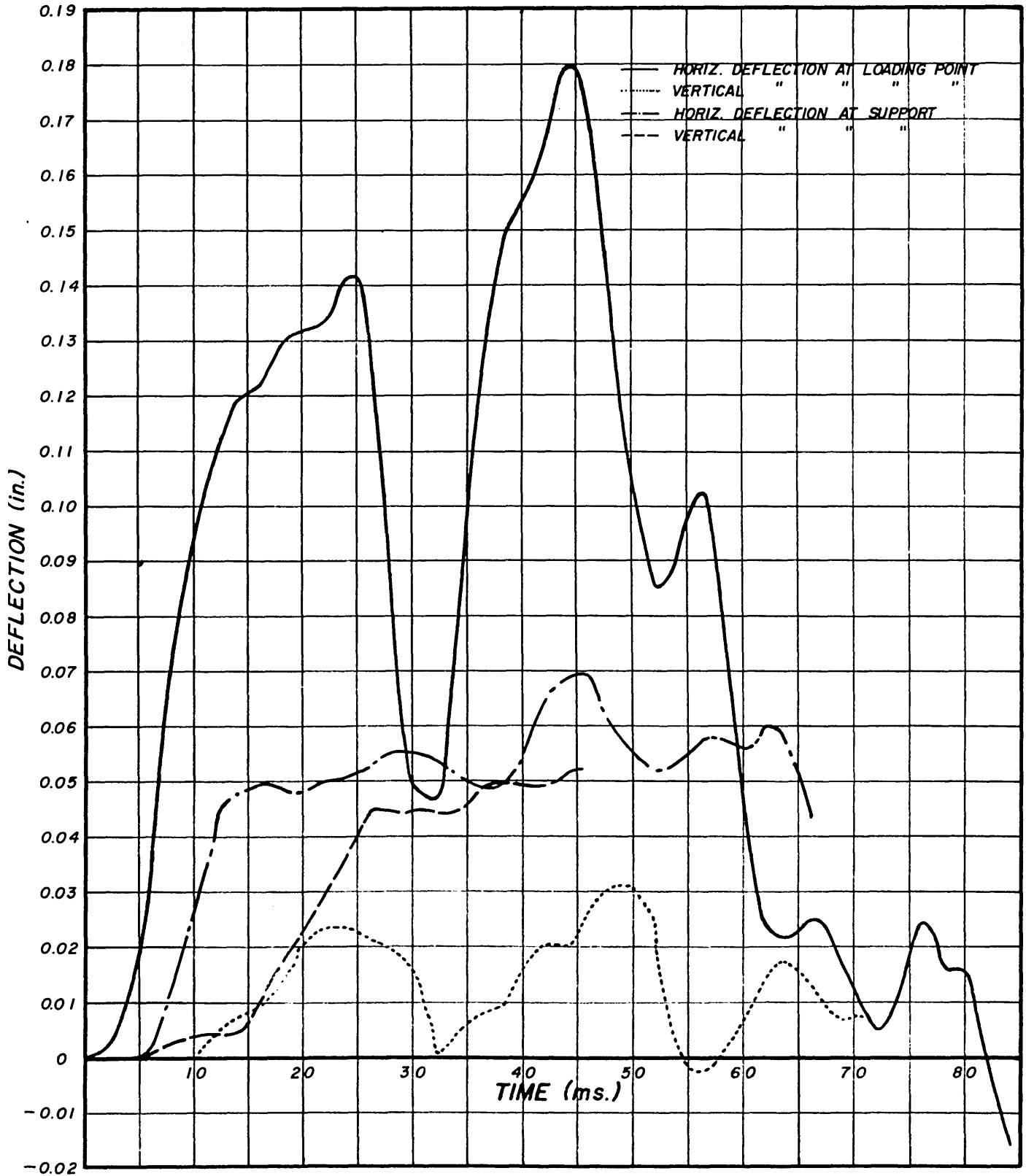


Figure 76 - Observed Deflections vs Time for Test No. 4 on Wall #4

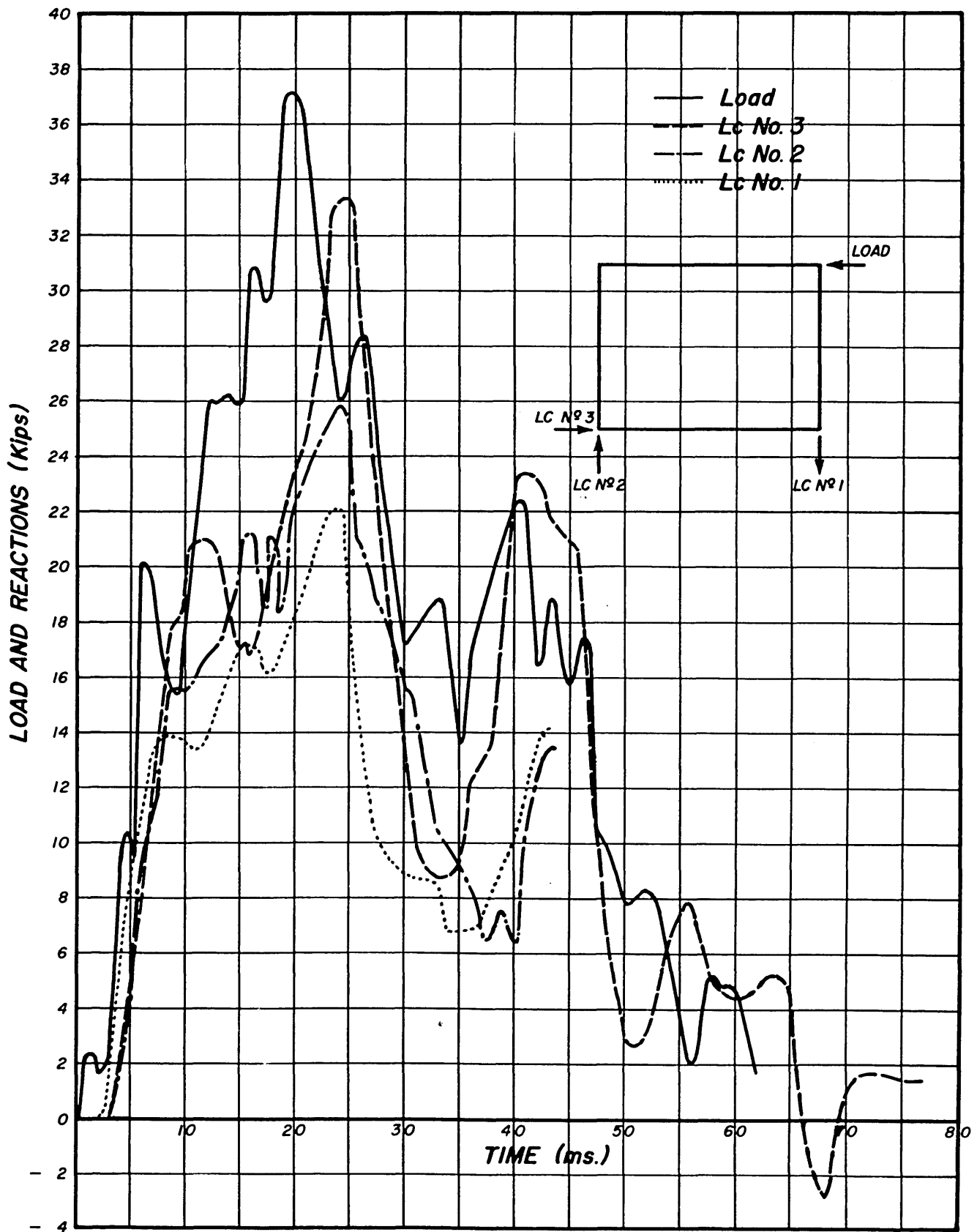


Figure 77 - Observed Load and Reactions vs Time for Test No. 5 on Wall #4 ...

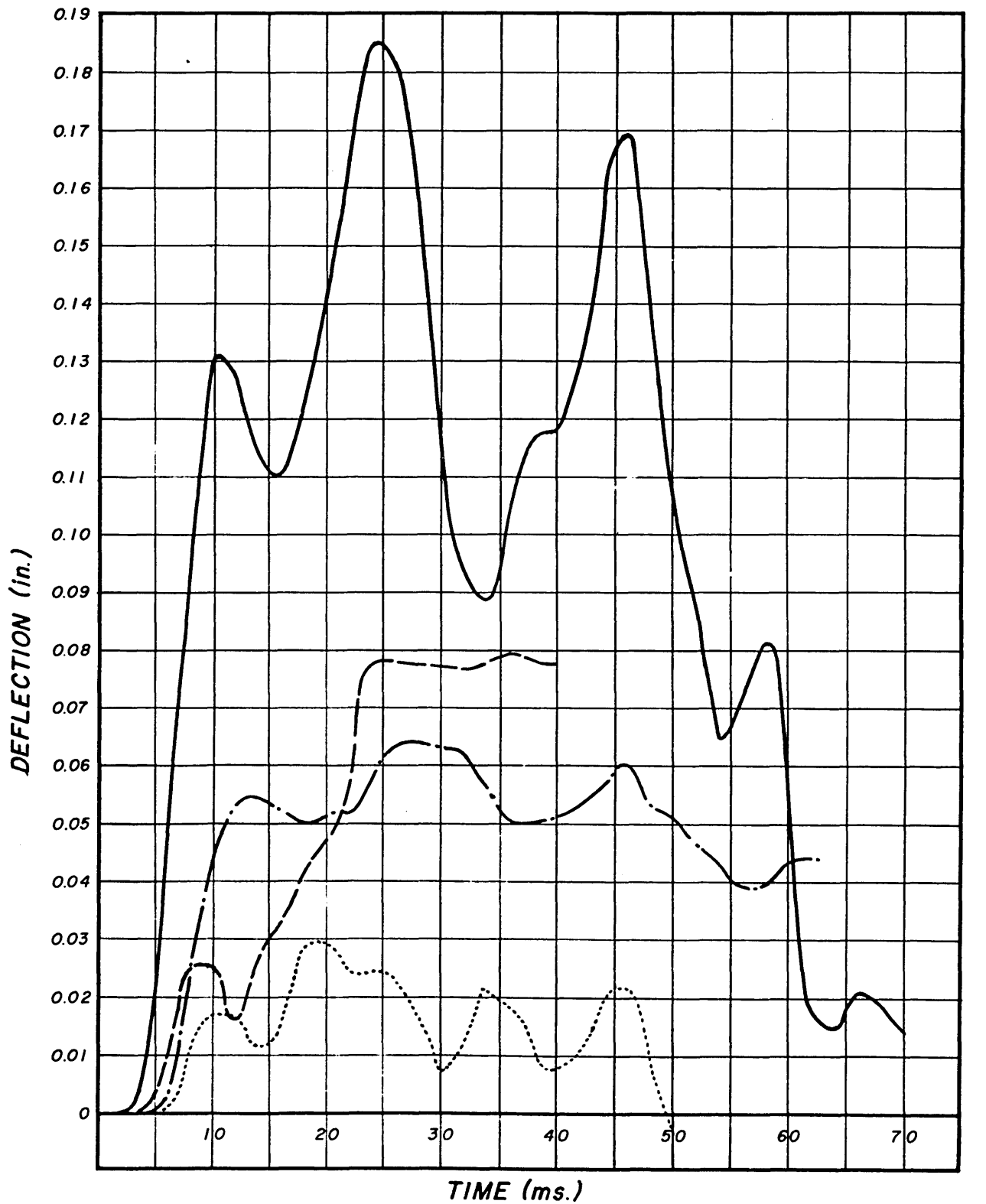


Figure 78 - Observed Deflections vs Time for Test No. 5 on Wall #4

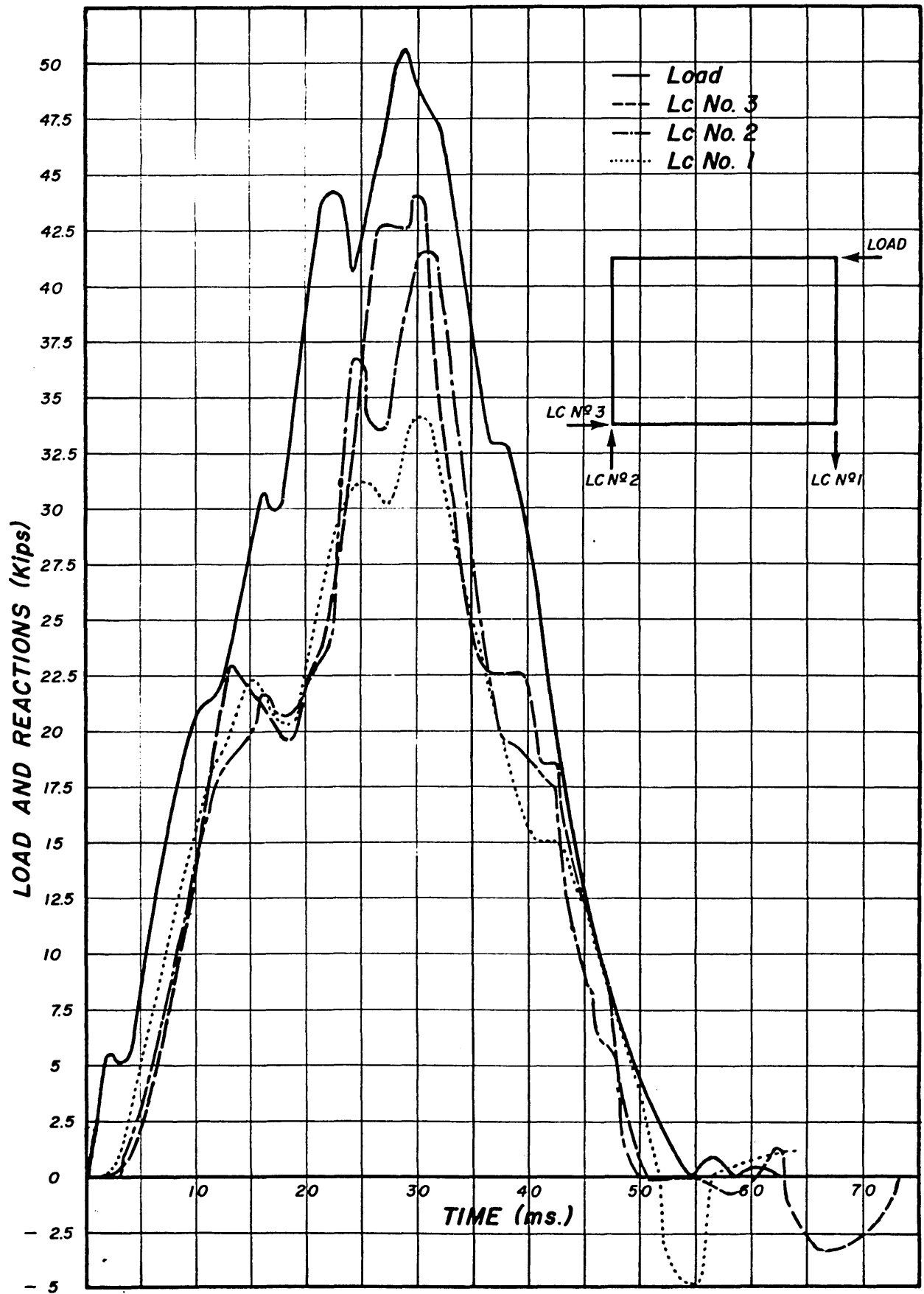


Figure 79 - Observed Load and Reactions vs Time for Test No. 6 on Wall #4

15/151

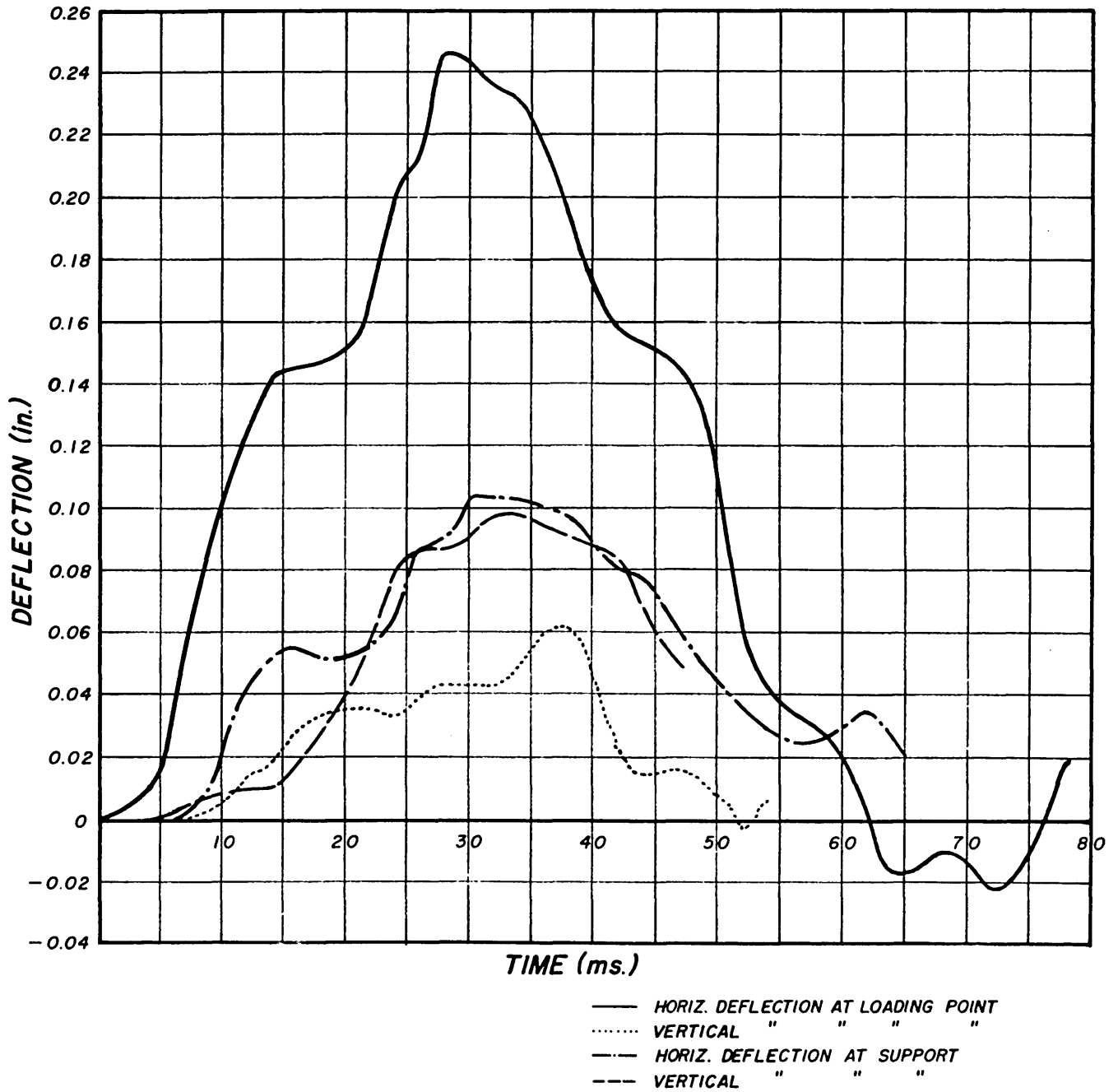


Figure 80 - Observed Deflections vs Time for Test No. 6 on Wall #4

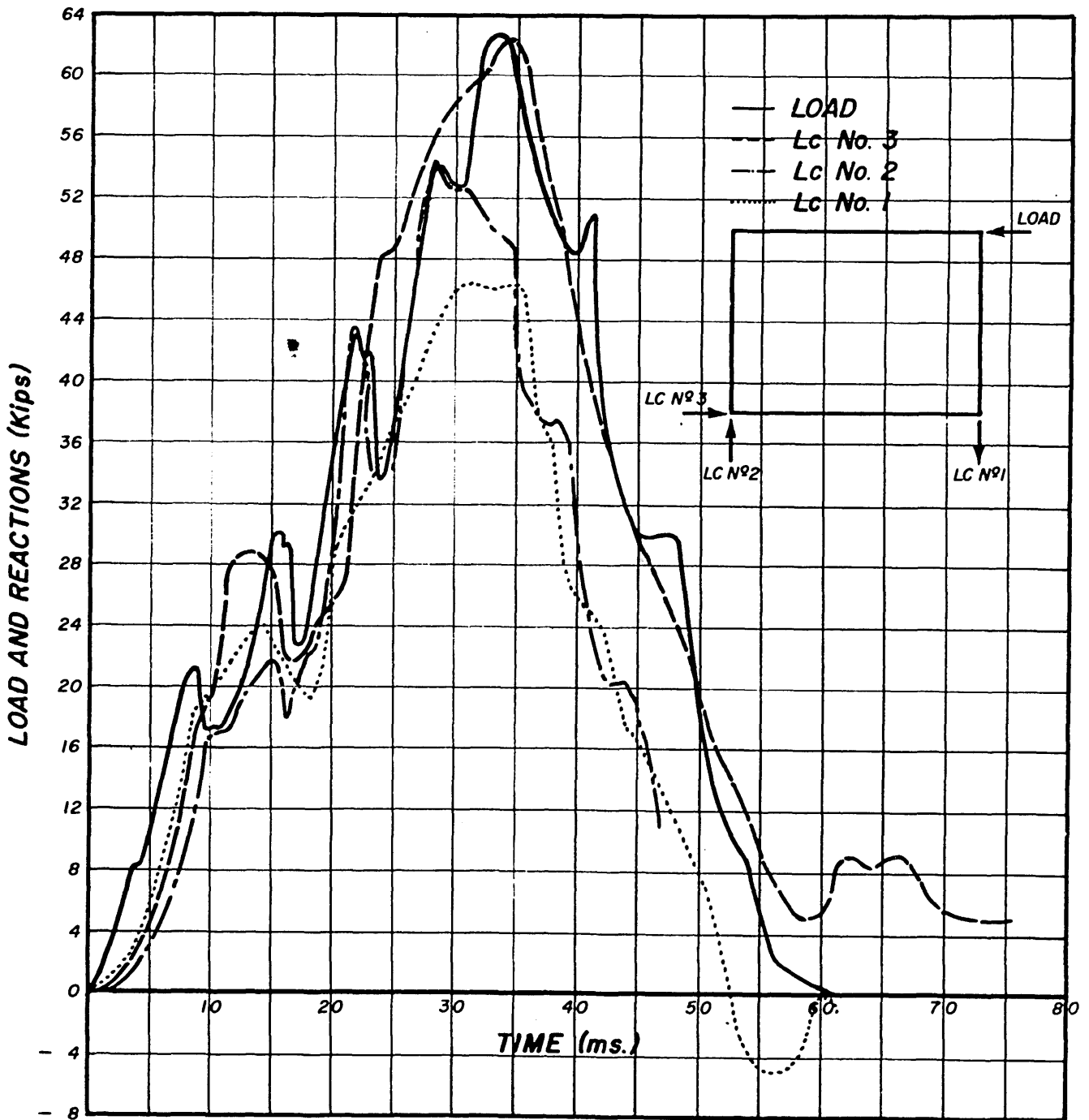


Figure 81 - Observed Load and Reactions vs Time for Test No. 7 on Wall #1

153

153

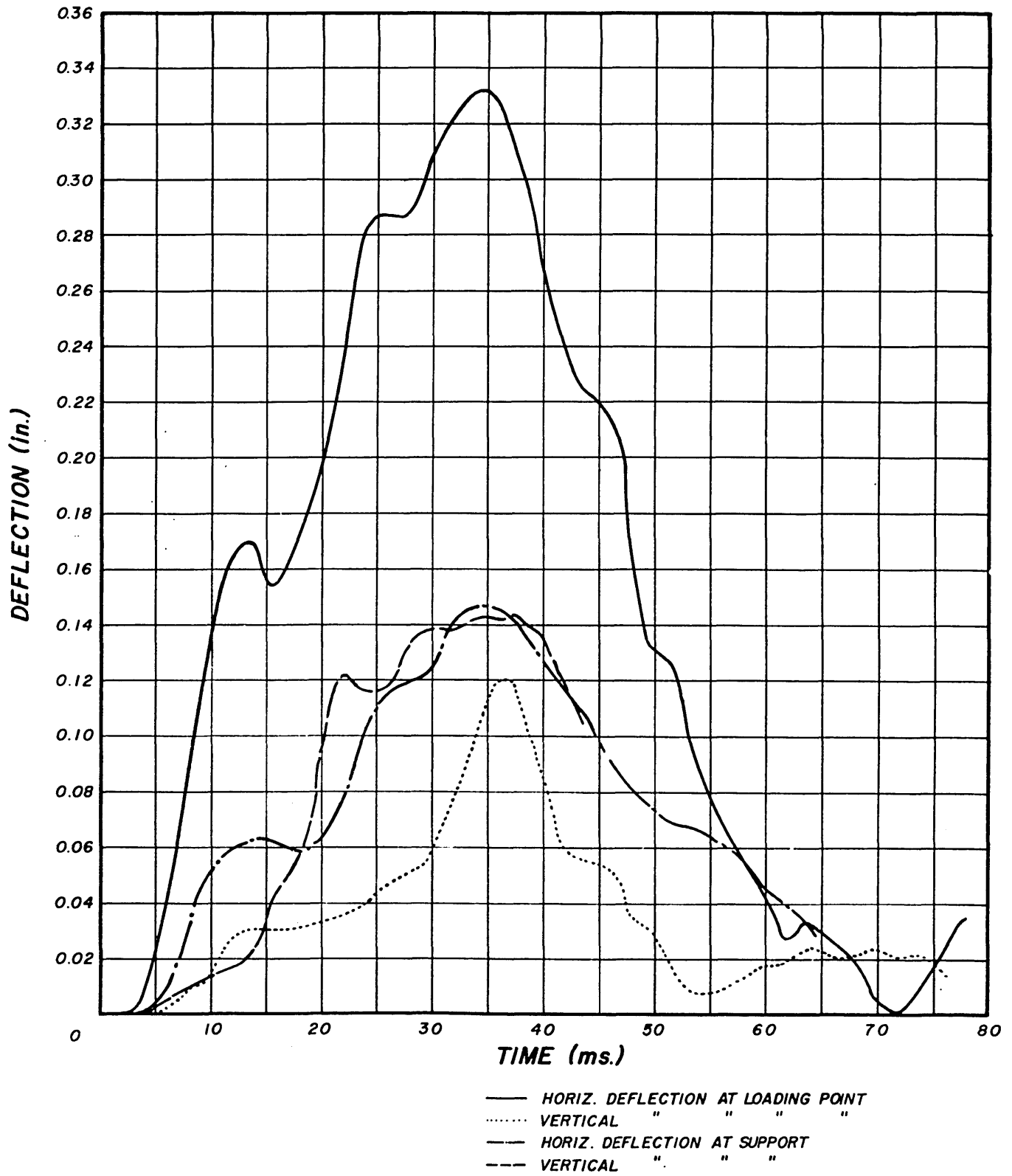


Figure 82 - Observed Deflections vs Time for Test No. 7 on Wall #4

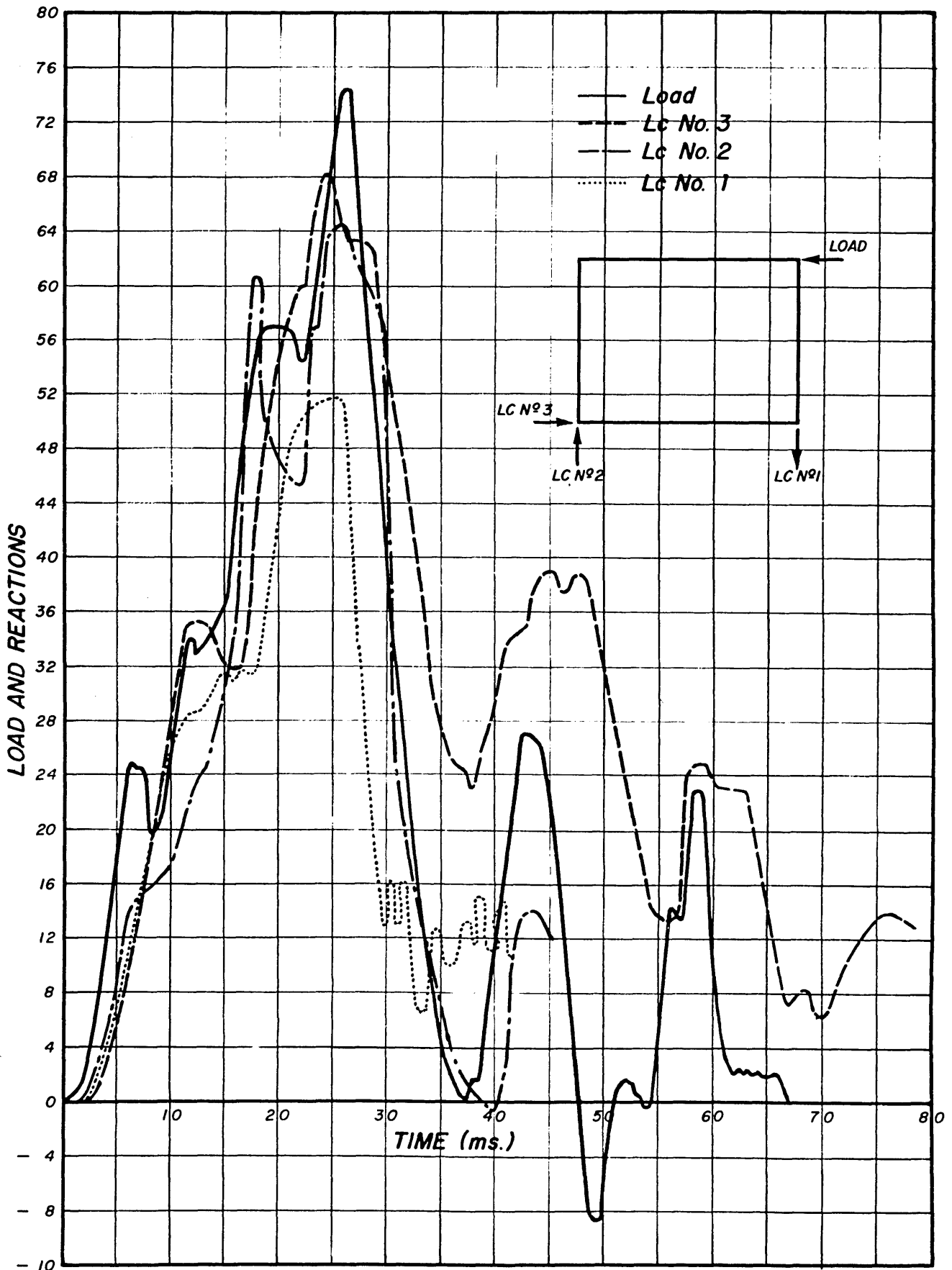


Figure 83 - Observed Load and Reactions vs Time for Test No. 9 on Wall #4

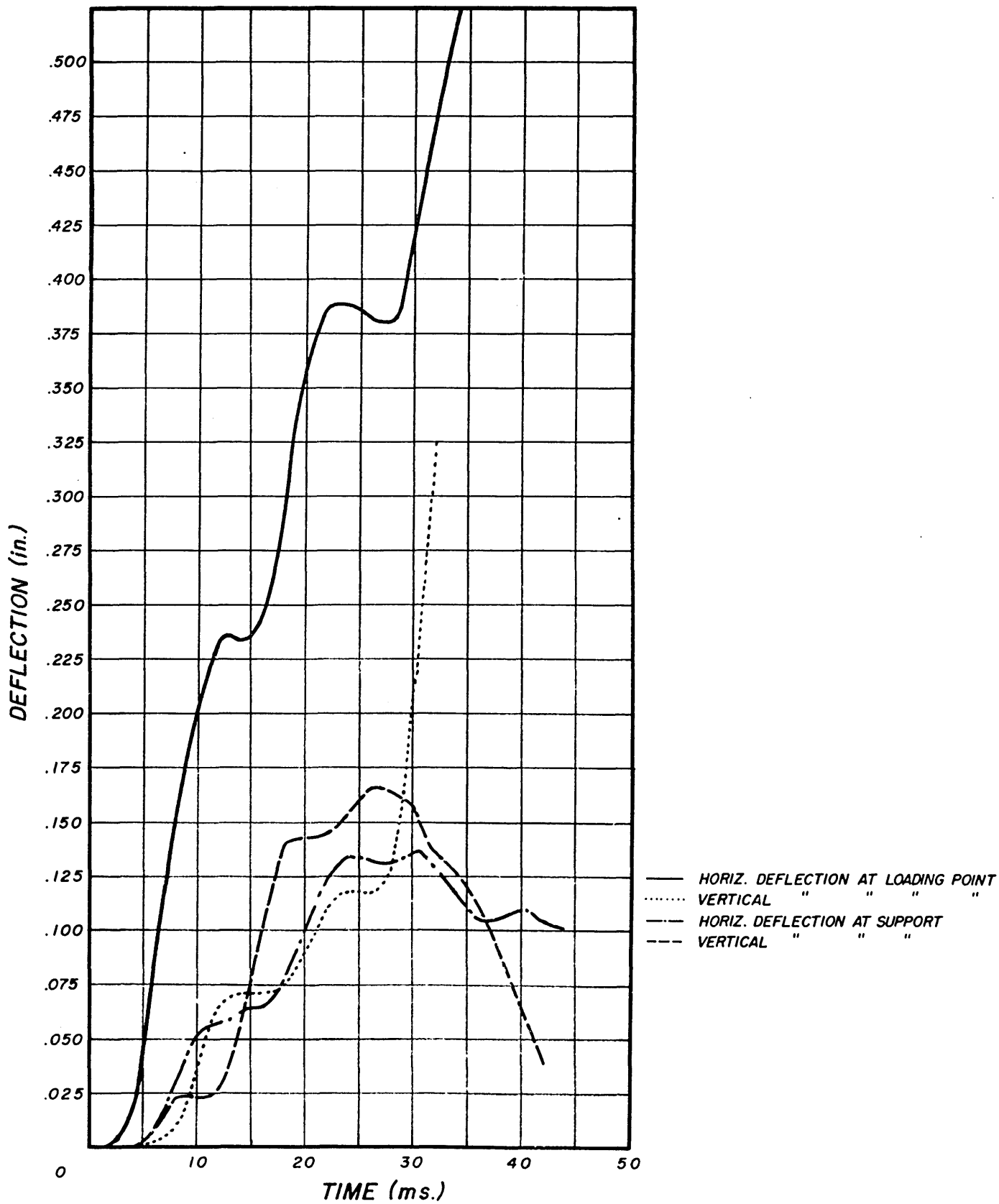


Figure 84 - Observed Deflections vs Time for Test No. 9 on Wall #4

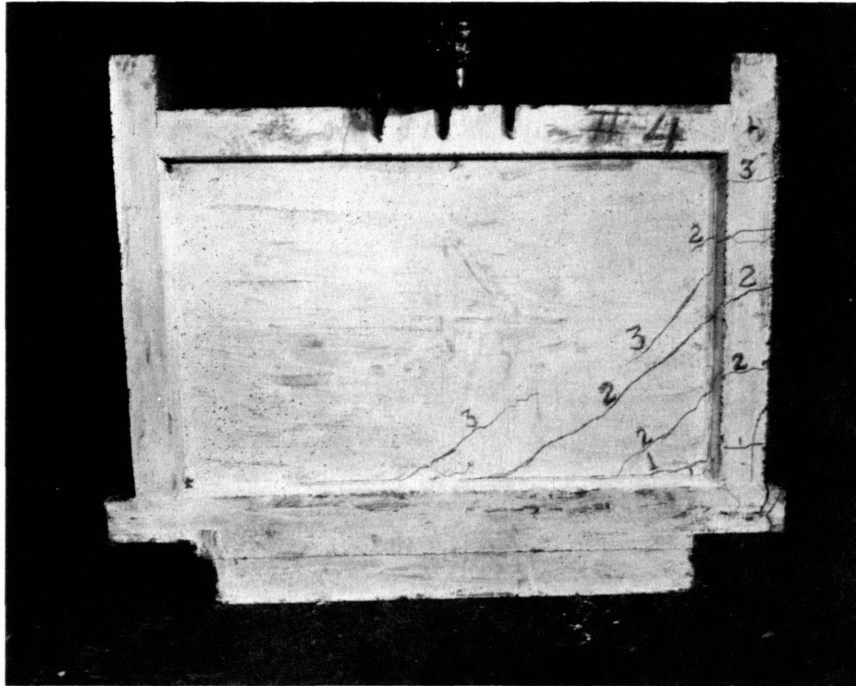


Figure 85 - Crack Pattern of Specimen #4 After Failure of the Connection Between the Reinforcement of the Tension Column and the Support Plate



Figure 86 - Crack Pattern (After Failure) of the Repaired Specimen #4

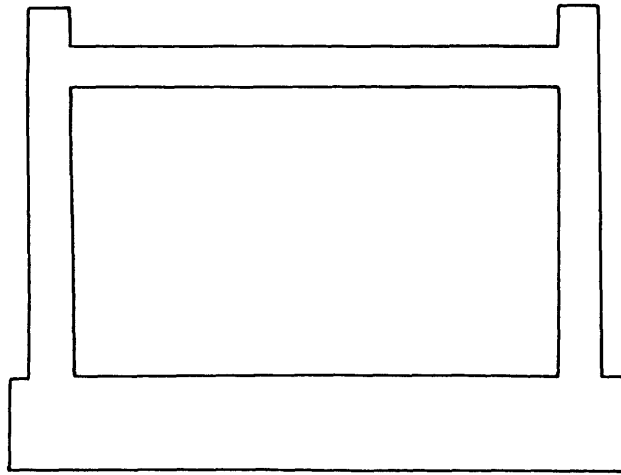


Figure 87(a) - Actual Wall

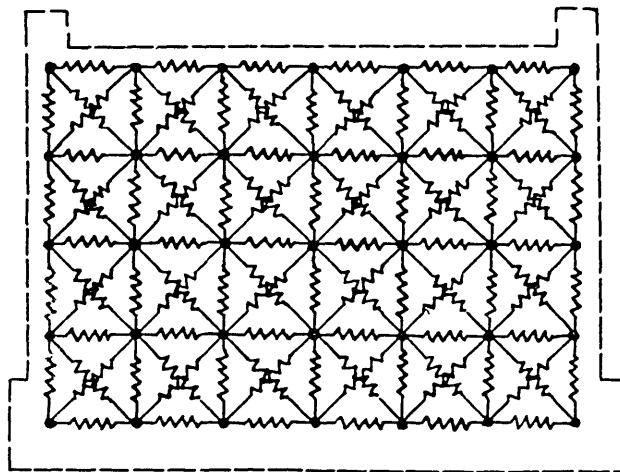


Figure 87(b) - Dynamic Model

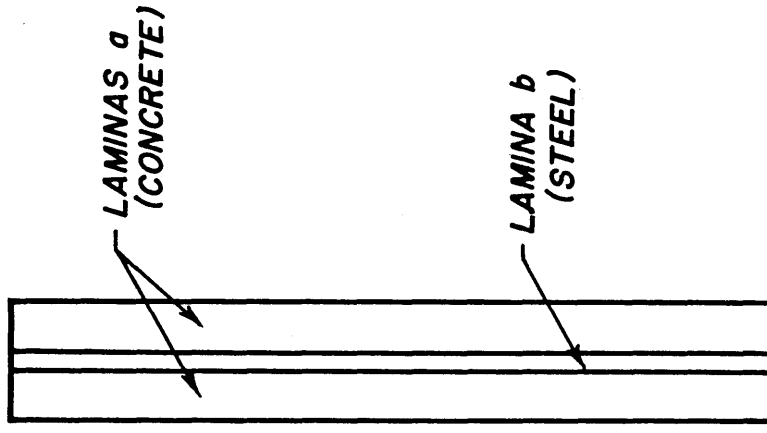


Figure 88 - Laminated Plate of Concrete and Steel

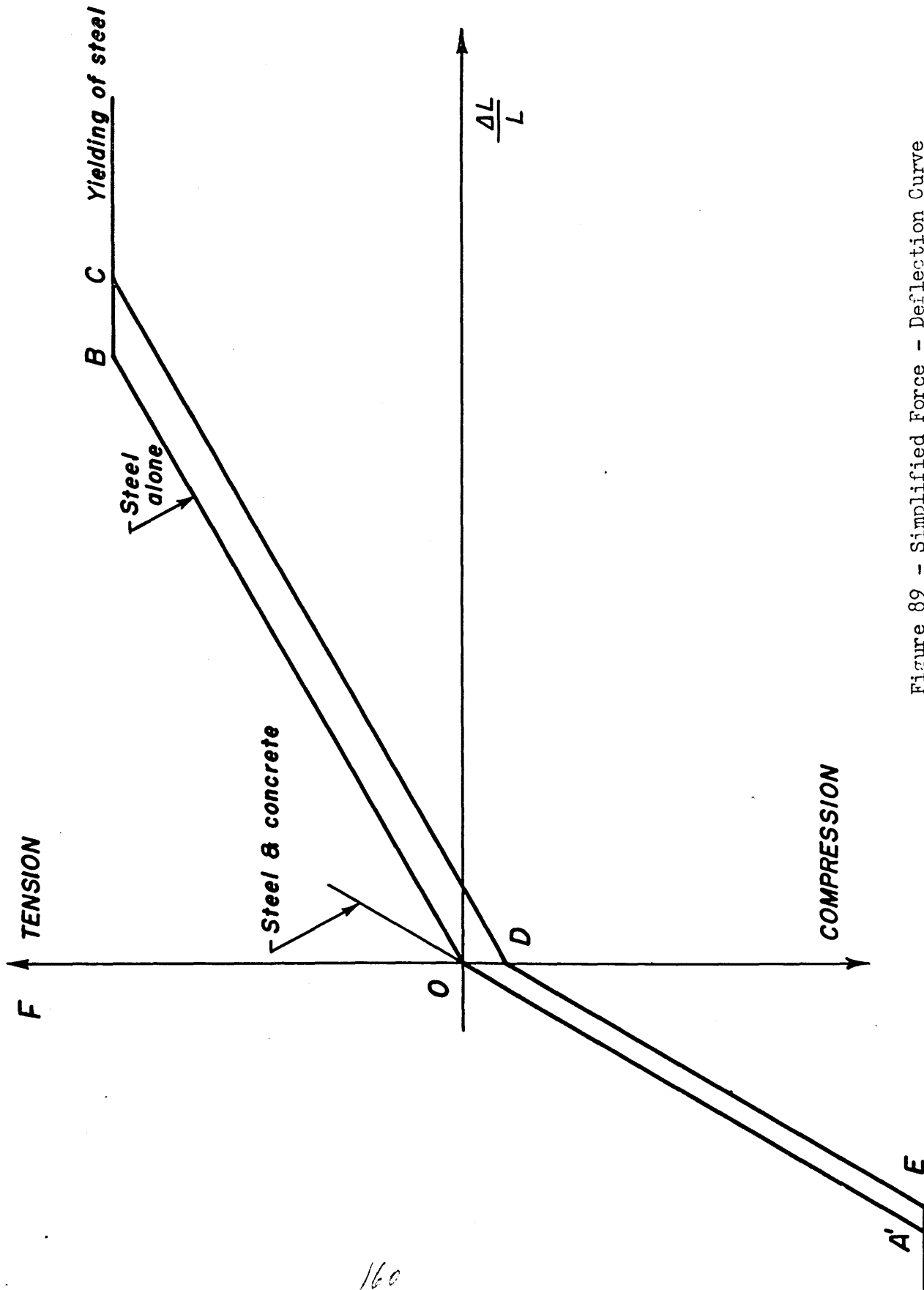


Figure 89 - Simplified Force - Deflection Curve of a Reinforced Concrete Bar

160

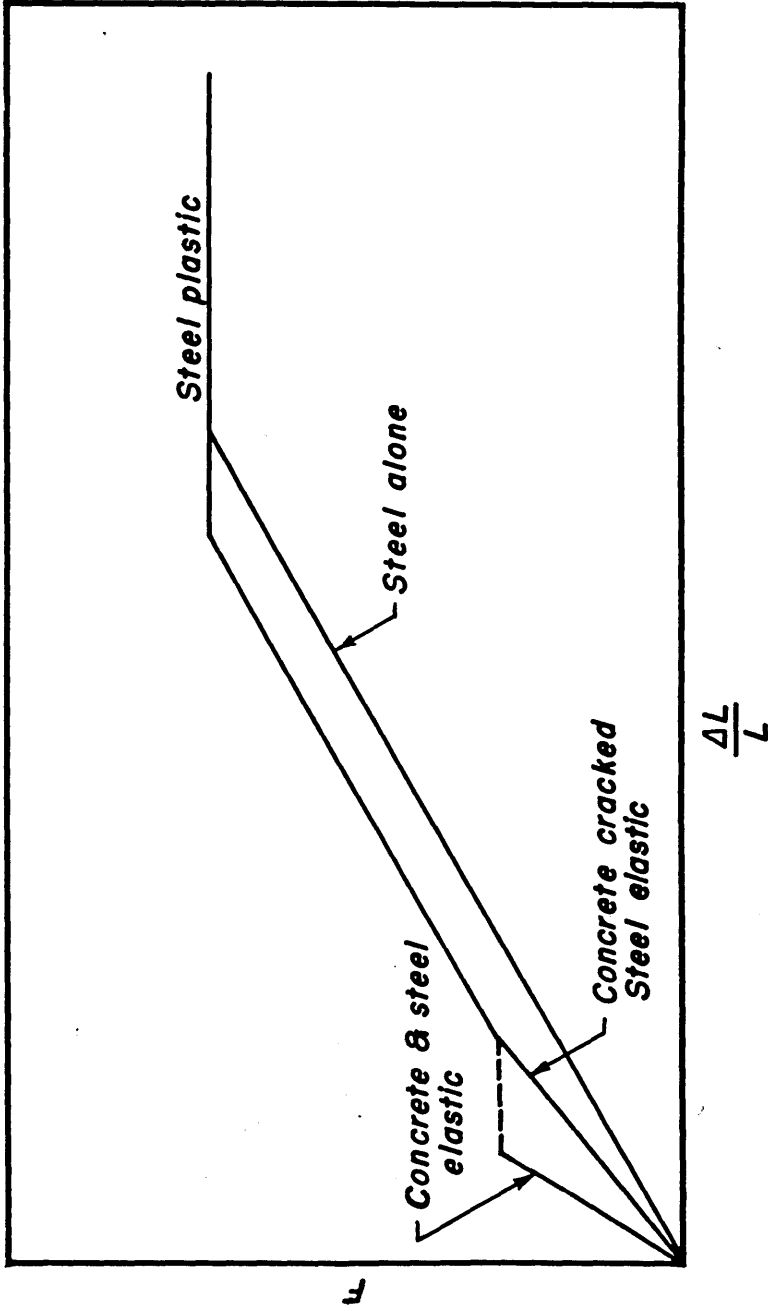


Figure 90 - Simplified Force-Deflection Curve of a Reinforced Concrete Bar - including collaboration of concrete between cracks

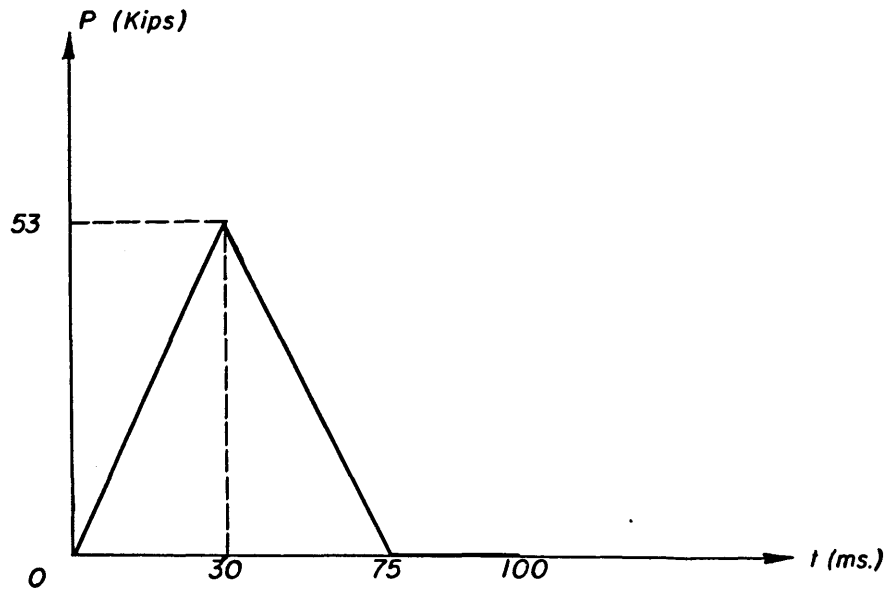


Figure 91 Applied Load Curve

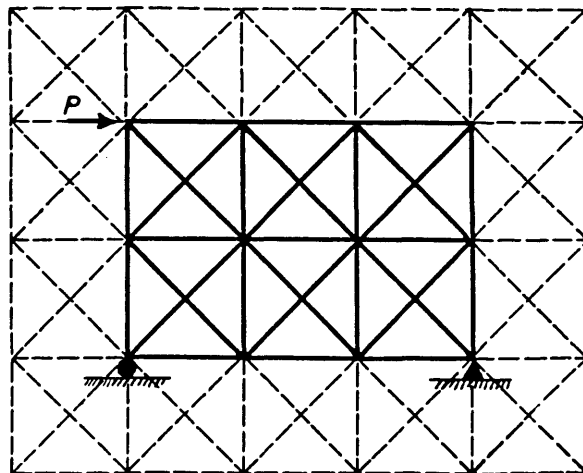


Figure 92 Dynamic Model

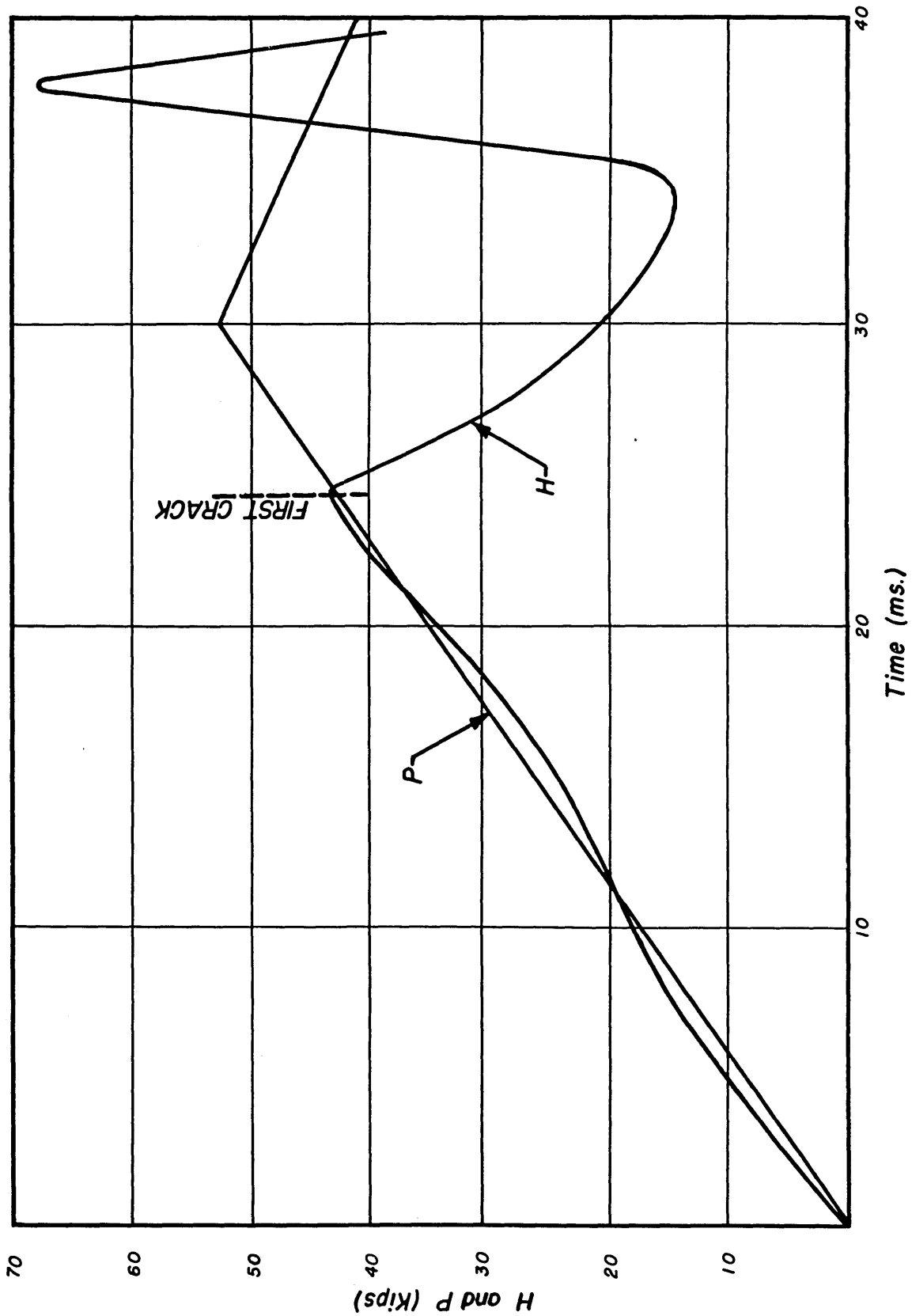


Figure 93 - Horizontal Reaction vs Time

163
7/6/72

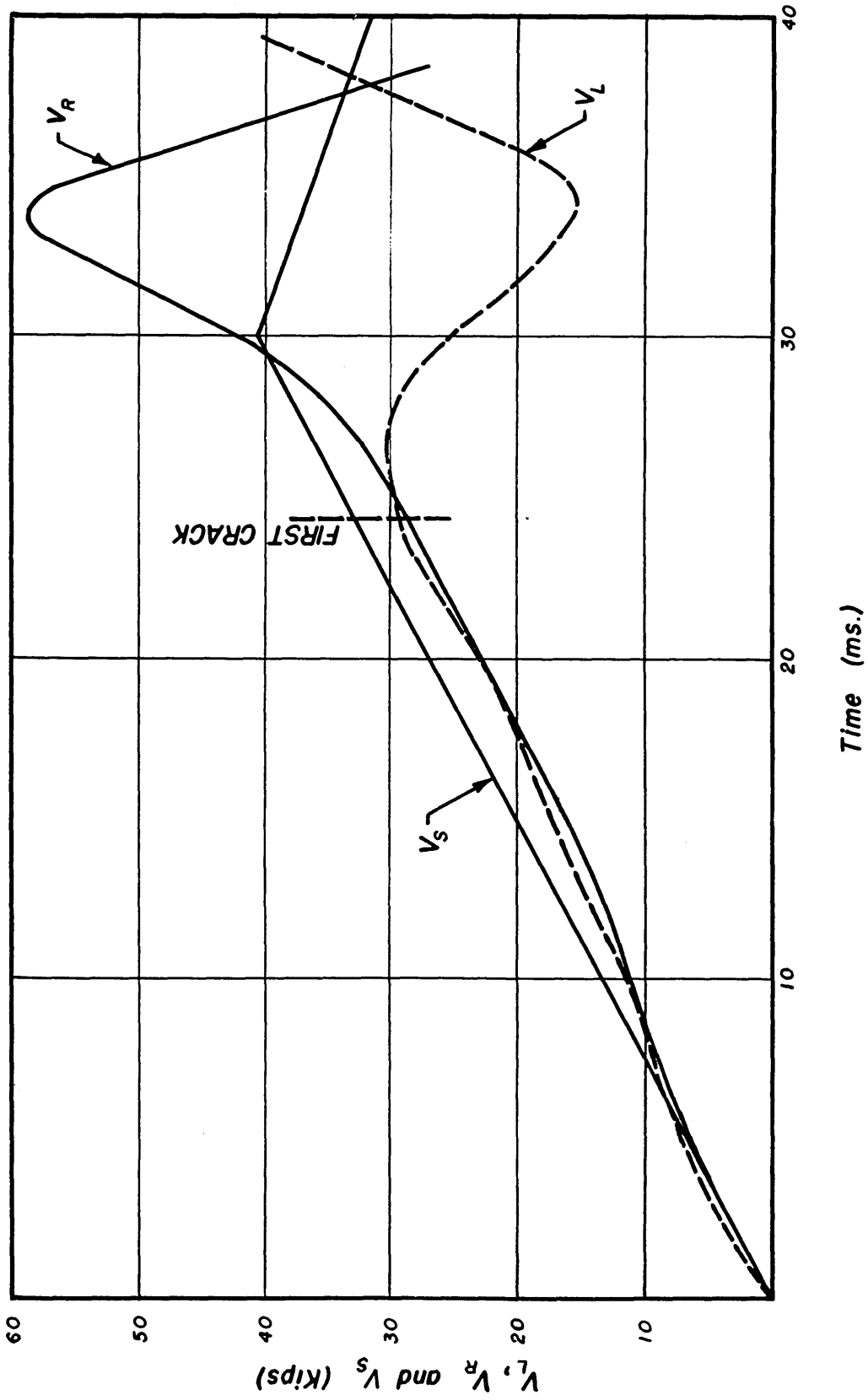


Figure 94 - Vertical Reactions vs Time

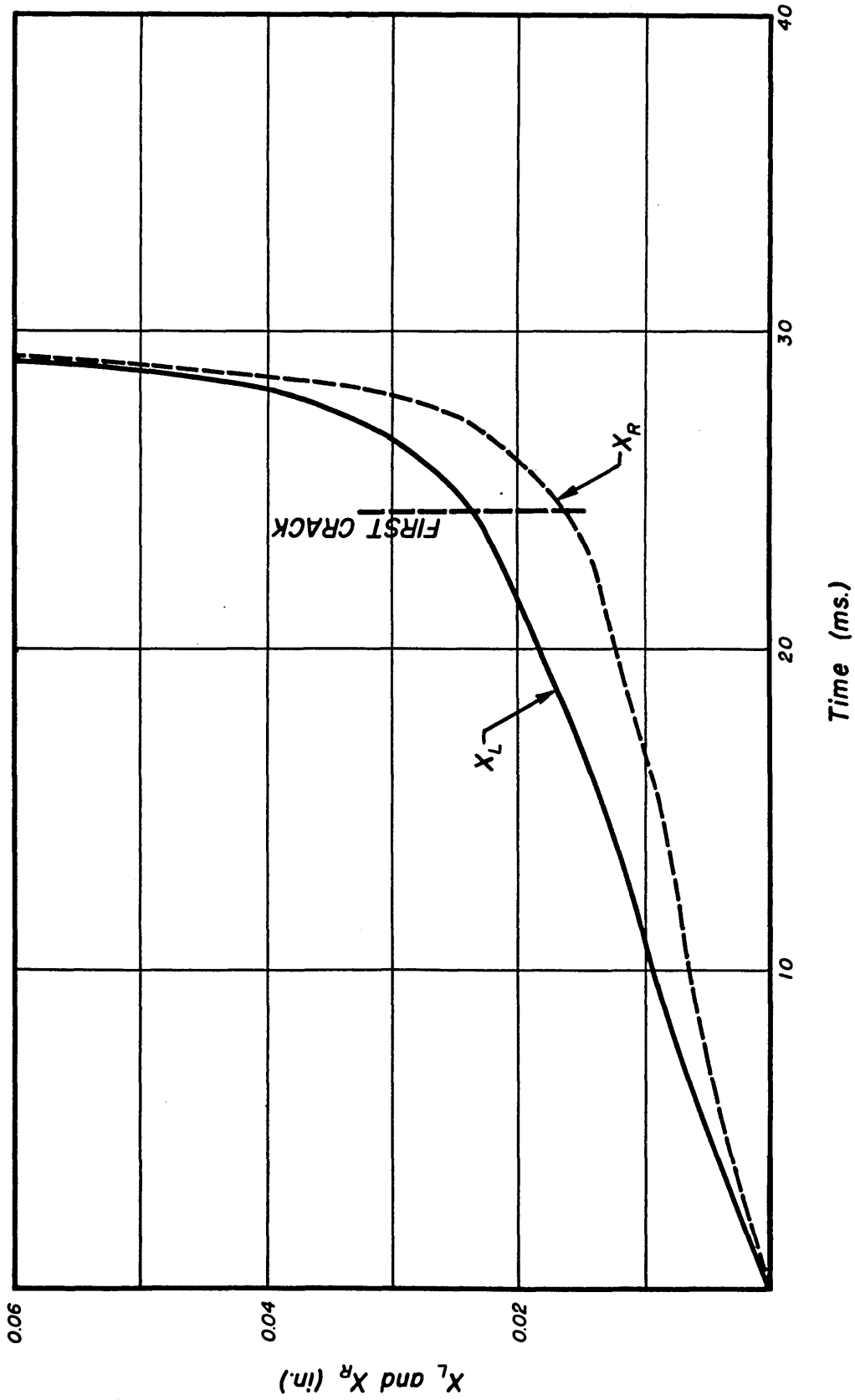


Figure 95 - Horizontal Displacements vs Time

165

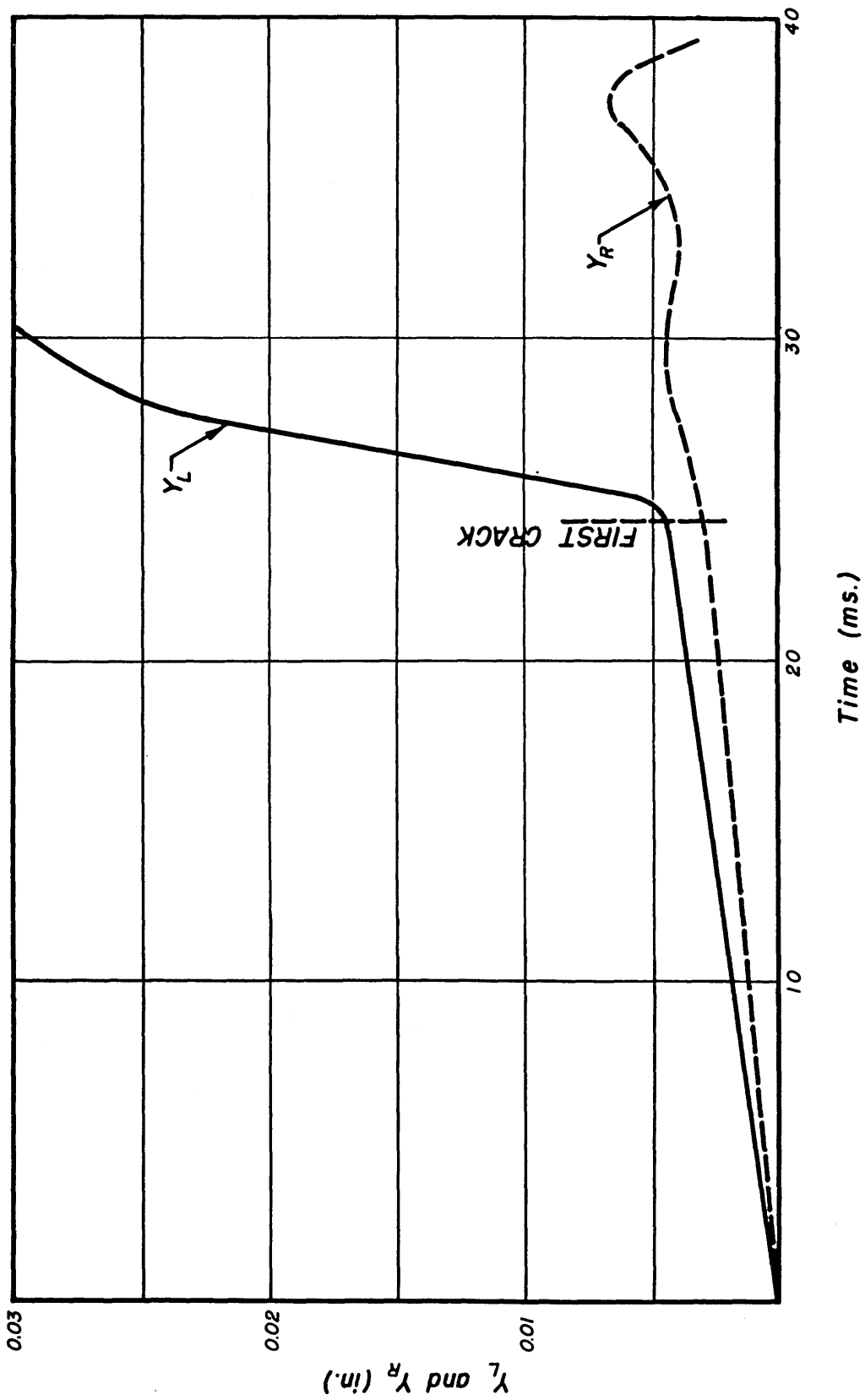


Figure 96 - Vertical Displacements vs Time.

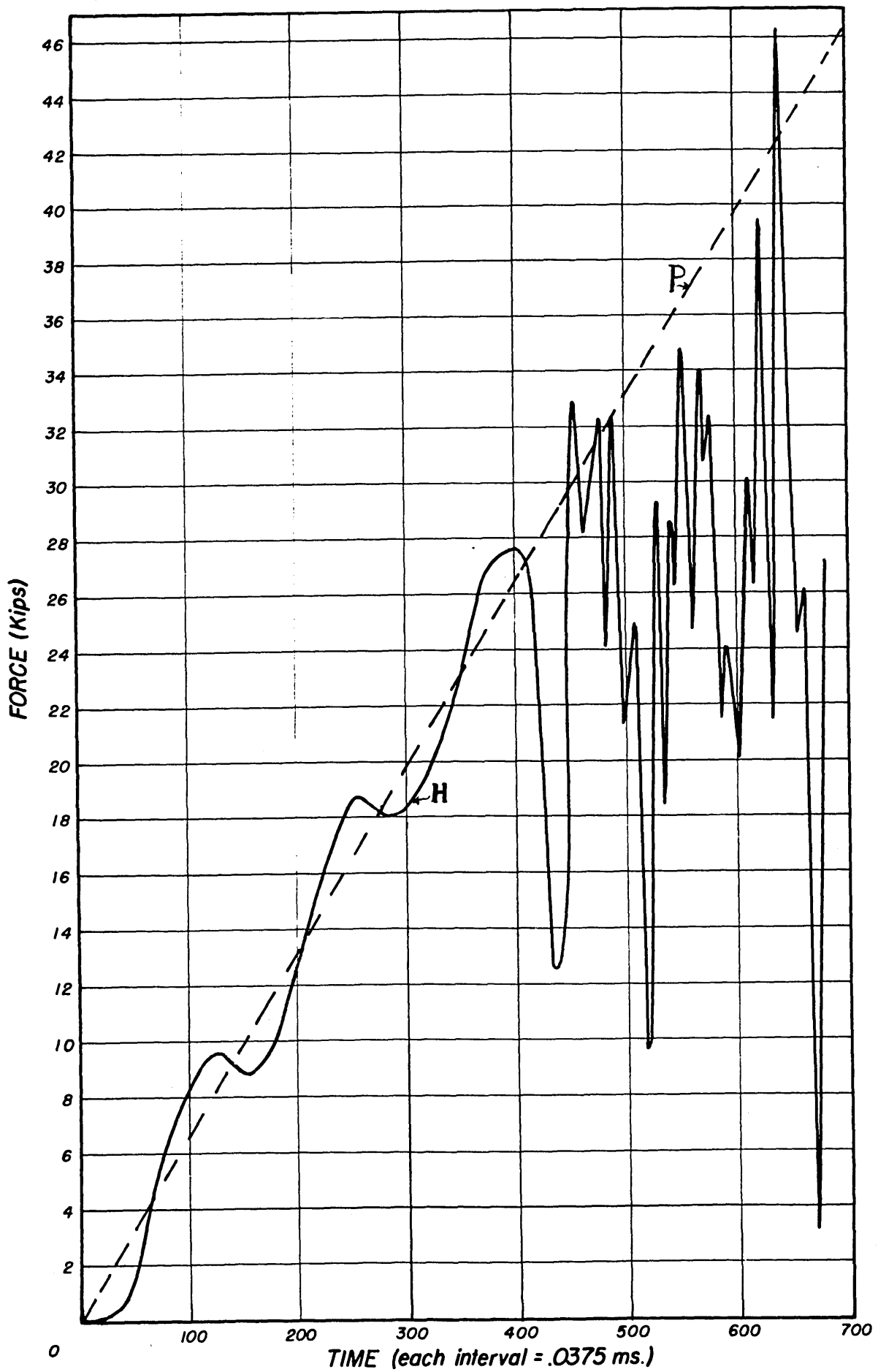


Figure 97 - Horizontal Reaction vs Time

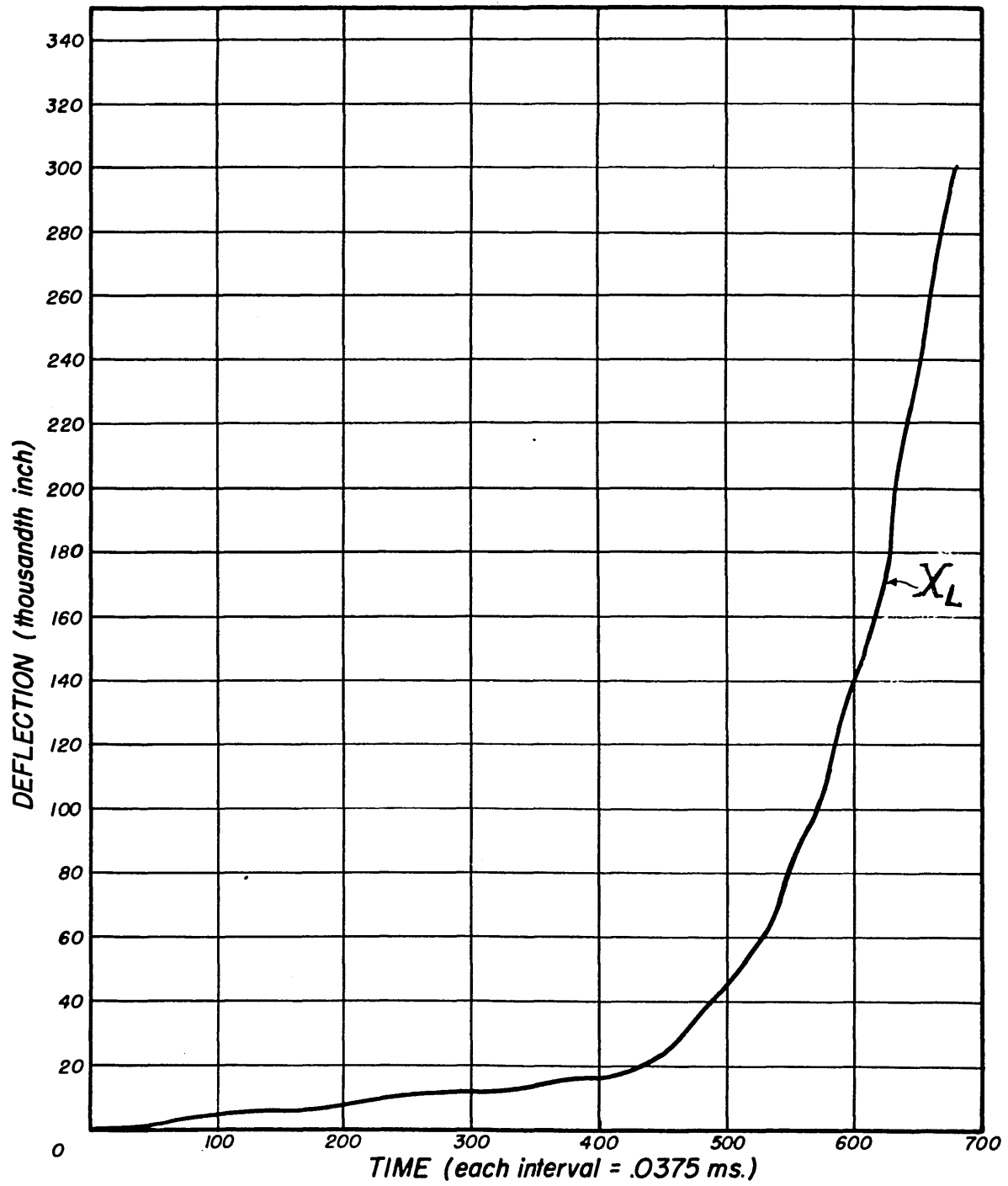


Figure 98 - Horizontal Displacements vs Time

168 g.

APPENDIX A
GENERAL PROGRAM AND CODING FOR
WHIRLWIND I

As it was established in Chapter VI, the writing of the general program and coding for Whirlwind I was undertaken by Mr. Shui-Ho, and the following description is a summary of his work.

NOMENCLATURE

In this appendix the following nomenclature is employed.

- a = side of the square grid
- A_2 = transformed net area of bounding beam of column.
- E_c = modulus of elasticity of concrete.
- h = time interval from t_{n-1} to t_n , or t_n to t_{n+1} , etc.
- K_d = spring stiffness of diagonal bar.
- K_e = spring stiffness of exterior bar.
- K_i = spring stiffness of interior bar.
- m = mass of the particle considered.
- M = mass of the mass point.
- P_q = the component force of the mass point in the q direction.
- P_n = value of the applied load on the mass point at time t_n in that direction, etc.
- q = the independent displacement coordinate of the mass point.
- q_n = displacement at time t_n .
- q_{n+1} = displacement at time t_{n+1} .
- q_{n-1} = displacement at time t_{n-1} .

- \dot{q}_{n+1} = velocity of the mass point at time t_{n+1} in that direction, etc.
- \ddot{q}_{n+1} = acceleration of the mass point at time t_{n+1} in that direction, etc.
- R_q = the component of resisting force on the mass point in the q-q direction generated by the displacement of all mass points.
- R_{n+1} = value of developed resistance on the mass point at time t_{n+1} in that direction, etc.
- t = transformed wall thickness.
- t_{n-1}, t_n, t_{n+1} = three successive values of independent time variable.

I. LATTICE ANALOGY FOR ELASTIC BEHAVIOR OF REINFORCED CONCRETE SHEAR WALLS

A. Dynamic Analogy

According to the lattice analogy method, the wall is replaced by a pin connected lattice (truss). In order for the lattice unit in Figure A-1(b) to be equivalent to the plate unit in Figure A-1(a) the following conditions must be satisfied:

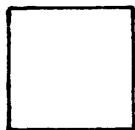


Figure A-1(a)

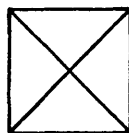


Figure A-1(b)

- 1) The deformations of the units must be the same under direct uniform stress.
- 2) The deformation must be the same under the Poisson's ratio effect.
- 3) The deformation must be the same under a pure shear loading condition.
- 4) The deformation must be the same under a pure moment loading condition.

As the wall is subjected to dynamic loads it is necessary to replace the equivalent lattice with massless springs and masses. A simplified model

was shown in Figure 87(b). The continuous distribution of the actual system is approximated by a number of concentrated masses, and these masses are coupled by interconnecting weightless springs. For a square grid assuming that the Poisson's ratio equal to one-third and neglecting the effect of pure moment, as shown in Mr. Finerman's report (21) the spring stiffnesses can be found as:

$$K_i = 3/4 \cdot t \cdot E_c \quad (A-1)$$

$$K_e = \left(3/8 t + \frac{A_2}{a} \right) E_c \quad (A-2)$$

$$K_d = 3/8 t \cdot E_c \quad (A-3)$$

B. Equation of Motion

The equation of motion for each mass point can be developed from the dynamic equilibrium as:

$$P_q + R_q - m(\ddot{q}) = 0 \quad (A-3)$$

If the x and y directions are chosen as the two independent coordinates to specify the location of the mass point at any instant, the resisting bar forces at the mass point can be derived as follows and according to Figure A-2.

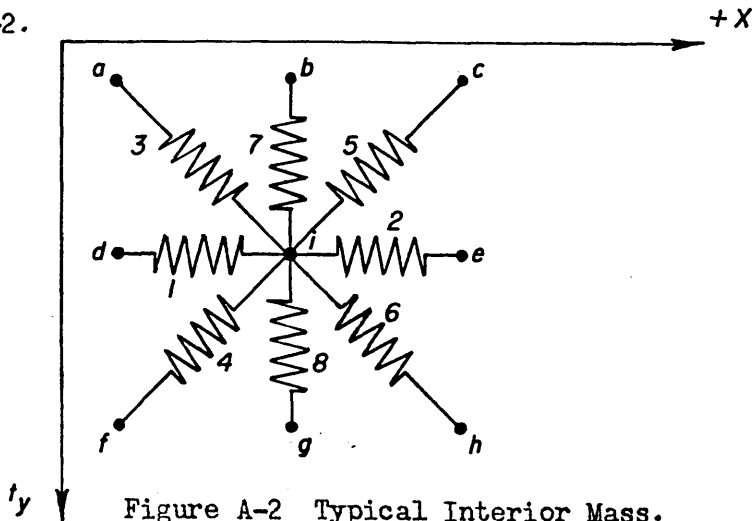


Figure A-2 Typical Interior Mass.

$$F_1 = K_1 [x_i - x_d] \quad (A-4)$$

$$F_2 = K_2 [x_e - x_i] \quad (A-5)$$

$$F_3 = K_3 [(x_i - x_a) + (y_1 - y_a)] \quad (A-6)$$

$$F_4 = K_4 [(x_i - x_f) + (y_f - y_1)] \quad (A-7)$$

$$F_5 = K_5 [(x_c - x_i) + (y_1 - y_c)] \quad (A-8)$$

$$F_6 = K_6 [(x_h - x_i) + (y_h - y_i)] \quad (A-9)$$

$$F_7 = K_7 [y_i - y_b] \quad (A-10)$$

$$F_8 = K_8 [y_g - y_i] \quad (A-11)$$

In the above equations, effective diagonal spring stiffness (equal to half the actual stiffness) is implied and only components of force rather than total force are considered. The two equations defining the horizontal and vertical motion of the interior mass point are:

$$P_x + R_x - m(\ddot{x}) = 0 \quad (A-12)$$

$$P_y + R_y - m(\ddot{y}) = 0 \quad (A-13)$$

where

$$R_x = -F_1 + F_2 - F_3 - F_4 + F_5 + F_6 \quad (A-14)$$

$$R_y = -F_7 + F_8 - F_3 + F_4 - F_5 + F_6 \quad (A-15)$$

C. Numerical Integration

The open type formula used to predict the value in the succeeding time interval was the Acceleration Impulse Equation

$$q_{n+1} = 2q_n - q_{n-1} + (h)^2 \ddot{q}_n \quad (A-16)$$

and the closed type formula used to correct the predicted value was the Linear Acceleration Equation

$$q_{n+1} = q_n + \dot{q}_n(h) + \frac{h^2}{6} (2 \ddot{q}_n + \ddot{q}_{n+1}) \quad (A-17)$$

where if t_{n-1}, t_n, t_{n+1} = three successive values of independent time variable

q_{n+1} = displacement at time t_{n+1}

q_n = displacement at time t_n

q_{n-1} = displacement at time t_{n-1}

\dot{q}_{n+1} = velocity at time t_{n+1}

\ddot{q}_{n+1} = acceleration at time t_{n+1}

h = time interval from t_{n+1} to t_n , or t_n to t_{n+1} , etc.

D. Principal Tensile Stress

The cracking stress of concrete varies between $0.06(f'_c)$ and $0.10(f'_c)$ for statically applied loads. With f'_c equal to 3000 psi, a criterion stress of 400 psi is adopted as the dynamic cracking stress.

The principal tensile stress at the segment center can be obtained directly from the displacement as

$$\sigma_m = \frac{\sigma_x + \sigma_y}{2} + \left[\left(\frac{\sigma_x - \sigma_y}{2} \right)^2 + (\tau_{xy})^2 \right]^{1/2} \quad (A-18)$$

For a Poisson's ratio equal to one-third, the corresponding stresses can be expressed as

$$\sigma_x = \frac{3E_c}{8} (3\epsilon_x + \epsilon_y) \quad (A-19)$$

$$\sigma_y = \frac{3E_c}{8} (3\epsilon_y + \epsilon_x) \quad (A-20)$$

$$\tau_{xy} = \frac{3E_c}{8} \gamma_{xy} \quad (A-21)$$

where according to Figure A-3

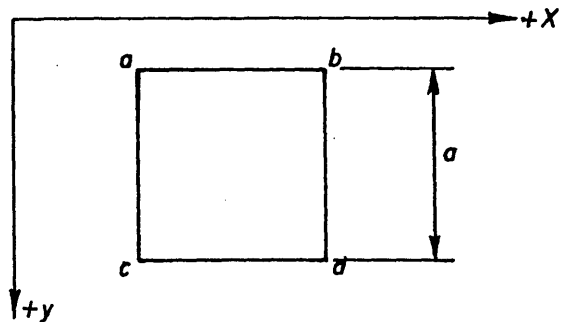


Figure A-3. Typical Plate Segment

$$\epsilon_x = \frac{1}{2a} \left[(x_b - x_a) + (x_d - x_c) \right] \quad (\text{A-22})$$

$$\epsilon_y = \frac{1}{2a} \left[(y_c - y_a) + (y_d - y_b) \right] \quad (\text{A-23})$$

$$\gamma_{xy} = \frac{1}{2a} \left[(x_c - x_a) + (x_d - x_b) + (y_b - y_a) + (y_d - y_c) \right] \quad (\text{A-24})$$

In general the first crack may occur at the center of any segment or in the most highly stressed tension column. The stresses at the tensile column can be found from the equation

$$\sigma_t = \frac{E_c}{a} (y_d - y_b) \quad (\text{A-25})$$

II. LATTICE ANALOGY FOR CRACKED REINFORCED CONCRETE WALLS

According to what was established in Chapter VI, after cracking has occurred, assuming 45° crack, all bars except the diagonal which is parallel to the crack will be modified based on the reinforcing steel of the wall unless the bar is subjected to compressive force. For the diagonal which is parallel to the crack, bar area will be reduced only if the tensile stress exceeds the allowable cracking value.

III. PLANNING FOR THE WHIRLWIND I PROGRAM

Before coding a program, it is essential to lay out the major routines of the complete program and all the equations involved.

The major operations of the program are as follows.

A). "Compute load P_n for use in acceleration impulse equation"

As the load curve may not be represented by formulas, it is decided to store the value of load for each time interval in the computer memories. Instead of computing the load from formulas, the computer will pick up the proper value of the applied load from the memories at each time interval.

B). "Predict the deflection q_{n+1} for each mass point from the acceleration impulse equation"

$$q_{n+1} = 2 q_n - q_{n-1} + (h)^2 \ddot{q}_n$$

where

$$\ddot{q}_n = \frac{P_n}{M} + \frac{R_n}{M}$$

The values of q_{n+1} can be obtained directly from this equation. For the loaded mass point, P_n can be picked up from the computer memories while for all other mass points P_n will be equal to zero. At the first time interval, use $P_0 = \frac{P_1}{6M}$ instead of $P_0 = 0$ to balance the error introduced by assuming $q_{n-1} = 0$ in the equation. After computing the value q_{n+1} for each mass point in the x direction, repeat the operations and compute the value q_{n+1} for each mass point in the y direction.

C). "From the predicted values of q_{n+1} calculate the resistances R_{n+1} for each mass point"

The spring forces between the masses are calculated from the deflections according equations (A-4) to (A-11) and the resistances R_{n+1} for each mass point can be obtained from equations (A-14) and (A-15).

The analysis involved is rather tedious after cracking has occurred. For convenience in programming, the analysis is broken down into several portions.

As discussed in Chapter VI after stress in center of a segment exceeds the cracking stress of concrete, all bar areas of the lattice segment except the diagonal which is parallel to the crack will be reduced. It is not likely that compression failure will appear in the shear wall; in order to simplify the analysis, straight line relationship of force against elongation is assumed for each individual spring as shown in Figure A.4 where

ab - represents the force-elongation curve of the bar before cracking.

The bar area is based on the transformed area of the plate segment.

bc - represents the state of cracking. When the stress at center of segment exceeds the cracking stress of concrete, the bar area is reduced and the bar force drops down from point b to c.

cd - represents the force-elongation curve of the cracked bar.

de - represents the state of plastic elongation of the cracked bar.

ef - represents the force-elongation curve of the cracked bar after the plastic elongation.

fg - represents the force-shortening curve of the bar. When the gap of the crack is less than zero (i.e. $e = 0$), the bar force is in compression and the cracked bar will behave as an uncracked element.

gh - represents a state of plastic shortening of the bar.

hi - represents the force-shortening curve of the bar after the plastic shortening.

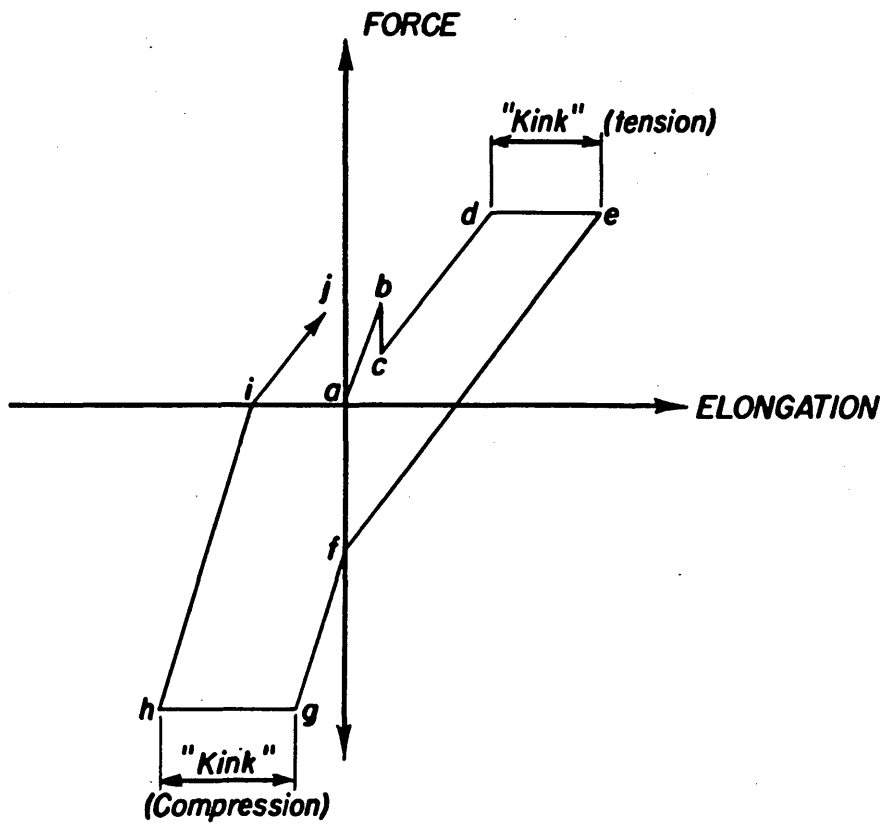


Figure A.4 - Typical Force-Elongation Curve I

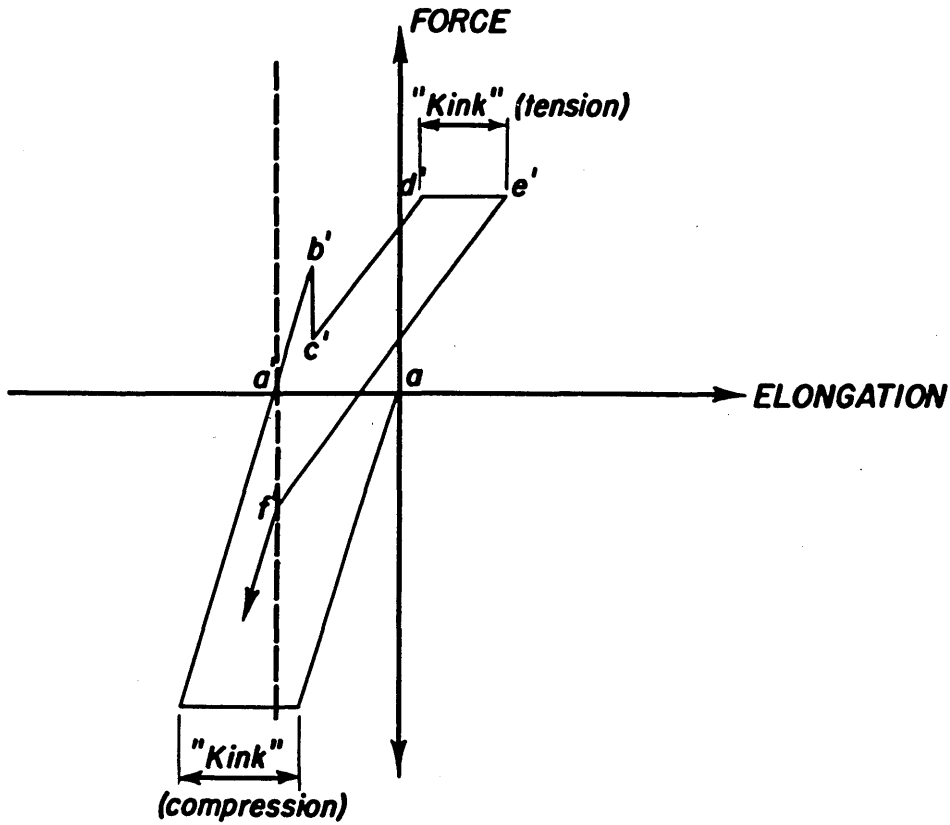


Figure A.5 - Typical Force-Elongation Curve II

ij - represents the force-elongation curve of the cracked bar. The bar force is in tension and the bar will behave as a crack element again.

If plastic shortening has occurred before cracking starts, the force elongation curves will have the same shape except that the origin "a" will move to point "a'" as shown in Figure A-5. For the diagonal which is parallel to the crack, the cracking state (bc) in Figure A-4) will depend on the tensile force at the bar instead of the stress at the center of the segment.

1st Resistance Routine for Horizontal Lattice Bar

As shown in Figure A-6 the horizontal lattice bar between the masses consists of two independent springs. The upper spring represents the equivalent resistant force in the upper segment and the lower spring represents the equivalent force in the lower segment.

For lattice bar at the edge, the outer spring will represent the equivalent resistance force of the bounding beam. For each lattice bar, the following storages are required from the computer memories.

- a - storage to store the value of "kink" (compression) for the whole lattice bar.
- b - storage to store the value of "kink" (tension) for each spring.
- c - storage to store the index for each spring indicating whether the spring is in plastic or elastic condition.
- d - storage to store the index for the edge spring indicating whether the bounding beam is cracked or not. This storage is required for the lattice bar at the edges only.

In the following discussion tensile forces are taken as positive bar forces; subsequently the "kink" (tension) will be a positive value. The operations involved in this portion of the routine are:

- a) Assuming no crack has occurred compute bar force between the two horizontal masses from the equation

$$F = K_L \left[x_b - x_a - \text{"Kink" (compression)} \right]$$

where K_L is the spring stiffness of the whole lattice bar and kink (compression) is a negative value.

- b) If the bar force is in compression, compare this value with the allowable compressive force for the bar:

- 1) If still remains in elastic condition, no correction is required.
- 2) If newly plastic, reduce the bar force to the allowable value.
- 3) If already plastic since the last time interval, reduce the bar force to the allowable value and compute the value of "kink" (compression).

- c) If the bar force is in tension, check each spring independently.

- 1) If no crack occurred in the corresponding segment (or bounding beam) except for the edge spring, no correction is necessary. For edge spring, compare the spring force with the cracking tensile force for the bounding beam; no modification if cracking has not taken place. Otherwise reduce the spring area (stiffness) and recompute the spring force.
- 2) If crack has occurred in the corresponding segment (or bounding beam), reduce the spring area (stiffness) and re-compute the spring force. Compare this value with the allowable tensile force for the modified spring.

- i) if still remains in elastic condition, no further correc-

tion is required.

ii) if newly plastic, reduce the spring force to the allowable value.

iii) if already plastic since the last time interval, reduce the spring force to the allowable value and compute the value of "kink" (tension) for the spring.

3) Correct the bar force with the modified spring forces.

d) A counting system set up for the above operations to compute force at each horizontal lattice bar.

2nd Resistance Routine for Vertical Lattice Bar

This portion of routine is about the same as for the horizontal lattice bar except that the system concerned is in the vertical direction.

3rd Resistance Routine for Diagonal Lattice Bar

For each diagonal bar only one spring is implied and the storages required from the computer memories are

- a) Storage to store the value of "kink" (compression) for the bar.
- b) Storage to store the value of "kink" (tension) for the bar.
- c) Storage to store the index indicating whether the bar is in plastic or elastic condition.
- d) Storage to store the index indicating whether the bar is cracked or not.

The following operations are involved in this portion of the routine:

- a) Assuming no crack has occurred compute the diagonal bar force from the equation (see Figure A-6)

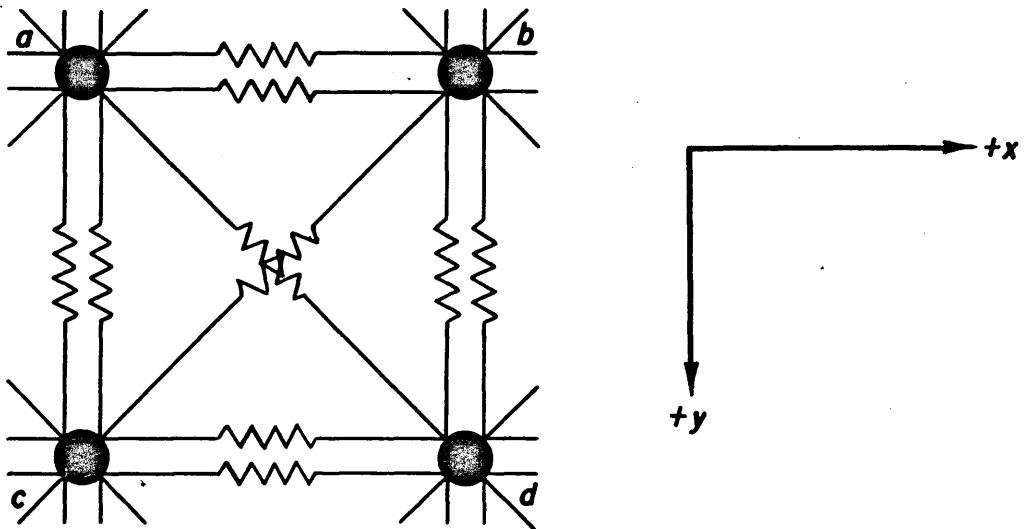


Figure A.6 - Typical Interior Lattice Segment

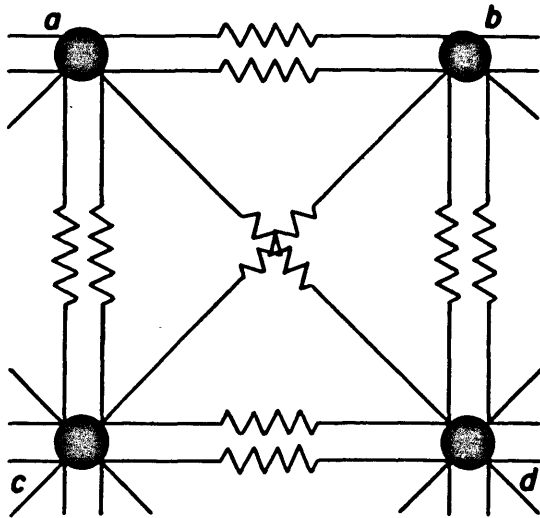


Figure A.6 - Typical Exterior Lattice Segment

$$F = K_L \left[(x_d - x_a) + (y_d - y_a) - \text{"kink" (compression)} \right]$$

- b) If the bar force is in compression, compare this value with the allowable compressive force of the bar.
- i) If still remains in elastic condition, no correction is required.
 - ii) If newly plastic, reduce the bar force to the allowable value.
 - iii) If already plastic since the last time interval, reduce the bar force to the allowable value and compute the value of "kink" (compression).
- c) If the bar force is in tension and no crack has occurred in the segment, no correction is required.
- d) If the bar force is in tension and crack has occurred in the segment, assuming that the direction of the crack is at 45 degrees:
- i) If the crack is parallel to this diagonal bar, compare the bar force with the cracking tensile force for the bar.
 - (1) If the bar force is greater than the cracking tensile force, no correction is required.
 - (2) If the bar force is greater than the cracking tensile force, the diagonal will crack and only the reinforcing steel contributes resisting force to the system. Reduce the bar area (spring stiffness) and re-compute the bar force.
 - ii) If the crack is perpendicular to this diagonal bar, reduce the bar area as the diagonal is cracked. Re-compute the bar force and compare this value with the allowable tensile force for the cracked bar:

- (1) If still remains in elastic condition, no further correction is required.
- (2) If newly plastic, reduce the bar force to the allowable value.
- (3) If already plastic since the last time interval, reduce the bar force to the allowable value and compute the value of "kink" (tension) for the bar.

e) A counting system setup for the above operations to all diagonal lattice bars.

D). "Compute load P_{n+1} for use in linear acceleration equations."

In this special case instead of computing the load from formulas, the computer will pick up the proper value of the applied load from the memories at time interval t_{n+1} .

E). "With the values of R_{n+1} and P_{n+1} , calculate the corrected values q_{n+1} for each mass point from the linear acceleration equation."

$$q_{n+1} = q_n + \dot{q}_n + \frac{h^2}{6} (2 \ddot{q}_n + \ddot{q}_{n+1})$$

where $\dot{q}_n = \dot{q}_{n-1} + h/2 (\ddot{q}_{n-1} + \ddot{q}_n)$

$$\ddot{q}_n = \frac{P_n}{M} + \frac{R_n}{M} \text{ and}$$

$$\ddot{q}_{n+1} = \frac{P_{n+1}}{M} + \frac{R_{n+1}}{M}$$

F). "Calculate the new values of resistance R_{n+1} for each mass point from the corrected values q_{n+1} , and compute the corrected values q_{n+1} again from the linear acceleration equation. Repeat this operation for three times."

G). "To store the values q_{n+1} , \dot{q}_{n+1} , \ddot{q}_{n+1} for use in the next time interval."

H). "Determine the stresses at the center of all segments: Compare these values with the cracking stress of concrete. If cracking has taken place compute direction of the crack."

The maximum principal stress at the segment is given by Eq. (A-18).

If cracking has taken place, compute and store the direction of the crack. The direction of crack is

$$\theta = \frac{1}{2} \tan^{-1} \frac{2\tau_{xy}}{\sigma_y - \sigma_x} \quad \text{where } \theta \leq \pm 90$$

and counterclockwise is considered as positive direction.

I). "Compute the stresses at the tensile column and compare these values with the cracking stress of concrete".

This is obtained from Eq. (A-25)

J). "With the values of resistance R_{n+1} and load P_{n+1} predict the deflection q_{n+2} for each mass point from the acceleration impulse equation."

i.e., start a new cycle of the above operations for the next time interval.

K). "Repeat the above operations until computer stops at certain specified deflection or after the dynamic load is over."

L). "Print out results"

- 1) Time
- 2) Applied Load
- 3) Horizontal support reaction
- 4) Vertical support reaction
- 5) Deflection in the x direction for each mass point
- 6) Deflection in the y direction for each mass point
- 7) The principal stresses at the center of the plate segments.

The direction and location of the cracks are also printed out at the last time interval to give a general picture of the cracked wall.

IV. CODING FOR THE WHIRLWIND I PROGRAM

A. General

Two systems of instructions are involved in the present high speed digital computer, Whirlwind I.

1) Whirlwind System. This system consists of the fundamental instructions to the computer. It is generally used in the counting system and used as index (e.g. indicating crack or plastic condition, etc.)

2) Comprehensive System. This system consists of the approved instructions for the computer. It is generally used as the arithmetical instruction in programming.

B. Storage Arrangement

The storage system of this program is shown in Figure A-7 and A-8). Contents of the storage are:

Comprehensive System

Registers x1	Horizontal displacements x
y1	Vertical displacements y
r1	Horizontal resistances $\frac{R_x}{M}$
r2	Vertical resistances $\frac{R_y}{M}$
x2	Horizontal displacements at previous time
y2	Vertical displacements at previous time
z1	Horizontal and vertical acceleration \ddot{x} and \ddot{y}
z2	Horizontal and vertical velocities times h, $\dot{x}(h)$ and $\dot{y}(h)$

e2 Principal tensile stresses
 e3 Direction of cracks
 e5 Horizontal bar forces
 e6 Vertical bar forces
 e7 Diagonal bar forces ($\theta = -45^\circ$)
 e8 Diagonal bar forces ($\theta = +45^\circ$)
 a1 "kink" (tension) for lower springs
 a2 "kink" (tension) for upper springs
 a3 "kink" (compression) for horizontal bars
 b1 "kink" (tension) for right springs
 b2 "kink" (tension) for left springs
 b3 "kink" (compression) for vertical bars
 Registers d1 "kink" (tension) for diagonals ($\theta = -45^\circ$)
 d2 "kink" (tension) for diagonals ($\theta = +45^\circ$)
 d3 "kink" (compression) for diagonals ($\theta = -45^\circ$)
 d4 "kink" (compression) for diagonals ($\theta = +45^\circ$)
 q3 Applied loads

Whirlwind System

Registers e4 Crack indexes for segments and bounding beams
 a4 Plastic indexes for lower springs
 a5 Plastic indexes for upper springs
 b4 Plastic indexes for right springs
 b5 Plastic indexes for left springs
 d5 Plastic indexes for diagonals ($\theta = -45^\circ$)
 d6 Plastic indexes for diagonals ($\theta = +45^\circ$)

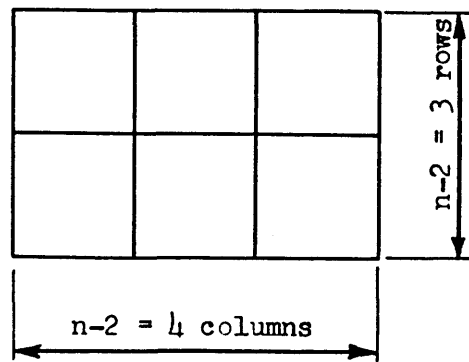
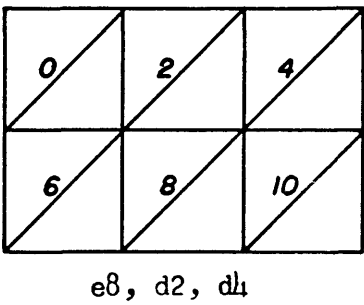
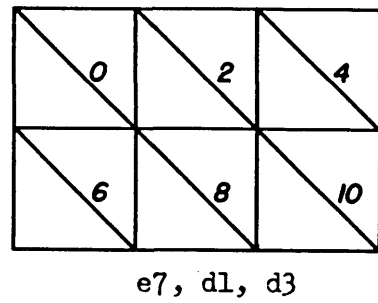
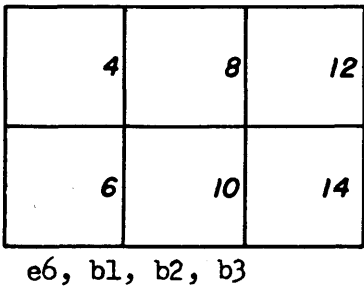
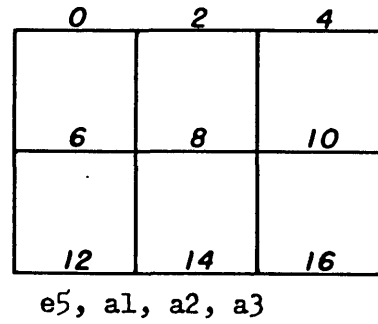
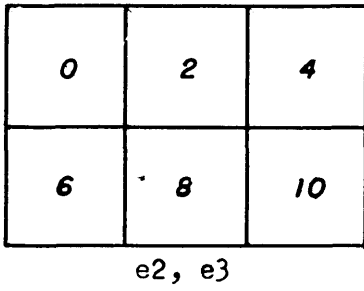
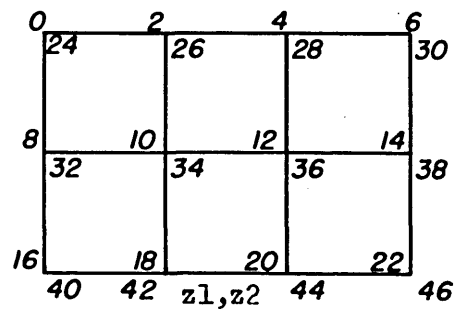
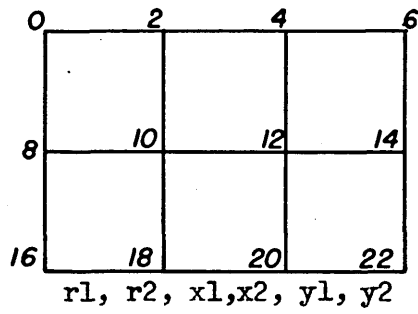
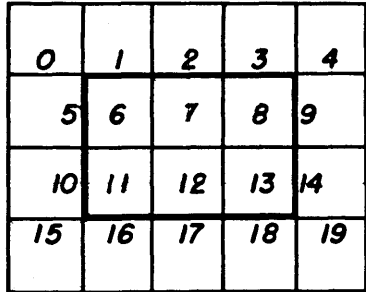
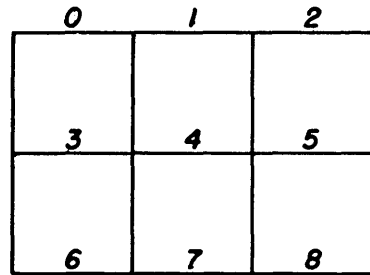


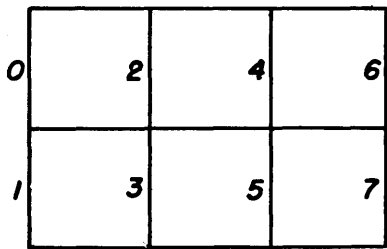
Figure A.7 - Details of the Storage Arrangement. Comprehensive System
(Each Number Occupies Two Registers)



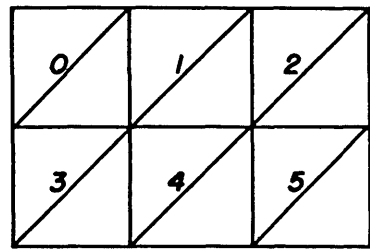
e4



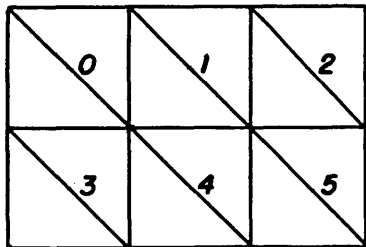
a4, a5



b4, b5



d6, d8



d5, d7

Figure A.8 - Details of the Storage Arrangement. Whirlwind System:
(Each Number Occupies One Register)

d7 Crack indexes for diagonals ($\theta = -45^\circ$)

d8 Crack indexes for diagonals ($\theta = +45^\circ$)

C. Field Arrangement

The computer core memory consists of six fields each of 1024 registers. The Whirlwind I computer is designed to operate with a full complement of 2048 registers of storage and combination of any two fields can be engaged at a time. In addition, huge memory called Auxiliary Drum is also available as extra storage.

In this program, all instructions and data are first stored in the Auxiliary Drum and will be distributed into six fields in the following order:

1) Group A (registers 0 - 1024):

- Field 0 The main program except the resistance routine.
- Field 2 Resistance routine, horizontal bar force computation.
- Field 3 Resistance routine, vertical bar force computation.
- Field 4 Resistance routine, diagonal bar force computation.
- Field 5 Resistance routine, resistance computation for mass points.

2) Group B (registers 1024 - 2048):

- Field 1 Constant and storage.

D. Overall Program (see Figure A-9)

Step A

Load Computation. Pick up P_n for use in acceleration impulse.

Proceed to Step B.

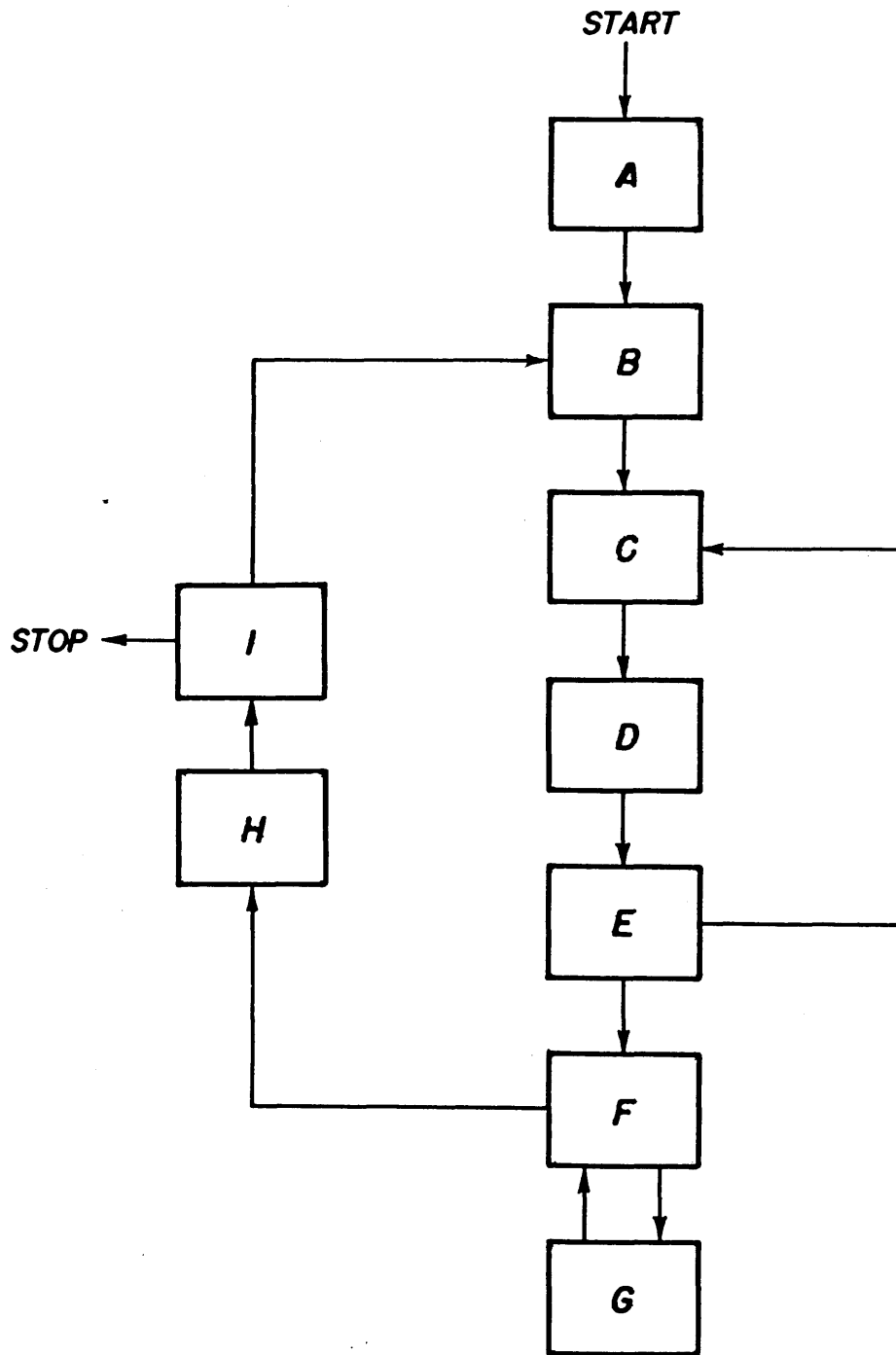


Figure A.9 - Block Diagram of Overall Program

Step B

Integration Routine. Predict q_{n+1} for each mass point from the acceleration impulse equation. Proceed to Step C.

Step C

Resistance Routine. Calculate R_{n+1} from the predicted values q_{n+1} for each mass point. Proceed to Step D.

Step D

Load Computation. Pick up P_{n+1} for use in linear acceleration equations. Proceed to Step E.

Step E

Integration Routine. Calculate the corrected values q_{n+1} for each mass point from the linear acceleration equation. Proceed to Step C to recorrect q_{n+1} . After performing this complete operation four times proceed to Step F.

Step F

Load Computation. Pick up P_{n+1} for use in acceleration impulse equations at next time interval. Proceed to step H. At every fourth time interval, before proceeding to Step H, enter Step G.

Step G

Print Out Subroutine. Print out the results of this time interval on the oscilloscope. Return to Step F.

Step H

Tensile Stress Computation. Compute the stresses at center of all segments. If cracking has taken place compute direction of the crack. Proceed to Step I.

Step I

Stopping Device. After the loading is over or if the wall fails, stop the computer and print out results. Otherwise, proceed to Step B.

E. Explanation of the Program

1) Load Computation

- m1 Compute $\frac{P_n}{M}$ for next time interval. Print out results and stop the computer at a specified time interval, if the loading is over.
- m2 Compute $\frac{P_{n+1}}{M}$.
- m3 Compute P_o ($= \frac{P_1}{6M}$). Used in the first time interval only.

2) Integration Routine

a) Acceleration Impulse Equation

- n1 Compute q_{n+1} from the equation.
- n3 A simplified routine for the first time interval to skip the unnecessary operations.
- n4 Counter for the mass point, check column.
- n5 Reset for next column and next row.
- n6 Counter for the mass point, check row.
- n8 Reset support deflections = 0.
- n7 Change field and proceed to the resistance routine.

b) Linear Acceleration Equation

- n2 Compute q_{n+1} from the equation.
- n10 Counter for the number of iterations (recorrection of q_{n+1}).
- n11 Counter for the mass point, check column.
- n12 Reset for next column and row.
- n13 Counter for the mass point, check row.

- n15 Reset n2.
- n16 Obtain resistance from the resistance routine.
- n17 Reset certain instructions for the fourth iteration.
- n18 Used in the fourth iteration only. Store $\dot{q}_{n+1}(h)$ and \ddot{q}_{n+1} .
- n19 Used in the fourth iteration only. Additional instructions for n12 when resetting n18 for next mass point.
- n20 After four iterations, reset the whole operation.

3) Resistance Routine

a) Horizontal Bar

- f1 Subroutine consists of all operations for a typical spring.
- f2 Subroutine of checking tensile stress for the edge spring.
- f3 Subroutine of checking compressive stress for the whole bar.
- a8 Compute bar force.
- a9 Counter for the bar, check column and row.
- a10 Reset for next column.
- a11 Reset for next interior row.
- a12 Reset for the bottom row.
- a13 Reset the whole operations. Change field and proceed to compute forces for the vertical bars.

b) Vertical Bar

- f4 Subroutine consists of all operations for a typical spring.
- f5 Subroutine of checking tensile stress for the edge spring.
- f6 Subroutine of checking compressive stress for the whole bar.
- b8 Compute bar force.
- b9 Counter for the bar, check column and row.
- b10 Reset for next row.

- b11 Reset for next interior column.
- b12 Reset for the right column
- b13 Reset the whole operation. Change field and proceed to compute forces for the diagonal bars.

c) Diagonal Bar

- f7 Subroutine consists of all operations for a typical bar.
- f8 Subroutine of checking tensile stress for the bar.
- f9 Subroutine of checking compressive stress for the bar.
- d11 Compute bar force.
- d12 Counter for the bar, check column and row. After completing computation for diagonals in one direction, reset the whole operation for diagonals in other direction.
- d13 Reset for next column.
- d14 Reset for next row.
- d15 Reset the whole operation. Change field and proceed to compute resistances.

d) Resistance Computation

- k2 Compute $\frac{R_x}{M}$ and $\frac{R_y}{M}$ at left upper corner.
- k3 Compute $\frac{R_x}{M}$ and $\frac{R_y}{M}$ for interior mass point at upper edge.
- k4 Counter for mass point at upper edge.
- k5 Compute $\frac{R_x}{M}$ and $\frac{R_y}{M}$ at right upper corner.
- k6 Reset k3 for next mass point.
- k7 Counter for the mass point, check row.
- k8 Compute $\frac{R_x}{M}$ and $\frac{R_y}{M}$ for mass point at left column.
- k9 Compute $\frac{R_x}{M}$ and $\frac{R_y}{M}$ for typical interior mass point

- k10 Counter for the typical interior mass point, check column.
- k11 Reset k9 for next mass point.
- k12 Compute $\frac{R_x}{M}$ and $\frac{R_y}{M}$ for mass point at right column.
- k13 Counter for the mass point, check and reset for next row.
- k14 Compute $\frac{R_x}{M}$ and $\frac{R_y}{M}$ at left lower corner.
- k15 Compute $\frac{R_x}{M}$ and $\frac{R_y}{M}$ for interior mass point at lower edge.
- k16 Counter for mass point at lower edge.
- k17 Compute $\frac{R_x}{M}$ and $\frac{R_y}{M}$ at right lower corner.
- k18 Reset k16 for next mass point.
- k19 Reset the whole operation. Change field and leave the resistance routine.

4) Tensile Stress Computation

- g1 Compute principal tensile stress.
- g2 LSR FU8 RAPID SQUARE ROOT SUBROUTINE.
- g3 Counter for the segment, check column.
- g4 Reset for next column.
- g5 Counter for the segment, check row.
- g6 Reset for next row.
- g8 Compute direction of cracks.
- g9 LSR FU7 ARC TANGENT SUBROUTINE.
- h1 Reset the whole operation. Check time interval, proceed to the print out routine at every fourth time interval.

5) Print Out Routine

- h2 Compute support reactions.

- h3 Reset the whole routine.
- p1 LSR OS4 SCOPE MRA DECIMAL FOMAT SUBROUTINE.
- p2 Counter for number of values to be printed.
- p3 Print out one value.
- p4 Reset for next value.
- p5 Set up the oscilloscope

6) Stopping Device

- m1 Stop the computer at the specified time interval when loading is over.
- g10 Stop the computer when deflection exceeds the specified value.

F. Preparation of Tapes

The program is introduced to the machine by means of punched tapes. For the details of the tape the reader is referred to the report of Mr. Shui Ho, "The Theoretical Analysis for the Dynamic Behavior of Shear Walls", Department of Civil and Sanitary Engineering of the Massachusetts Institute of Technology, May 20, 1957.

V. EQUIVALENT WALL PROPERTIES FOR THE DYNAMIC MODEL

Wall size: 66" x 44"

Grid size: 22" x 22"

Areas: Top edge and columns = 32.5 in²
 Bottom edge = 80.25 in²

Columns: Interior segment = 22 x 22 x 2 = 968 in³
 Exterior segment = 1/2 x 968 + 22 x 32.5 = 1199 in³
 Bottom segment = 1/2 x 968 + 22 x 80.25 = 2249.5 in³
 Bottom corner = 1/4 x 968 + 22 x 1/2 (32.5 + 80.25) = 1482.25 in³
 Upper corner = 1/4 x 968 + 22 x 32.5 = 957 in³

Masses: Interior segment = 968 x $\frac{.150}{12 \times 12 \times 12}$ x $\frac{1}{32.2 \times 12}$
 = 0.2174632 x 10⁻³ k-sec²/in

Exterior segment = 1199 x $\frac{.150}{12 \times 12 \times 12}$ x $\frac{1}{32.2 \times 12}$
 = 0.2693578 x 10⁻³ k-sec²/in

Bottom segment = 2249.5 x $\frac{.150}{12 \times 12 \times 12}$ x $\frac{1}{32.2 \times 12}$
 = 0.5053548 x 10⁻³ k-sec²/in

Bottom corner = 1482.25 x $\frac{.150}{12 \times 12 \times 12}$ x $\frac{1}{32.2 \times 12}$
 = 0.3329905 x 10⁻³ k-sec²/in

Upper corner = 957 x $\frac{.150}{12 \times 12 \times 12}$ x $\frac{1}{32.2 \times 12}$
 = 0.2149920 x 10⁻³ k-sec²/in

Transformed thickness of wall: #2 at 9.8" c-c

$$p = \frac{As}{bd} = \frac{0.05 \text{ (one direction)}}{9.8 \times 2} = 0.00255102\%$$

$$E_c = 3000 \text{ k.s.i.}$$

$$n = 10$$

$$t_w = t \left[1 + (n-1) P_w \right] = 2 \left[1 + 9 \times 0.00255102 \right] = 2.0459184 \text{ in}$$

Transformed thickness of edge: $4\#4$

$$P_w = \frac{4 \times 0.2}{37.5} = 0.02133333\%$$

$$t_e = 7.5 (1 + 9 \times 0.02133333) = 8.939999775 \text{ in}$$

Transformed thickness of Bottom edge: $4\#4$

$$P_w = \frac{4 \times 0.2}{12 \times 7.5} = 0.008$$

$$t_b = 7.5 (1 + 9 \times 0.008) = 8.099999993 \text{ in}$$

Bar areas:

$$A_2 \text{ (edge)} = 8.939999775 \times 5 - 2.0459184 \times 2.5 = 39.585203 \text{ in}^2$$

$$A_2' \text{ (bottom edge)} = 8.099999993 \times 12 - 2.0459184 \times 4.875 = 87.2261477 \text{ in}^2$$

$$A_1 \text{ (interior)} = 3/8 \times a \times t_w$$

$$\text{Interior bar} = 2A_1 = 3/4 \times a \times t_w$$

$$\text{Exterior bar} = A_1 + A_2 = 3/8 \times a \times t_w + A_2$$

$$\text{Bottom bar} = A_1 + A_2' = 3/8 \times a \times t_w + A_2'$$

$$\text{Diagonal bar} = A_1 \times 2 = 3/8 \times a \times t_w \times 2$$

$$\text{Stiffnesses (concrete): } \frac{F}{e} = \frac{AE}{L}$$

$$\text{Interior spring} = 3/4 t_w B_c = 3/4 \times 2.0459184 \times 3000 = 4601.316 \text{ k/in}$$

$$\begin{aligned} \text{Exterior spring} &= (3/8 t_w + A_2/a) B_c = (3/8 \times 2.0459184 + 39.585203 \times \\ &1/22) \times 3000 = 7699.6404 \text{ k/in} \end{aligned}$$

$$\begin{aligned} \text{Bottom spring} &= (3/8 t_w + A_2'/a) B_c \\ &= (3/8 \times 2.0459184 + 87.2261477 \times 1/22) \times 3000 \\ &= 14196.9 \text{ k/in} \end{aligned}$$

$$\text{Diagonal spring} = 3/8 t_w E_c = 3/8 \times 2.0459184 \times 3000 = 2300.2582 \text{ k/in}$$

Effective stiffnesses (concrete):

Interior spring = 4601.3160 k/in

Exterior spring = 7699.6406 k/in

Bottom spring = 14196.1329 k/in

Diagonal spring = 1150.6291 k/in

Stiffnesses (steel):

Edge spring = $\frac{1}{22} \times 4 \times 0.2 \times 30000 = 1090.9091$ k/in

Typical interior spring = $1/2 (0.05 \times \frac{22}{9.8}) \times \frac{30000}{22} = 153.0612$ k/in

Effective stiffnesses (steel):

Edge spring = 1090.9091 k/in

Typical interior spring = 76.5306 k/in

Bottom spring = 1090.9091 k/in

Diagonal spring = 76.5306 k/in

Allowable compressive forces (concrete): $f_c' = 4000$ p.s.i. = 4 k.s.i.

Interior bar = $4 (2 \times 3/8 \times a \times tw)$

$$= 3 \times 22 \times 2.0459184$$

$$= 135.0306144 \text{ k}$$

Exterior bar = $67.5153072 + 39.585203 \times 4$

$$= 225.8561192 \text{ k}$$

Bottom bar = $67.5153072 + 87.2261477 \times 4$

$$= 416.419898 \text{ k}$$

Effective diagonal bar = $1/2 \times 135.0306144$

$$= 67.5153072 \text{ k}$$

Allowable tensile forces (concrete): $f_t' = 0.4$ k.s.i.

Top edge and columns = 39.585203×0.4

$$= 15.8340812 \text{ k}$$

$$\text{Bottom edge} = 87.2261477 \times 0.4$$

$$= 34.8904591 \text{ k}$$

$$\text{Effective diagonal bar} = (3/8 \times a \times tw) \times 0.4$$

$$= 6.7515307 \text{ k}$$

$$\text{Allowable tensile forces (steel): Panel} \text{ --- } f'_y = 39.3 \times 1.33 = 52.229 \text{ k.s.i.}$$

$$\text{Frame} \text{ --- } f'_y = 47 \times 1.33 = 62.51 \text{ k.s.i.}$$

$$\text{Edge spring} = 4 \times 0.2 \times 62.51$$

$$= 50.008 \text{ k}$$

$$\text{Bottom spring} = 50.008 \text{ k}$$

$$\text{Typical interior spring} = 1/2 \left(0.05 \times \frac{22}{9.8} \right) \times 52.229$$

$$= 2.9312194 \text{ k}$$

$$\text{Effective diagonal spring} = 2.9312194 \text{ k}$$

APPENDIX B

GENERAL PROGRAM AND CODING FOR IBM 704

The general programming and coding for IBM 704 was undertaken by Mr. Christopher Calladine and the following description is a summary of his work.

In its general structure, the program is similar to that described in Appendix A, and this discussion will only include points which may be considered as modification of the program described previously.

NOMENCLATURE

In this appendix the following nomenclature is used.

a = $1/2$ of the side of the square grid.

A_1 = side bar area per element = $3/4 at$.

A_d = diagonal bar area per element = $\frac{3}{4} \sqrt{2} at$.

A_E = edge bar area = $A_b \left[\frac{1 + (n-1) p_b}{1 + (n-1) p} \right]$

E = $E_c [1 + (n-1) p]$ is the transformed modulus of elasticity of the bars.

m = ρ_s / ρ_c = Density of Steel/Density of Concrete.

n = $\frac{E_s}{E_c}$ = Young Modulus for Steel/ Y.M. for Concrete.

p = proportional area of steel in wall each way.

t = wall thickness

A_b, p_b, A_s, b, d are defined in Figure B-1.

M_N = Mass of Central Element = $\rho_c 4a^2 t [1 + 2p(m-1)]$

M_B = Mass of Edge Element = $\rho_c \left\{ [A_b + at] 2a + (m-1) 2a \times [A_b p_b + at \cdot 2p] \right\}$

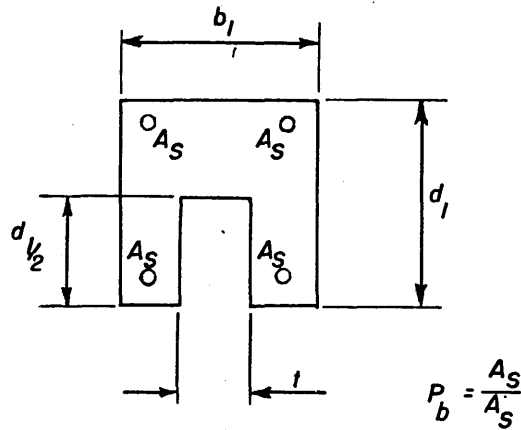


Figure B-1

$$M_C = \text{Mass of Corner Element} = \frac{M_N}{4} + \rho_c \left[(b_1 d_1 + b_2 d_2) a - \frac{d_1 a t}{2} - \frac{d_2 a t}{2} + \frac{d_1 d_2 t}{4} + (A_{s_1} + A_{s_2}) a (m-1) \right]$$

I. COMPUTATION OF THE ACCELERATIONS OF THE MASS-POINTS

A. Uncracked Wall

In order to compute the resistance R_{n+1} for each mass point from the predicted values of q_{n+1} (see item II, part C of Appendix A) the operator technique was used. This technique basically consists in the following:

Consider the system shown in Figure B-2, whose members are unstrained and whose mass point may be considered to be undeflected.

If the eight external mass-points are held fixed and the central point is moved a small distance in the x direction, the following forces will act upon the fixed mass points.

Point 1 :	$x_0/4a$	$A_d E$	in direction	1-9
3 :	$x_0/4a$	$A_d E$	in direction	9-3
4 :	x_0/a	$A_1 E$	in direction	9-4
5 :	$x_0/4a$	$A_d E$	in direction	9-5

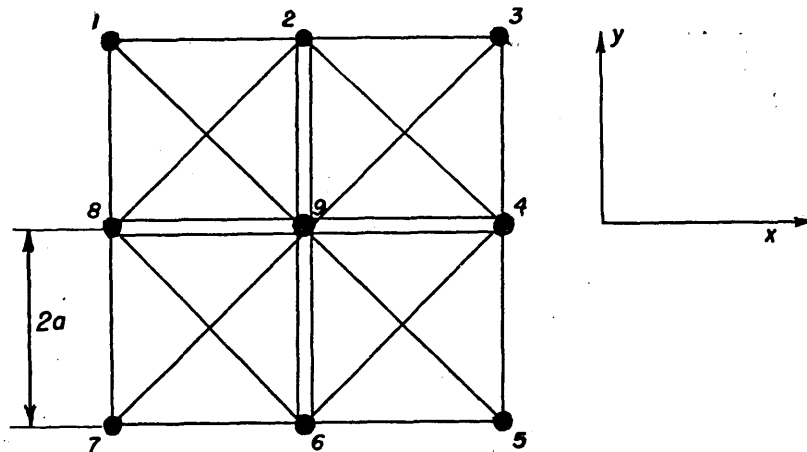


Figure B-2

$$\begin{aligned}
 7 &: x_9/4a \quad A_d \quad E \quad \text{in direction} \quad 7-9 \\
 8 &: x_9/a \quad A_1 \quad E \quad \text{in direction} \quad 8-9 \\
 9 &: 2x_9/a \quad A_1 \quad E + \frac{x_9}{\sqrt{2}a} \quad A_d \quad E \quad \text{in direction} \quad 9-8
 \end{aligned}$$

Substituting for A_1 and A_d the values given in the nomenclature, we have the following components of force.

Point	Horizontal Force	Vertical Force
1	$+ 3/16 x_9 Et = + x_9 \beta$	$- 3/16 x_9 Et = - x_9 \beta$
3	$3/16 x_9 Et = + x_9 \beta$	$+ 3/16 x_9 Et = + x_9 \beta$
4	$3/4 x_9 Et = + 2x_9 \alpha$	
5	$3/16 x_9 Et = + x_9 \beta$	$- 3/16 x_9 Et = - x_9 \beta$
7	$3/16 x_9 Et = + x_9 \beta$	$+ 3/16 x_9 Et = + x_9 \beta$
8	$3/4 x_9 Et = + 2x_9 \alpha$	
9	$- 9/4 x_9 Et = 4 \gamma x_9$	

where $\alpha = 3/8 Et$, $\beta = 3/16 Et$, $\gamma = -(\alpha + \beta) = - 9/16 Et$.

A similar set of reactions can be found for a displacement of point (9) in the y-direction.

The whole wall system may now be analyzed by superimposing solutions of this type for each mass point. If a means of storing accumulated totals of forces is available, then the resulting forces at each mass point can be built up by the use of the above operation for each mass point.

At mass points on the boundaries of the grid system the effects will necessarily be modified. The constants concerned may in this case be evaluated by the use of a method similar to that described above.

Figure B-3 and B-4 show the complete operations for displacements in the x and y directions. The forces computed are divided by the corresponding masses to give the desired accelerations.

In the program all the operator constants are divided by the mass of the central element M_N , thus giving the accelerations directly. Edge accelerations are found by multiplying the computed values by

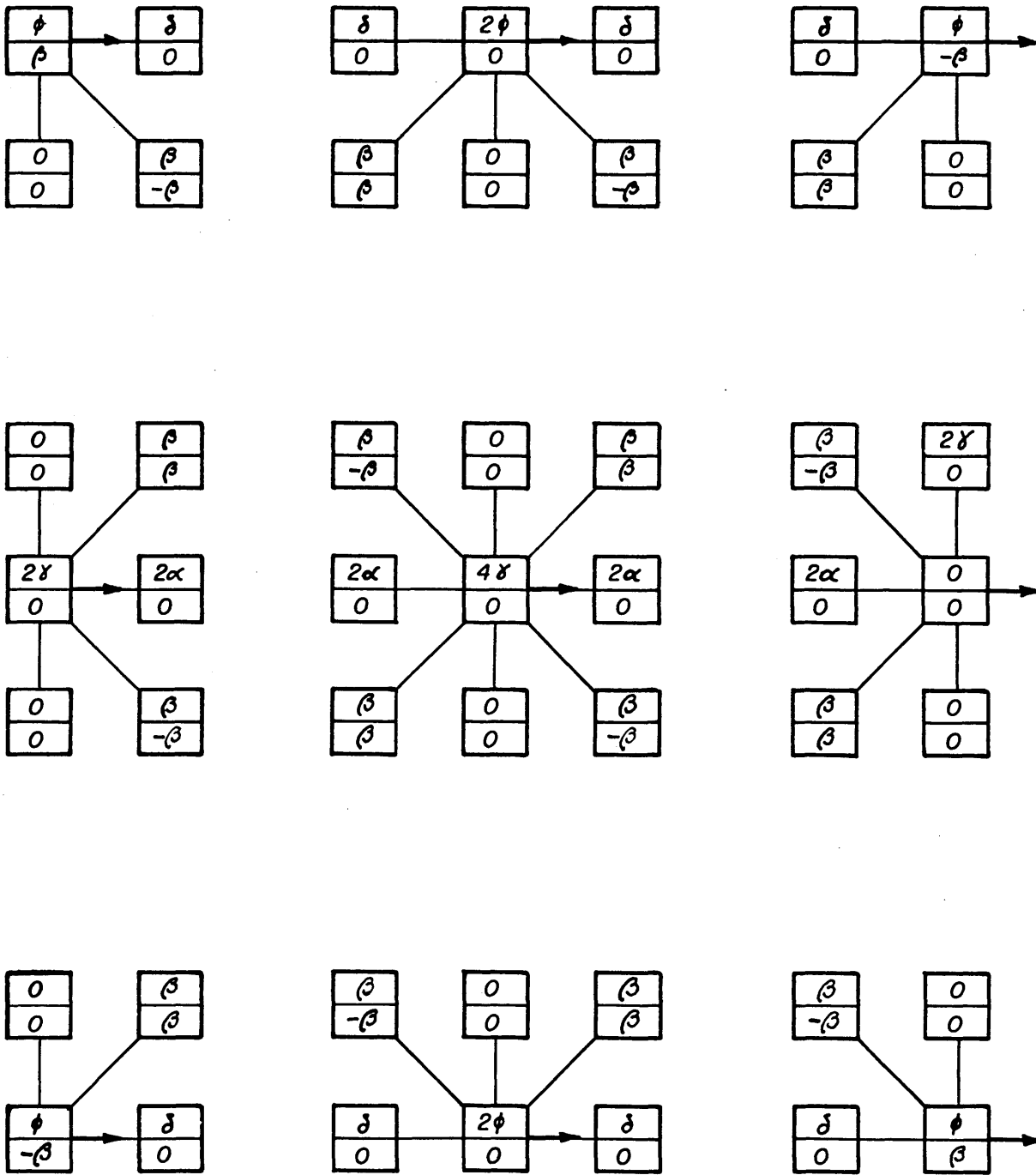
$\frac{M_N}{\text{the mass of the corresponding element}}$

B. Cracked Wall

The effect of a 45° crack across an element has already been discussed in Chapter VI and Appendix A.

In the computation of accelerations from deflections of the mass points, the system is first analyzed as if there were no cracks, and the solution is then modified by replacing the forces as originally computed in the bars by the forces resulting from an analysis of the bars that are assumed to be cracked.

A flow diagram of the subroutine which deals with cracked bars



$$\left. \begin{aligned} \delta &= \alpha + \epsilon \\ \phi &= \delta - \epsilon \end{aligned} \right\} \epsilon = \frac{A_E E}{2a}$$

Figure B-3 Operators for the Contributions to Forces in the x and y directions resulting from unit deflection in the x direction. The upper members in the square refer to x-multipliers, the lower, to y.

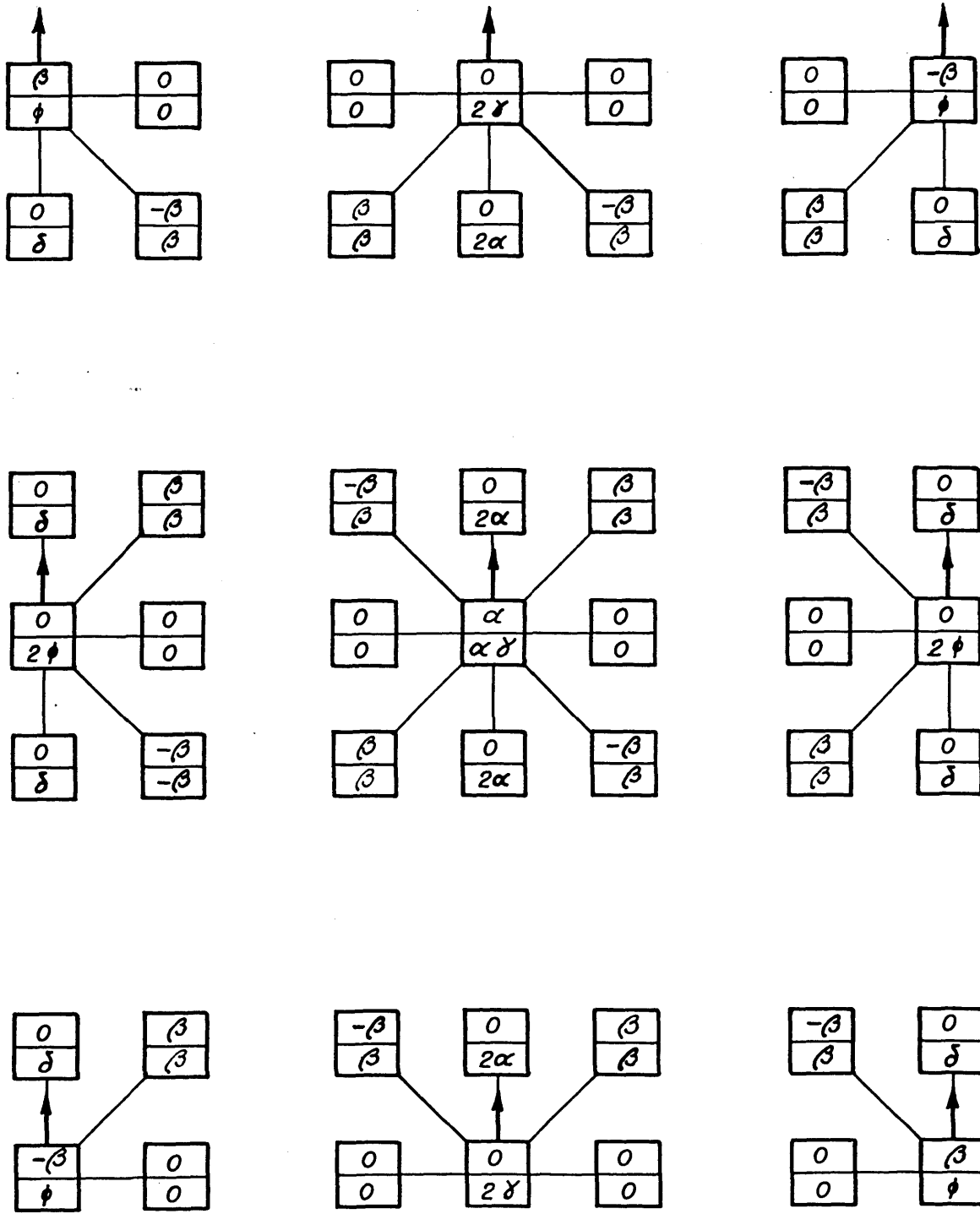


Figure B-4 Operators for the contributions to forces in the x and y-directions resulting from unit deflection in the y direction. The upper members in the squares refer to x-multipliers, the lower to y.

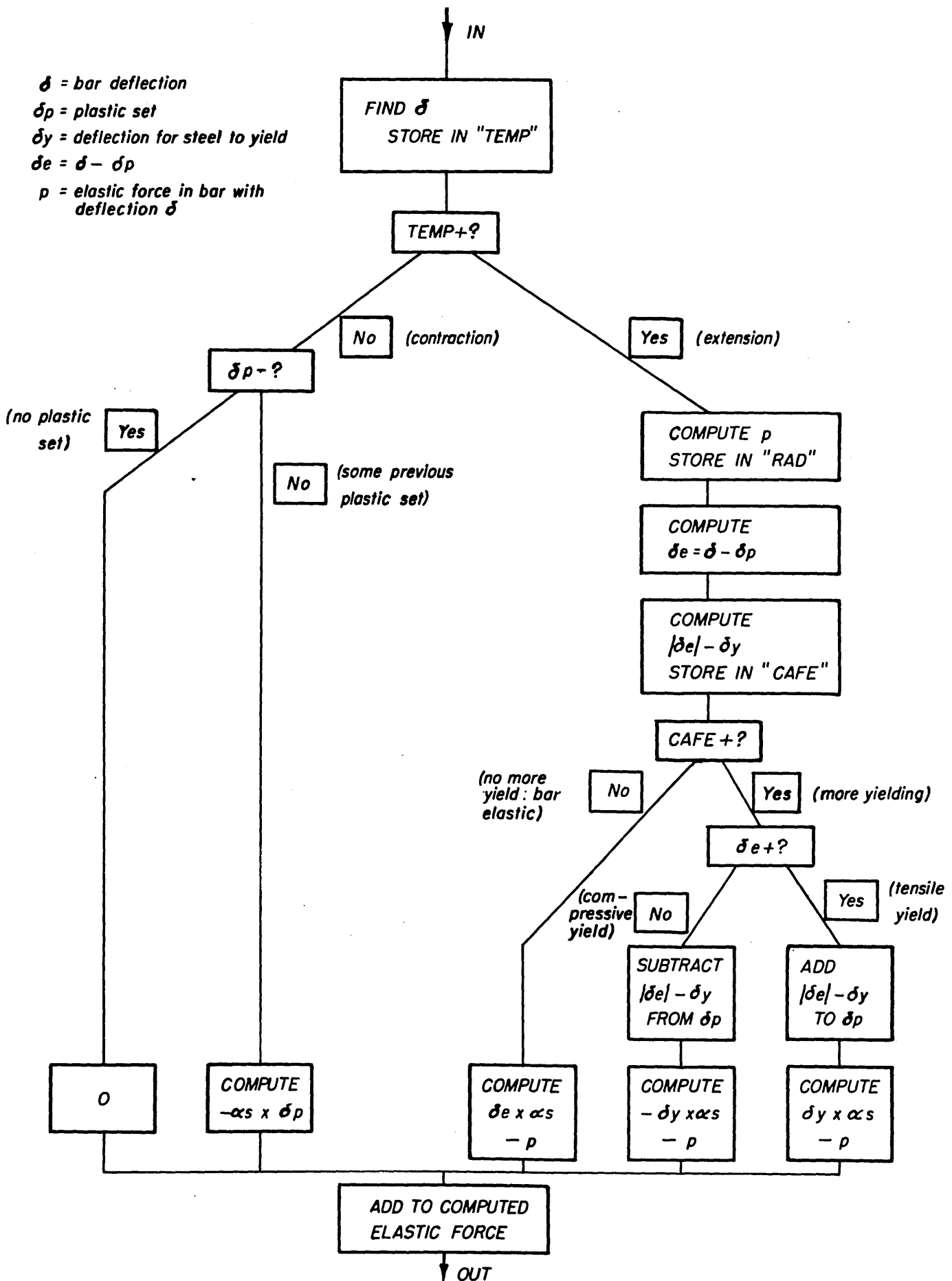


Figure B-5 Flow diagram for the programme which computes the difference in force due to cracking

is shown in Figure B-5 and the following is a brief explanation of the different possibilities that it was necessary to consider for a given bar deflection (δ).

1. δ is Negative. In this case, we have contraction, and the following two cases must be considered:

a) If the plastic set δ_p was negative just before this δ was considered, it means that no previous tension plastic set occurred and we have the situation given in Figure B-6

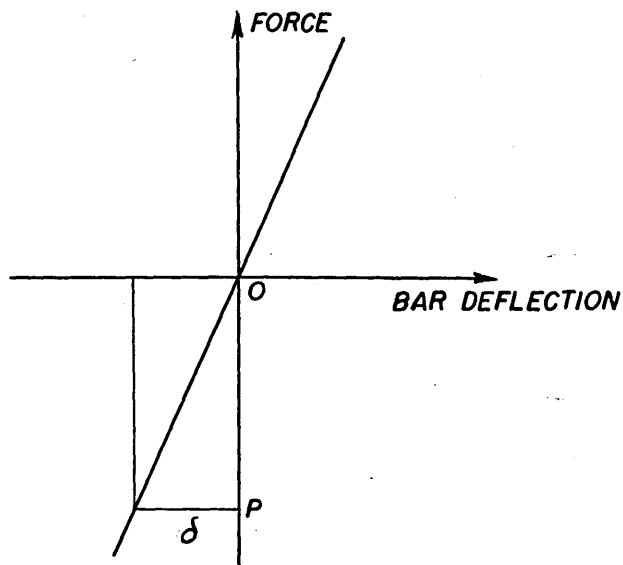


Figure B-6

b) If δ_p was positive, we have the situation illustrated in Figure B-7 by point F.

From this figure it can be seen that if we had computed the force assuming the bar was elastic, the value obtained would be that shown by point P. However, the actual value is given by P_e and in order to obtain this it is necessary to add to the elastic force P the value PP_e which is equal to OP' . This value is directly $\alpha_s \times p$.

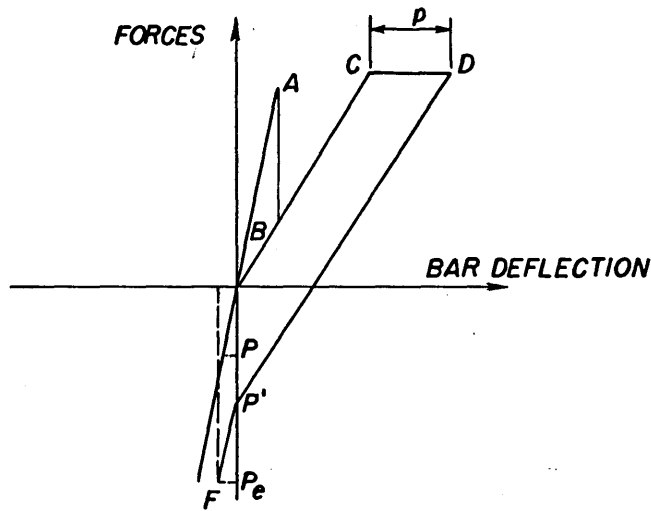


Figure B-7

2. δ is Positive. In this case we have extension and depending on whether $[|\delta_e| - \delta y]$ is positive or negative, the following two cases must be considered:

- a) If $[|\delta_e| - \delta y]$ is negative we have the case illustrated in Figure B-8, where we can see that the exact value of the force is P_e . The value computed assuming the bar is uncracked was P . Therefore, in order to obtain the exact value $P_e = \delta_e \times \alpha_s$, it is necessary to add to the computed value P the value $[\delta_e \cdot \alpha_s - P]$

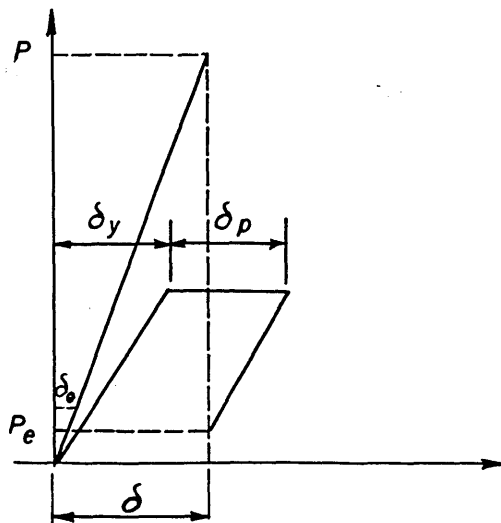


Figure B-8

b) If $[|\delta_e| - \delta_y]$ is positive we have to consider two new possibilities, depending on whether δ_e is positive or negative.

i) If δ_e is negative, we have the situation shown in Figure

B-9 where in order to obtain the exact value of the force

$P_e = (-\alpha_s \times \delta_y)$ it is necessary to add to the computed

elastic value P the value $[-\alpha_s \delta_y - P]$.

In order to obtain the new plastic set δ_p it is necessary

to subtract from the former δ_p the value $(|\delta_e| - \delta_y)$.

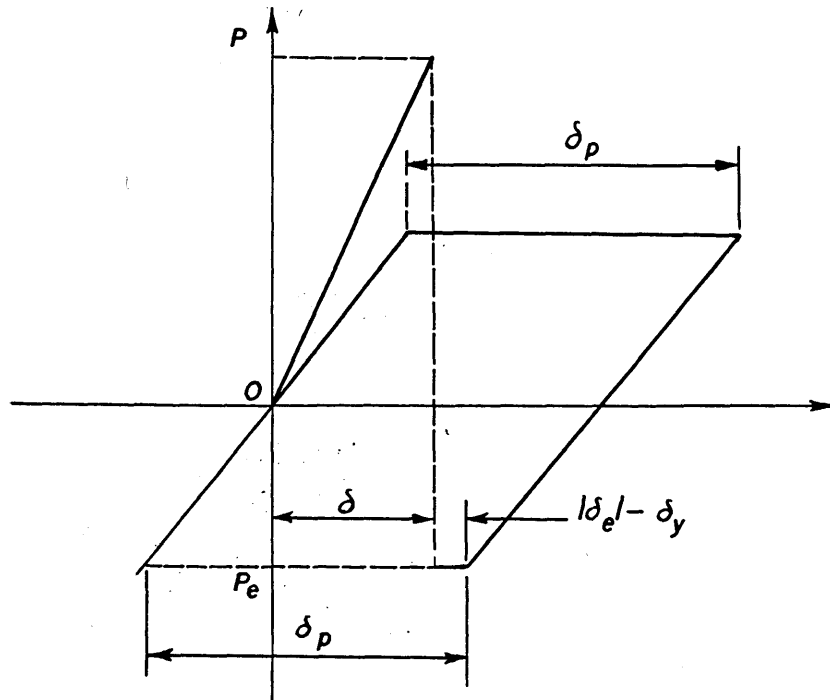


Figure B-9

ii) If δ_e is positive we have the situation shown in Figure

B-10 and the exact value P_e may be obtained by adding to

the computed force P the value $(\delta_y \times \alpha_s - P)$ and in order

to obtain the value of the plastic set for the next step

it is necessary to add to δ_p the value $[|\delta_e| - \delta_y]$

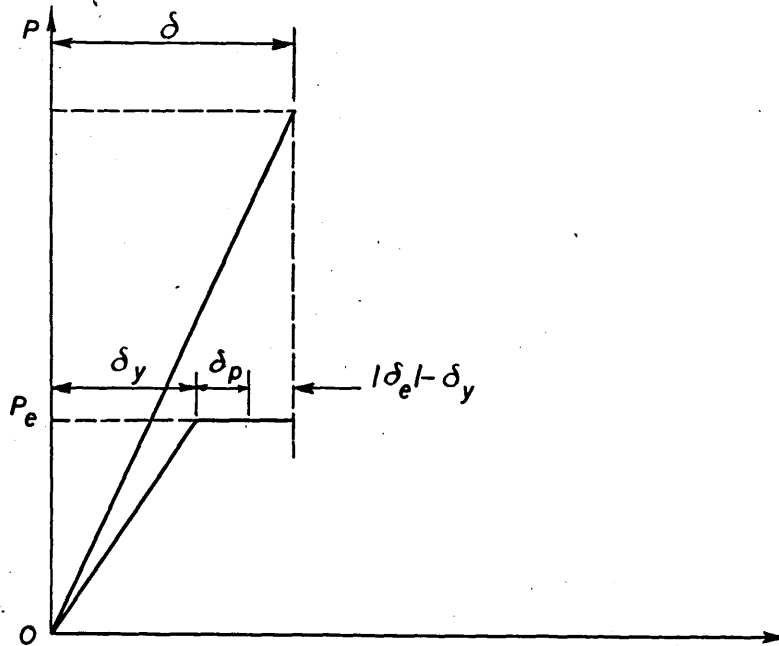


Figure B-10

II. THE ITERATIVE SOLUTION OF THE EQUATIONS OF MOTION OF THE POINT MASSES

As already explained in Appendix A, three equations are used.

Acceleration Impulse Equation.

$$q_{n+1} = 2q_n - q_{n-1} + h^2 \ddot{q}_n \quad (B-1)$$

Linear Acceleration Equation.

$$q_{n+1} = q_n + \dot{q}_n h + \frac{h^2}{6} (2 \ddot{q}_n + \ddot{q}_{n+1}) \quad (B-2)$$

Velocity Equation.

$$\dot{q}_n = \dot{q}_{n-1} + h/2 (\ddot{q}_{n-1} + \ddot{q}_n) \quad (B-3)$$

First, with \ddot{q}_n ; q_n ; \dot{q}_{n-1} ; \ddot{q}_{n-1} ; q_{n-1} known, \dot{q}_n is computed from (B-3).

Equation (B-1) is then used to obtain an estimate of q_{n+1} . This estimate

is then used to compute the accelerations \ddot{q}_{n+1} by use of the processes described above. Substitution of this value, and the value of \dot{q}_n in(2) gives a second estimate of q_{n+1} . Again \ddot{q}_{n+1} is computed, and a third estimate of \ddot{q}_{n+1} is obtained. These iterations are continued until an adequate convergence is obtained. First trial was made with 3 iterations. Figure B-11 is a "Flow Diagram" showing how the equations are used.

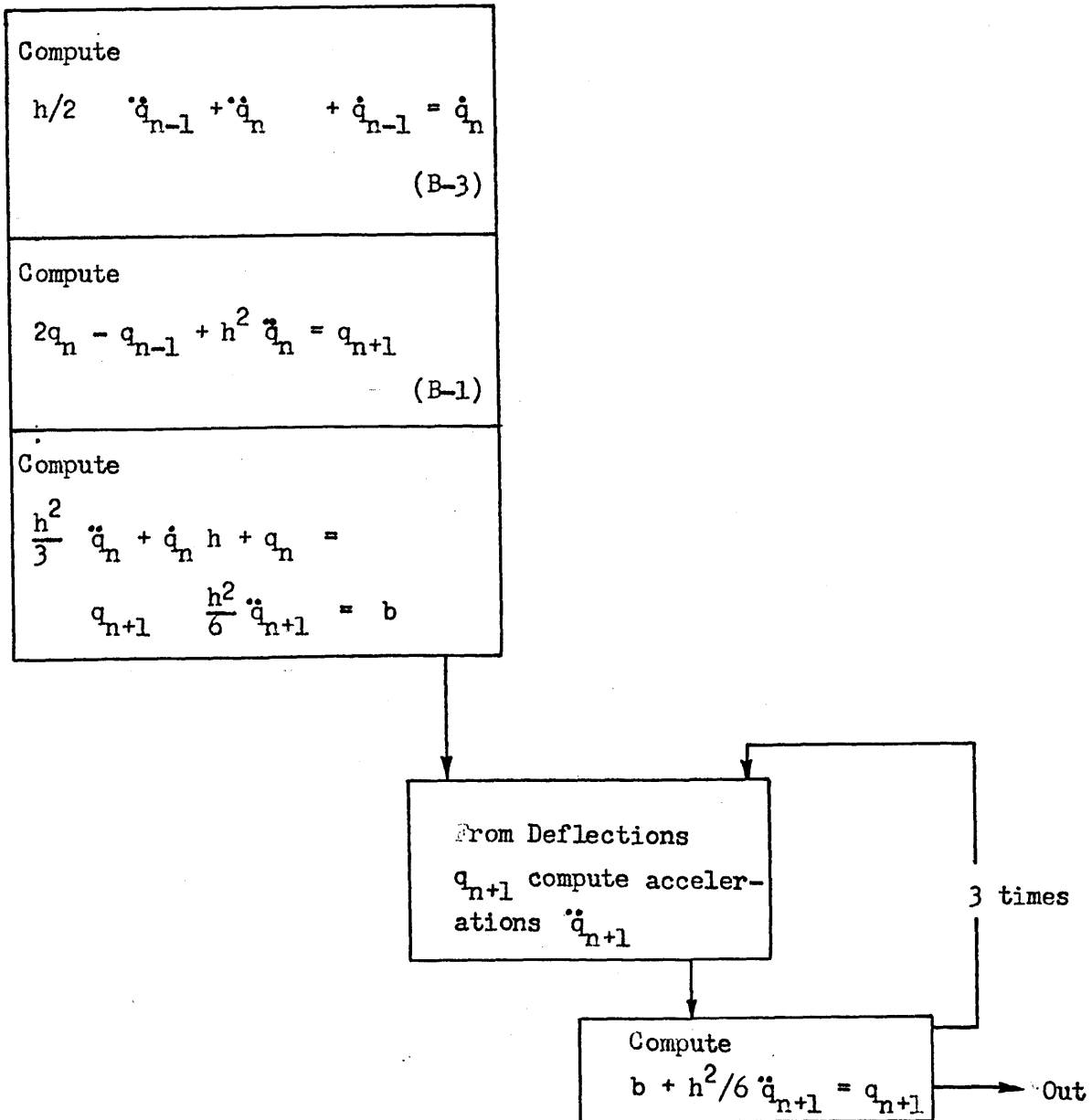


Figure B-11

III. PROGRAM FOR THE IBM 704 BASED ON SCHEMATIC FLOW DIAGRAM

A. Key to the Overall Flow Diagram

The following is a description necessary in order to interpret the flow diagram of Figure B-11.

- Wall : Starts program off. Reserves space for final Stop, and for Dump Stop.
- Num 1 : Reserves all storage space used: the size of the matrices being determined by the input data.
- Orig : Fills in with -0 the blocks which will contain the amounts of plastic yield in the bars.
- Fill : Sets up Reference Grid.
- CAL : Computes all constants subsequently used -- bar stiffnesses, element masses, etc. Points out column headings and results at zero time. Applies equation 2 for the top left-hand corner for the first time interval.
- PO3 : Sets counter for r iterations: i.e. put CHECK = r + 1
- Rout : Computes \ddot{q}_{n+1} from q_n , assuming the wall uncracked and of uniform section (i.e. no heavier edge beams). Sets corner accelerations = 0 at points of rigid support.
- CF10 : Checks the indicators for cracking of the wall anywhere. If there is any cracking, control is transferred to CRAX; if not, control is transferred to BOUND.
- CF1 : Checks for the last iteration of the current time interval. If the iterative procedure is over, control is transferred to CF2. Otherwise control is transferred to BOUND.
- CF2 : Stores the corner accelerations before they are set to zero by ROUT
- Crax : Modifies \ddot{q}_{n+1} wherever there is cracking.

- Bound : Modifies \ddot{q}_{n+1} to take account of the additional mass of the edge beams. Applies equation 2: i.e. makes estimates of q_{n+1} .
- Stres : Computes the principal tensile stress in each panel of the wall and in the edge beams. If the breaking stress is reached, a record of the time is made in appropriate registers. For wall cracks, the angle of the crack in each segment is also recorded.
- Mast : Master control. Sets the force for the next time interval. Increases TIM, the time-interval counter, by 1. If the end of the computation is reached control is transferred to PRO.
- PRO : Prints out the sequence of cracking and the angles of the wall cracks.
- OUTP : Collects required deflections, and assembles together with the corner reactions for printing. Prints out the results at certain predetermined times.
- Pl : Applies equations 1 and 3, and finds three terms of equation 2 (See BOUND)

IV. CONTROL REGISTERS

- CHECK Counts the number of iterations per time interval.
- CATCH Current results are printed out when CATCH = 1. Any new crack puts CATCH = 1.
- CUT Results are printed out when CUT = 0. Each successive time interval CUT is reduced by 1. CUT is set to S-1 after a "CUT = 0" point and to q-1 after a "CATCH = 1" point.
- TEST +1 or -1. When positive, the routines deal with forces, velocities and accelerations in the x-direction; when negative, in the y-direction.
- SPLIT Originally set to 0, it is set to +1 on the occurrence of any crack, and x acts as an overall cracking indicator.

TIM Counts the time-intervals. Originally 0, it contains +1 during the computations of the first time interval, +2 during the second, etc.

TCO +1 or -1. When TIM is odd, TCO is +1

When TIM is even, TCO is -1.

As q_n during one time-interval becomes q_{n-1} during the next, etc, it is necessary to have an indicator to decide what information is to be used in the application of each equation. This control is achieved by using TCO.

Parameters r = number of iterations per interval

s = number of time intervals elapsing between normal points.

q = number of time intervals after the occurrence of a crack at which a print is made.